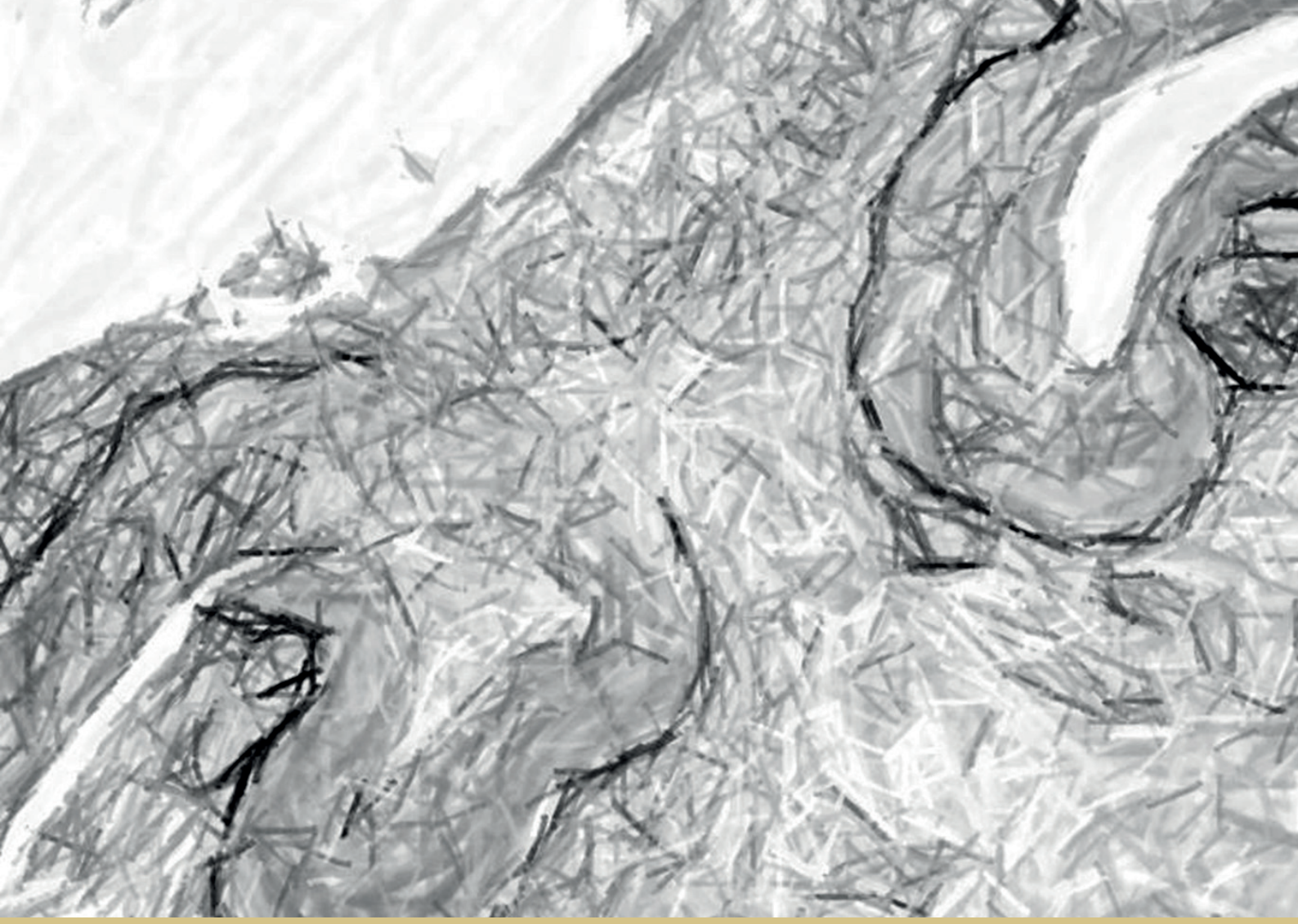

Beatriz Maria Pinto da Cruz Costa

EVALUATION OF THE CELLULAR, HUMORAL AND MOLECULAR EFFECTS OF THE TEDUGLUTIDE ADMINISTRATION ON AN ANIMAL MODEL OF INTESTINAL ANASTOMOSIS

Doctoral Programme in Health Sciences, Medicine, supervised by Professor Doctor Francisco José Franquera Castro e Sousa, Professor Doctor Maria Filomena Rabaça Roque Botelho, and Professor Doctor Ana Bela Sarmento Antunes da Cruz Ribeiro, and presented to the Faculty of Medicine of the University of Coimbra

December 2017

· U C ·

Universidade de Coimbra

EVALUATION OF THE CELLULAR, HUMORAL AND MOLECULAR EFFECTS OF THE TEDUGLUTIDE ADMINISTRATION ON AN ANIMAL MODEL OF INTESTINAL ANASTOMOSIS

AVALIAÇÃO DOS EFEITOS CELULARES, HUMORAIS E MOLECULARES DA ADMINISTRAÇÃO DO TEDUGLUTIDE NUM MODELO ANIMAL DE ANASTOMOSE INTESTINAL

Doctoral Programme in Health Sciences, Medicine, supervised by Professor Doctor Francisco José Franquera Castro e Sousa, Professor Doctor Maria Filomena Rabaça Roque Botelho, and Professor Doctor Ana Bela Sarmento Antunes da Cruz Ribeiro, and presented to the Faculty of Medicine of the University of Coimbra

December 2017

· U C ·

UNIVERSIDADE DE COIMBRA

Publications

The following original articles and abstracts have been published in peer-scientific indexed journals, within the scope of the present PhD thesis:

Original articles

Costa BP, Gonçalves AC, Abrantes AM, Alves R, Matafome P, Seiça R, Sarmento-Ribeiro AB, Botelho MF, Castro-Sousa F: Intestinal epithelial stem cells: Distinct behavior after surgical injury and teduglutide administration. *J Invest Surg*. 2017;31:1-10. Doi 10.1080/08941939.2017.1294217.

Costa BP, Gonçalves AC, Abrantes AM, Matafome P, Seiça R, Sarmento-Ribeiro AB, Botelho MF, Castro-Sousa F: Effects of teduglutide on histological parameters of intestinal anastomotic healing. *Eur Surg*. 2017;49(5):218-227. Doi 10.1007/s10353-017-0478-9.

Costa BP, Gonçalves AC, Abrantes AM, Alves R, Matafome P, Seiça R, Sarmento-Ribeiro AB, Botelho MF, Castro-Sousa F: Teduglutide effects on gene regulation of fibrogenesis on an animal model of intestinal anastomosis. *J Surg Res*. 2017;216:87-98. Doi 10.1016/j.jss.2017.04.022.

Costa BP, Gonçalves AC, Abrantes AM, Matafome P, Seiça R, Sarmento-Ribeiro AB, Botelho MF, Castro-Sousa F: Intestinal inflammatory and redox responses to the perioperative administration of teduglutide in rats. *Acta Cir Bras*. 2017;32(8):648-661. Doi 10.1590/s0102-865020170080000007.

Costa BP, Gonçalves AC, Abrantes AM, Matafome P, Seiça R, Sarmento-Ribeiro AB, Botelho MF, Castro-Sousa F: Tissular growth factors profile after teduglutide administration on an animal model of intestinal anastomosis. *Nutr Hosp*. 2018;35(1):xxx-xxx. Doi 10.20960/nh.1326 *(Accepted for publication in July 21, 2017)*.

Abstracts

Beatriz P. Costa, Margarida Abrantes, Augusta Cipriano, Ângela Jesus, Mário Ruivo, Paulo Teixeira, Lígia Castro, Cristina Gonçalves, Ana Bela Sarmento Ribeiro, Maria Filomena Botelho, F. Castro Sousa: Avaliação dos efeitos da administração do *Glucagon-like Peptide 2* num modelo animal de anastomose intestinal - Análise preliminar. *Revista Portuguesa de Cirurgia.* 2015;32 (Supl. março):93 (oral presentation at the XXXV Congresso Nacional de Cirurgia, Figueira da Foz, Portugal).

Costa BP, Sarmento-Ribeiro AB, Gonçalves AC, Botelho F, Abrantes M, Castro-Sousa F: Response of putative intestinal epithelial stem cells to surgical injury and teduglutide administration on an animal model. *Clin Nutr.* 2015;34 (Supp1):S19 [oral communication at the 37th European Society for Clinical Nutrition and Metabolism (ESPEN) Congress, Lisbon, 2015].

Costa BP, Sarmento-Ribeiro AB, Gonçalves AC, Botelho F, Abrantes M, Castro-Sousa F: Tissular growth factors profile after teduglutide administration on an animal model of intestinal anastomosis. *Clin Nutr.* 2015;34 (Supp1):S26 [outstanding abstract and poster at the 37th European Society for Clinical Nutrition and Metabolism (ESPEN) Congress, Lisbon, 2015].

Acknowledgments & Agradecimentos

Considero meu dever testemunhar o meu profundo reconhecimento perante todos aqueles que, com o seu encorajamento e orientação, contribuíram para esta Tese.

Ao meu orientador Professor Doutor Francisco José Franquera Castro Sousa, Professor Catedrático de Cirurgia da Faculdade de Medicina da Universidade de Coimbra, Director do Serviço de Cirurgia III/A dos Hospitais da Universidade de Coimbra do Centro Hospitalar e Universitário de Coimbra, meu Mestre e Amigo, Professor e Cirurgião notável que, pela excelência das qualidades científicas e técnicas, determinação e inconformismo, adquiriu indiscutível prestígio nacional e internacional, expresso profundo reconhecimento e respeito.

Às minhas co-orientadoras Professora Doutora Maria Filomena Rabaça Roque Botelho e Professora Doutora Ana Bela Sarmento Antunes da Cruz Ribeiro, pela ajuda inestimável na orientação desta tese, incentivo e tempo que me dedicaram.

Ao Professor Doutor Júlio Fortunato Soares Leite, Director do Serviço do Serviço de Cirurgia A/B do Centro Hospitalar e Universitário de Coimbra, Regente da Unidade Curricular de Clínica Cirúrgica do Mestrado Integrado em Medicina da Faculdade de Medicina da Universidade de Coimbra, cirurgião de reconhecidas qualidades técnicas e humanas e com elevada vocação didáctica, expresso o meu agradecimento.

À Professora Doutora Raquel Seiça, pelo permanente incentivo, disponibilidade, amizade e apoio.

À Doutora Margarida Abrantes, à Doutora Ana Cristina Gonçalves, à Dra Maria Augusta Cipriano, ao Doutor Paulo Matafome, à Mestre Raquel Alves e à Dra Lígia Prado e Castro pela prestimosa colaboração no estudo experimental.

À Doutora Bárbara Paiva, Doutora Mafalda Laranjo, Dr. João Casalta, Sra. Técnica Superior de Anatomia Patológica Ângela Jesus, Srs. Técnicos Superiores de Anatomia Patológica Mário Ruivo e Paulo Teixeira e Dra. Lisete Lemos.

A todos os meus colegas do Serviço de Cirurgia A do Centro Hospitalar e Universitário de Coimbra. Um agradecimento especial aos Srs Dr. Helder Soriano de Carvalho, Dr. António Milheiro, Dr. Carlos Mesquita, Dra. Gorete Jorge, Dr. José Carlos Campos, Prof. Doutor José Guilherme Tralhão, Dr. Alexandre Monteiro, Dra. Mónica Martins, Doutor Henrique Alexandrino, Dr. António Manso, Dr. Marco Serôdio, Dr. Ricardo Martins, Dr. Miguel Fernandes, Dr. Manuel Rosete e Dra. Marisa Tomé.

Aos restantes profissionais do Serviço de Cirurgia A e do Bloco Operatório do Centro Hospitalar e Universitário de Coimbra, incluindo enfermeiros, assistentes técnicos e operacionais, pela sua dedicação, carinho e amizade.

Aos meus professores e alunos.

À minha família e aos meus amigos, um especial agradecimento pelo apoio permanente nos momentos mais difíceis.

Aos meus pais, Maria Fernanda e Carlos, pelo profundo amor e incondicional apoio.

Bem hajam!

"*Surgery is an Art and a Science in which the Hands are at the service of the Intelligence*"

Jean d'Ormesson

Table of Contents

Table of Contents

Abbreviations & Acronyms

[Glp2]: Concentration of glucagon-like peptide 2

[GSH]: Cellular reduced glutathione content

α-Sma: α-smooth muscle actin

σ: Spearman's correlation coefficent

$\Delta C_{T:}$ Threshold cycle

Δψmt: Mitochondrial membrane potential

A

ACS-NSQIP: American College of Surgeons National Surgical Quality Improvement Program

Adam: A desintegrin and metalloprotease (adamalysin)

Adamts: A desintegrin and metalloprotease with thrombospondin motifs

AKT: Protein-kinase B

Alcam: Activated leukocyte cell adhesion molecule

APC: Allophycocyanin

Arg: Arginine

ARRIVE: Animal Research: Reporting In Vivo Experiments

ASA: American Society of Anesthesiology

ATP: Adenosine triphosphate

AUC: Area under the curve

auROC: Area under the Receiver Operating Characteristic Curve

AV: Annexin-V

B

Bcl2: B-cell chronic lymphocytic leukemia/lymphoma 2

bFGF: Basic fibroblast growth factor

Bmi1: Bmi1 protooncogene, Polycomb ring finger (B-cell-specific Moloney murine leukemia virus insertion site 1)

Bmi1: B-cell-specific Maloney murine leukemia virus insertion site 1

Bmp: Bone morphogenic protein

Bmp4: Bone morphogenic protein 4 ligand

C

cAMP-PKA-CREB: Cyclic adenosine monophosphate-Protein kinase A-cyclic adenosine monophosphate response element-binding protein

CD166: Cluster of differentiation 166

CD24: Cluster of differentiation 24

CD31: Cluster of differentiation 31

CD44: Cluster of differentiation 44

CD45: Cluster of differentiation 45

CD90/Thy-1: Cluster of differentiation 90/Thymocyte differentiation antigen 1

cDNA: Complementary deoxyribonucleic acid

CI: Confidence interval

CK18: Cytokeratin 18

Col1a1: Collagen, type I, alpha 1, mRNA

Col3a1: Collagen, type III, alpha 1, mRNA

Col4a1: Collagen, type IV, alpha 1, mRNA

Col5a1: Collagen, type V, alpha 1, mRNA

COPD: Chronic obstructive pulmonary disease

Cox2: Cyclooxygenase 2

CTGF: Connective tissue growth factor

Ctgf: Connective tissue growth factor, mRNA

cWnt: Canonical Wingless

CXCL5: C-X-C motif chemokine ligand 5

D

DCF: 2',7'-dichlorofluorescein

$DCFH_2$: 2',7'-dichlorodihydrofluorescein

$DCFH_2$-DA: 2',7'-dichlorodihydrofluorescein diacetate

DHR 123: dihydrorhodamine 123

DDR: Discoidin domain receptors

DMEM: Dulbecco's modified eagle's medium

DMSO: Dimethyl sulfoxide

DNA: Deoxyribonucleic acid

E

Early ap: Early apoptosis index

EDTA: Ethylenediaminetetraacetic acid

EGF: Epidermal growth factor

Egf: Epidermal growth factor, mRNA

EIA: Competitive enzyme immunoassay

ELISA: Enzyme-linked immunosorbent assay

EMA: European Medicines Agency

Epcam: Epithelial cell adhesion molecule

EPO: Erythropoietin

ErbB: Erythroblastic leukemia viral oncogene

ERK: Extracellular signal-regulated kinase

ESPEN: European Society for Clinical Nutrition and Metabolism

F

Fab: Antigen-binding fragment

FACS: Fluorescence-activated cell sorting

Fc: Crystallizable fragment

FDA: United States Food and Drug Administration

FGF2: Fibroblast growth factor 2

Fgf2: Fibroblast growth factor 2, mRNA

FGF7: Fibroblast growth factor 7 (keratinocyte growth factor 1, KGF1)

Fgf7: Fibroblast growth factor 7, mRNA

FGF-R1: Fibroblast growth factor receptor 1

FITC: Fluorescein-isothiocyanate

FL: Fluorescence detector

G

G&S: Gordon-Sweet's protocol

GALT: Gut-associated lymphoid tissue

GFRP: Growth factor-rich plasma

GH: Growth hormone

GLP-1: Glucagon-like peptide 1

GLP-2 MMB: GLP-2 mimetibody construct

GLP-2: Glucagon-like peptide 2

GLP-2R: Glucagon-like peptide 2 receptor

Glp2r: Glucagon-like peptide 2 receptor, mRNA

GM-CSF: Granulocyte-macrophage colony-stimulating factor

Gpr49: G Protein-coupled receptor 49

Grp78: 78 KDa glucose-regulated protein

GSH: Reduced glutathione

GSK3β: Glycogen synthase kinase 3 β

H

Hb: Hemoglobin

H&E: Hematoxylin-eosin

H_2O: Water

H_2O_2: Hydrogen peroxide

HB-EGF: Heparin-binding epidermal-like growth factor

Hbegf: Heparin-binding EGF-like growth factor, mRNA

HBOT: Hyperbaric oxygen therapy

HBSS: Hank's balanced salt solution

Hepes: 4-(2-hydroxyethyl)piperazine-1-ethanesulfonic acid solution

Hif: Hypoxia-inducible factor 1

Hippo-YAP: Hippo-Yes-associated protein 1

$HO^{\cdot}$: Hydroxyl radical

Hopx: Homeodomain-only protein

Hprt1: Hypoxanthine phosphoribosyltransferase 1, mRNA

HR: Hazard ratio

I

ic[GSH]: Cellular reduced glutathione content

IESC: Intestinal epithelial stem cells

IFN-γ: Interferon-γ

Ig: Immunoglobulin

Igf1: Insulin-like growth factor 1, transcript variant 1, mRNA

IGF-1: Insulin-like growth factor 1

IGF-BP: Insulin-like growth factor binding protein

IL: Interleukin

IL-1α: Interleukin-1 alpha

IL-2R: Interleukin-2 receptor

IL-4: Interleukin-4

IL-6: Interleukin-6

IM: Intramuscular

IMAGinE: International Multispecialty Anastomotic Leak Global Improvement Exchange

iNOS: Inducible nitric oxide synthase

IO: Intraoperative

IP: Intraperitoneal

IQR: Interquartile range

J

JC-1: 5,5',6,6'-tethrachloro-1,1',3,3'-tethraethylbenzimidazolcarbocyanine iodide

JC1 A/M: JC-1 aggregates/monomers ratio

K

Kgf: Keratinocyte growth factor

L

Lap: Laparotomy

Late ap: Late apoptosis/necrosis index

LCA: Leucocyte common antigen

Lgr5/Gpr49: Leucine-rich repeat-containing G-protein coupled receptor 5

Lgr5: Leucine-rich repeat-containing G-protein coupled receptor 5

Lrig1: Leucine-rich repeats and immunoglobulin-like domains 1

M

MALT: Mucosal-associated lymphoid tissue

MAPK: Mitogen-activated protein kinase

MCP-1: Macrophage chemo-attractant protein-1

MFI: Mean intensity of fluorescence

MMP: Matrix metalloproteinases

Mmp1: Matrix metallopeptidase 1 (interstitial collagenase), mRNA

Mmp 12: Matrix metallopeptidase 12, mRNA

Mmp 13: Matrix metallopeptidase 13, mRNA

Mmp 14: Matrix metallopeptidase 14 (membrane inserted), mRNA

Mmp 2: Matrix metallopeptidase 2, mRNA

Mmp 3: Matrix metallopeptidase 3, mRNA

Mmp 9: Matrix metallopeptidase 9, mRNA

MO: Mercury orange dye

MMLV: Moloney strain of murine leukemia virus

mRNA: Messenger ribonucleic acid

mTOR: Mammalian target of rapamycin

mTORC1: Mammalian target of rapamycin complex 1

Mψ: mitochondrial membrane potential

N

NCBI: National Center for Biotechnology Information

N.t.: Not tested

NF-κB: Nuclear factor-kappa-light-chain-enhancer of activated B cells

NO: Nitric oxide

NOS: Nitric oxide synthase

NSAID: Non-steroid anti-inflammatory drugs

O

$ONOO^-$: Peroxynitrite

OR: Odds ratio

P

p: value of significance

PAS-AB: Periodic acid schiff-alcian blue

PBS: Phosphate buffered saline

PCR: Polymerase chain reaction

PDGF: Platelet-derived growth factor

Pdgfb: Platelet-derived growth factor beta polypeptide, mRNA

PE: Phycoerythrin

Pecam-1: Platelet and endothelial cell adhesion molecule-1

Peroxides: Cytosolic peroxides level

PerCP-Cy5.5: Peridinin cholorophyll protein complex with cyanin-5.5

PGE2: Prostaglandin E2

PI: Propidium iodide

PI3K: Phosphatidylinositol 3-kinase

PPAR-γ: Peroxisome proliferator activator receptor-γ

Pro-MMP: Pro-metalloproteinase

PRP: Platelet-rich plasma

Q

qRT-PCR: Quantitative real-time reverse-transcription polymerase chain reaction

R

Reac Sp: Reactive species generation in the mitochondria

Ref: Reference

Res: Resection

RNA: Ribonucleic acid

ROC: Receiver Operating Characteristic

ROS: Reactive oxygen species

RR: Relative risk

RS: Reactive species

R-spondins: Roof plate-specific spondins

RT: Room temperature

S

Sc: Subcutaneous

SDF-1: Stromal cell-derived factor-1

SMC: Smooth muscle cells

SPSS: Statistical Package for Social Sciences

STAT3: Signal transducer and activator of transcription-3

STEPS: Study of Teduglutide Effectiveness in Parenteral Nutrition-Dependent Short-bowel Syndrome Subjects

T

Tcf4: Transcription factor 4

Ted: Teduglutide

Tert: Telomerase reverse transcriptase

TGF-β: Transforming growth factor-β

Tgfb1: Transforming growth factor, beta 1, mRNA

Th1: T-helper 1 lymphocytes

Th2: T-helper 2 lymphocytes

Timp1: TIMP metallopeptidase inhibitor 1, mRNA

Timp2: TIMP metallopeptidase inhibitor 2, mRNA

Timp: Tissue inhibitor of matrix metalloproteinases

tKGF: Truncated keratinocyte growth factor

TNF-α: Tumour necrosis factor-alpha

Tpl2: Tumor progression locus 2

Trem2: Triggering receptor expressed on myeloid cells 2

Tris: Tris(hydroxylmethyl)aminomethane

U

UK: United Kingdom

USA: United States of America

USP: United States Pharmacopeia

V

VEGF: Vascular endothelial growth factor

Vegfa: Vascular endothelial growth factor A, transcript variant 2, mRNA

Vs.: Versus

VSM: Vascular smooth muscle

W

Wnt: Wingless

Wnt3: Wingless ligand 3

Abstract & Resumo

Abstract

Despite recent progresses in surgical technique and perioperative care, failure of intestinal anastomotic healing remains one of the most feared complications in digestive surgery, exerting a profound adverse impact on the operative morbidity and mortality rates, oncologic and functional outcomes, and socioeconomic costs.

Teduglutide is an enterotrophic analogue of glucagon-like peptide 2 (GLP-2) approved for the pharmacological rehabilitation of short-bowel syndrome.

Present study aimed to clarify the potential of teduglutide as a promoting strategy for the improvement of intestinal anastomotic healing, on an animal model, through the influence on the cellular, humoral and molecular mediators of repair.

An experimental rat model of standard small-bowel anastomosis was used with evaluation at the third and seventh postoperative days. Structural assessment of the anastomosis included the macroscopic integrity and the histological and immunohistochemical examination of healing parameters, comprising reepithelialization, neoangiogenesis and fibroplasia. Cellular and molecular mediators of anastomotic healing were analyzed, including: putative epithelial stem cells response (using Lgr5, Bmi1 and the panel CD24/CD44/CD166/Grp78 surface markers by flow cytometry); cellular viability and death (with double staining with annexin-V/propidium iodide by flow cytometry); oxidative stress [quantification of cytosolic peroxides with 2',7'-dichlorodihydrofluorescein diacetate ($DCFH_2$-DA) probe, mitochondrial reactive species with dihydrorhodamine 123 (DHR 123) probe, total intracellular reduced glutathione with mercury orange staining and mitochondrial membrane potential with 5,5',6,6'-tethrachloro-1,1',3,3'-tethraethylbenzimidazolcarbocyanine iodide (JC-1) probe, by flow cytometry]; local and systemic inflammatory response (tissue and plasma concentrations of interleukine-1α, macrophage chemo-attractant protein-1, tumor necrosis factor-α, interferon-γ and interleukine-4 by flow cytometric multiplexed bead assay); gene expression of main extracellular matrix components (*Collagen, type I, alpha 1: Col1a1; Collagen, type III, alpha 1: Col3a1; Collagen, type IV, alpha 1: Col4a1; Collagen, type V, alpha 1: Col5a1*) and remodeling factors, matrix metalloproteinases (*Mmp*; *Mmp1* and *Mmp13*, *Mmp2* and *Mmp9*, *Mmp3*, *Mmp12* and

Mmp14) and tissue inhibitors of metalloproteinases 1 and 2 (*Timp*; *Timp1* and *Timp2*); gene expression of growth factors and receptor potentially implicated on anastomotic repair (*Insulin-like growth factor 1, transcript variant: Igf1; Vascular endothelial growth factor A, transcript variant 2: Vegfa; Transforming growth factor, beta 1: Tgfb1; Connective tissue growth factor: Ctgf; Fibroblast growth factor 2: Fgf2; Fibroblast growth factor 7: Fgf7; Epidermal growth factor: Egf; Heparin-binding epidermal-like growth factor: Hbegf; Platelet-derived growth factor beta polypeptide: Pdgfb; Glucagon-like peptide 2 receptor: Glp2r*) by quantitative real-time reverse-transcription polymerase chain reaction (qRT-PCR); and Glp-2 plasma levels (by competitive enzyme immunoassay).

Teduglutide had no apparent relevant impact on the rate or severity of intestinal anastomotic leakage. A favorable influence of teduglutide on the reepithelialization and neoangiogenesis events of the proliferative phase of anastomotic repair was documented. Teduglutide was associated with an increase of subepithelial myofibroblasts density score, but no significant effect on the goblet, Paneth and glial cellular indexes was observed.

This growth factor was associated with an enhancement of type III collagen deposition on the submucosa at the seventh postoperative day, although with simultaneous reduction of type I collagen level in that layer, and a non-significant reduction of global anastomotic collagen content.

Teduglutide inhibited the gene modulation of fibrolysis in the predominantly inflammatory phase of anastomotic repair, while repressed the fibrogenesis in the proliferative stage. Teduglutide induced the upregulation of gene expression of *Timp1*, *Timp2* and *Col4a1*, and the downregulation of *Mmp3* and *Mmp12*, at the third postoperative day; and the repression of gene expression of *Timp1*, *Col3a1, Col4a1* and *Col5a1*, at the seventh day.

Teduglutide contributed to the expansion of the putative crypt base columnar stem cells pool at the seventh day and to the concomitant depletion of the putative "position +4" stem cells fraction. An increase (non-significant) of the overall putative intestinal epithelial stem cells was also observed in teduglutide-treated animals.

Teduglutide was associated with a non-significant prooxidative effect, with an increase of the cytosolic peroxides and mitochondrial reactive species levels and a reduction of the cellular reduced glutathione content. Those effects were coincident with an increase of cellular viability indexes and a non-significant decrease of early apoptotic events. No relevant influence on mitochondrial membrane potential was verified. A non-significant increase of tissue levels of the anti-inflammatory interleukin-4 at the seventh day, and a significant reduction of plasma levels of interferon-γ at the third day were observed in teduglutide-treated animals.

Teduglutide induced the upregulation of the gene expression of *Igf1*, *Vegfa* and *Ctgf* and the downmodulation of *Fgf2*, *Fgf7*, *Tgfb1* and *Glp2r*.

To conclude, the present study reflects the complexity of the intestinal anastomotic repair and points to a favorable influence of teduglutide on this process that deserves additional investigation.

Keywords: Teduglutide; Surgical anastomosis; Anastomotic leak; Reepithelialization; Physiologic angiogenesis; Extracellular matrix; Growth factor; Adult stem cells; Inflammation; Oxidative stress

Resumo

Apesar dos recentes progressos da técnica cirúrgica e suporte peri-operatório, a falência da cicatrização anastomótica intestinal constitui, ainda, uma das mais temíveis complicações da cirurgia digestiva, com um importante impacto adverso na mortalidade e morbilidade operatórias, resultados oncológicos e funcionais e custos económico-sociais.

O teduglutide é um análogo enterotrófico do *glucagon-like peptide 2* (GLP-2) aprovado para a reabilitação farmacológica na síndroma do intestino curto.

Este estudo procurou analisar as potencialidades do teduglutide como estratégia adjuvante da cicatrização anastomótica intestinal, num modelo animal, através da sua influência nos mediadores celulares, humorais e moleculares do processo reparativo.

Foi utilizado um modelo experimental de anastomose intestinal estandardizada, em rato, com avaliação ao terceiro e ao sétimo dias pós-operatórios. A avaliação estrutural da anastomose incluiu a integridade macroscópica e os exames histológico e imunohistoquímico dos parâmetros de cicatrização, tais como reepitelização, neoangiogénese e fibroplasia. Foram analisados os seguintes mediadores celulares e moleculares da cicatrização anastomótica: resposta das putativas células estaminais epiteliais (usando os marcadores de superfície Lgr5, Bmi1 e o painel CD24/CD44/CD166/Grp78 por citometria de fluxo); viabilidade e morte celular (com marcação dupla com anexina V/iodeto de propídeo, por citometria de fluxo); stresse oxidativo [quantificação de peróxidos citoplasmáticos com sonda de diacetato de 2',7'-diclorodihidrofluoresceína ($DCFH_2$-DA), espécies reactivas mitocondriais com sonda de dihidrorodamina 123 (DHR 123), glutatião reduzido intracelular com marcação com alaranjado de mercúrio e potencial de membrana mitocondrial com sonda de iodeto de 5,5',6,6'-tetracloro-1,1',3,3'-tetraetilbenzimidazolcarbocianina (JC-1), por citometria de fluxo]; resposta inflamatória local e sistémica (concentrações tecidulares e plasmáticas de interleucina-1α, *macrophage chemo-attractant protein-1*, factor de necrose tumoral-α, interferon-γ e interleucina-4 por citometria de fluxo; expressão génica de componentes da matriz extracelular (*Collagen, type I, alpha 1: Col1a1; Collagen, type III, alpha 1: Col3a1; Collagen, type IV, alpha 1: Col4a1; Collagen, type V, alpha*

1: Col5a1) e respectivos factores de remodelação, metaloproteinases (Mmp) da matriz 1, 13, 2, 9, 3, 12 e 14 (*Mmp1* e *Mmp13*, *Mmp2* e *Mmp9*, *Mmp3*, *Mmp12* e *Mmp14*) e inibidores tecidulares das Mmp 1 e 2 (*Timp1* e *Timp2*); assim como dos factores de crescimento potencialmente implicados na reparação anastomótica (*Insulin-like growth factor 1, transcript variant: Igf1; Vascular endothelial growth factor A, transcript variant 2: Vegfa; Transforming growth factor, beta 1: Tgfb1; Connective tissue growth factor: Ctgf; Fibroblast growth factor 2: Fgf2; Fibroblast growth factor 7: Fgf7; Epidermal growth factor: Egf; Heparin-binding epidermal-like growth factor: Hbegf; Platelet-derived growth factor beta polypeptide: Pdgfb; Glucagon-like peptide 2 receptor: Glp2r*) por transcrição reversa quantitativa da reacção em cadeia da polimerase em tempo real; e da concentração plasmática do Glp-2 (por imunoensaio enzimático competitivo).

O teduglutide não teve impacto relevante aparente na incidência e gravidade da deiscência anastomótica mas exerceu uma influência favorável nos processos de reepitelização e de neoangiogénese da fase proliferativa da cicatrização. Associou-se, ainda, a um aumento da densidade de miofibroblastos subepiteliais, sem modificação significativa dos índices de células caliciformes, de Paneth e gliais.

Este factor de crescimento associou-se ao aumento da deposição de colagéneo III na submucosa ao sétimo dia pós-operatório, embora com redução concomitante do colagéneo I na mesma camada, e à redução não significativa do teor global de colagéneo na anastomose.

O teduglutide inibiu a modulação génica da fibrólise na fase predominantemente inflamatória da reparação enquanto, pelo contrário, reprimiu a fibrogénese na fase proliferativa. O teduglutide aumentou a expressão génica de *Timp1*, *Timp2* e *Col4a1* e, reduziu a de *Mmp3* e *Mmp12*, ao terceiro dia pós-operatório; e diminuiu a expressão génica do *Timp1*, *Col3a1, Col4a1* e *Col5a1*, ao sétimo dia.

O teduglutide induziu a expansão das putativas células estaminais colunares basais das criptas e, concomitantemente, a depleção das células da "posição +4". Nos animais tratados com teduglutide, observou-se, ainda, um aumento global não significativo das putativas células epiteliais intestinais.

O teduglutide associou-se a um efeito pro-oxidativo não significativo, com aumento dos níveis de peróxidos citoplasmáticos e de espécies reactivas mitocondriais e redução do glutatião reduzido celular. Estes efeitos foram acompanhados por um aumento do índice de viabilidade celular e uma redução não significativa dos eventos apoptóticos precoces. Não se verificou influência significativa no potencial de membrana mitocondrial. Nos animais tratados com teduglutide, observou-se um aumento não significativo dos níveis tecidulares da citocina anti-inflamatória interleucina-4 ao sétimo dia, assim como uma redução significativa da concentração plasmática de interferon-γ ao terceiro dia.

O teduglutide promoveu o aumento da expressão génica do *Igf1*, *Vegfa* e *Ctgf* e a repressão do *Fgf2*, *Fgf7*, *Tgfb1* e *Glp2r*.

Em conclusão, o presente estudo reflecte a complexidade da cicatrização anastomótica intestinal e sugere uma influência favorável do teduglutide neste processo que justifica uma investigação adicional.

Palavras-chave: Teduglutide; Anastomose cirúrgica; Fístula anastomótica; Reepitelização; Angiogénese fisiológica; Matriz extracelular; Factor de crescimento; Células estaminais adultas; Inflamação; Stresse oxidativo

Chapter 1

Introduction

1.1. Intestine structure and function

The intestine is characterized by a highly differentiated structure composed of four distinct layers: mucosa, submucosa, *muscularis propria* and serosa (Fig. 1.1). Mucosa consists of a single layer of columnar epithelium resting on the *lamina propria*, which contains loose connective tissue with blood and lymphatic vessels and some lymphoid tissue, and is separated from submucosa by the *muscularis mucosae*. In the small intestine, mucosa is organized in millions of villi and crypts of Lieberkühn that markedly increase its surface area. Submucosa contains connective tissue with blood vessels, lymphatics and the Meissner's plexus of the enteric nervous system. *Muscularis propria* includes two concentric layers of smooth muscle (an inner circular and an outer longitudinal) and, between both, the Auerbach's plexus. Serosa consists in a delicate sheet of loose connective tissue covered outside by the mesothelium (Piscaglia, 2014; Lloyd and Gabe, 2008).

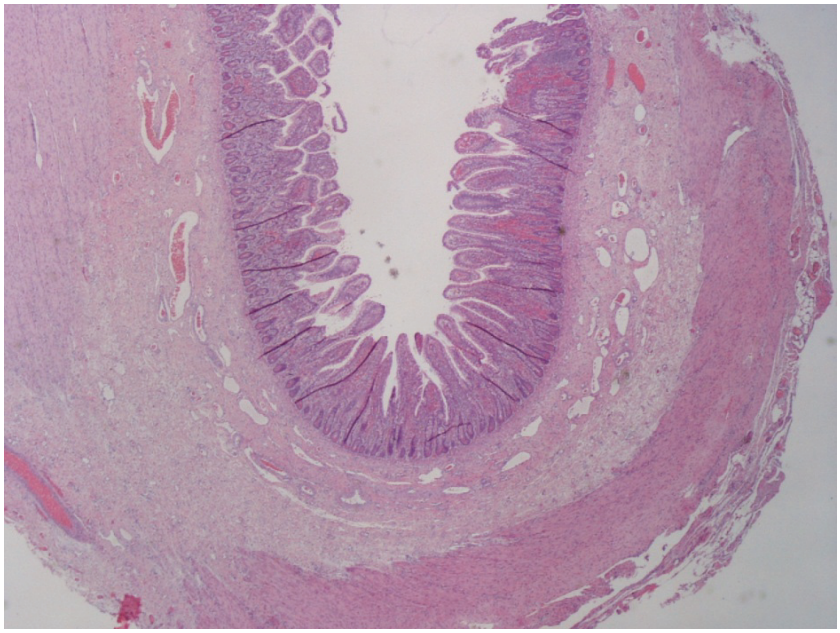

Figure 1.1. Cross-section of human small bowel (hematoxylin-eosin staining; original magnification 2x). Intestinal wall is subdivided into four layers: mucosa, submucosa, *muscularis propria* and serosa (image kindly provided by M.A. Cipriano)

The gut is an organ with complex and intricate absorptive, digestive, defense, neuromotor, endocrine and metabolic functions. These functions include digestion and absorption of water, macro and micronutrients; defense (maintenance of the barrier function and participation on local and systemic immune processes) and modulation of the inflammatory response; mixture and propulsion of chyme (with stationary motility and propulsive peristalsis); clearance of microorganisms and particles; production of peptides with endocrine, paracrine and autocrine properties; metabolism of amino acids and synthesis of apoproteins. Small intestine is the largest endocrine organ and produces peptides that regulate the metabolism of glucose; appetite and food ingestion; gastric, biliary and pancreatic secretions; gastrointestinal motility and immune function (Lindberg *et al.*, 2008; O'Mahony L, 2008).

The intestinal epithelium covering constitute the largest surface of contact of the human body with the external environment, with a total area over 200 m^2 (Lopetuso *et al.*, 2013). The Gut-associated Lymphoid Tissue (GALT) is one of the greatest lymphoid organs, containing up to 70% of the body's total number of immune cells, and acting as an inductor for the Mucosal-associated Lymphoid Tissue (MALT) (Fay *et al.*, 2017; O'Mahony, 2008; Garcia Lorenzo Mateos *et al.*, 2007; Wiest *et al.*, 2003). The GALT comprises intraepithelial lymphocytes, lamina propria lymphocytes, Peyer's Patches, and mesenteric lymph nodes. Peyer's Patches interact with epithelial cells to induce the local immune responses to luminal antigens, mediating the interplay between antigen presenting cells and T cells and the release of cytokines from activated T cells (Fay *et al.*, 2017).

Intestinal microbioma is constituted by a population of approximately 40 trillion of bacteria, of over 1,000 different species, predominantly (80%) of two dominant phyla (Firmicutes and Bacteroidetes) (Fay *et al.*, 2017; Cabrera-Perez *et al.*, 2017). Bacteriophagic particles, viruses, fungi and archaea are also constituents of gut microbioma. Firmicutes are Gram-positive bacterial taxa constituted by many commonly recognized genera (such as Clostridia, Streptococcaceae, Staphylococcaceae, Enterococcaceae, and Lactobacillae). Bacteroidetes, on the other hand, are Gram-negative bacteria composed mainly of Bacteroides species, which are obligate anaerobes. Human intestinal microbiota seems to be analogous to that of

mice, with concordances until the genus (for Firmicutes) and species levels (for Bacteroidetes) (Cabrera-Perez *et al.*, 2017). Gut microbiota-host multidirectional interactions play a relevant role in the homeostasis preservation. Intestinal dysbiosis, defined as a disturbance of microbial composition and/or activity, seems to contribute for the development of several diseases, due to its adverse impact on gut barrier, immunity and endocrine function (Bachmann *et al.*, 2017).

Regardless of the constant exposure to physical, biochemical, microbiological, and other forms of injury, the intestine maintains a relative state of homeostasis with preservation of the structure and function.

1.2. Intestinal anastomotic leakage

1.2.1. Definition and incidence

Despite recent progresses in surgical technique and perioperative care, failure of intestinal anastomotic healing, with subsequent leakage, dehiscence, stenosis or bleeding, remains a major source of morbidity and mortality in digestive surgery (Guyton *et al.*, 2016; Bosmans *et al.*, 2015; Shogan *et al.*, 2013; Thompson *et al.*, 2006). However, definition and reporting of anastomotic complications have been characterized by significant inconsistence. Furthermore, pathophysiology of intestinal anastomotic repair is still poorly understood (Guyton *et al.*, 2016; Chadi *et al.*, 2016; Vallance *et al.*, 2016; Bosmans *et al.*, 2015; Shogan *et al.*, 2013).

Intestinal anastomotic leakage is one of the most ominous postoperative complications (Guyton *et al.*, 2016). According to the International Multispecialty Anastomotic Leak Global Improvement Exchange (IMAGinE), anastomotic leakage may be defined as a defect in the integrity of a surgical junction between two hollow viscera leading to a communication between the intra and extraluminal compartments (Chadi *et al.*, 2016; Shogan *et al.*, 2013). This event may lead to a variety of anatomic and clinical consequences, ranging from a small contained abscess with spontaneous resolution to

a generalized peritonitis requiring urgent reoperation, and from a purulent discharge from a wound or drain to a life-threatening septic shock (Shogan *et al.*, 2013). Anastomotic leakage may be classified, in accordance with the impact on the clinical management, as grade A (that does not imply an active therapeutic intervention), B (that demands nonoperative radiological or endoscopic treatment) or C (that requires reoperation) (Shogan *et al.*, 2013).

Intestinal anastomotic fistula develops in 1 to 9% of cases, although this is probably an underestimated and underreported incidence. Rates of anastomotic leakage vary from 0.02 to 4% in enteroenteric and ileocolonic anastomosis, 0 to 2% in colocolonic anastomosis and 1 to 20% in colorectal, coloanal and ileoanal anastomosis (Chadi *et al.*, 2016). The risk of disruption varies according to the anastomotic site. It is usually lower in small bowel and higher in colon and rectum, particularly in most distal locations (Hyman, 2009; Turrentine *et al.*, 2015) (Fig. 1.2).

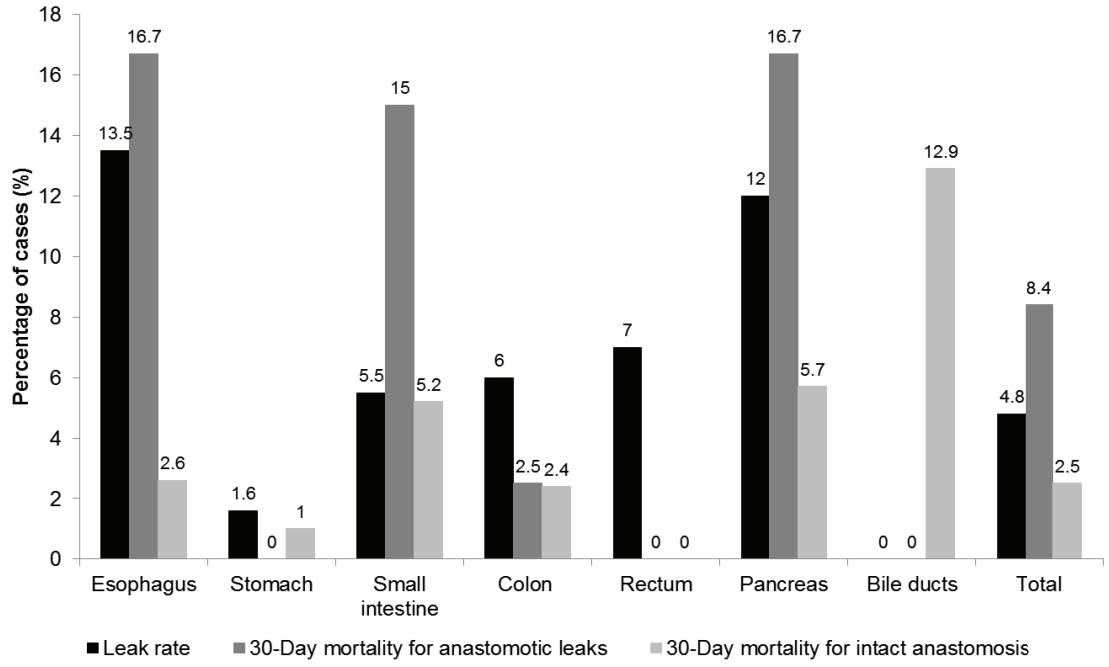

Figure 1.2. Frequency and mortality of gastrointestinal anastomotic leaks by anatomic site. Retrospective review of 2,237 adult surgical gastrointestinal tract procedures with anastomosis prospectively collected from the American College of Surgeons National Surgical Quality Improvement Program database and published by Turrentine FE *et al* in 2015 (Turrentine *et al.*, 2015)

1.2.2. Diagnosis and management

Early diagnosis and intervention are critical for the successful management of the anastomotic leakage and for the minimization of its deleterious consequences (Chadi *et al.*, 2016). Nevertheless, timely diagnosis may constitute a major challenge since the initial clinical and radiological signs are often nonspecific (Chadi *et al.*, 2016).

Most (79.4%) of the gastrointestinal fistula were identified within 30 days after surgery (median time of 11 days and mean of 28 days) and 94.3% within 90 days (Turrentine *et al.*, 2015). Anastomotic leakage with mechanic and structure-related causes tend to be diagnosed earlier, whereas those with ischemia-related origin tend to present later (Chadi *et al.*, 2016).

Surgeon's intraoperative evaluation has a low accuracy for detection of anastomotic leakage in gastrointestinal surgery (Guyton *et al.*, 2016; Shogan *et al.*, 2013). After colorectal surgery, surgeons' clinical risk assessment has a sensitivity of 38 to 62% and a specificity of 46 to 52%, not significantly influenced by the respective training level (Karliczeck *et al.*, 2009). After colon cancer resection, the predictive capacity was also low (area under the receiver operating characteristic curve [auROC]=0.40, p=0.243) (Sammour *et al.*, 2017).

The well-established intraoperative anastomotic air leak test, when feasible, seems to be effective in predicting satisfactory healing if it demonstrates an intact anastomosis (Vallance *et al.*, 2016; Chadi *et al.*, 2016). Intra-operative endoscopy may allow the assessment of the anastomosis integrity and has been shown to be safe and reliable, but the potential benefit of its routine use remains to be determined (Vallance *et al.*, 2016). Intraoperative imaging may also be useful (Hirst *et al.*, 2014).

Computerized tomography with luminal contrast and water-soluble contrast studies are the current preferred techniques for the diagnosis of intestinal anastomotic leakage, but are characterized by variable sensitivity and specificity and logistical constraints (Chadi *et al.*, 2016; Hirst *et al.*, 2014).

Several biomarkers of ischemia, inflammation and microbiological aggression, in the systemic circulation and in the peritoneal drainage fluid, were evaluated for the diagnosis of anastomotic disruption. Most commonly evaluated parameters were C-

reactive protein, procalcitonin and total leucocytes count, in the systemic circulation, and interleukin-6, interleukin-10 and tumor necrosis factor-α, in the peritoneal drainage fluid. These biomarkers are considered poor predictors of anastomotic leakage when isolated, but its combination showed improvement in the diagnostic accuracy (Su'a *et al.*, 2017). Notwithstanding, serum C-reactive protein at the third postoperative day seemed to be a useful negative predictive test for the development of anastomotic leakage following colorectal surgery, with a pooled area under the curve of 0.81 (95% confidence interval [CI] 0.75 to 0.86); derived cut-off value was 172 mg/l, which corresponded to a high negative predictive value (97%) and a negative likelihood ratio of 0.26 to 0.33 (Singh *et al.*, 2014). In a recent study, procalcitonin revealed high specificity and negative predictive values for anastomotic leakage in colorectal surgery at the third and fifth postoperative days (auROC of 0.775 and 0.862, respectively) and its combination with C-reactive protein significantly improved the diagnosis at the fifth day (auROC=0.901) (Giaccaglia *et al.*, 2016). Combination of plasma C-reactive protein and calprotectin at the third postoperative day after colorectal surgery yielded sensitivity of 100%, specificity of 89%, positive likelihood ratio of 9.09 (95% CI 4.34-16), negative likelihood ratio of 0.00 (95% CI 0.00-0.89) (p<0.001) and a high negative predictive value (100%) (Reisinger *et al.*, 2014). Furthermore, preoperative intestinal fatty acid-binding protein levels can be used for anastomotic leakage risk assessment as they predicted colorectal anastomotic disruption at a cut-off level of 882 pg/ml with sensitivity of 50%, specificity of 100%, positive likelihood ratio of "infinite" (95% CI 4.01-"infinite"), and negative likelihood ratio of 0.50 (95% CI 0.26-0.98) (p<0.0001) (Reisinger *et al.*, 2014). Those biomarkers might be advantageous in providing real-time monitoring of leakage development and be useful as discharge criteria in enhanced recovery after surgery programs. Nevertheless, implementation of those parameters in the daily practice deserves additional investigation.

New strategies, including several diagnosis scores and decision algorithms, have been developed for detection of anastomotic leakage in the postoperative period of colorectal cancer surgery, such as the Diacole score based in 13 clinical signs and symptoms and proposed by Rojas-Machado SA *et al* in 2016 (Rojas-Machado *et al.*, 2016). The ongoing Condor (Early Complication Detection After Colorectal

Surgery) prospective study is also expected to contribute for the development of a new diagnostic score (Kornmann *et al.*, 2016). Those indexes require validation and further evaluation to determine whether they translate into improved patient outcomes. Further research is needed to address this important area.

After an early diagnosis, an optimized multidisciplinary approach is necessary, based on medical, radiologic, endoscopic and/or surgical interventions. Management often implies reoperation in a hostile abdomen, creation of an intestinal stoma, and the need for subsequent operations to restore intestinal continuity (Hyman, 2009).

Recent advances in the management of anastomotic leakage comprise the more widespread use of non-operative strategies, including guided percutaneous drainage, endoluminal stenting, endoscopic vacuum-assisted drainage and over-the-scope-clip system application, and also of minimally invasive approaches (laparoscopic or endoscopic) in operative interventions (Chadi *et al.*, 2016; Vallance *et al.*, 2016; Sparreboom *et al.*, 2016a).

1.2.3. Consequences

Intestinal anastomotic leakage has an important negative impact on the morbidity and mortality rates, reoperation and readmission indexes, lengths of hospital stay, long-term oncological outcomes, functional results, patients' quality of life, economic costs and surgeon-patient relationships (Gessler *et al.*, 2017; Scarborough *et al.*, 2017; Chadi *et al.*, 2016; Midura *et al.*, 2015; Shogan *et al.*, 2013; Luján *et al.*, 2011; Hyman, 2009).

In a retrospective review of 2,237 adult surgical gastrointestinal tract procedures with anastomosis prospectively collected from the American College of Surgeons National Surgical Quality Improvement Program (ACS-NSQIP) database, anastomotic leaks were associated with higher overall morbidity (98.0 *vs.* 28.4%; $p<0.0001$), return to the operating room (45.8 *vs.* 4%; $p<0.0001$), length of stay (13 *vs.* 5 days; $p\leq0.0001$), 30-day mortality (8.4 *vs.* 2.5%; $p<0.0001$), long-term mortality (36.4 *vs.* 20.0%; $p\leq0.0001$) and risk of death (adjusted hazard ratio [HR]=1.77; $p=0.008$); and decreased survival (log-rank test, chi-square=23.1; $p<0.0001$); as well as, increased hospitalization costs (chi-square [2]=359.8; $p<0.0001$; mean $16,085.39 hospital cost

for patients who had an intact anastomosis and did not experience complications, and mean $56,349.12 for those who experienced an anastomotic leak) (Turrentine *et al.*, 2015).

In a retrospective study of 99,879 patients submitted to colorectal surgery, anastomotic leaks had a 30-days overall incidence of 6.18% and incurred additional length of stay and hospital costs of 7.3 days and $24,129, respectively (only within the first hospitalization); higher 30-day readmission rates (1.3 times) and postoperative infection rates (0.8–1.9 times) were also observed ($p<0.001$ for both) (Hammond *et al.*, 2014).

In a meta-analysis of 34 nonrandomized studies analyzing the oncologic impact of anastomotic leakage following restorative colorectal cancer surgery, involving 78,434 patients, increased local recurrence (relative risk [RR] 1.90, 95% CI 1.48-2.44, $I^2=78\%$) and reduced overall survival (RR 1.36, 95% CI 1.24-1.50, $I^2=74\%$), cancer-specific survival (RR 1.41, 95% CI 1.19-1.68, $I^2=56\%$), and disease-free survival (RR 1.40, 95% CI 1.20-1.63, $I^2=86\%$) were documented (Ha *et al.*, 2017). Similar results were observed by Wang S *et al* (Wang *et al.*, 2017) after curative anterior rectum resection for rectal cancer, with greater local recurrence and decreased overall and cancer-specific survival. Additionally, Nachiappan S *et al*, prospectively verified a significantly reduced overall survival after anastomotic leakage treated with reoperation following elective colorectal cancer resection (HR 2.74, 95% CI 1.67-4.52, $p<0.001$) (Nachiappan *et al.*, 2015). In a multicentric prospective study, anastomotic leakage after surgery for colorectal cancer constituted an independent predictor of the quality of life ($\beta=-0.42$, $p<0.001$) (Di Cristofaro *et al.*, 2014). Other authors reported also deterioration of the quality of life with anastomotic leakage after colorectal cancer surgery (Brown *et al.*, 2014; Marinatou *et al.*, 2014; Ashburn *et al.*, 2013). Anastomotic leakage constitutes an important indicator of the surgical quality of care and has aroused an increasing interest in performance metrics (Nikolian *et al.*, 2017).

1.2.4. Etiology

Pathogenesis of the failure of intestinal anastomotic repair is multifactorial and insufficiently known. Interference of non-recognized determinant factors may explain

failures of anastomoses performed in a technically correct manner and in the absence of other apparent risk conditions (Guyton *et al.*, 2016).

Differences in the cytokines response in early and late anastomotic leakages, with increased plasma concentrations of interleukin-1β, interleukin-6, interleukin-8 and interleukin-10 within the first five postoperative days in the first case and no significant modifications in late-onset dehiscence, may support the theory of different pathological mechanisms of disruption (Ellebæk *et al.*, 2014).

A successful intestinal anastomosis requests a meticulous surgical technique and compliance with fundamental surgical principles, including the absence of ischemia, excessive tension and distal obstruction, adequate serosal incorporation and apposition; and an uncompromised waterproof-sealed lumen (Tabola *et al.*, 2017; Guyton *et al.*, 2016).

Nevertheless, at present moment, the blood perfusion adequate to the anastomotic healing is not accurately defined and there are no direct unequivocal evidences that the increase of tension prevents healing. In a recently published experimental study, tissue hypoxia was not a distinctive feature of the disrupted anastomotic tissues, even after segmental devascularization and the assertion that hypoxia plays a major role in the pathogenesis of anastomotic leak was considered still unconfirmed (Shakhsheer *et al.*, 2017). At the present, intraoperative assessment of tissue perfusion with fluorescence real-time angiography is feasible and alters surgical strategy in a non-negligible proportion of patients, but its impact on the incidence of anastomotic dehiscence is still unknown (Mizrahi *et al.*, 2017; Chadi *et al.*, 2016; Vallance *et al.*, 2016). In a recent study, fluorescence angiography during laparoscopic left-sided or anterior rectum resection implied revision of the surgical plan in 8% of cases, without postoperative development of leakage (Jafari *et al.*, 2015).

Multiple technical aspects of anastomotic surgery have been extensively described and analyzed, including handsewn *versus* stapled and compression anastomosis, everting *versus* inverting, single *versus* double-layer anastomosis, anastomotic configuration, and suture types and materials, but none was considered highly determinant in the

outcome and no individual method of anastomosis construction was found to be superior (Kar *et al.*, 2017; Guyton *et al.*, 2016; Herrle *et al.*, 2016; Gustafsson *et al.*, 2015; Slieker *et al.*, 2013; Neutzling *et al.*, 2012; Choy *et al.*, 2011). Thus, surgical technique is left to the surgeon's preference (Guyton *et al.*, 2016). However, although handsewn anastomosis is nonstandardized, a single-layer continuous technique using inverting sutures with slowly absorbable monofilament material seems preferable (Slieker *et al.*, 2013).

In spite of extensive experimental research in the field of intestinal surgery (Nordentoft *et al.*, 2015; Vakalopoulos *et al.*, 2013), anastomotic sealing with tissue adhesives has not yet shown convincing results and has not been implemented into the regular clinical practice (Vakalopoulos *et al.*, 2017; Vakalopoulos *et al.*, 2013).

Nowadays, there is no high-level clinical evidence demonstrating benefits of sutureless dynamic compression anastomoses (including biofragmentable anastomotic rings, compression anastomotic rings, compression anastomotic clips and magnetic anastomoses) (Tabola *et al.*, 2017; Bobkiewicz *et al.*, 2017; Graves *et al.*, 2017; Slesser *et al.*, 2016; Li *et al.*, 2016; D'Hoore *et al.*, 2015; Massomi *et al.*, 2013), intraluminal devices (Bakker *et al.*, 2017; Lee *et al.*, 2015; Morks *et al.*, 2011) or external coating (with fibrin sealants, hyaluronic acid/carboxymethylcellulose, omental pedicle grafts and others) (Nasiri *et al.*, 2017; Pommergaard *et al.*, 2012; Hao *et al.*, 2008) to reduce leakage rates. Nevertheless, the prophylactic transanal decompression tube is considered a likely effective and safe method of preventing anastomotic leakage after rectal cancer surgery (Zhao *et al.*, 2017a).

Anastomotic fistula may occur after technically well-constructed anastomoses. Highly experienced and specialized surgeons working in high-volume centers continue to experience anastomotic leaks (Guyton *et al.*, 2016; Shogan *et al.*, 2013).

Emerging evidence suggests that gut microbiota has a strong influence on the intestinal anastomotic healing (Bachmann *et al.*, 2017). After injury, gut microbiota supports epithelial cells migration, adhesion, restitution and proliferation; mucosal barrier integrity; immune cells activation; and vascularization. Akkermansia *muciniphila* and Lactobacillus species seem to reinforce wound healing and gut barrier function, stimulating prorestitutive signalling and increasing cellular migration and proliferation.

Reactive oxygen species and formyl peptide receptors are considered key molecular mediators of microbiota regulation of wound healing process. Microbiota-host cell interactions also modulate β-catenin signaling and, subsequently, the epithelial cell proliferation (Bachmann *et al.*, 2017).

Gut microbiota seems to be influenced by the intestinal resection and anastomosis process and, also, by the perioperative management (including antibiotics prescription and mechanical bowel preparation), with emergence of species with a more aggressive tissue-destroying phenotype, such as Enterococcus. Lower levels of the usually cytoprotective Lactobacillaceae bacteria have also been evident in perianastomotic tissues (Bachmann *et al.*, 2017). Shogan BD *et al* (Shogan *et al.*, 2014) demonstrated that the colon anastomotic injury induced significant changes in the anastomotic tissue-associated microbiota, including a 500-fold and 200-fold increase in the relative abundance of Enterococcus and Escherichia/Shigela, respectively, with minimal repercussion in luminal microbiota. Functional profiling predicted the prevalence of bacterial virulence-associated pathways in postanastomotic tissues (Shogan *et al.*, 2014). A correlation between the bacterial family Lachnospiraceae, low microbial diversity and intestinal colon anastomotic leakage, possibly in association with the body mass index, was found by van Praagh JB *et al* (van Praagh *et al.*, 2016). The relative abundance of the Lachnospiraceae family (phylum Firmicutes) may be explained by the higher abundance of mucin-degrading Ruminococci in anastomotic failure cases (van Praagh *et al.*, 2016). Gelatinase GelE of Enterococcus *faecalis*, a highly prevalent bacterium in leaking anastomotic tissues (Shogan *et al.*, 2014), disrupts the intestinal integrity, induces inflammation and degrades collagen (Bachmann *et al.*, 2017). The distinct core microbiota of the elderly, with greater proportion of Bacteroides species and distinct abundance patterns of Clostridium groups may contribute to the increased risk of leakage in those individuals (Bachmann *et al.*, 2017).

1.2.5. Risk factors and prevention

Numerous patient, disease and operation-related risk factors of anastomotic leakage have been recognized in clinical studies (Nikolian *et al.*, 2017; Rencuzogullari *et al.*, 2017; van Rooijen *et al.*, 2016; Midura *et al.*, 2015) (Table 1.1).

Table 1.1. Clinical relevant risk factors for gastrointestinal anastomotic leakage described in the literature [a]

Patient-related factors	Disease-related factors	Laboratorial factors	Operation-related factors	Other factors
Male gender[1-11]	Neoadjuvant treatment	Hyperglycemia / high hemoglobin A1c[7]	Emergent/urgent operation[1,4,11]	Lack of mechanical bowel preparation*[7]
Young age[3]	*Chemotherapy*[1,6,9]	Anemia[1,5]	Blood transfusions[1,5,9,11]	Lack of selective gut decontamination*[7]
Smoking history[1,3,4,6,7,11]	*Radiotherapy*[1,8,11]	Leukocyte count > 12,000/mm^3 [11]	Blood loss[5,9,11]	Antibiotics omission*[2]
Alcohol excess[1,11,12]	*Bevacizumab*[11]	Thrombocytosis[4]	Prolonged operating time[4,5,6,9,11]	Number of hospital beds*[2]
Obesity[1,2,4,9,11]	Neoplasia	Hypoproteinemia[2]	Intraoperative complications[1,2,5,10]	Contaminated/infected wounds[7]
Malnutrition[7,11,12]	*Distal location*[11]	Hypoalbuminemia[1,3]	Intraoperative hypotension[15]	Perioperative fluid overload (>8 l infusion in the first 3 days)[14]
ASA classification $\geq$3[1,3,7,9,11]	*Advanced stage*[11]	Abnormal sodium[12]	Low central venous oxygen saturation[15]	
Comorbidities	*Metastatic disease*[11]		Other concomitant surgical procedures[1]	
Diabetes mellitus[1,3,5,7]	*Great size*[9,11]		Rectum anastomosis[12]	
COPD[1,7]			Low rectal anastomosis[1,8,9,10]	
Cardiovascular disease[1,12]			Elective rectal cancer surgery*[3]	
Renal disease[1]			High ligation of inferior mesenteric artery*[10]	
Liver disease[1]			Splenic flexure mobilization*[3]	
Overall comorbidities[1,10,11]			Mechanical anastomosis*[1]	
Medications			Stapler firing $\geq$ 3**[9]	
Steroids[1,6,12]			Open approach colectomy[6]	
Immunosuppressors[4,11]			Emergency colectomy for bleeding*[3]	
Anticoagulants[2]				
Non-selective NSAID[13]				

ASA, American Society of Anesthesiology; COPD, Chronic obstructive pulmonary disease; NSAID, Non-steroid anti-inflammatory drugs. *Colorectal surgery; **Laparoscopic anterior rectum resection. [a]From references: 1. Rojas-Machado *et al.*, 2016, 2. Frasson *et al.*, 2015, 3. Parthasarathy *et al.*, 2016, 4. Nikolian *et al.*, 2017, 5. van Rooijen *et al.*, 2016, 6. Midura *et al.*, 2015, 7. Rencuzogullari *et al.*, 2017, 8. Pommergaard *et al.*, 2014, 9. Qu *et al.*, 2015, 10. Trencheva, *et al.*, 2013, 11. McDermott *et al.*, 2015, 12. Turrentine *et al.*, 2015, 13. Smith *et al.*, 2016, 14. Boesen *et al.*, 2013, 15. Futier *et al.*, 2010

There are no evidences that minimally invasive approaches (including laparoscopic and robotic interventions) (Juo *et al.*, 2014) and standardized enhanced recovery after surgery protocols (Wang *et al.*, 2014; Li *et al.*, 2013) increase the risk of intestinal anastomotic leakage. Through the analysis of 8,442 cases of the National Surgical Quality Improvement Program database, Kiran RP *et al* (Kiran *et al.*, 2015) demonstrated that combined preoperative mechanical bowel preparation with oral antibiotics (but not without) significantly reduces anastomotic leaks after colorectal surgery (odds ratio=0.57, 95% CI 0.35-0.94). Combined preoperative mechanical bowel preparation with oral antibiotics (and isolated oral antibiotics) was also associated with a significant reduction of anastomotic leak risk in a more recent analysis of 32,359 cases of the same database (Koller *et al.*, 2017). Recently, Garfinkle R *et al* (Garfinkle *et al.*, 2017) showed, on a conditional logistic regression of matched patients extracted from an analysis of 40,446 cases, that oral antibiotic preparation alone was protective of anastomotic leak (odds ratio=0.60, 95% CI 0.34-0.97). Similar results were obtained in others studies (Scarborough *et al.*, 2015). A systematic review and meta-analysis suggested that, in elective gastrointestinal surgery, a combination of perioperative selective decontamination of the digestive tract and perioperative intravenous antibiotics may reduce the rate of anastomotic leakage compared with use of intravenous antibiotics alone (Roos *et al.*, 2013).

Influence of new advances in perioperative care (such as surgical prehabilitation protocols, perioperative nutrition support and rational goal-directed perioperative fluid therapy) in the incidence of anastomotic complications need to be further evaluated.

Recently, Rojas-Machado *et al* (Rojas-Machado *et al.*, 2016) proposed the Procole prognostic score (Prognostic Colorectal Leakage) for colorectal cancer surgery as a good predictive indication. The Reveal (Predictive Factors of Anastomotic Leakage after Colorectal Surgery) study of predictive factors after colorectal surgery is also ongoing (Jongen *et al.*, 2016).

Development of prognostic indexes and predictive nomograms may be very important to estimate the risk of anastomotic leakage, but they require previous prospective external validation (Sammour *et al.*, 2017; Rojas-Machado *et al.*, 2016; Frasson *et al.*,

2015). The identification of high-risk cases may allow the secondary prevention of anastomotic disruption (including the use of adjuvants of repair, anastomotic reinforcement and other strategies) and the establishment of adequate criteria for selective proximal virtual or classical diverting ostomies. These data may allow a more accurate risk assessment in the clinical practice and also risk adjustment for quality of care control (Nikolian *et al.*, 2017). Nevertheless, although those numerous potential risk factors may contribute to anastomotic failure, the underlaying mechanisms remain poorly understood and speculative (Guyton *et al.*, 2016).

Anastomotic leakage remains a critical, expensive and potentially life-threatening complication and an ongoing challenge (Guyton et al., 2016). An evidence-based and integrated approach based on the understanding of the pathophysiology and on clinical trials is necessary to prevent anastomotic complications. Surgical research for improvement of the understanding of the cellular, molecular and biochemical pathways of anastomotic healing and for the development of new preventive and early diagnostic strategies is needed. Great interest emerged on innovative perioperative interventions to improve anastomotic repair, especially in high-risk conditions.

1.3. Intestinal anastomotic healing

Intestinal anastomotic healing is a continuous multicellular multimolecular dynamic process involving complex interactions between multiple signaling networks and rigorous spacial and temporal control. Repair progression requires the coordinated interplay of specific cell types, cell surface receptors, extracellular matrix proteins and bioactive factors (Rijcken *et al.*, 2014; Greaves *et al.*, 2013; Thompson *et al.*, 2006). Inadequate anastomotic healing may conduct to fistula and dehiscence, when insufficient, or to fibrosis and stenosis, when uncontrolled and excessive (Rijcken *et al.*, 2014).

Traditionally, the wound healing model considers three overlapping phases: inflammatory, proliferative and reparative (Rijcken *et al.*, 2014; Greaves *et al.*, 2013) (Fig. 1.3).

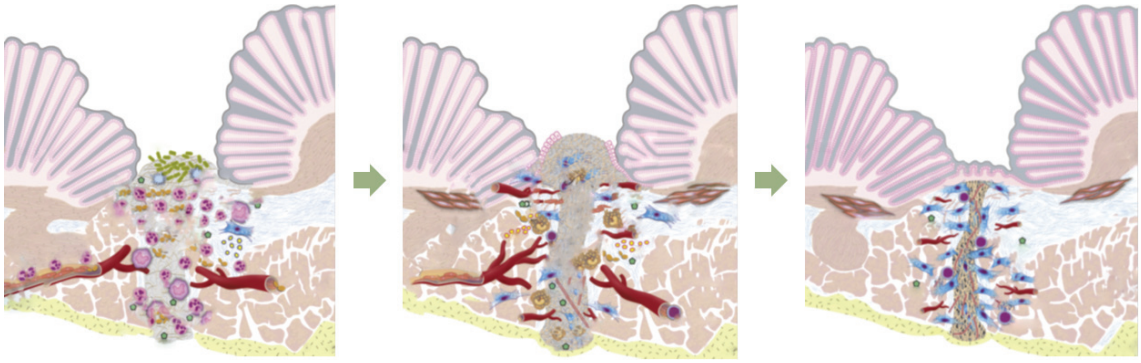

Figure 1.3. Graphic representation of the classical model of the intestinal anastomotic healing. Anastomosis repair develops in three overlapping phases. Inflammatory stage (*left*) is characterized by inflammatory cells infiltration, extracellular matrix degradation, wound debridement and provisional closure. Proliferative phase (*middle*) comprises the reepithelialization, angiogenesis and fibroplasia processes. Reparative stage (*right*) develops with remodeling of extracellular matrix, wound maturation and contraction. Adapted from Rijcken E *et al.*, 2014

1.3.1. Inflammatory, proliferative and remodeling phases

Inflammatory phase

In the inflammatory stage, during the first one to four days, the coagulation process origins thrombin, an inducer of platelet degranulation, and triggers the release of bioactive mediators that stimulate the recruitment and activation of inflammatory cells. Influx of inflammatory cells to the wound site is facilitated by vasodilation and increase of vascular permeability. These cells participate in the wound debridement, extracellular matrix degradation, antigen presentation, phagocytosis and release of reactive oxygen species, inflammatory cytokines, chemokines and growth factors that amplify the repair process. Neutrophils are the most abundant inflammatory cells in the early stages, followed by monocytes and classically activated macrophages (M1), which are considered the most important regulatory cell type in the exudative phase (Rijcken *et al.*, 2014; Greaves *et al.*, 2013; Delavary *et al.*, 2011). Provisional wound closure and debridement were therefore ensured (Rijcken E *et al.*, 2014). Molecular mediators of inflammatory phase of repair include vasoactive amines (histamine and serotonin), plasma proteases (bradykinin and complement factors), coagulation factors

(such as fibrinopeptides and platelet-activating factor), arachidonic acid metabolites (thromboxanes, prostaglandins and leukotrienes), cytokines (interleukins and tumor necrosis factor-α), growth factors (platelet-derived growth factor, transforming growth factor β, vascular endothelial growth factor and insulin-like growth factor) and reactive oxygen and nitrogen species (Rijcken *et al.*, 2014; Greaves *et al.*, 2013).

Proliferative phase

Proliferative phase is characterized by reepithelialization, angiogenesis and fibroplasia and occurs, generally, between the second and the fourteenth postoperative days (Rijcken *et al.*, 2014; Greaves *et al.*, 2013). Activated macrophages (M2) contribute to the transition of inflammatory to proliferative phase of healing, suppressing the inflammatory response and the adaptive T-helper 1 lymphocytes (Th1)-immunity and favoring a T-helper 2 lymphocytes (Th2) response, which has been related to fibrogenesis. M2 macrophages constitute a relevant source of transforming growth factor β and promote angiogenesis and extracellular matrix deposition (Delavary *et al.*, 2011).

Reepithelialization process begins within minutes to hours of injury, to obtain the reestablishment of the epithelial continuity, and is based on restitution, crypt stem cells proliferation and differentiation, and crypt fission (Bloemendaal *et al.*, 2016; Rijcken *et al.*, 2014; Greaves *et al.*, 2013; Iizuka M and Konno S, 2011). Restitution occurs along the exposed and new basement membrane and implies cellular adhesion and cytoskeletal remodeling (Rijcken *et al.*, 2014; Iizuka and Konno, 2011). Neighboring epithelial cells suffer reorganization of the actin cytoskeleton, lose their columnar polarity, acquire a flattened morphology and migrate into the wound to restore barrier integrity (Iizuka and Konno, 2011).

Molecular mediators of intestinal epithelial wound repair include growth factors (transforming growth factor α, transforming growth factor β, epidermal growth factor, heparin-binding epidermal growth factor, hepatocyte growth factor, fibroblast growth factor 2, keratinocyte growth factor, insulin-like growth factors 1 and 2, cytokines, chemokines and their receptors, prostaglandin E2, cyclooxygenases 1 and 2, toll-like

receptors 2, 5 and 9, hypoxia-inducible factor and dietary factors such as glutamine (Iizuka and Konno, 2011). Most important involved signaling pathways were Rho family, for modulation of cytoskeletal actin reorganization; extracellular signal-regulated kinase (ERK)1/ERK2, mitogen-activated protein kinase (MAPK) and phosphatidylinositol 3-kinase (PI3K)/Akt, for regulation of epithelial proliferation and survival; nuclear factor-κB (NF-κB), for epithelial cells protective function; signal transducer and activator of transcription-3 (STAT3) for regulation of immune homeostasis and triggering receptor expressed on myeloid cells 2 (Trem2) for promotion of M2 macrophages activation (Iizuka and Konno, 2011).

Angiogenesis is the complex process of ingrowth of new microvessels in the wound that restores microcirculation and allows reestablishment of adequate perfusion, normoxia and nutrient delivery to the regenerating tissue. Endothelial cells from the capillaries in the margin migrate into the wound, suffer pseudopodia, proliferate and form new capillaries (Greaves *et al.*, 2013). Fibroblast growth factor 2 is the most important pro-angiogenic factor in the early phase after injury, decreasing then towards the seventh day (Greaves *et al.*, 2013). Vascular endothelial growth factor is determinant to the angiogenesis and is upregulated in the first three to seven days after the injury, promoting endothelial cell migration and proliferation, and vascular permeability (Greaves *et al.*, 2013). Other important angioproliferative factors include tissue hypoxia, nitric oxide, tumor necrosis factor-α and angiopoietin 1. Proangiogenic effects of hypoxia are mediated through hypoxia-inducible factor 1, which upregulates the vascular endothelial growth factor, endothelial nitric oxide synthase and heme oxygenase 1 expressions (Greaves *et al.*, 2013).

In the proliferative phase, fibroplasia, the process of extracellular matrix deposition and basement membrane restoration, provides a scaffold for further cellular influx, adhesion and differentiation during the healing process (Greaves *et al.*, 2013). Fibrogenesis results from the activation and synergy of mesenchymal cells, mainly fibroblasts and myofibroblasts, that are the key effectors of tissue repair (Greaves *et al.*, 2013; Speca *et al.*, 2012). Number of fibrogenic cells in the wound increase by proliferation, transdiferentiation and desdiferentiation between fibroblast, myofibroblast and smooth muscle phenotypes, epithelial-to-mesenchymal and

endothelial-to-mesenchymal transitions and migration from non-affected tissues to the wound (chemotaxis and chemokinesis) (Greaves *et al.*, 2013; Speca *et al.*, 2012).

Fibroblasts, the most important cell type in the wound at the fourth day, produce a collagen-rich extracellular matrix that gradually replace temporary fibrin matrix and increase tissue biomechanical strength (Speca *et al.*, 2012; Thompson *et al.*, 2006). Myofibroblasts (subepithelial myofibroblasts and intersticial cells of Cajal) are highly contractile cells with a phenotype between fibroblasts and smooth muscle cells that participate in tissue growth and repair (Speca *et al.*, 2012). Myofibroblasts produce high levels of extracellular matrix and basement membrane components, particularly collagen, glycosaminoglycans, tenascin and fibronectin, and participate in the modulation of the inflammatory reaction by the secretion of chemokines and cytokines (Speca *et al.*, 2012). Myofibroblasts generate traction forces and initiate wound closure and contraction (Greaves *et al.*, 2013). Other cells types involved in the fibrogenesis are stellate cells, pericytes, local and bone marrow-derived stem cells (Greaves *et al.*, 2013; Speca *et al.*, 2012).

Extracellular matrix is an active and dynamic structure that participates in the regulation of the inflammatory response and the healing process by focal adhesions with immune and non-immune cells (Speca *et al.*, 2012). It has anchorage-related functions and constitutes a reservoir for mediators such as cytokines, chemokines and growth factors (including vascular endothelial growth factor, transforming growth factor β and fibroblast growth factor 2) (Gattazzo *et al.*, 2014). Extracellular matrix assists endothelial cell proliferation and migration and determines the outcome of vessel organization (Greaves *et al.*, 2013). Extracellular matrix degradation is mediated by the fine balance between matrix-degrading enzymes (including matrix metalloproteinases) and their inhibitors (such as tissue inhibitors of matrix metalloproteinases) (Speca *et al.*, 2012). Adequate wound tension and cytokines profile constitute determinant factors of the mechanical properties of extracellular matrix, with an important role in the restoration of mechanotransduction and tissue homeostasis (Gattazzo *et al.*, 2014; Greaves *et al.*, 2013).

Most important molecular mediators of fibrogenesis process include growth factors (transforming growth factor β1, connective tissue growth factor, platelet-derived

growth factor, insulin-like growth factors 1 and 2, epidermal growth factor and vascular endothelial growth factor), cytokines, chemokines, reactive oxygen species, endothelins 1, 2 and 3, components of the renin-angiotensin system, peroxisome proliferator activator receptor-γ (PPAR-γ), mammalian target of rapamycin (mTOR), matrix metalloproteinases (MMPs) and tissue inhibitors of metalloproteinases (TIMPs) (Speca S *et al.*, 2012).

Remodeling phase

In the reparative phase, the last and longest phase of wound healing process, which may elapse up to six months (Rijcken *et al.*, 2014), extracellular matrix undergoes continuous synthesis, breakdown and remodeling by proteolytic enzymes (including matrix metalloproteinases), leading to wound maturation and contraction (Greaves *et al.*, 2013). Extracellular matrix acquires progressively a predominantly collagenous structure, with reduced cellularity (Greaves *et al.*, 2013). Deposited collagen suffers rearrangement and cross-linking and type III collagen is replaced by type I collagen (Delavary *et al.*, 2011). Remodeling is mainly promoted by transforming growth factor β and platelet-derived growth factor (Rijcken *et al.*, 2014) and is influenced by the predominance of a Th2 or a Th1 response (Delavary *et al.*, 2011).

1.3.2. Particularities of intestinal healing

Despite fundamental similarities, the healing process of the intestinal anastomosis differs from that of the cutaneous tissue. Intestinal anastomotic wound environment is characterized by the particular microbiota, the biomechanical stress resultant from motility and mass propulsion, and the higher susceptibility to vascular perfusion disturbances (Thompson *et al.*, 2006).

Gut microbiota composition, including aerobic and anaerobic microorganisms, is different from the skin flora (Rijcken *et al.*, 2014) and seems to exert a relevant influence on the anastomotic healing process (Bachmann *et al.*, 2017).

The importance of mechanical forces in the intestinal healing process was demonstrated by Kovalenko PL *et al* (Kovalenco *et al.*, 2012) who verified that the repetitive deformation may favor mucosal repair via ERK signaling, whereas the increase of luminal pressure may inhibit it by an ERK-independent mechanism. Loss of the repetitive distension may decrease mucosal healing in the defunctionalized bowel. Moreover, the increased luminal pressure above anastomoses (or in a spastic bowel disease) could further inhibit mucosal restoration, despite peristaltic reccuring strain (Kovalenco *et al.*, 2012).

Collagen in the gastrointestinal tract includes subtypes I, III and V and is produced by fibroblasts and smooth muscle cells, while, in the skin, only subtypes I and III are produced and solely by fibroblasts (Bosmans *et al.*, 2015).

In comparison with cutaneous repair, intestinal anastomotic healing is characterized by a proportionally faster increase of the physical strength (especially in small intestine), possibly as a result of differences in the degree of expression and time course of proinflammatory and antiinflammatory cytokines and growth factors between these two wound sites (Zubaidi *et al.*, 2015; Bosmans *et al.*, 2015; Alzoghaibi and Zubaidi, 2014; Alzoghaibi, 2013; Zubaidi *et al.*, 2010). The intestinal serosal layer, nonexistent in the skin, provides a matrix for fibroblasts and has an important role in the wound strength (Bosmans *et al.*, 2015).

Collagenase activity exerts a relevant role the intestinal anastomotic repair and it is responsible for the low wound biomechanical strength in the early postoperative period (Bosmans *et al.*, 2015). In fact, in the first two to three days of the postoperative period, a transient reduction of the anastomotic strength occurs, due to the degradation of collagen by the proteinase activity in the wound (Thompson *et al.*, 2006). Thereafter, strength increases by synthesis and deposition of new collagen in the predominantly proliferative phase of the healing process. Tensile strength, a rarely used measure for anastomosis assessment, reflects the suture-holding capacity of the preexisting collagen of perianastomotic tissue, in all the surface area of the wound edge, and correlates with collagen synthesis after the fourth postoperative day. Tensile strength is regained at a slower rate than the bursting pressure. Bursting pressure reflects the weakest site of the anastomosis and is usually used as an evaluation

parameter only in first few days after the operation. Bursting pressure of a small intestine anastomosis is approximately 50% of normal at the second and third postoperative days and approaches 100% at the seventh day, whereas a tensile strength similar to the unwounded tissue is reached only four weeks after surgery (Thompson *et al.*, 2006).

A better understanding of the pathophysiology of intestinal anastomotic disturbances, insufficiently known at the present (Guyton et al., 2016), may lead to more targeted and efficacious preventing interventions, with a potential relevant clinical and socioeconomic impact.

1.4. Adjuvant interventions on intestinal anastomotic healing

Numerous experimental studies have been undertaken on the role of adjuvants of intestinal anastomotic healing, either in standard or high-risk contexts (Yauw *et al.*, 2015) (Table 1.2).

The perioperative strategies to improve anastomosis repair described in those studies included pharmacological interventions, nutrients and probiotics administration, stem cell-based therapies, anastomotic reinforcement, among many others (Yauw *et al.*, 2015).

The most studied pharmacologic interventions included the administration (topic or systemic) of growth factors and hormones (granulocyte-macrophage colony-stimulating factor, insulin-like growth factor, platelet-rich plasma, growth hormone and erythropoietin), matrix metalloproteinases (mmp) inhibitors, prostacyclin analogues, antibiotics, allopurinol, superoxide dismutase, β-D-glucan and aprotinin (Yauw *et al.*, 2015). Nutrients manipulation comprised short-chain fatty acids, glutamine, arginine, vitamin A/retinoid acid, vitamin C and zinc supplementation. Other types of adjuvant interventions included the use of tissue adhesives (cyanoacrylates, fibrin glues, polyethylene glycol adhesives and albumin-based adhesives) and alternative forms of

anastomotic reinforcement, hyperbaric oxygen therapy, ischemic preconditioning and electromagnetic field stimulation (Vakalopoulos *et al.*, 2017; Yauw *et al.*, 2015).

Table 1.2. Potential adjuvant strategies for intestinal anastomotic healing analyzed in experimental studies[a]

Type	Description
Pharmacological adjuvants	
Growth factors	Insulin-like growth factor, keratinocyte growth factor, granulocyte-macrophage colony-stimulating factor, epidermal growth factor, basic fibroblast growth factor, vascular-endothelial growth factor, heparin-binding epidermal growth factor, glucagon-like peptide 2, platelet-derived growth factor, transforming growth factor β, platelet-rich plasma
Hormones	Growth hormone, erythropoietin, melatonin, anabolic steroids, estrogen, progesterone, ghrelin, leptin, triiodothyronine, adrenomedullin, somatostatin analogues (octreoctide, lanreotide), placental lactogenic hormone, somatomammogenic chorionic hormone, thyroid stimulating hormone
Active peptides	Matrix metalloproteinases inhibitors (aprotinin, nafomostat mesylate, soybean trypsin inhibitor, others), prostaglandins (E1, E2); β-D-glucan, activated protein C, antithrombin III, caffeic acid phenethyl ester, pentadecapeptide BPC 157, calcitonin gene-related peptide, s-methylisothiourea hemisulphate, poly-L-lysine and poly-L-glutamate, enterosan; coagulation factor XIII, flavonoids, neurotensin, pancreatic polypeptides, substance P, carnitine, catalase, adenosine triphosphate, amelogenin, aminoguanidine, β-aminopropionitrile, neurokinin 1 receptor antagonist, parthenolide, regenerating agent 11
Antioxidants	Allopurinol, superoxide dismutase, diosmine+hesperidine, N-(3(aminomethyl)benzyl)acetamidine
Vasodilators	Prostacyclin analogues (iloprost, others), sildenafil, bosentan, nitroglycerine, papaverine, talafadil, trapidil, perflurane
Other drugs	Pentoxifylline, acetylcysteine, simvastatin, ranitidine, famotidine, ketotifen, piroxicam, flurbiprofen, nifedipine, dopamine, bromopride, neostigmine, phenytoin, low molecular weight heparin, lisinopril, mesalasine, montelukast, tacrolimus, tranexamic acid, amifostine, bupivacaine
Antibiotics/antiseptics	Neomycin, metronidazole, gentamicin, levamizol, cephalosporins, noxythiolin, levamisole, amikacin, doxycycline, imipenem, penicillin, taurolidine, kanamycin+chloramphenicol, kanamycin+cephalotin, penicillin/streptomycin/chlorostrep (chloramphenicol and dihydrostreptomycin); chlorhexidine, iodine, silver-nanoparticle-coated sutures; and others
Organic compounds	Polyphenols (reversatrol, proanthocyanidins), ethyl pyruvate, guar gum, honey, tualang honey, gingko biloba extract, aloe vera, algae, oxidized cellulose, castor oil, copaiba oil, shark cartilage, thymoquinone, extracts of aroeira do sertão, *Schinus terebinthifolius*, *Jatropha gossypiifolia*, *Passiflora edulis*
Other compounds	Chitosan, propolis, vinpocetine, cholera toxin, interleukin 2, methylene blue, pyrrolidine dithiocarbamate, taurocholate, cartilage bone marrow extract, radioprotective treatments (WR-2721 and ribose-cysteine) and others
Nutrients	
	Glutamine, short-chain fatty acids (mostly butyrate), arginine, branched-chain amino acid mixture, glycine, methionine; vitamin A/retinoic acid, vitamin B5, vitamin C, zinc; whey, lactulose, ketone bodies, kefir, polyphosphate; and others
Probiotics	
Stem cell therapy	
	Adipose stem cells, bone marrow-derived mesenchymal stem cells
Anastomotic reinforcement	
	Tissue adhesives (cyanoacrylates, fibrin glues, polyethylene glycol adhesives and albumin-based adhesives); biological coating (omentum, peritoneum, collagen fleece, small intestine submucosa, amniotic membrane and others); synthetic matrixes and patches (polyglactin, polyglycolic acid, polypropylene, alginate and others)
Other therapies	
	Hyperbaric oxygen, ischemic preconditioning, electromagnetic field stimulation, positively charged diethylaminoethyl cross-linked dextran bead particles/electrical stimulation, laser stimulation, radiofrequency, extracorporeal shockwave therapy, hyperoxygenated solution lavage, other types of oxygen supplementation, ozone gas, circadian rhythm alteration

[a] From references Vakalopoulos *et al.*, 2017; Hyoju *et al.*, 2017; Zhao *et al.*, 2017b; Kızıltan *et al.*, 2016; Aznan *et al.*, 2016; De la Portilla *et al.*, 2016; Yauw *et al.*, 2015; Sipahi *et al.*, 2014; Silva *et al.*, 2014; Cueto *et al.*, 2014; Vakalopoulos *et al.*, 2013; Pommergaard *et al.*, 2012

Pharmacologic adjuvants

In a systematic review of 75 experimental studies on colorectal anastomosis repair published in 2014 (Oines *et al.*, 2014), 56 different adjuvant substances were tested.

Subsequent meta-analysis identified seven compounds with the potential to reproducibly improve anastomotic healing under non-complicated conditions, including the growth factors and hormones insulin-like growth factor 1, growth hormone and erythropoietin; broad-spectrum inhibitors of matrix metalloproteinases [associated with an increase of the weighted mean of bursting pressure of 48 mmHg (95%CI 31-66)]; immunomodulators, such as iloprost and tacrolimus [that increased the mean bursting pressure by 60 mmHg (95% CI 30-89) and 29 mmHg (95% CI 4-53), respectively]; and hyperbaric oxygen therapy [that enhanced the mean bursting pressure by 24 mmHg (95% CI 13-34) on the third and fourth postoperative days]. In those studies, anastomotic healing could be improved by various mechanisms, including the stimulation of epithelialization, angiogenesis and fibrogenesis, and the inhibition of the degradation of extracellular matrix, among others (Oines *et al.*, 2014).

Another systematic review of 65 preclinical studies and 48 compounds was recently undertaken and the meta-analysis suggested that postoperative hyperbaric oxygen therapy significantly improved colonic anastomotic healing in rat models complicated by bowel ischemia, with a significant increase of the bursting pressure by a mean of 28 mmHg (95% CI 17-39 mmHg, $p<0.00001$) (Nerstrom *et al.*, 2016). Favorable effects of granulocyte-macrophage colony-stimulating factor were demonstrated in the context of segmental ischemia and obstructive jaundice (Nerstrom *et al.*, 2016). Iloprost was found to be beneficial for the early healing of colonic anastomosis in rats with intestinal obstruction and in those exposed to chemotherapy. Positive actions of N-acetylcysteine after ischemia/reperfusion injury and radiotherapy were also verified (Nerstrom *et al.*, 2016).

Matrix metalloproteinases inhibitors have been shown to improve the biomechanical properties in animal models of colonic anastomotic healing (Krarup *et al.*, 2017; Krarup *et al.*, 2013; Ågren *et al.*, 2011), preventing the collagen degradation and preserving the integrity of extracellular matrix (Krarup *et al.*, 2013). Although selective metalloproteinases inhibition seems to increase the breaking strength and to reduce the anastomotic leakage in experimentally obstructed colon (Krarup *et al.*, 2017), on the contrary, non-selective inhibition was found to increase anastomotic disruption, possibly by impending reepithelialization (Rehn *et al.*, 2015). In humans, broad

spectrum matrix metalloproteinases inhibitors were associated with detrimental side effects, mainly the musculoskeletal syndrome, due to the high structural homology and overlapped substrate specificity of metalloproteinases (Amar *et al.*, 2017; Cui *et al.*, 2017). Future research should focus on the development of new generation matrix metalloproteinases inhibitors (with high specificity and selectivity for the targeted metalloproteinases), determination of the ideal timing and duration of the administration, and appropriate delivery system (probably by topical administration).

Iloprost is a stable analogue of prostaglandin I_2, which is a potent endogenous vasodilator and also a cryoprotective compound on the intestinal epithelium. Iloprost may improve intestinal anastomotic healing (Oines *et al.*, 2014) through the stimulation of intestinal perfusion and angiogenesis (Galanopoulos *et al.*, 2011).

Hyperbaric oxygen therapy (HBOT) seems to improve colorectal anastomotic healing, particularly in the context of ischemia (Nerstrom *et al.*, 2016; Boersema *et al.*, 2016; Yildiz *et al.*, 2013). Oxygen may stimulate collagen synthesis, matrix deposition, angiogenesis, epithelialization, and eradication of some bacteria. Besides, hyperbaric oxygen therapy may act through the inhibition of inducible nitric oxide synthase protein (iNOS) expression and the suppression of proinflammatory agents (Boersema *et al.*, 2016). Logistical issues and potential side effects (including middle ear and pulmonary barotraumas, central nervous system and pulmonary oxygen toxicities, ocular adverse events, increase of blood pressure, pulmonary edema and hypoglycemia in diabetics) may limit hyperbaric oxygen therapy clinical applications (Heyboer *et al.*, 2017).

Anastomotic reinforcement

The external reinforcement of colonic anastomoses failed to show convincing results in a systematic review of 40 studies and 20 different coating materials (Pommergaard *et al.*, 2012). In humans, fibrin glue has shown positive, however not significant, results; omental pedicle grafts demonstrated no benefit and hyaluronic acid/carboxymethylcellulose use was considered deleterious (Pommergaard *et al.*, 2012). Other coating materials were evaluated only in preclinical context and

demonstrated overall contradictory results, despite some positive effects of the coating with amniotic membrane, polypropylene mesh and collagen matrix-bound coagulation factors (Pommergaard *et al.*, 2012).

Tissue adhesives are among the most studied strategies as gastrointestinal anastomotic sealants, mostly on animal but, also, in clinical studies (Vakalopoulos *et al.*, 2013). According to the systematic review of 48 clinical and experimental studies published by Vakalopoulos KA *et al* in 2013 (Vakalopoulos *et al.*, 2013), results for the sealing of small intestine and colorectal anastomoses remain inconclusive and predominantly based on animal research. Promising results of fibrin glue sealing on small intestine anastomosis were documented and, for colorectal anastomoses, fibrin glue appeared more advantageous than cyanoacrylates (Vakalopoulos *et al*, 2013). Nevertheless, in some experimental studies, cyanoacrylate glues showed encouraging effects, particularly in high-risk conditions (Boersema *et al.*, 2017; Wu *et al.*, 2015; Wu *et al.*, 2014).

Nordentoft T *et al* (Nordentoft *et al.*, 2015) demonstrated in a systematic review of 28 experimental studies that fibrin glue did not have a consistently positive influence on the healing of gastrointestinal anastomoses and considered plausible that the potential positive effects of fibrin glue sealing were related mainly to its mechanical effect. Likewise, Stergios K *et al* (Stergios *et al.*, 2017) found no evidence to support the use of fibrin sealants as adjunct of colorectal anastomotic healing in the context of severe diabetes.

Furthermore, the ideal tissue adhesive has not yet been found (Vakalopoulos *et al.*, 2017). In a recent experimental research, cyanoacrylates exhibited mild clinical and immunohistopathological effects while maintaining high anastomotic strength and were considered promising as colonic anastomotic sealants. On the contrary, albumin based adhesives (gelatin-resorcinol-formaldehyde and glutaraldehyde-albumin glues) were considered the least suitable. Polyethylene glycol adhesives (polyethylene glycol, trilisine amine, blue dye and N-hydroxy succinimide) and fibrin glue showed low mechanical strength (Vakalopoulos *et al.*, 2017).

Regardless numerous experimental studies in colorectal surgery, anastomotic sealing with tissue adhesives has not yet been applied into the everyday clinical practice (Vakalopoulos *et al.*, 2017).

Despite extensive research, no substantial evidence was documented to justify the implementation of any of the referred promoting strategies of intestinal anastomotic repair for routine clinical use. Growth factors and hormones (insulin-like growth factor, growth hormone, granulocyte-macrophage colony-stimulating factor and erythropoietin), reinforcement with tissue adhesives, hyperbaric oxygen therapy (HBOT), inhibitors of matrix metalloproteinases and iloprost were the most promising interventions (Vakalopoulos et al., 2017; Nerstrom et al., 2016; Oines et al., 2014; Vakalopoulos et al., 2013; Pommergaard et al., 2012). Logistical constraints, absence of approval for human application and the risk of undesired side-effects, such as the potential development of anastomotic strictures, peritoneal adhesions and carcinogenesis, were some of the limitations of the described adjuvants. Unfortunately, at the moment, no convincing conclusions were drawn about its clinical applicability, efficacy and safety. More experimental and clinical studies are needed before those strategies can be recommended for clinical practice. Research on anastomotic healing may benefit also from a more systematic approach.

1.5. Growth factors as promoters of intestinal anastomotic healing

Several experimental studies analyzing the effects of growth factors, hormones and analogues on the gastrointestinal anastomotic healing suggested potential interferences in every phases of the repair process (Rijcken *et al.*, 2014). Insulin-like growth factor 1, vascular endothelial growth factor, epidermal growth factor, heparin-binding epidermal growth factor, basic fibroblast growth factor, transforming growth factor β and platelet-derived growth factor participate in the cellular migration and proliferation, angiogenesis and extracellular matrix synthesis; and its exogenous administration appears to increase the mechanical strength of intestinal anastomosis (Rijcken *et al.*, 2014; Oines *et al.*, 2014).

In present investigation, a literature search was conducted including all relevant articles published between January 1, 2000 and July 22, 2017. Prospective controlled

studies that investigated a growth factor or hormone with the purpose of promoting intestinal anastomotic healing under uncomplicated or complicated conditions were included. The search was performed using the PubMed version of Medline database and two different syntaxes (search #1 and search #2, described in the Supplementary Table S1). Articles selected through title and abstract screening were then subjected to full-text analysis. Review articles and studies on other types of anastomosis (for example, gastrojejunal, esophagojejunal, pancreatojejunal and bilioenteric anastomosis) were excluded.

A total of 395 and 111 records were identified in search #1 and in search #2, respectively. Article titles and abstracts were screened and 39 eligible articles were identified. Cross-references from the included studies were manually reviewed and 10 other articles were found. Evaluation of the reporting quality and of the internal or external validity was not formally performed.

A comprehensive review of 49 experimental studies was undertaken (Table 1.3). In fourteen articles (28.6%), full-text was unavailable and only the abstract was analysed.

Nineteen growth factors and hormones were assessed for potential improvement of intestinal anastomotic healing. They included insulin-like growth factor 1, granulocyte-macrophage colony-stimulating factor, basic fibroblast growth factor, epidermal growth factor, vascular endothelial growth factor, platelet-derived growth factor, heparin-binding epidermal growth factor, glucagon-like peptide 2, transforming growth factor β, erythropoietin, growth hormone, melatonin, leptin, ghrelin, octreotide, lanreotide, thyroid hormone, adrenomedullin and nandrolone. Effects of platelet-rich plasma and growth factor-rich plasma were also analyzed. Majority of studies were performed in a rodent model (*n*=43; 87.8%), were conducted in high risk context (*n*=32; 65.3%), involved colonic anastomosis (*n*=38; 77.6%), recurred to systemic administration of the drug (*n*=30; 61.2%) and reported clearly beneficial effects of the investigated compound (*n*=42; 85.7%). Complicated anastomotic conditions included ischemia, hypoxia, intra-abdominal sepsis, chemotherapy (systemic or intraperitoneal), radiotherapy, pharmacological immunosuppression (corticosteroid treatment or other), intestinal obstruction, obstructive jaundice, open abdomen and chemically-induced colitis.

Most investigated compounds were insulin-like growth factor 1, granulocyte-macrophage colony-stimulating factor, platelet-rich plasma, growth hormone and erythropoietin. All seem to potentially increase the bursting pressure of the anastomosis (Table 1.3).

Insulin-like growth factor 1, growth hormone and granulocyte-macrophage colony stimulating factor were shown to be beneficial to intestinal anastomotic healing in most of the experimental studies. In humans, insulin-like growth factor 1 is used in cases of growth hormone insensitivity and severe insulin-resistance and is associated with relevant side effects, such as hypoglycemia, hyperplasia of lymphoid tissues, retinal edema and severe myalgias (Frysak *et al.*, 2015; Rosenbloom, 2009). Growth hormone is approved for the treatment of adult patients with short-bowel syndrome, but is associated with relevant adverse effects, including peripheral edema, arthralgias, sleep disturbances and others (Pironi *et al.*, 2016).

Granulocyte-macrophage colony-stimulating factor is a pleiotropic cytokine that activates granulocyte and macrophage cell lineages. It is also known to have an important function in wound repair (Rho *et al.*, 2015), with influence on inflammation, reepithelialization, neovascularization (Mann *et al.*, 2006) and immune response (Yan *et al.*, 2017). In a previously mentioned systematic review and meta-analysis of pre-clinical studies, Nerstrom M *et al* (Nerstrom *et al.*, 2016) assessed the efficacy of therapeutic agents against colonic anastomotic leakage on high-risk conditions; positive effects of granulocyte-macrophage colony-stimulating factor were found in the context of segmental ischemia and obstructive jaundice, although it failed to shown a significant favorable influence in chemotherapy (Nerstrom *et al.*, 2016). Nowadays, granulocyte-macrophage colony-stimulating factor is approved for the treatment of adults with acute myeloid leukemia and submitted to bone marrow/peripheral blood stem cell transplantation and its potential side effects included fluid retention, respiratory and cardiovascular symptoms, renal and hepatic dysfunctions (Francisco-Cruz *et al.*, 2014).

Platelet-rich plasma (PRP) is an autologous blood-derived product enriched in platelets, growth factors, adhesive proteins, angiogenic factors, chemokines, cytokines, clotting factors and their inhibitors, membrane proteins and immune mediators, and used in a variety of clinical applications (Pavlovic *et al.*, 2016). Most important growth

factors comprised in the platelet-rich plasma are vascular endothelial growth factor, platelet-derived growth factor, fibroblast growth factor, epidermal growth factor, insulin-like growth factor, transforming growth factor β and hepatocyte growth factor. These bioactive molecules are involved in clotting, inflammation, chemotaxis, mitogenesis, cellular differentiation and host defense. Growth factor-rich plasma is characterized, in comparison with platelet-rich plasma, by a moderate platelet concentration and absence of leucocytes and fibrin scaffold (Giusto *et al.*, 2017). In humans, platelet-rich plasma is being increasingly used as a biological enhancer for tissue healing in the treatment of musculoskeletal soft tissue injuries, with a low incidence of side effects, although with insufficient clear evidences of benefit (Moraes *et al.*, 2014). Heterogeneity of platelet-rich plasma preparations may influence their biological properties and impair the evaluation of efficacy (Kaux *et al.*, 2017). Overall, results of platelet-rich plasma and growth factor-rich plasma as adjuvants of anastomotic healing were inconsistent (Giusto *et al.*, 2017) (Table 1.3).

Platelet-derived growth factor, transforming growth factor β, epidermal growth factor, basic fibroblast growth factor, vascular endothelial growth factor and platelet-derived formulas were clinically studied for the topical treatment of diabetic lower-extremity ulcers (Martí-Carvajal *et al.*, 2015; Barrientos *et al.*, 2014) and its safety profiles were considered unclear (Martí-Carvajal *et al.*, 2015).

Erythropoietin (EPO) is the main hormonal regulator of erythropoiesis and recombinant erythropoietin emerged as the leading drug for the treatment of anemia from chronic kidney disease and other causes. Side effects of erythropoietin include arterial hypertension, vascular access thrombosis and major adverse cardiovascular events, including myocardial infarction and stroke (Palmer *et al.*, 2014).

A previously referred meta-analysis (Oines *et al.*, 2014) identified pharmacologic compounds with the potential to improve colonic anastomotic healing under non-complicated conditions, including insulin-like growth factor 1, growth hormone and erythropoietin, which were associated with an enhancement of the weighted mean anastomotic bursting pressure of 61 mmHg (95% CI 43-79), 21 mmHg (95% CI 7-35) and 45 mmHg (95% CI 14-76), respectively (Oines *et al.*, 2014).

Table 1.3. Animal studies on the potential promoting effects of the exogenous administration of growth factors, hormones and analogues on the intestinal anastomotic healing published from 2000 (*n*=49)

Study	Drug	Location	Context	Species	Sample size	Dosage and schedule	Route	Time of evaluation	Effect
Fuchs TF *et al*, 2012	IGF-1	Colon	Normal	Rats	48	IO	Local (coated suture)	Day 3	Beneficial
Rijcken E *et al*, 2010	IGF-1	Colon	Dextran sodium sulphate colitis	Rats	120	IO	Local (coated suture)	Days 1,3 and 7	Beneficial
Inglin RA *et al*, 2008	IGF-1	Colon	Mycophenolate mofetil	Rats	63	1 mg/kg/day from day 0	IP	Days 2,4 and 6	Beneficial
Zacharakis E *et al*, 2008	IGF-1	Colon	5-fluouracil	Rats	80	2 mg/kg at days 0,2,4 and 6	IP	Day 7	Beneficial
Zacharakis E *et al*, 2007	IGF-1	Colon	Normal	Rats	40	2 mg/kg at days 0,2,4 and 6	IP	Day 7	Beneficial
Mantzoros I *et al*, 2006[b]	IGF-1	Colon	Hydrocortisone	Rats	80	2 mg/kg at days 0,2,4 and 6	IP	Day 7	Beneficial
Egger B *et al*, 2001	IGF-1 and tKGF	Colon	Normal	Rats	72	1 mg/kg/day from 12 h before	IP	Days 2,4 and 6	Beneficial
Liu Y *et al*, 2012[b]	GM-CSF	Colon	Oxaliplatin	Rats	60	IO	Local	Days 2,3,5 and 7	Beneficial
Cetinkaya K *et al*, 2005	GM-CSF	Colon	IP mitomicin-C	Rats	81	50 μg	Local	Day 3	Beneficial
Gulcelik MA *et al*, 2005	GM-CSF	Colon	Jaundice	Rats	86	50 μg	Local	Day 3	Beneficial
Dinc S *et al*, 2004a[b]	GM-CSF	Small intestine	Radiotherapy	Rats	160	50 μg, IO	Local	Days 3 and 7	Beneficial
Dinc S *et al*, 2004b	GM-CSF	Small intestine	Ischemia	Rats	144	50 μg, IO	Local	Days 3 and 7	Beneficial
Erdem E *et al*, 2002	GM-CSF	Colon	5-fluorouracil	Rats	45	50 μg, IO	Local	Day 3	Beneficial (only after 5-FU)
Dinc S *et al*, 2002	GM-CSF	Colon	Long term methylprednisolone	Rats	80	50 μg, IO or 50 μg, SC	Local or SC	Day 3	Beneficial
Demirer S *et al*, 2001[b]	GM-CSF	Colon	Normal	Rats	40	100 μg/kg 2 days before	SC	Days 3 and 7	Not beneficial
Şenocak R et al, 2017	EGF	Small intestine	Ischemia	Rabbits	16	2 μg/kg IO ± 2 μg/Kg/day IP	Local and IP	Day 4	Beneficial
Sakallioglu AE *et al*, 2004	EGF	Colon	Dexamethasone	Rats	60	1 μg/kg/day throughout 4 days	Local (EGF-loaded sponge)	Day 7	Beneficial
Hirai K *et al*, 2016	bFGF	Small intestine	Normal	Rats	90	30 μg, IO	Local (bFGF-impregnated sheet)	Days 1, 3, 7, 14 and 28	Beneficial
Günes HV *et al*, 2006[b]	bFGF	Colon	Long-term methyprednisone	Rats	80	5 μg/kg/day, 3 days after	SC		Not beneficial
Adas G *et al*, 2011	VEGF-A and FGF-2 (gene therapy)	Colon	Ischemia	Rats	40	1 μg VEGF-A and 1 μg bFGF, IO	Local (plasmid delivery)	Day 4	Beneficial (VEGF-A, FGF-2 and combination)
Ishii M *et al*, 2009	VEGF-A	Colon	Normal	Rabbits		10 μg, IO	Local	Days 3,4 and 7	Beneficial
Radulescu A *et al*, 2011	HB-EGF	Small intestine	Normal	Mice	149	800 μg/kg/day	Enteral	Days 3 and 6	Beneficial
Redstone HA *et al*, 2010	GLP-2 and GLP-2 MMB	Colon	Hypoxia	Rats	48	GLP-2 100 μg/kg or 2 mg/kg, 2 id, on days 0 and 3	SC	Day 5	Not clearly beneficial
Saribeyoglu K et al, 2003b	PDGF-BB	Colon	Ischemia	Rats	40		Intraabdominal	Day 4	Beneficial (only in ischemia)
Migaly J et al, 2004b	TGF-β1 (gene therapy)	Colon	Normal	Rats	24	At day 0 or 3	Local (plasmid delivery)	Day 6	Beneficial (only when administered at the 3rd day)
Giusto G *et al*, 2017	PRP and GFRP	Small intestine	Normal	Pigs	8[a]	IO	Local	Day 8	Not beneficial (except increased epithelialization after PRGF)
Sozutek A *et al*, 2016	PRP	Colon	Intra-abdominal sepsis	Rats	50	IO	Local	Day 7	Beneficial
Zhou B *et al*, 2014	PRP	Colon	Open abdomen	Rats	30	IO	Local	Day 7	Beneficial (only in open abdomen)
Yamaguchi R *et al*, 2012	PRP	Small intestine	Normal	Rats	48	IO	Local	Day 5	Beneficial only in low-dose. Deleterious in high-dose

Table 1.3. Animal studies on the potential promoting effects of the exogenous administration of growth factors, hormones and analogues on the intestinal anastomotic healing published from 2000 (*n*=49) - *Continued*

Study	Drug	Location	Context	Species	Sample size	Dosage and schedule	Route	Time of evaluation	Effect
Fresno L *et al*, 2010	PRP	Small intestine	Normal	Pigs	35	IO	Local	Days 1,2,3,4 and 7	Not clearly beneficial
Yol S *et al*, 2008	PRP	Colon	Normal	Rats	30	IO	Local	Day 7	Beneficial
Ozel Turkcu U *et al*, 2012	EPO	Colon	Radiotherapy	Rats	32	500 IU/Kg/day 7 days	IM	Day 7	Beneficial
Kaemmer DA *et al*, 2010	EPO	Colon	Normal	Rats	20	5 IU/g, 24 h before and at day 0	SC	Days 3 and 5	Beneficial at day 5
Faruquzzaman SK, 2009[b]	EPO	Colon	Intestinal obstruction	Pigs	20	500 IU/kg	SC		Beneficial only in obstruction
Moran M *et al*, 2007	EPO	Colon	Intestinal obstruction	Rats	40	500 IU/kg/day, 7 days	SC	Day 7	Beneficial only in obstruction
Küper MA *et al*, 2016	GH	Colon	Everolimus	Rats	48	2.5 mg/Kg/day 7 days before and 7 days after	SC	Day 7	Beneficial in normal and everolimus contexts
Adas M et al, 2013	GH and hyperbaric oxygen	Colon	Ischemia	Rats	80	GH 2 mg/Kg/day from day 0 to 4; hyperbaric O_2 3 hours after surgery and continued for 4 days	SC	Day 4	Beneficial in combination
Wang P *et al*, 2009	GH and fibrin glue	Small intestine	Traumatic shock with peritonitis	Pigs	163	2 IU/Kg/day, 7 days	SC	Day 10	Fibrin glue and combination beneficial; GH not beneficial
Tei TM *et al*, 2006	GH	Colon	Normal	Rats	22	2 mg/kg/day, 7 days before and 4 days after	SC	Day 4	Beneficial
Yarimkaya A *et al*, 2003[b]	GH or nandrolone	Colon	Ischemia	Rats	70			Day 3 and 7	Beneficial
Cağlikülekçi M *et al*, 2002[b]	GH	Small intestine	Obstructive jaundice	Rats	40	2 mg/kg/day	SC	Day 7	Beneficial in jaundice and normal contexts
Ozen IO *et al*, 2007[b]	Melatonin	Small intestine and colon	Bacterial peritonitis	Rats	32	5 and 10 mg/kg/day, 5 days starting in the day before			Beneficial (dose-dependent effect)
Ozdogan M *et al*, 2005[b]	Melatonin	Colon	Normal	Rats		1 mg/kg or 10 mg/kg, at day 0,1 and 2		Days 3 and 7	Not beneficial
Ceran C *et al*, 2013	Ghrelin	Colon	Normal	Rats	20	10 ng/kg/day, 7 days	IP	Day 7	Beneficial
Karaman K *et al*, 2012	Thyroid hormone (T3)	Colon	Normal	Rats	30	400 μg/100 g at day 1	SC	Days 3 and 7	Beneficial at day 7
Karatepe O *et al*, 2011	Adrenome-dullin	Colon	Ischemia	Rats	40	2 μg/day from day 0 to 3	SC	Day 7	Beneficial
Colak T *et al*, 2007[b]	Octreoctide	Colon	5-fluorouracil	Rats	40	20 μg/kg/day	SC	Day 7	Beneficial
Demetriades H *et al*, 2002	Lanreotide	Small intestine	Intestinal obstuction	Rats	16	5.4 mg/kg, 2 days before	IM	Day 7	Beneficial
Tasdelen A *et al*, 2004	Leptin	Colon	Ischemia	Rats	48	1 mg/kg, 2 id	IP	Day 7	Beneficial in normal and ischemic contexts

bFGF, Basic fibroblast growth factor; EGF, Epidermal growth factor; EPO, Erythropoietin; GH, Growth hormone; GFRP, Growth factor-rich plasma; GLP-2, Glucagon-like peptide 2; GLP-2 MMB, GLP-2 mimetibody construct; GM-CSF, Granulocyte-macrophage colony-stimulating factor; HB-EGF, Heparin-binding epidermal-like growth factor; IGF-I, Insulin-like growth factor 1; PDGF, Platelet-derived growth factor; PRP, Platelet-rich plasma; tKGF, Truncated keratinocyte growth factor; TGF-β, Transforming growth factor β; VEGF, Vascular endothelial growth factor. IM, intramuscular; IO, intraoperative; IP, intraperitoneal; SC, subcutaneous. [a] Six anastomosis *per* animal [b] Article full-text not retrievable

In spite of some promising results, numerous experimental studies on growth factors as promoters of intestinal anastomotic healing are characterized by poor quality, including low internal validity (high risk of selection, performance and detection bias) and reporting quality (Bosmans et al., 2016; Yauw et al., 2015). Its interpretation is hampered by the heterogeneity of animal models, anatomic localizations of the anastomosis, surgical techniques, context (normal or high-risk), evaluated endpoints and outcome measures, and studied growth factors, including type and administration schedule (dosage, route of delivery, timing and duration). Safety profiles and high cost may constitute additional disadvantages of these drugs. Therefore, further research is necessary to support the use of growth factors in this context.

1.6. Glucagon-like peptide 2 and teduglutide

Glucagon-like peptide 2

Glucagon-like peptide 2 (GLP-2) is a potent and relatively specific gastrointestinal growth factor with intestinotrophic, antisecretory and transit-modulating properties (Drucker and Yusta, 2014).

GLP-2 is a 33-amino acid peptide produced in the enteroendocrine L cells of the intestine, predominantly located in the distal ileum and colon, with glucagon-like peptide 1 (GLP-1), intervening peptide 2 and glicentin, after cleavage of proglucagon by prohormone convertase 1 and 3 (Drucker and Yusta, 2014; Janssen *et al.*, 2013) (Fig. 1.4).

GLP-2 is produced in response to nutritional, hormonal and neural stimulation (Drucker and Yusta, 2014). Secretion occurs in a biphasic pattern in humans (Janssen *et al.*, 2013; Marathe *et al.*, 2013). Early postprandial secretion elapses between 30 to 60 minutes and is probably due to the stimulation by neural and endocrine pathways; second peak develops between 90 to 120 minutes by direct stimulation of intestinal L cells by digested nutrients (including glucose, fatty acids and dietary fibers) (Janssen *et al.*, 2013; Marathe *et al.*, 2013). After ingestion of nutrients, plasma levels of GLP-2 and GLP-1 increase two to five-fold, depending of the size and composition of the meal

(Janssen *et al.*, 2013). Plasma concentrations of GLP-2 increase, also, in response to intestinal injury or major resection (Drucker and Yusta, 2014).

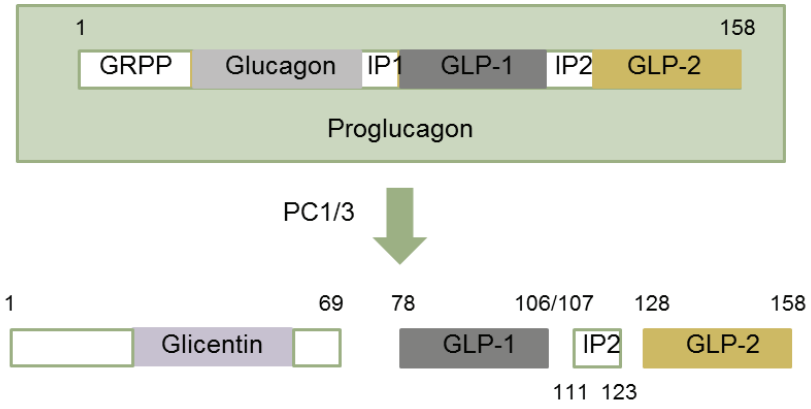

Figure 1.4. Peptide products of the posttranslaccional processing of proglucagon in enteroendocrine cells of the intestine. Proglucagon is cleaved by proconvertases 1 and 3 leading to the formation of GLP-2, GLP-1, IP-2 and glicentin. GLP-2, Glucagon-like peptide 2; GLP-1, Glucagon-like peptide 1; GRPP, Glicentin-related pancreatic polypeptide; IP-2, Intervening peptide 2; PC1/3, Prohormone convertase 1/3. Adapted from Janssen P *et al.*, 2013

After release, biologically active GLP-2(1-33) is rapidly degraded, through cleavage at the alanine residue in position "2" from the N-terminus, by the ubiquitously expressed exopeptidase dipeptidylpeptidase IV, resulting in the generation of its metabolite GLP-2(3-33) (Drucker and Yusta, 2014; Janssen *et al.*, 2013). GLP-2(3-33) is a pharmacological antagonist of glucagon-like peptide 2 receptor (GLP-2R), although it exerts also a weak agonist activity (Drucker and Yusta, 2014). The enzymatic inactivation and the renal clearance control the elimination of bioactive GLP-2 (Drucker and Yusta, 2014).

In preclinical models, inhibition of dipeptidylpeptidase IV activity slightly increases the effects of GLP-2, but treatment with this enzyme inhibitors does not significantly expand the mucosal epithelium in normal rats (Drucker and Yusta, 2014).

The activity of GLP-2 is transduced through a G protein-coupled receptor (glucagon-like peptide 2 receptor - GLP-2R) expressed almost exclusively in the intestinal tract, stomach and central nervous system (in rodents). GLP-2R expression is considered high in the proximal small intestine, particularly in jejunum, and decrease distally along the longitudinal axis (Drucker and Yusta, 2014; Baldassano *et al.*, 2013; Janssen *et al.*, 2013). Nevertheless, the study of El-Jamal N *et al* (El-Jamal *et al.*, 2014) did not confirm the decreasing gradient of GLP-2R toward the distal gut. More limited expression of GLP-2R was also observed in the lung, cervix, vagal afferents and heart (Drucker and Yusta, 2014; Janssen *et al.*, 2013), as well as in the liver, pancreas, spleen, bladder, mesenteric fat and lymph nodes (El-Jamal *et al.*, 2014). GLP-2R is highly selective for GLP-2 and reacts only weakly to equimolar concentrations of structurally related peptides such as glucagon, GLP-1 and glucose-dependent insulinotropic polypeptide (Drucker and Yusta, 2014). In the intestine, at the cellular level, GLP-2R was identified in subepithelial myofibroblasts, enteric neurons and some enteroendocrine cells, but, surprisingly, was not detected in crypt epithelial cells and enterocytes, which seem to constitute the main targets of GLP-2 action *in vivo* (Drucker and Yusta, 2014; Janssen *et al.*, 2013; Dubé *et al.*, 2007).

Signaling pathways transducing the multiple actions of GLP-2 in the target cells of the intestine remain largely unknown. Most GLP-2 effects are indirect and secondary to endocrine, paracrine, autocrine and neural signals activated by the GLP-2R (Drucker and Yusta, 2014; Janssen *et al.*, 2013; Rowland and Brubaker, 2011).

GLP-2 demonstrates a complex and indirect mechanism of action with intricate signaling pathways and multiple mediators' participation (including insulin-like growth factors 1 and 2, ErbB superfamily of ligands, keratinocyte growth factor, vasoactive intestinal polypeptide, endothelial nitric oxide synthase, and vascular endothelial growth factor) (Drucker and Yusta, 2014; Janssen *et al.*, 2013; Brinkman *et al.*, 2012; Rowland and Brubaker, 2011; Bulut *et al.*, 2008; Dubé *et al.*, 2007). According to the proposed model for the mechanism of action on intestinal epithelial crypt cells, GLP-2 acts via GLP-2R binding on subepithelial myofibroblasts, leading to the release of insulin-like growth factor 1 and, likely, other growth factors, such as ErbB ligands (Rowland and Brubaker, 2011). Insulin-like growth factor 1 binds to the insulin-like

growth factor 1 receptor (IGF-1R) located on crypt epithelial cells and transactivates the ErbB receptor, leading to proliferative responses including phosphatidylinositol-3-kinase (PI3K/Akt) and canonical Wingless (cWnt)/β-catenin signaling (Rowland and Brubaker, 2011) (Fig. 1.5).

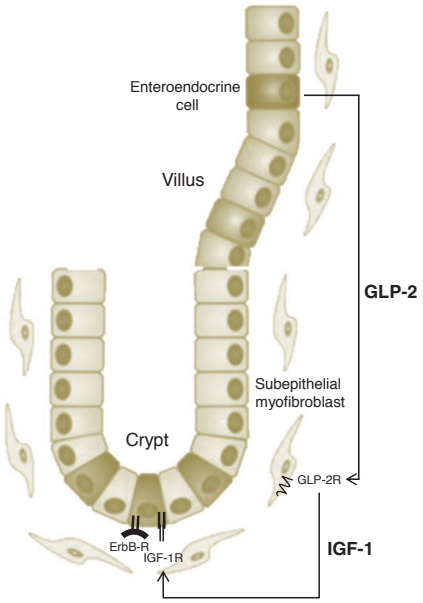

Figure 1.5. Proposed mechanism for the action of GLP-2 on the intestinal crypt cells. GLP-2 activates the GLP-2R on the subepithelial myofibroblasts leading to the release of IGF-1 (and likely other growth factors, such as ErbB ligands), which then binds to the IGF-1R expressed on the crypt epithelial cells. IGF-1R may transativate the ErbB-R and origin proliferative responses. ErbB-R, ErbB receptor, GLP-2, Glucagon-like peptide 2; GLP-2R, Glucagon-like peptide 2 receptor; IGF-1, Insulin-like growth factor 1; IGF-1R, Insulin-like growth factor 1 receptor. Adapted from Rowland and Brubaker, 2011

PI3K/Akt signaling activates β-catenin in intestinal epithelial stem and progenitor cells via phosphorylation at Ser552, through a mechanism involving Ras activation and glycogen synthase kinase 3β (GSK3β) phosphorylation. Role of the IGF-1R and/or ErbB receptor expressed by the subepithelial myofibroblasts has not been established, but it may mediate the autocrine effects of myofibroblasts-derived factors, leading to

the release of other growth factors. Several studies suggest also a dose-dependent activation of the cAMP-protein kinase A-cAMP response elements (CRE) B (cAMP-PKA-CREB) pathway by the ligand binding to GLP-2R and inhibition of GSK3β and B-cell lymphoma 2 (Bcl-2) (Rowland and Brubaker, 2011).

Main biological effects of GLP-2 are related to the regulation of energy absorption and maintenance of intestinal mucosa morphology, function and integrity (Janssen *et al.*, 2013). Physiological actions of endogenous GLP-2 receptor signaling include the adaptation of intestinal mucosal growth to refeeding (via the activity of ErbB ligands), the resistance to injury and the antimicrobial mucosal defense mechanisms (through the Paneth cell functions). Proglucagon-derived axis seems to play an important role in the normal human intestinal development and function (Drucker and Yusta, 2014; Janssen *et al.*, 2013).

Several studies, particularly of animal but also clinical experimentation, have suggested that exogenous GLP-2 administration may induce expansion of intestinal absorption surface (through stimulation of proliferation in the epithelial crypt cells and inhibition of apoptosis in the crypt and villi); improvement of macronutrients digestion and absorption (increasing the expression and activity of digestive enzymes and transporters); reduction of intestinal permeability and reinforcement of barrier function (upregulating tight junction proteins *zonula occludens*-1 and occludin); stimulation of mesenteric perfusion (predominantly in the pancreas, duodenum and jejunum) and portal blood flow; inhibition of gastrointestinal motility, gastric acid hypersecretion and intestinal chloride secretion; repair after injury; anti-inflammatory and antioxidant effects; proangiogenic actions; and increase of distraction enterogenesis (Drucker and Yusta, 2014; Janssen *et al.*, 2013; Sueyoshi *et al.*, 2013; Dubé *et al*, 2007). Extra-gastrointestinal effects of GLP-2 administration seems to include the stimulation of glucagon secretion (without significant modification of glucose homeostasis), inhibition of bone reabsorption, control of the appetite, and reduction of food intake, gut motility and blood pressure (after direct administration in the central nervous system of rodents) (Drucker and Yusta, 2014).

Potential for GLP-2 to induce carcinogenesis remains controversial (Drucker and Yusta, 2014; Trivedi *et al.*, 2012). Several studies have demonstrated that the

enterotrophic effects of GLP-2 and its analogues are exerted indirectly through multiple mediators (including insulin-like growth factor 1, ErbB ligands and receptors), with activation of signaling pathways that have been implicated in the development of intestinal cancer (Trivedi *et al.*, 2012), namely phosphatidylinositol 3 kinase/protein kinase B and β-catenin (Kannen *et al.*, 2013). Previous experimental studies suggested that sustained pharmacological GLP-2 (and its analogues) administration may promote, rather induce, tumor growth in rodent models of carcinogen-induced and inflammation-associated carcinogen-induced neoplasia (Drucker and Yusta, 2014; Trivedi *et al.*, 2012). Ability of exogenous or endogenous GLP-2R signaling to modify the growth of preexisting intestinal tumors depends on the precise experimental model used (Drucker and Yusta, 2014; Trivedi *et al.*, 2012).

Activation of GLP-2R signaling seems to protect the small and large bowels in several experimental models of intestinal injury, including short-bowel syndrome and major small-bowel resection, parenteral nutrition and fasting-associated gut hypoplasia, chemical enteritis and/or colitis, postchemotherapy and postradiotherapy enteritis, antigen-induced inflammatory bowel disease, infectious enteritis, ischemic insult, immune-mediated hypersensitivity lesion, sepsis, mucosal dysfunction and reduced barrier function (Drucker and Yusta, 2014; Janssen *et al.*, 2013). Degree of mucosal protection was highly dependent on the specific models and timing of GLP-2 administration (Drucker and Yusta, 2014).

Teduglutide

Teduglutide [GLP-2(2-33)] is a long-acting dipeptidylpeptidase IV-resistant equivalent of GLP-2(1-33), obtained through the substitution of alanine by glycine at position "2" that confers higher biological potential and longer half-life (Drucker and Yusta, 2014; Yazbeck *et al.,* 2009; Drucker *et al.*, 2002) (Table 1.4).

Table 1.4. Glucagon-like peptide 2 and teduglutide amino acid sequences[a]

Peptide	Amino acid sequence
Human (Homo sapiens) GLP-2	His - **Ala** - Asp - Gly - Ser - Phe -Ser - Asp - Glu - Met - Asn - Thr -Ile - Leu - Asp - Asn - Leu - Ala -**Ala** - Arg - Asp -Phe - Ile - Asn -Trp - Leu - Ile - Gln - Thr - Lys - Ile - Thr - Asp
Rat (*Rattus norvegicus*) GLP-2	His - **Ala** - Asp - Gly - Ser - Phe -Ser - Asp - Glu - Met - Asn - Thr -Ile - Leu - Asp - Asn - Leu - Ala -**Thr** - Arg - Asp -Phe - Ile - Asn -Trp - Leu - Ile - Gln - Thr - Lys - Ile - Thr - Asp
Teduglutide	His - **Gly** - Asp - Gly - Ser - Phe -Ser - Asp - Glu - Met - Asn - Thr -Ile - Leu - Asp - Asn - Leu - Ala -Ala - Arg - Asp -Phe - Ile - Asn -Trp - Leu - Ile - Gln - Thr - Lys - Ile - Thr - Asp

[a] From references Drucker and Yusta, 2014; Drucker *et al.*, 2002. Ala, Alanine; Arg, Arginine; Asn, Asparagine; Asp, Aspartate; Glu, Glutamate; Gln, Glutamine; Gly, Glycine; His, Histidine; Ile, Isoleucine; Leu, Leucine; Lys, Lysine; Met, Methionine; Phe, Phenylalanine; Ser, Serine; Thr, Tryptophan

In human, half-life of teduglutide is increased compared with native GLP-2 (thirty minutes *versus* seven minutes and, following subcutaneous injection, 180 to 330 minutes *versus* 60 to 90 minutes, respectively) (Berg *et al.*, 2014; Naimi *et al.,* 2013).

Teduglutide is currently accepted for pharmacological rehabilitation of patients with short-bowel syndrome associated intestinal failure (Burness and McCormak, 2013) and also considered a promising medication for moderate-to-severe Crohn's disease (Blonski *et al.*, 2013). In short-bowel context, teduglutide seems to increase energy, fluid, mineral and electrolyte absorption, weight gain, lean body mass, bone density, plasma levels of citrulline, urine output and creatinine clearance; and to decrease parenteral nutrition and/or fluid therapy requirements (Drucker and Yusta, 2014). Several studies have demonstrated that, in patients with short-bowel syndrome, teduglutide treatment is safe, well tolerated and efficacious, with improvement of intestinal absorption and reduction of parenteral support requirements (Naberhuis *et al.*, 2016; Austin *et al.*, 2016). In the study STEPS (Study of Teduglutide Effectiveness in Parenteral Nutrition-Dependent Short-bowel Syndrome Subjects) II, 93% of the patients who completed 30 months of treatment achieved clinical response (defined as a reduction of weekly parenteral support volume of at least 20% from baseline), with a mean parenteral support reduction of 66% (corresponding to 7.6±4.9 l/week), and 33% obtained full enteral autonomy (Schwartz *et al.*, 2016). Teduglutide was recently approved by the European Medicines Agency for treatment of patients with short-bowel syndrome related parenteral support dependence despite optimized medical and dietetic treatment, aged more than one year and who are stable following a period of postsurgical intestinal adaptation (Kim and Keam, 2017; Billiauws *et al.*,

2017). Furthermore, in the recently published guidelines of the European Society for Clinical Nutrition and Metabolism, teduglutide was considered the first choice for carefully selected patients with chronic intestinal failure who are candidates for growth factor treatment (Pironi *et al.*, 2016).

Adverse events associated with treatment with GLP-2 analogues include headache, nausea, vomiting, abdominal pain, abdominal distention, ostomal site complications, injection site complaints, nasopharyngitis and development of non-neutralizing antibodies (Drucker and Yusta, 2014; Janssen *et al.*, 2013). Proproliferative and antiapoptotic activities of GLP-2 rise concerns about its carcinogenic risk (Drucker and Yusta, 2014; Trivedi *et al.*, 2012), particularly at long-term and emphasize the importance of careful screening and follow-up of human subjects treated with GLP-2 analogues (Drucker and Yusta, 2014). Nevertheless, as mentioned before, the potential for GLP-2 and its analogues to induce carcinogenesis remains controversial (Drucker and Yusta, 2014; Trivedi *et al.*, 2012; Iakoubov *et al.*, 2009; Koehler *et al.*, 2008; Thulesen *et al.*, 2004). Tumor promotion effects seem to be associated with the exposition to teduglutide plasma concentrations much higher than those obtained with the daily recommended dose (Kim and Keam, 2017). Furthermore, there have been no reports of intestinal dysplasia in patients with short-bowel syndrome-associated intestinal failure treated for up to two years with teduglutide (Schwartz *et al.*, 2016).

Teduglutide has a considerable therapeutic potential, particularly in short-bowel syndrome (preventing or minimizing the parenteral nutrition dependence), but also in others types of acute and chronic intestinal dysfunction, such as inflammatory bowel diseases, radiation and chemotherapy enteropathies, necrotizing enterocolitis, and ischemia/reperfusion lesions (Drucker and Yusta, 2014; Yazbeck et al., 2009; Wallis et al., 2007). However, cellular and molecular mechanisms underlying biological action of GLP-2, precise therapeutic indications, optimal administration methods and adverse effects remain unclear and additional studies are required.

Chapter 2

Framework, hypothesis & objectives

2.1. Framework & hypothesis

Regardless of continuous improvements in surgical technique and perioperative care, intestinal anastomotic failure remains, as mentioned before, one of the most serious postoperative complications, due to its incidence and deleterious consequences (Guyton *et al.*, 2016; Chadi *et al.*, 2016; Vallance *et al.*, 2016; Bosmans *et al.*, 2015; Shogan *et al.*, 2013).

Anastomotic failure has a multifactorial etiology and its pathogenesis continues to be insufficiently understood (Guyton *et al.*, 2016; Chadi *et al.*, 2016; Vallance *et al.*, 2016; Bosmans *et al.*, 2015; Shogan *et al.*, 2013). Therefore, further research on the underlying pathophysiological mechanisms of intestinal wound healing and on innovative perioperative management to improve anastomotic repair, especially in high-risk context, persists necessary.

Glucagon-like peptide 2 (GLP-2) is a gastrointestinal growth factor with a relevant role on the control of energy absorption and on the preservation of intestinal mucosa morphology and function (Drucker and Yusta, 2014). GLP-2 demonstrates a complex, indirect and poorly understood mechanism of action with intricate signaling pathways and multiple mediators' participation (Drucker and Yusta, 2014; Janssen *et al.*, 2013; Rowland and Brubaker, 2011). GLP-2 exogenous administration has been associated with intestinotrophic, antisecretory, transit-modulating and antiinflammatory effects (Drucker and Yusta, 2014).

Teduglutide is a long-acting equivalent of GLP-2 (Drucker and Yusta, 2014) currently accepted for pharmacological rehabilitation of patients with short-bowel syndrome associated intestinal failure and considered safe, well tolerated and efficacious in this context (Kim and Keam, 2017; Billiauws *et al.*, 2017; Naberhuis *et al.*, 2016; Austin *et al.*, 2016).

Intestinal anastomotic repair is a complex and well-orchestrated multicellular multimolecular process, regulated by cytokines, chemokines, growth factors, reactive oxygen species and other factors (Nerstrom *et al.*, 2016; Rijcken *et al.*, 2014; Oines *et al.*, 2014), and thus, susceptible to the influence of GLP-2 and its analogues. Intestinotrophic and cytoprotective properties of GLP-2, particularly the promotion of

epithelial proliferation, neoangiogenesis and blood perfusion, suggest a potential favorable influence on the inflammatory and proliferative phases of intestinal anastomotic healing. In fact, previous experimental studies indicated potential beneficial effects on anastomotic repair from the exogenous administration of growth factors that are considered mediators of the GLP-2 intestinotrophic actions, including insulin-like growth factor 1, epidermal growth factor, heparin-binding epidermal growth factor, fibroblast growth factor 7/keratinocyte growth factor and vascular endothelial growth factor (Nerstrom *et al.*, 2016; Rijcken *et al.*, 2014; Oines *et al.*, 2014; Drucker and Yusta, 2014; Janssen *et al.*, 2013; Rowland and Brubaker, 2011).

Knowledge of the potential influence of teduglutide on the intestinal anastomotic repair is relevant, not only for patients with short-bowel syndrome undergoing intestinal anastomosis (including autologous intestinal reconstruction procedures) during treatment with this growth factor, but also to explore its potential role as a perioperative adjuvant strategy. Relative specificity of the GLP-2 effects, consequence of the predominant gastrointestinal expression of its receptor (GLP-2R) (El-Jamal *et al.*, 2014; Drucker and Yusta, 2014; Janssen *et al.*, 2013; Baldassano *et al.*, 2013) may constitute an advantage in this context.

Any anastomotic healing-promoting intervention could have a potential enormous positive clinical and socioeconomic impact. As referred previously, albeit numerous experimental studies on this subject, results were insufficient to allow the translation into the daily practice. GLP-2 seems to be critically involved in the physiologic process of intestinal anastomotic repair and, therefore, teduglutide may represent a new therapeutic resource, particularly in high-risk conditions.

In regard to this framework, it was hypothesized that teduglutide may interfere with the cellular, humoral and molecular mediators of intestinal repair and exert a favorable influence on the anastomotic healing (Fig. 2.1).

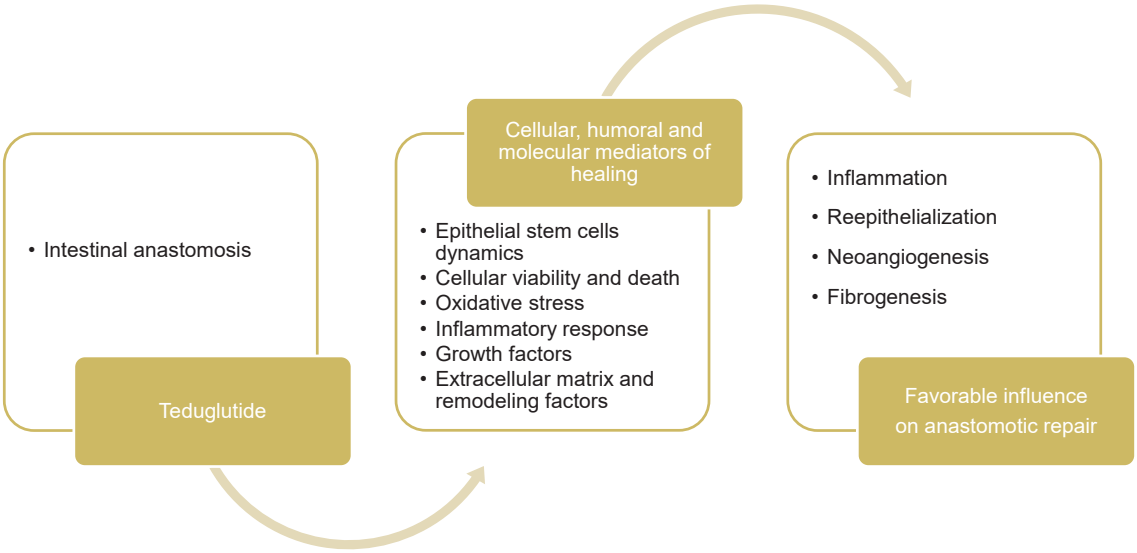

Figure 2.1. Schematic representation of the hypothesized influence of teduglutide exogenous administration on the intestinal anastomotic repair process

2.2. Objectives

The present study aimed to analyze the effects of teduglutide administration on the early stages of the intestinal anastomotic healing on an animal model and to elucidate about the underlying cellular, humoral and molecular mechanisms.

An experimental rat model of standard intestinal anastomosis was proposed with evaluation at the third and the seventh postoperative days, corresponding presumably to the predominantly inflammatory and proliferative phases, respectively (Rijcken *et al.*, 2014). Experiment outline includes the evaluation of the anastomosis outcome with an anastomotic complication score and the assessment of structural parameters of anastomotic healing, including inflammatory cells influx, reepithelialization, neoangiogenesis and fibroplasia. Analysis of the cellular, humoral and molecular mediators of anastomotic healing was programmed, including cellular viability and death, oxidative stress, local and systemic inflammatory response, growth factors, putative intestinal epithelial stem cells, extracellular matrix components and remodeling factors. Correlation of the results with Glp-2 plasma concentrations and Glp-2 receptor (Glp-2r) tissue gene expression was also planned.

The ultimate goal of this experiment was to better understand the intestinal repair and to anticipate the role of teduglutide as a promoting strategy of the anastomotic healing.

For this purpose, the following five specific objectives were addressed:

- To analyse the response of putative intestinal epithelial stem cells to teduglutide treatment in the contex of intestinal anastomosis repair – **Chapter 3**;

- To evaluate the influence of teduglutide administration on the intestinal anastomosis outcome, at the macroscopic and microscopic levels – **Chapter 4**;

- To investigate the effects of teduglutide on the cellular viability and death processes, oxidative stress and mitochondrial function, and inflammatory response on the context of intestinal anastomotic healing – **Chapter 5**;

- To study the response of tissue growth factors involved in the intestinal anastomotic repair to the teduglutide postoperative administration – **Chapter 6**;

- To assess the effects of teduglutide short-term administration on the fibrogenesis process of the intestinal anastomotic healing – **Chapter 7**.

Chapter 3

Response of putative intestinal epithelial stem cells to teduglutide on an animal model of intestinal anastomosis

This chapter was partially published as:

Costa BP, Gonçalves AC, Abrantes AM, Alves R, Matafome P, Seiça R, Sarmento-Ribeiro AB, Botelho MF, Castro-Sousa F: Intestinal epithelial stem cells: Distinct behavior after surgical injury and teduglutide administration. *J Invest Surg.* 2017;31:1-10. Doi 10.1080/08941939.2017.1294217.*

Costa BP, Sarmento-Ribeiro AB, Gonçalves AC, Botelho F, Abrantes M, Castro-Sousa F: Response of putative intestinal epithelial stem cells to surgical injury and teduglutide administration on an animal model. *Clin Nutr.* 2015;34 (Supp1):S19 (oral communication at the 37th European Society for Clinical Nutrition and Metabolism Congress, Lisbon, 2015).

*Commented on: Sipos F, Muzes G: Teduglutide-induced stem cell function in intestinal repair. *J Invest Surg.* 2017;0:1-3. Doi 10.1080/08941939.2017.1300715.

3.1. Abstract

Previous studies suggest that intestinal epithelial stem cells (IESC), critical drivers of homeostasis and regeneration, include two subpopulations: crypt-based columnar and "position +4" stem cells, identified by Lgr5 and Bmi1 biomarkers, respectively. Teduglutide is an enterotrophic long-acting counterpart of glucagon-like peptide 2. This study investigated the response of putative IESC to surgical injury and teduglutide administration on an animal model of intestinal resection and anastomosis. Wistar rats (*n*=62) were distributed into four groups: "*Ileal Resection and Anastomosis*" *versus* "*Laparotomy*", subsequently subdivided into "*Postoperative Teduglutide Administration*" *versus* "*No Treatment*"; and sacrificed at third or seventh postoperative days, with ileal sample harvesting. Flow cytometry was used to analyze IESC with monoclonal antibodies against Lgr5, Bmi1 and also CD44, CD24, CD166 and Grp78 surface markers. Surgical trauma induced an increase of putative epithelial stem cells population at third day (9.2±2.8 *vs.* 5.5±2.7%, p=0.0001), which was more intense and involved all subpopulations after ileal resection. At seventh day, teduglutide was significantly associated with higher proportion of $Lgr5^{+}/Bmi1^{-}$ cells (5.9±0.4 *vs.* 2.8±1.9%, p=0.005) and, on the contrary, lower percentage of $Lgr5^{-}/Bmi1^{+}$ cells (0.03±0.04 *vs.* 1.87±0.22%, p=0.049) after ileal resection; and higher proportion of $Lgr5^{+}/Bmi1^{+}$ cells (1.8±0.6 *vs.* 1.2±1.3 %, p=0.028) after isolated laparotomy. After surgery, $Lgr5^{+}/Bmi1^{-}$ and $Lgr5^{-}/Bmi1^{+}$ subpopulations demonstrated an inverse correlation and both correlated negatively with Grp78 labeling index. $Lgr5^{-}/Bmi1^{+}$ and $CD44^{+}/CD24^{low}/CD166^{+}/Grp78^{+}$ cells proportions exhibited a high grade positive correlation. Those observations support the existence of two epithelial stem cells subpopulations with distinct behavior after surgical injury and teduglutide treatment.

3.2. Introduction

Intestinal epithelium is one of the most dynamic sites of cell turnover, demonstrating a relevant self-renewing capacity, achieved by crypt stem cell proliferation and crypt-to-villus multilineage differentiation, which constitutes the basis of tissue homeostasis and repair (Barker, 2014; Vanuytsel *et al.*, 2013; Tesory *et al.*, 2013; Barker *et al.*, 2012). Resident stem cells located in the crypt base provide rapidly proliferating transit-amplifying cells that differentiate and give origin to all the seven cellular types of the epithelium (Barker, 2014) (Fig. 3.1).

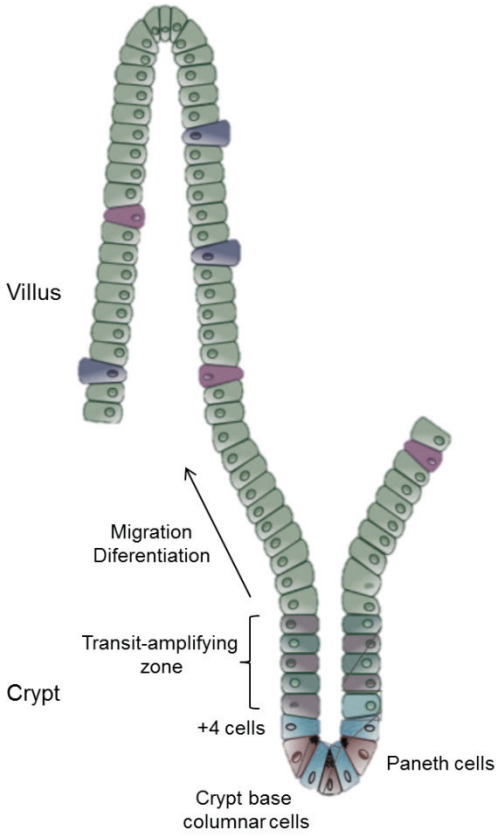

Figure 3.1. Crypt-to-villus architecture of the intestinal epithelium. Stem cells located at the crypt base (crypt base columnar and "+4" cells) provide rapidly proliferating transit-amplifying cells that differentiate and migrate up to the villus tip, where they undergo anoikis. Differentiated epithelial cells comprise enterocytes, enteroendocrine cells, goblet cells, Paneth cells, tuft cells, microfold (M) cells and cup cells. Under homeostatic conditions, transit along the crypt-villus axis takes three to five days. Paneth cells constitute an exception because they are renewed only every three to six weeks and follow a downward migratory path from the transit-amplifying compartment to the crypt bottom. Adapted from Barker N, 2014 and Smith RJ *et al.*, 2017

Recently, an unifying model of adult intestinal epithelial stem cells (IESC) emerged, considering two functionally different populations, coexisting and interconvertible, corresponding to crypt base columnar stem cells and "position +4" stem cells, respectively (Barker, 2014; Clevers, 2013; Barker *et al.*, 2012; Rizk and Barker, 2012; Yan *et al.*, 2012). Crypt base columnar cells, intercalated between Paneth cells at the base of the crypts, are considered actively cycling cells, very sensitive to canonical wingless (wnt) signaling and susceptible to radiation injury, which give origin to transit-amplifying cells on an everyday basis, ensuring the homeostatic self-renewal. "Position +4" stem cells, localized preferentially at the fourth position from the crypt base, immediately above the Paneth cells compartment, are considered slow-cycling reserve cells that guarantee injury-induced regeneration (Barker, 2014; Clevers, 2013; Barker *et al.*, 2012; Rizk and Barker, 2012; Yan *et al.*, 2012; Tian *et al.*, 2011) (Fig. 3.2).

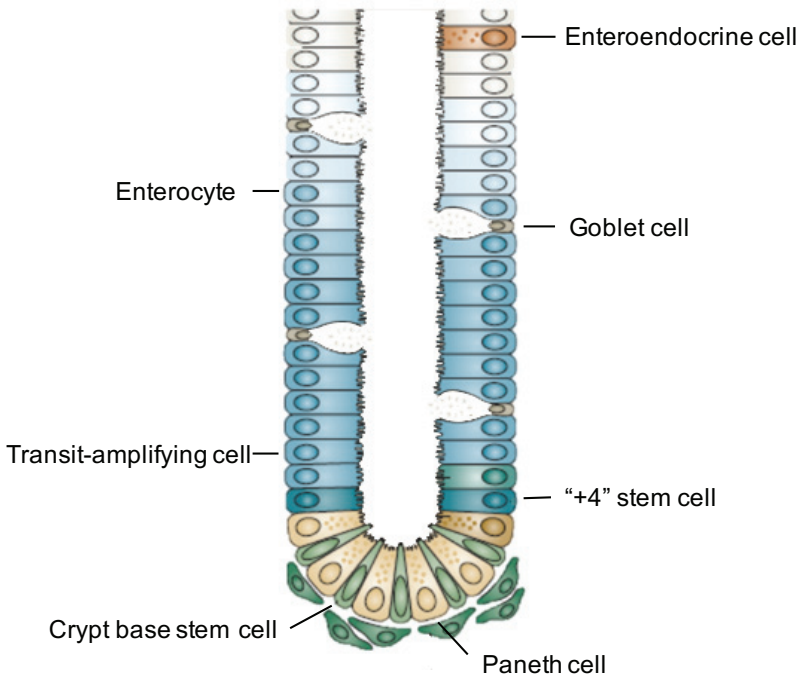

Figure 3.2. Model of adult intestinal epithelial stem cells. Two functionally different epithelial stem cells populations are considered to exist: crypt base columnar and "position +4" stem cells. Crypt base columnar stem cells, intercalated with Paneth cells at the base of the crypts, are considered actively cycling cells and continuously generate rapidly proliferating transit-amplifying cells, which subsequently differentiate into the mature lineages of the villi, ensuring the homeostatic self-renewal of the epithelium. "Position +4" stem cells, localized immediately above the Paneth cells, are considered slow-cycling reserve cells that can restore the crypt base columnar cells compartment following injury. Adapted from Barker N, 2014

Stem cells homeostasis is maintained by a neutral drift clone dynamics, guaranteed by the stem cell niche and the complex interplay among multiple signaling pathways, including wnt, hedgehog, bone morphogenic protein (bmp), notch, hippo-yap and ephB/ephrin B (Table 3.1; Fig. 3.3) (Bloemendaal *et al.*, 2016; Barker, 2014; Gracz and Magness, 2014; Vanuytsel *et al.*, 2013).

Table 3.1. Intestinal epithelial stem cell signaling pathways[a]

Signaling pathway	Upward gradient (from crypt base)	Function
Wnt	Decreasing	Most important factor in the maintenance of the self-renewing phenotype of IESC; Induction of Paneth cells differentiation; Regulation of crypt-to-villus migration (through cell-contact dependent EphB/Ephrin signaling).
Notch	Decreasing	Preservation of IESC self-renewal (in synergism with wnt); Promotion of absorptive lineage commitment through lateral inhibition (and inhibition of secretory lineage differentiation).
Hedgehog	Increasing	Sensing of the epithelial integrity; Confinement of the wnt responsive compartment to the base of crypts (through bmp4); Maturation and homing of underlying stromal cells; Modulation of the proinflammatory response.
Bmp	Increasing	Prevention of IESC overproliferation and maintenance of an undifferentiated state; Differentiation of enteroendocrine cells; Complete maturation of the secretory cell lineage.
Hippo/Yap	Increasing	Suppression of the proliferation of differentiated cells through wnt and notch inhibition (prevention of uncontrolled proliferation without differentiation)
EphB/Ephrin	Decreasing for EphB3 and EphB4; Increasing for EphB1 and EphB2	Coordination of cellular migration; Modulation of actin cytoskeleton.

Bmp, Bone morphogenic protein; Bmp4, Bone morphogenic protein 4 ligand; IESC, Intestinal epithelial stem cells; Hippo-Yap, Hippo-Yes-associated protein; Wnt, Wingles. [a] From references Bloemendaal *et al.*, 2016; Gracz and Magness, 2014; Vanuytsel *et al.*, 2012

The stem cell niche is the complex and dynamic microenvironment in which epithelial stem cells reside and that regulates its behavior during tissue homeostasis and regeneration (Smith *et al.*, 2012). The stem cell niche is constituted by epithelial and mesenchymal components, including Paneth cells, subepithelial myofibroblasts, smooth muscle cells of the *muscularis mucosa*e, lymphatic and vascular endothelial cells, bone-marrow derived stromal cells, neural cells, intraepithelial lymphocytes, extracellular matrix, mesenchymal stem cells, among others (Tesori *et al.*, 2013; Roth *et al.*, 2012). In the niche, the bidirectional dynamic regulatory network between epithelial and

mesenchymal cells includes the hedgehog, bmp and wnt pathways. Hedgehog signaling from differentiated epithelial cells induces stromal synthesis of Bmp ligands. Active Bmp signaling within epithelial cells contributes to the maintenance of the differentiated state and the reduction of proliferative activity. Production of canonical wnt ligands by Paneth and pericryptal mesenchymal cells promotes epithelial stem cells self-renewal. Secretion of Bmp antagonists by the underlying mesenchymal cells protects epithelial stem cells from the differentiation induced by bmp ligands (Smith *et al.*, 2017).

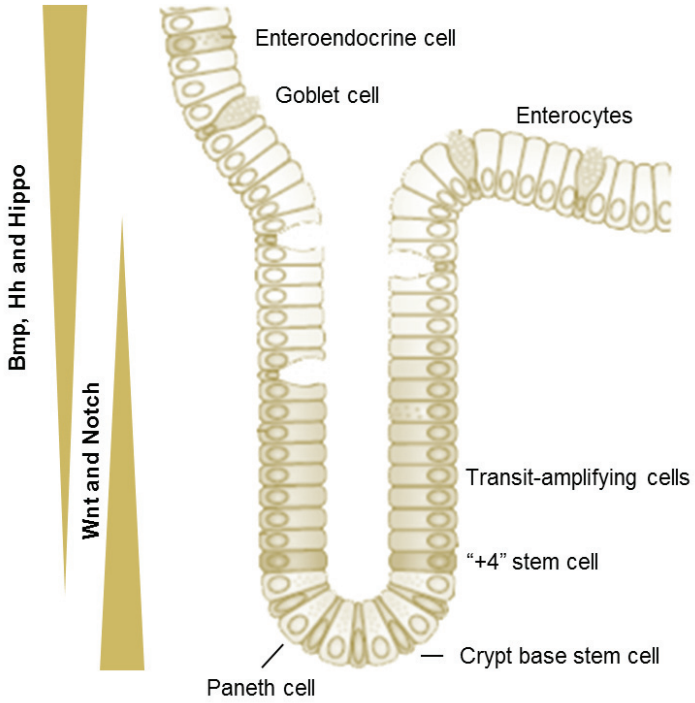

Figure 3.3. Proposed signaling pathways in the crypt-villus axis. Wingless (wnt) and notch signaling are highly active at the base of the crypts, contributing to the stem cell renewal. On the contrary, bone morphogenic protein (bmp), hedgehog (Hh) and hippo signaling are predominant at the villi, inducing differentiation, and their activity decrease towards the crypts. Hh signaling from the differentiated epithelial cells induces the synthesis of bmp ligands in the mesenchymal cells, in a paracrine way, which contribute to the maintenance of the differentiated state and to the inhibition of proliferation. Production of wnt ligands by Paneth cells and pericryptal mesenchymal cells promotes epithelial stem cells self-renewal and induces the Paneth cells differentiation. Secretion of bmp antagonists by the underlying pericryptal mesenchymal cells protects epithelial stem cells from the differentiation induced by bmp ligands. Adapted from Bloemendaal ALA *et al.*, 2016 and Smith RJ *et al.*, 2017

According to genetic marking and lineage tracing studies, leucine-rich repeat-containing G-protein coupled receptor 5 (*Lgr5*/*Gpr49*) and B-cell-specific Moloney

murine leukemia virus insertion site 1 (*Bmi1*) seem to be markers that identify the two functionally different intestinal epithelial stem cells (Yan *et al.*, 2012).

Lgr5 is a wnt/β-catenin target gene that encodes an orphan G-protein coupled receptor for the wnt agonists roof plate-specific spondins (R-spondins) 1 to 4 (Barker, 2014; Clevers, 2013; Tesori *et al.*, 2013; Kemper *et al.*, 2012; Barker *et al.*, 2012). Lgr5 has been considered a specific marker of crypt base columnar epithelial stem cells (Barker *et al.*, 2012; Barker, 2010; Sato *et al.*, 2009; Barker *et al.*, 2007).

Bmi1 is a polycomb ring finger oncogene that encrypt a polycomb group protein, component of the transcriptional polycomb repressive complex 1, considered to be involved in the modulation of the stem cell self-renewal, pluripotency and lineage specification in several tissues (Barker *et al.*, 2012; Rajasekhar *et al.*, 2007). *Bmi1* is the most widely recognized marker of "position +4" intestinal epithelial stem cells (Rizk and Barker, 2012; Sangiorgi *et al.*, 2008). Nevertheless, specificity of *Bmi1*, as well as that of other proposed markers of "position +4" epithelial stem cells such as *Tert*, *Hopx* and *Lrig1*, has been challenged by the expression analysis with single-molecule *in situ* hybridization techniques (Koo *et al.*, 2014; Clevers, 2013;).

Teduglutide is a long-acting counterpart of glucagon-like peptide 2 (GLP-2), which is a relatively specific gastrointestinal growth factor crucial for the maintenance of intestinal mucosa morphology, function and integrity (Drucker and Yusta B, 2014; Burness and McCormak, 2013).

Regeneration of the epithelial architecture after the intestinal disruption triggered by surgical resection and anastomosis is based on a wound repair process that includes restitution, crypt stem cell proliferation and differentiation, and crypt fission (Bloemendaal *et al.*, 2016; Rijcken *et al.*, 2014; Iszuka *et al.*, 2011). Influence of teduglutide on crypt base columnar and "position +4" stem cells dynamics in the perioperative context of intestinal resection is not yet well understood.

This study aimed to analyze the response of putative intestinal epithelial stem cells to surgical injury and teduglutide short-term administration on an animal model of intestinal resection and anastomosis.

3.3. Methods

3.3.1. Ethical statement

Study protocol was approved by the institution's Ethics Committee (Official Letter nº 32-06-09) and was implemented in consonance with the institutional and national guidelines respecting animals' protection in experimental research. Experiment was conducted according to the "Animal Research: Reporting in Vivo Experiments" (ARRIVE) guidelines (Kilkenny *et al.*, 2010a; Kilkenny *et al.*, 2010b).

3.3.2. Animals

Adult male Wistar *albinus* rats (Rattus *norvegicus albinus*) weighting 250 to 300 g were acclimatized to the laboratory environment for five days before the experimental study, kept in temperature (22±1°C) and humidity (50±10%) controlled ventilated cages, with light/dark cycles of 12 hours, and maintained on water and standard rodent diet (5L79 Purina rat and mouse 18% chow; Charles River Laboratories, Wilmington, Massachusetts, USA) *ad libitum*. Animals were supplied by the animal colony of the Laboratory for Experimental Research of the Faculty of Medicine, University of Coimbra, Coimbra, Portugal.

3.3.3. Study Design

Rats were randomly assigned into four different experimental groups: (1) "*Res Ted* +", (2) "*Res Ted* –", (3) "*Lap Ted* +" and (4) "*Lap Ted* –". Group "*Res Ted* +" rats were submitted to standard ileal resection and anastomosis (*Res*), teduglutide postoperative administration (*Ted*) and sacrifice at the third or seventh day, respectively (two subgroups) (Fig. 3.4). In group "*Lap Ted* +", a laparotomy was performed (*Lap*; without resection), teduglutide was administered and sacrifice occurred at the third or seventh day, respectively (two subgroups). Group "*Res Ted* –" rats were subjected to intestinal resection and anastomosis, and were sacrificed at the third or seventh postoperative days, respectively (two subgroups). Finally, in group "*Lap Ted* –", laparotomy was

performed and sacrifice occurred at the third or seventh days, respectively (two subgroups). "*Lap*" and "*Ted -*" groups were considered controls. Expected number of animals to be involved in the study corresponded to approximately eight for each subgroup.

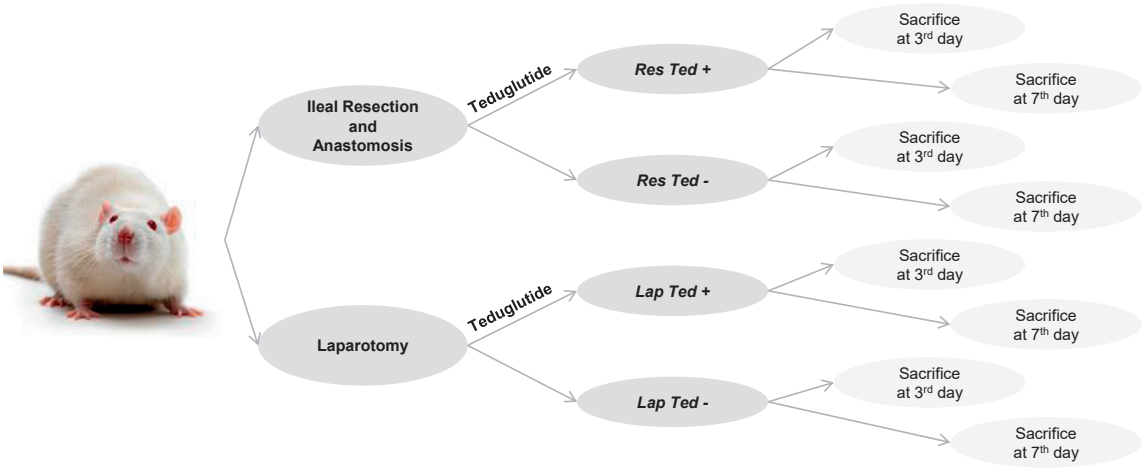

Figure 3.4. Study design. Adult male Wistar *albinus* rats were randomly distributed into four groups: "*Ileal Resection and Anastomosis*" ("*Res*") *versus* "*Laparotomy*" ("*Lap*"), each one splited into "*Postoperative Teduglutide Administration*" ("*Ted +*") *versus* "*No Treatment*" ("*Ted -*"). Evaluation was performed at the moments of the operation and sacrifice, at the third or seventh postoperative days (eight subgroups), with ileal segment harvesting and blood collection. Tissue baseline values of "*Ileal Resection and Anastomosis*" groups were considered for comparison with postoperative results of the "*Laparotomy*" groups; tissue samples recovered at the sacrifice in these animals corresponded to the perianastomotic segments.

3.3.4. Operative Procedures

All the operative procedures were accomplished by the same investigator after a period of two hours solid fasting (water was never restricted), with clean surgical technique, under anesthesia with intraperitoneal injection of a combination of ketamine hydrochloride (75 mg/kg; Pfizer Inc., New York, USA) and chlorpromazine (3 mg/kg; Laboratórios Vitória, Amadora, Portugal).

In "*Res*" groups, a 10-cm length ileal resection was performed, preserving distal 5 cm, after a 3-cm midline laparotomy. Continuity was reestablished by a standardized end-to-end anastomosis with eight equidistant full-thickness polydioxanone United States Pharmacopeia (USP) 6/0 stitches (PDS II; Ethicon, Johnson-Johnson Intl, Cincinnati,

USA). Abdominal wall was closed with two running sutures (muscle-aponeurotic and cutaneous) of braided coated polyglactin 910 USP 4/0 (Surgilactin, Sutures Limited, Wrexham, UK) and natural silk USP 4/0 (Surgisilk, Sutures Limited, Wrexham, UK), respectively. In "*Lap*" groups, a 3-cm midline laparotomy (without resection) was performed, with mild manipulation of the small-bowel. In the first postoperative day, ingestion was restricted to water with 5% glucose (at a 1:1 ratio) and, then, *ad libitum* oral hydration and chow were reassumed.

Rats were monitored on a daily basis throughout the entire length of the experiment. Quotidian evaluation included the activity grade, sleep patterns, food and water ingestion, elimination and other. Operative morbidity and mortality were recorded. A daily health score of the animals was calculated, as described previously by van Landeghem L *et al* (Van Landeghem *et al.*, 2012a), by the sum of points attributed by the four following parameters: activity (active = 1 and stationary = 0), posture (normal = 1 and hunched = 0), pelage (normal grooming, smooth and healthy-looking fur = 1 and lack of grooming and rough fur = 0) and dehydration (none = 1 and dehydrated = 0; dehydration was tested by gently raising a small piece of dorsal skin and was considered to be present if the skin stayed up in a tent or only slowly retracted back to normal shape). Overall health score, ranging from "0" to "4", was determined every day during the three or seven day-time courses following the operation (according to the study groups). Any rat assigned an overall health score of "0" was euthanized in accordance with the protocol. Survival data corresponded to those animals that did not fulfilled the health score criteria for euthanasia.

At the third or the seventh postoperative days, animals were sacrificed by cervical displacement and subjected to relaparotomy with ileal resection (10-cm length, retaining distal 3 cm). During relaparotomy, the peritoneal cavity was carefully inspected.

3.3.5. Drug regimen

In "*Ted* +" groups, teduglutide (American Peptide Company, Sunnyvale, California, USA) was administered subcutaneously during the postoperative period (from the

operation day) at 200 μg/kg body weight *per* day, diluted in 0.25 ml phosphate buffered saline pH 7.4 (PBS pH 7.4, Gibco, Life Technologies, Carlsbad, California, USA) after reconstitution in agreement with the manufacturer's recommendations.

Teduglutide, [Gly2]GLP-2 peptide, was purchased in a lyophilized form. Purity of the product was 98.8% (as confirmed by high performance liquid chromatography and mass spectral analysis), molecular weight was 3752.1 Da and the white lyophilized powder contained 91.8% of peptide. Lyophilized peptide was stored in a freezer at -20°C under dry conditions for maximum stability and was warmed to room temperature prior to opening and dissolving. Necessary amount of peptide for the day was aliquoted, the vial was resealed tightly and the remaining was stored at -20°C. Peptide was dissolved in 5% ammonium hydroxide in water to a concentration of 1 mg/ml and the product was then diluted with phosphate buffered saline pH 7.4.

3.3.6. Tissue sampling

In "*Res*" groups, a 10-cm length ileal segment was carefully removed, opened at the mesenteric side, gently rinsed with normal saline solution and divided in four samples: one, the most distal, with 4 cm and three, with 2 cm. First 4-cm length ileal fragment was split into three similar longitudinal strips (each one corresponding to one third of the circumference) that were immediately subjected to further processing: tissue dissociation and cell separation procedures (for cellular characterization by flow cytometry, in this study), homogenization (for determination of tissue levels of cytokines by flow cytometric bead assay and for quantitative real-time reverse-transcription polymerase chain reaction - qRT-PCR), and fixation with 10% formaldehyde (Sigma-Aldrich, Sintra, Portugal) followed by paraffinization (for histological examination), respectively. Other three contiguous ileal specimens were retrieved and prepared for subsequent studies: one fixed in 10% formaldehyde for histological examination; one placed in a cryotube, frozen in liquid nitrogen and stored at -80°C; and the remaining preserved in RNA-*later* (Sigma-Aldrich, Sintra, Portugal), respectively and successively (Fig. 3.5 A). Samples for molecular studies were weighted

on a high-precision digital scale (Kern 770 Electronic Analytical Balance; Kern & Sohn GmbH, Ziegrlei, Balinger, Germany).

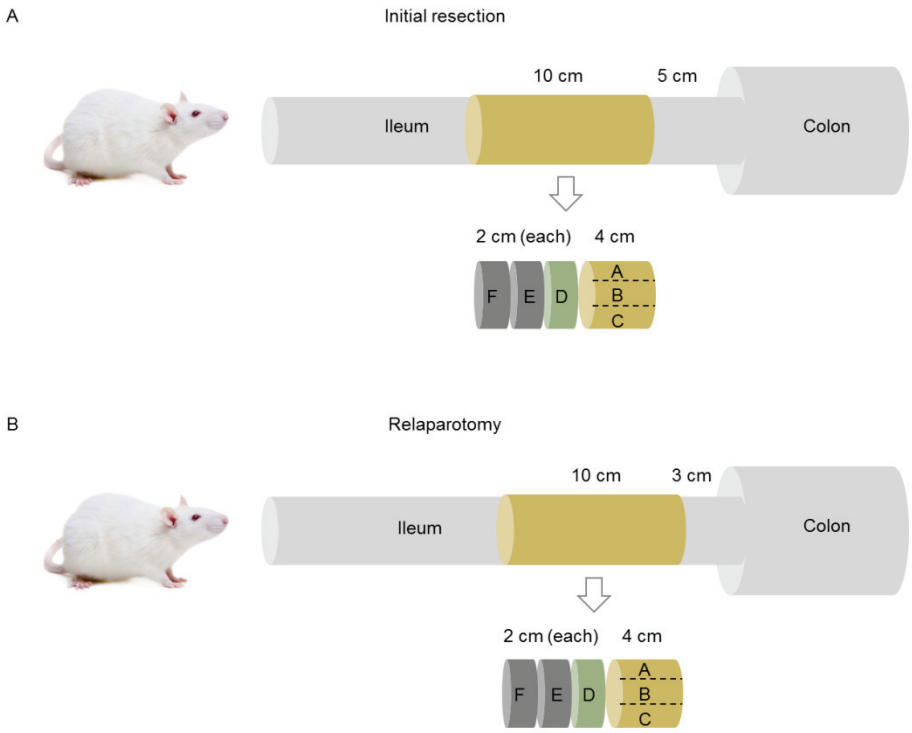

Figure 3.5. Tissue harvesting. A. Initial resection. A 10-cm length ileal resection was performed with preservation of distal 5 cm. Four contiguous ileal segments were recovered: one with 4-cm and three 2-cm length. Most distal sample was divided into three longitudinal strips for histological examination (A) and molecular studies (flow cytometry and qRT-PCR) (B and C); the other three contiguous specimens were prepared, fixed in 10% formaldehyde for histological examination (D), frozen in liquid nitrogen and stored at -80˚C (E), and preserved in RNA-*later* (F), respectively. **B. Relaparotomy.** A 10-cm ileal resection retaining distal 3 cm was undertaken. Four contiguous ileal segments (one with 4-cm and three 2-cm length) were retrieved. Most distal ileal sample, with the anastomosis in the middle, was divided into three longitudinal sections for histological examination (A) and molecular studies (flow cytometry and qRT-PCR) (B and C); the other three contiguous specimens were prepared, fixed in 10% formaldehyde for histological examination (D), frozen in liquid nitrogen and stored at -80˚C (E), and preserved in RNA-*later* (F), respectively.

In all groups, during relaparotomy, the procedure was analogous to the previously described (Fig. 3.5 B). In "*Res*" groups, distal samples recovered at the sacrifice corresponded to the anastomotic segment and included the anastomosis in the

middle. Tissue baseline values of "*Res*" groups were considered for comparison with postoperative results of the "*Lap*" group.

3.3.7. Intestinal tissue dissociation and cell separation procedure

Cells were isolated from one ileal longitudinal strip, immediately after excision, by a standardized adaptation of the collagenase/dispase isolation technique outlined by Evans GS *et al* (Evans *et al.*, 1992) and Dekaney CM *et al* (Dekaney *et al.*, 2007; Dekaney *et al.*, 2005), to obtain a cellular population predominantly constituted of epithelial and some stromal cells.

Summarily, the ileal sample was cleaned of mesentery, flushed with Hank's balanced salt solution (HBSS, Gibco, Life Technologies, Carlsbad, California, USA), cut into pieces of approximately 3 mm length and washed six times in 10 ml of HBSS on an orbital shaker (80 cycles/minute). Fragments were cut into 1 mm pieces and shaken vigorously in HBSS containing 2 ml of enzyme solution, on a shaking platform, for 25 minutes at room temperature. Enzyme solution contained 0.1 mg/ml of dispase type II (Gibco, Life Technologies) and 5 mg/ml of collagenase type IV (Gibco, Life Technologies) in HBSS.

Digested tissue was further disaggregated by vigorous up and down hand pipetting for five minutes, transferred to a conical tube and allowed to sediment under gravity for one minute; then, the supernatant was removed into a new tube and sedimentation was repeated twice. Subsequently, 4 ml of Dulbecco's Modified Eagle's Medium (DMEM) in fetal bovine serum 10% (DMEM 10%) (Gibco, Life Technologies) was added to supernatant, mixed and spin at 470x *g* for three minutes. Pellet was collected, resuspended in 4 ml of DMEN 10% and the procedure was repeated once. Cell pellets were combined in DMEN 10% and passed through a 70 μm filter to obtain a single cells suspension. Isolated cells in phosphate buffered saline (PBS, pH 7.4, Gibco, Life Technologies) were centrifuged at 1000x *g*, at room temperature, for five minutes, resuspended in 500 μl of PBS and distributed for ten different tubes for flow cytometry (50 μl/vial). Three vials were used for multiparameter flow cytometry

cellular immunophenotyping and the remaining for additional studies (four for oxidative stress study and one for cell viability and death evaluation).

3.3.8. Multiparameter flow cytometry cellular phenotyping

Characterization of the isolated cells from rats' ileum was performed by multicolor flow cytometry. Single cells suspensions were stained with monoclonal antibodies directed against cell surface markers using a direct immunofluorescence technique, following the manufacturer's instructions.

Identification of the putative epithelial stem cell populations was accomplished with the cell surface markers Lgr5 and Bmi1 (Barker *et al.*, 2014), markers of crypt base columnar and "position +4" stem cells, respectively. Epithelial stem cells population ($Lgr5^+$ and/or $Bmi1^+$ cells) was considered to include three fractions: $Lgr5^+/Bmi1^-$ [corresponding presumably to crypt base columnar stem cells (Barker *et al.*, 2012; Yan *et al.*, 2012; Sato *et al.*, 2009; Barker *et al.*, 2007)], $Lgr5^-/Bmi1^+$ [representing possibly putative "position +4" stem cells (Barker *et al.*, 2012; Rizk and Barker, 2012; Yan *et al.*, 2012; Sangiorgi *et al.*, 2008)] and $Lgr5^+/Bmi1^+$ (double positive) cells.

Additionally, putative intestinal epithelial stem cells were studied with a combination of CD44, CD24, CD166 and Grp78 surface markers according to Wang F *et al* (Wang *et al.*, 2013) (Fig. 3.6). These authors proposed the use of $CD44^+/CD24^{low}/CD166^+/Grp78^{-/low}$ and $CD44^+/CD24^{low}/CD166^+/Grp78^+$ combinations to identify putative epithelial stem cells and transit-amplifying cells, respectively (Wang *et al.*, 2013). Cytokeratin 18 (CK18), CD31 and CD45 surface markers were used to recognize the epithelial, endothelial and hematopoietic cellular differentiations, respectively; vimentin, α-smooth muscle actin (α-Sma) and desmin markers were used to label mesenchymal cells (Rekhtman and Bishop, 2011). Main characteristics of the stem cell surface markers and references of the monoclonal antibodies used in present study were included in Supplementary Tables S2 and S3, respectively. The flow cytometry panel used is represented in Supplementary Table S4. Antibodies combinations included: Anti-Lgr5 / Anti-Bmi1 + Anti-goat IgG Phycoerythrin (PE) / Anti-CD45 / Anti-CD31; Anti-desmin / Anti-CK18 / Anti-α-Sma + Goat anti-rabbit

IgG-Peridinin cholorophyll protein complex with cyanin-5.5 (PerCP-Cy5.5) / Anti-vimentin; Anti-78 KDa glucose-regulated protein (anti-Grp78) / Anti-CD166+Anti-goat IgG PE / Anti-CD24 / Anti-CD44.

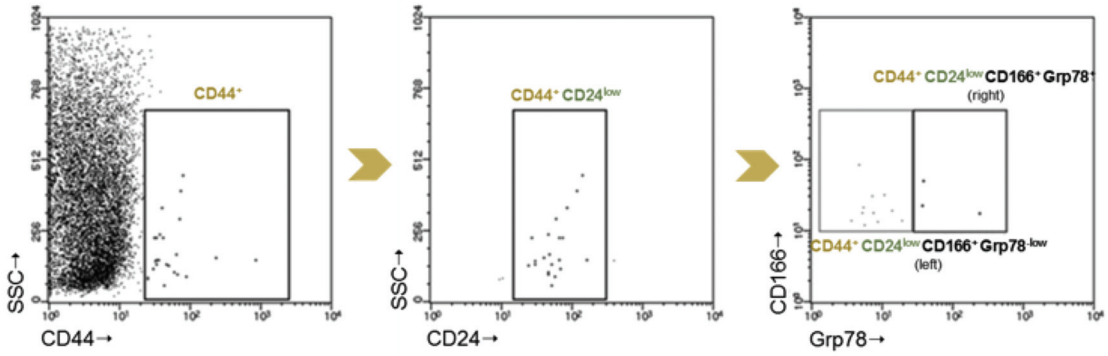

Figure 3.6. Fluorescence-activated cell sorting (FACS) strategy. Method for sequentially gating putative intestinal epithelial stem cells using CD44, CD24, CD166 and Grp78 surface markers, after intestinal tissue dissociation and cell separation procedures, as previous description of Wang *et al.* (Wang *et al.*, 2013). According to these authors, CD44 and CD24 markers may be used to select epithelial crypt cells and to exclude fractional differentiated cells in the lower crypt, respectively; combination of CD44, CD24 and CD166 may further exclude differentiated cells from the villi and crypts. The use of $CD44^{+}/CD24^{low}/CD166^{+}/Grp78^{-/low}$ and $CD44^{+}/CD24^{low}/CD166^{+}/Grp78^{+}$ combinations was proposed to identify putative epithelial stem cells and transit-amplifying cells, respectively. $CD44^{+}/CD24^{hi}/CD166^{+}$ fraction may correspond to secretory cells in the lower region of crypts as result of the high expression of CD24 and CD166 in that location (Wang *et al.*, 2013)

Isolated cells were resuspended in the staining medium at a concentration of one million of cells *per* 100 µl *per* tube and incubated with 0.5 µg of monoclonal antibodies according to the supplyer' concentrations, for 15 minutes, at room temperature, in the absence of light. Next, cells were incubated with 2 ml of lysis buffer (BD BioSciences, San Jose, California, USA) for 10 minutes, at room temperature, in the dark. Then, cells were washed with PBS pH 7.4 (Gibco, Life Technologies) by centrifugation at 300x *g* for five minutes and resuspended in 400 µl of that buffer solution. A similar process was followed for the secondary antibody staining.

Cells analysis and data acquisition were performed using a six-parameter, four-color, FACSCalibur flow cytometer (Becton Dickinson, San Jose, California, USA) and the CellQuest software (version 0.3, BD BioSciences, San Jose, California, USA). For each

sample, 5 x 10^4 events *per* tube were acquired. Results were analyzed and quantified using the Paint-a-Gate 3.02 program (BD BioSciences). Experiments were carried out in duplicate. Results were expressed in terms of percentage (%) of positive cells expressing each protein.

3.3.9. Statistical analysis

Statistical analysis was performed using the Statistical Package for Social Sciences (SPSS) version 18 software package (SPSS, Chicago, Illinois, USA). Type of distribution of variables was determined using Shapiro-Wilk and Kolmogorov-Smirnov-Lillifors tests. Data were indicated as medians and interquartile ranges (median ± IQR) or numbers (%). Non-parametric continuous variables were compared by Mann-Whitney U test, Wilcoxon matched pairs test, and analysis of variance by ranks (Kruskall-Wallis test) with pairwise comparisons (for comparisons across multiple groups). Correlations were determined by the Spearman's rank correlation coefficient (σ). Categorical variables were compared by Qui-square test. Differences were considered statistically significant at a level of 95% ($p<0.05$).

3.4. Results

3.4.1. Animals' postoperative course

Sixty-two animals were studied. There were two cases of mortality associated with anastomotic leakage (in "*Res Ted* -" and "*Res Ted* +" groups, respectively) and one of indeterminate etiology (in "*Res Ted* -" group), that were excluded from further analysis.

Fifty-nine animals completed the study and were included into the following groups: "*Res Ted* +" (15, eight of them sacrificed on the third day), "*Res Ted* –" (13, five sacrificed at third day), "*Lap Ted* +" (16, eight sacrificed on the third day) and "*Lap Ted* -" (15, seven sacrificed at third day) (Fig. 3.7).

Morbidity included one case of small scurf at the teduglutide injection site. Postoperative daily health score used by van Landeghem L *et al* (van Landeghem *et al.*, 2012a) amounted to four points in all animals except in the cases of mortality at day of death (two points).

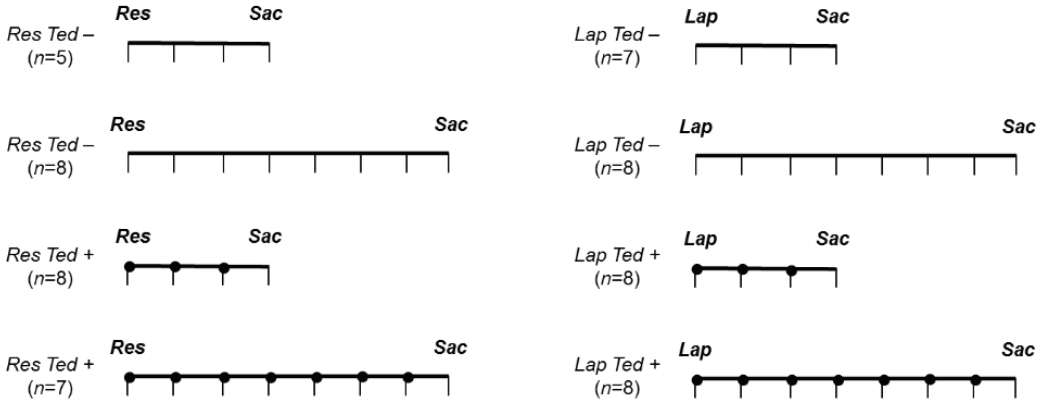

Figure 3.7. Distribution of the animals for the study groups. Adult male Wistar *albinus* rats were randomly allocated into four groups: "*Ileal Resection and Anastomosis*" ("*Res*") *versus* "*Laparotomy*" ("*Lap*"), each one subdivided into "*Postoperative Teduglutide Administration*" ("*Ted +*") *versus* "*No Treatment*" ("*Ted -*"). Evaluation was accomplished at the moments of the operation and sacrifice (*Sac*), at the third or seventh postoperative days (eight subgroups), with ileal segment harvesting and blood collection. Tissue baseline values of "*Ileal Resection and Anastomosis*" groups were considered for comparison with postoperative results of the "*Laparotomy*" groups; tissue samples recovered at the sacrifice in those animals corresponded to the peri-anastomotic segments.

3.4.2. Flow cytometry expression profile of cells isolated from rats' ileum at the baseline

In the flow cytometry analysis of rats' small intestine preparations derived from the initial ileal resection, surface markers of epithelial ($CK18^+$), mesenchymal ($vimentin^+$), smooth muscle ($desmin^+$) and hematopoietic ($CD45^+$) differentiation were demonstrated in 23.5±12.3 (18.7-49.7)%, 16.2±5.9 (11.7-21.6)%, 16.7±1.3 (9.3-19)% and 6.2±4.2 (1.9-16.9)% of isolated cells, respectively (Supplementary Figure S1).

Lgr5 and Bmi1 surface cell markers were expressed in 3.5±1.5 (2.1-5.5)% and 3.2±2.5 (1.2-5.9)% of all cells, respectively; nearly 26.7% of $Lgr5^+$ cells coexpressed the Bmi1

marker. In basal conditions, putative epithelial stem cells ($Lgr5^+$ and/or $Bmi1^+$ cells) amounted to 5.5±2.7 (3.1-9.7)%; approximately 48.7% of them were $Lgr5^+/Bmi1^-$, 34.5% $Lgr5^-/Bmi1^+$ and the remaining exhibited overlapping expression of those biomarkers.

3.4.3. Putative epithelial stem cells response to surgical injury

Surgical trauma induced a significant expansion of putative epithelial stem cells population ($Lgr5^+$ and/or $Bmi1^+$) at the third postoperative day (9.2±2.8 *vs.* 5.5±2.7%, p=0.0001), with normalization at the seventh. That response was significantly more intense after ileal resection, in comparison with isolated laparotomy (10.9±1.2 *vs.* 7.9±2.2%, p=0.036), and involved all the three subpopulations (predominantly $Lgr5^-/Bmi1^+$ cells), including $Lgr5^+/Bmi1^-$ cells that did not suffer any increase after laparotomy (Fig. 3.8-3.9).

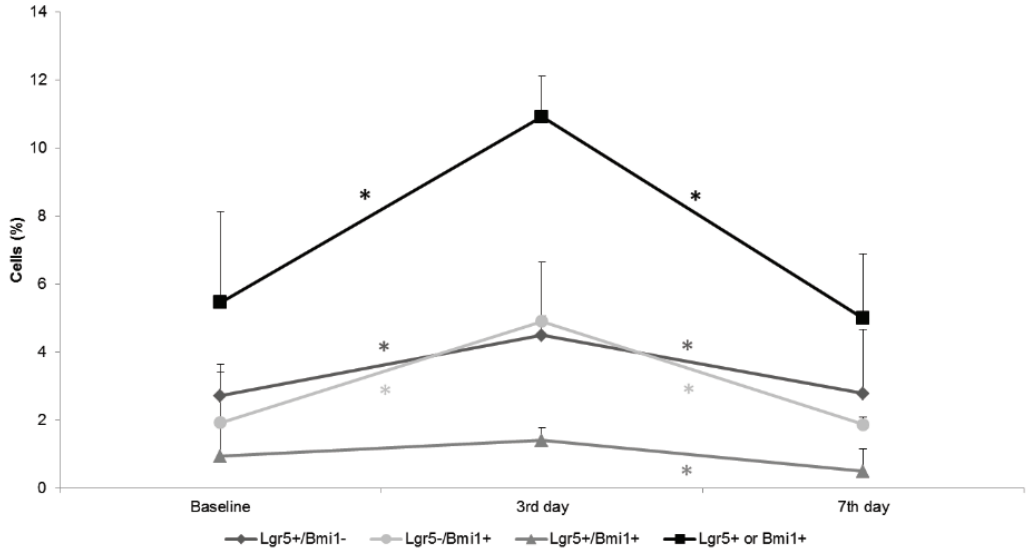

Figure 3.8. Evolution of epithelial stem cell markers expression after ileal resection. Putative intestinal epithelial stem cell markers (Lgr5 and Bmi1) expression, in cells isolated from rats' ileum, at third and seventh days after ileal resection and anastomosis, in animals not submitted to teduglutide administration (n=13), as detected by flow cytometry. Samples recovered at sacrifice corresponded to the anastomotic segment. Data were expressed as percentage of cells expressing the marker (median±interquartile range). * p<0.05

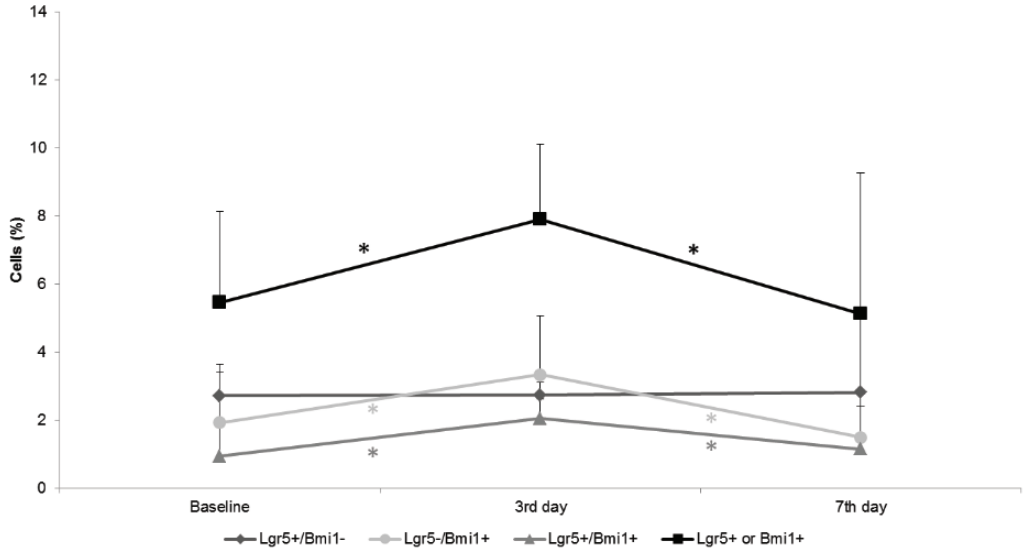

Figure 3.9. Evolution of epithelial stem cell markers expression after laparotomy. Putative intestinal epithelial stem cell markers (Lgr5 and Bmi1) expression, in cells isolated from rats' ileum, at third and seventh days after laparotomy, in animals not submitted to teduglutide administration (n=15), as detected by flow cytometry. Baseline values of rats submitted to ileal resection (n=13) were considered for comparison. Data were expressed as percentage of cells expressing the marker (median±interquartile range). * p<0.05

3.4.4. Putative epithelial stem cells response to teduglutide administration

After ileal resection and anastomosis, teduglutide administration was significantly associated with higher proportion of $Lgr5^+/Bmi1^-$ cells at the seventh day (5.9±0.4 *vs.* 2.8±1.9%, p=0.005) and lower percentage of $Lgr5^-/Bmi1^+$ cells at both moments (0.05±0.03 *vs.* 4.91±0.28%, p=0.003 at the third day; 0.03±0.04 *vs.* 1.87±0.22%, p=0.049 at the seventh day; Fig. 3.10-3.11). After isolated laparotomy, higher percentage of $Lgr5^+/Bmi1^+$ cells was observed in teduglutide-treated animals at the seventh day (1.8±0.6 *vs.* 1.2±1.3 %, p=0.028; Fig. 3.11). After laparotomy alone, teduglutide treatment was not associated with relevant modifications of the $Lgr5^+/Bmi1^-$ subpopulation.

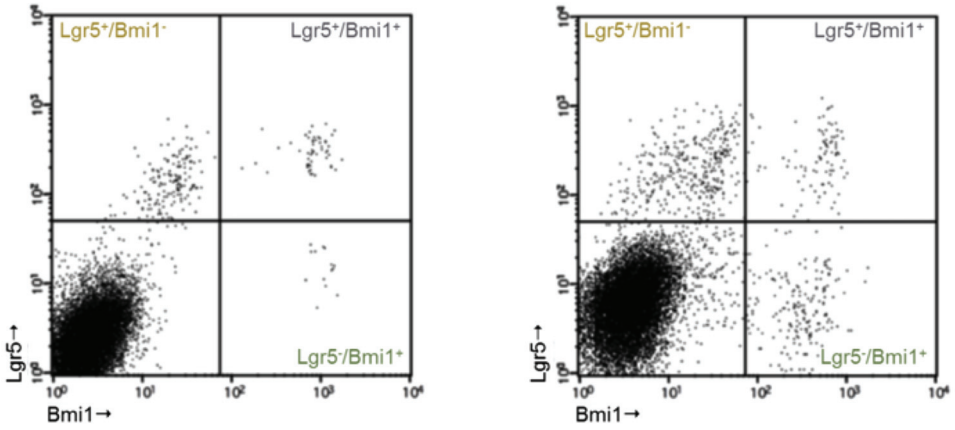

Figure 3.10. Dot plots. Representative dot plots of flow cytometry analysis of cells isolated from the ileum of a teduglutide-treated rat, at the baseline (*left*) and at the third day after intestinal resection and anastomosis (*right*), demonstrating the expression pattern of Lgr5 and Bmi1 surface markers. An increase of the proportion of $Lgr5^+$ and/or $Bmi1^+$ cells and of the $Lgr5^+/Bmi1^-$, $Lgr5^-/Bmi1^+$ and $Lgr5^+/Bmi1^+$ fractions was observed at the third day in comparison with baseline

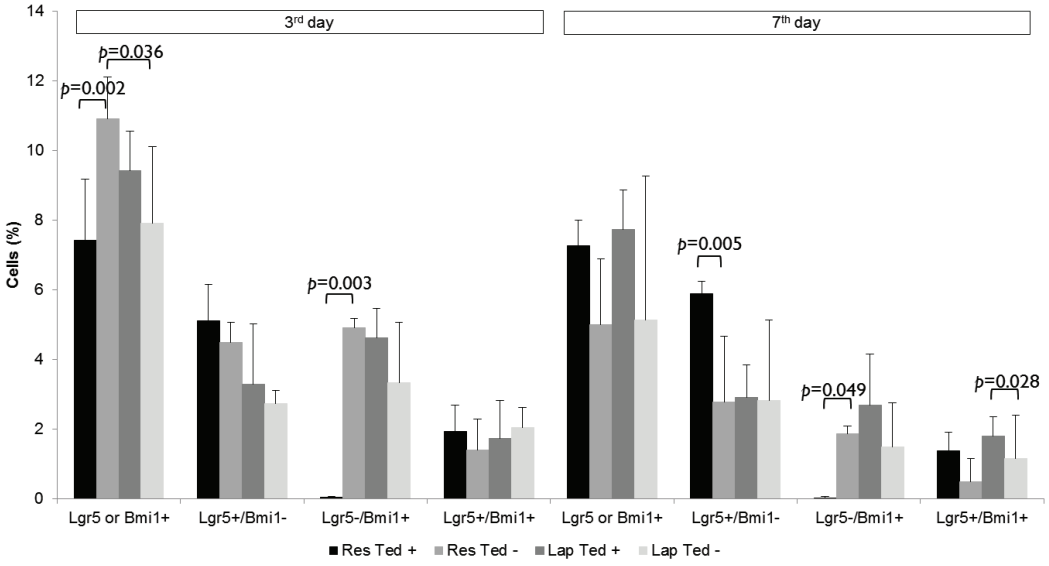

Figure 3.11. Expression of epithelial stem cells markers in the different groups of study. Expression of putative intestinal epithelial stem cell markers in cells isolated from rats' ileum, at third and seventh postoperative days, in the different study groups (n=59), as detected by flow cytometry analysis. Results were presented in percentage (%) of cells expressing the specific marker and corresponded to the median (±interquartile range) of each represented group. Kruskall-Wallis test was used for comparisons. *"Res"*, Ileal Resection; *"Lap"*, Laparotomy; *"Ted +"*, With postoperative teduglutide administration; *"Ted -"*, Without teduglutide administration

Considering all the studied animals (*n*=59), teduglutide postoperative administration was significantly associated with an enrichment of putative intestinal epithelial stem cells population at the seventh day after the operation (7.4±1.1 *vs.* 5±3.4%, *p*=0.0001); higher proportion of $Lgr5^{+}/Bmi1^{-}$ cells (3.8±3.1 *vs.* 2.8±1.8%, *p*=0.015) and $Lgr5^{+}/Bmi1^{+}$ cells (1.5±0.7 *vs.* 0.8±1.1%, *p*=0.001) was also observed at that time point (Fig. 3.12).

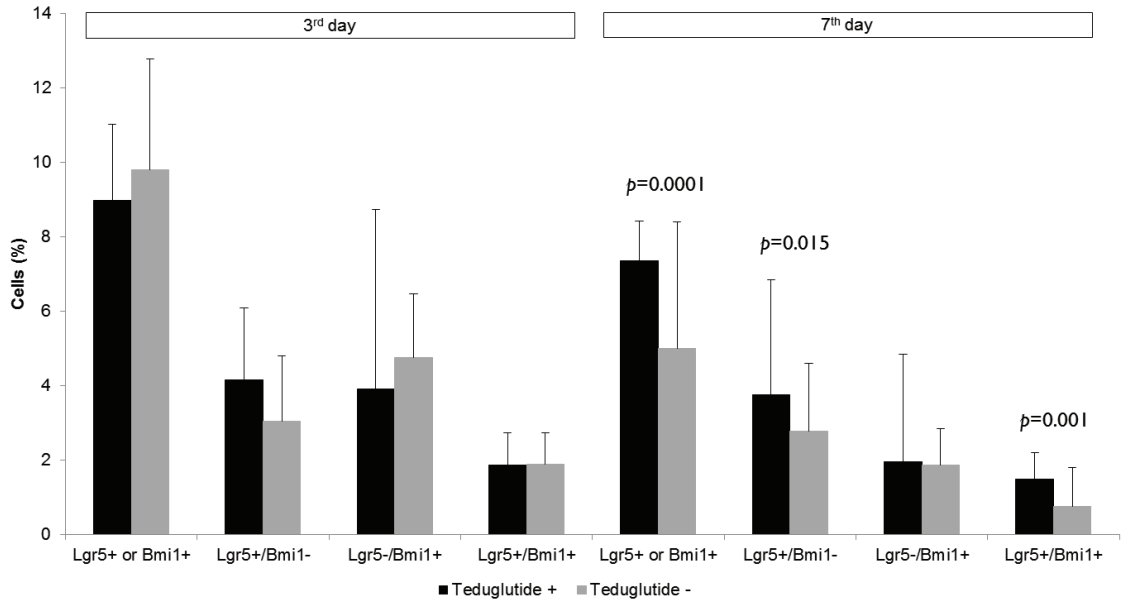

Figure 3.12. Expression of putative epithelial stem cells markers after surgery (ileal resection or isolated laparotomy). Expression profile of cells isolated from rats' ileum, at third and seventh postoperative days, after ileal resection and isolated laparotomy, according to the teduglutide administration in all groups (*n*=59), as detected by flow cytometry analysis. Results were presented in percentage (%) of cells expressing the specific marker (median±interquartile range). Mann-Whitney U test was used for comparisons. *"Teduglutide +",* With postoperative teduglutide administration; *"Teduglutide -",* Without teduglutide administration

3.4.5. Correlations profile of putative epithelial stem cells at the moment of sacrifice

After the operation, at the moment of sacrifice, putative epithelial stem cells pool ($Lgr5^{+}$ and/or $Bmi1^{+}$ cells) correlated mainly with $Lgr5^{-}/Bmi1^{+}$ fraction (σ=74.6%,

p=0.0001; Table 3.2). Moreover, at that moment, $Lgr5^+/Bmi1^-$ and $Lgr5^-/Bmi1^+$ subpopulations correlated inversely (σ=-30.4%, p=0.019), contrary to the observed in basal condition (σ=52.1%, p=0.003); particularly after ileal resection (σ=-69%, p=0.0001) and teduglutide administration (σ=-71.9%, p=0.0001). $Lgr5^+/Bmi1^-$ and $Lgr5^-/Bmi1^+$ fractions correlated negatively with Grp78 labeling index. $Lgr5^-/Bmi1^+$ and $CD44^+/CD24^{low}/CD166^+/Grp78^+$ cells proportions demonstrated a significant and high-grade correlation (σ=87.1%, p=0.0001) in the postoperative period. $CD44^+/CD24^{low}/CD166^+/Grp78^{-/low}$ cells did not correlated significantly with $Lgr5^+$, $Bmi1^+$ and $Lgr5^+/Bmi1^-$ fractions, demonstrating only a low grade correlation with $Lgr5^-/Bmi1^+$ and $Lgr5^+/Bmi1^+$ cells.

Table 3.2. Correlations between the proportion of putative epithelial stem cells at the moment of sacrifice[a]

(σ / p)	$Lgr5^+/Bmi1^-$ cells	$Lgr5^-/Bmi1^+$ cells	$Lgr5^+/Bmi1^+$ cells	$Lgr5^+$ or $Bmi1^+$ cells
$Lgr5^+/Bmi1^-$ cells		-30.4% p=0.019		
$Lgr5^-/Bmi1^+$ cells	-30.4% p=0.019		31.4% p=0.016	74.6% p=0.0001
$Lgr5^+/Bmi1^+$ cells		31.4% p=0.016		56.7% p=0.0001
$CD44^+/CD24^{low}/CD166^+/Grp78^{-/low}$ cells		26.9% p=0.039	39.6% p=0.002	31.6% p=0.015
$CD44^+/CD24^{low}/CD166^+/Grp78^+$ cells		87.1% p=0.0001	38.8% p=0.002	70.8% p=0.0001
$Grp78^+$ cells	-37.7% p=0.003	-43.7% p=0.001		-37.5% p=0.003

[a] Relevant correlations between the proportion of putative epithelial stem cells isolated from rats' ileum, at the moment of sacrifice, in all the studied animals (n=59), as determined by flow cytometry. Samples recovered at sacrifice in rats submitted to ileal resection corresponded to the anastomotic segment. Spearman's correlation coefficent (σ) and value of significance (p) were presented

3.5. Discussion

Intestinal epithelial stem cells have been characterized mainly by genetic lineage tracing strategies combined with transplantation and development of organotypic culture systems (Barker *et al.*, 2012). Until recently, the identification of putative epithelial stem cells using cell surface markers was hampered by the unavailability of reliable

antibodies for fluorescence-activated cell sorting or immunohistochemical analysis (Barker *et al.*, 2012; Rizk and Barker, 2012; Kemper *et al.*, 2012). In this study, analysis of the dynamics of putative intestinal epithelial stem cell populations was accomplished by flow cytometry with a combination of cell surface markers (Lgr5 and Bmi1). Cell separation method used in this experiment included mechanical tissue dissociation, enzymatic digestion, rotation, filtration and density-based steps. Procedure yielded a heterogeneous population including cells with epithelial, mesenchymal, muscle and hematopoietic differentiation. Interpretation of the results of the cellular characterization by flow cytometry must be cautious due to the heterogeneity of the isolated population, potential modifications of the cell surface phenotype induced by the isolation method, and non-specific antibody binding (Tomlinson *et al.*, 2013; Gracz and Magness, 2012).

Present study supports the existence of two functionally different putative epithelial stem cells subpopulations, identified by the Lgr5 and Bmi1 markers, with distinct behaviors after surgical injury and teduglutide treatment: $Lgr5^{+}/Bmi1^{-}$ and $Lgr5^{-}/Bmi1^{+}$ cells [corresponding presumably to crypt base columnar stem cells and to putative "position +4" stem cells, respectively (Barker *et al.*, 2012; Yan *et al.*, 2012)].

As outlined above, surgical injury, especially the ileal resection, induced a significant expansion of putative epithelial stem cells population ($Lgr5^{+}$ and/or $Bmi1^{+}$ cells) at the third postoperative day, which reverted at the seventh. The expansion of epithelial stem cells compartment observed after ileal resection, with increase of all three subpopulations, may have been related with activation of stem cells proliferation or cellular plasticity and lineage reversibility, as adaptive mechanisms after injury, contributing to the reestablishment of epithelial continuity. In reality, according to previous studies, crypt regeneration following injury seems to be based on the reactivation of reserve "position +4" stem cells (Tian *et al.*, 2011; Takeda *et al.*, 2011) or plasticity (dedifferentiation) of committed progenitors, the transit-amplifying cells (Tetteh *et al.*, 2016; Barker, 2014; Buczacki *et al.*, 2013; van Es *et al.*, 2012). As suggested formerly by other authors (Tetteh *et al.*, 2016; Buczacki *et al.*, 2013), the replenishment of Lgr5-positive stem cells pool may derive from plasticity of both their absorptive and secretory-lineage progeny. In present study, less intense aggression

induced by isolated laparotomy did not seem to be sufficient to significantly modify the $Lgr5^{+}/Bmi1^{-}$ fraction of putative crypt base columnar stem cells.

Postoperative teduglutide administration, during seven days, was significantly associated with expansion of intestinal epithelial stem cells population and higher proportions of $Lgr5^{+}/Bmi1^{-}$ cells and $Lgr5^{+}/Bmi1^{+}$ cells. Previously, other experimental studies suggested that Glp2 may stimulate epithelial stem cells and transit-amplifying cells proliferation, namely of cells at the positions "+3" to "+10" (after acute administration), "+15" to "+20" (after chronic treatment), "+1" to "+4" and "+4" from the crypt base (Rowland and Brubaker, 2011). Although the signaling networks responsible for the transduction of Glp-2 effects are still insufficiently known, Wnt/β-catenin, one of the most important epithelial stem cells signaling pathways, seem to be critically involved (Bloemendaal *et al.*, 2016; Drucker and Yusta, 2014; Janssen *et al.*, 2013; Rowland and Brubaker, 2011).

In this experiment, teduglutide treatment during seven days after ileal resection and anastomosis was significantly associated with enrichment of putative crypt base columnar stem population ($Lgr5^{+}/Bmi1^{-}$ cells) whereas, on the contrary, induced depletion of putative "position +4" stem cells ($Lgr5^{-}/Bmi1^{+}$ fraction).

Increase of $Lgr5^{+}/Bmi1^{-}$ fraction might have derived from proliferation on the same compartment, recruitment of the $Lgr5^{-}/Bmi1^{+}$ cells or plasticity of transit-amplifying cells to revert to a stem cell phenotype, as previously demonstrated in the literature (Tetteh *et al.*, 2016; Buczacki *et al.*, 2013; van Es *et al.*, 2012). $Lgr5^{-}/Bmi1^{+}$ cells might have constituted a reservoir that was activated after injury to replenish the $Lrg5^{+}/Bmi1^{-}$ pool, as described by others authors (Tian *et al.*, 2011; Takeda *et al.*, 2011), or to contribute directly to the transit-amplifying compartment. Similarly, Van Landegherm L *et al* (van Landegherm *et al.*, 2015; van Landegherm *et al.*, 2012b) demonstrated that insulin-like growth factor 1 (Igf 1), a critical mediator of the enterotrophic effects of Glp2 (Drucker and Yusta, 2014; Rowland and Brubaker, 2011; Bortvedt *et al.*, 2012), activates two intestinal epithelial stem cells populations, via distinct regulatory pathways, to promote growth of normal intestinal epithelium and crypt regeneration after irradiation. Indeed, according to those authors studies, Igf 1 increases the percentage of Sox9-low intestinal epithelial stem cells (actively cycling)

and percentage of those cells in M-phase, but does not expand Sox9-high cells (reserve intestinal epithelial stem cells) (van Landegherm *et al.*, 2015; van Landegherm L *et al.*, 2012b). According to Buczacki SJ *et al* (Buczacki *et al.*, 2013), approximately 20% of the intestinal $Lgr5^{+}$ cells are quiescent secretory precursors, coexpressing Lgr5 and all "position +4" markers, that can revert into actively cycling $Lgr5^{+}$ crypt base columnar stem cells upon injury, contributing to regeneration.

In this investigation, variations of putative epithelial stem cells pool ($Lgr5^{+}$ and/or $Bmi1^{+}$ cells) depended mainly of $Lgr5^{-}/Bmi1^{+}$ fraction, as demonstrated by a significant and high positive correlation, suggesting that "position +4" stem cells might constitute the main effectors of surgical injury stem-cells response.

Inverse correlation between $Lgr5^{+}/Bmi1^{-}$ and $Lgr5^{-}/Bmi1^{+}$ subpopulations after surgery, opposed to that observed in basal condition, was in accordance with a potential interconversion between putative crypt base columnar and "position +4" stem cells, particularly after ileal resection and teduglutide administration.

$Lgr5^{+}/Bmi1^{-}$ and $Lgr5^{-}/Bmi1^{+}$ subpopulations of putative epithelial stem cells correlated moderate and negatively with Grp78 labeling index, as expected. In reality, Grp78 is considered a marker of endoplasmic reticulum stress signaling that is induced at the transition from the stem cells to the transit-amplifying cells in the early phase of differentiation process (Heijmans *et al.*, 2013).

In 2013, Wang F *et al* (Wang *et al.*, 2013) described a method of isolation and characterization of putative intestinal epithelial stem cells based on a surface markers combination and a colony-formation assay, using immunohistochemistry, real-time reverse-transcription polymerase chain reaction and fluorescence-activated cell sorting. In 2016, Nefzger CM *et al* (Nefzger *et al.*, 2016) proposed also a combinational cell surface marker-mediated strategy for the isolation of putative crypt base columnar stem cells, transcriptionally and functionally equivalent to the putative intestinal stem cells extracted from Lgr5-Green fluorescent protein (Grp) models ($CD31^{-}/CD45^{-}/CD166^{low}/CD24^{med}/CD44^{high}/Grp78^{neg/low}/Epcam^{high}/EphB2^{high}$). In present study, $Lgr5^{-}/Bmi1^{+}$ subpopulation, the putative "position +4" stem cells, demonstrated a significant high positive correlation with $CD44^{+}/CD24^{low}/CD166^{+}/Grp78^{+}$ cells that were considered by Wang F *et al* (Wang *et al.*, 2013) to correspond to transit-amplifying

cells. Nevertheless, surprisingly, $CD44^{+}/CD24^{low}/CD166^{+}/Grp78^{-/low}$ cells, perceived by those authors as epithelial stem cells, did not demonstrated a significant correlation with $Lgr5^{+}/Bmi1^{-}$ cells and showed only a low-grade correlation with $Lgr5^{-}/Bmi1^{+}$ and $Lgr5^{+}/Bmi1^{+}$ cells.

In conclusion, the present study corroborates the existence of two functional putative epithelial stem cells subpopulations ($Lgr5^{+}/Bmi1^{-}$ and $Lgr5^{-}/Bmi1^{+}$) with distinct behavior after surgical injury and teduglutide administration. Surgical injury seems to induce an increase of putative epithelial stem cells population at the third day. Teduglutide administration during seventh days after surgical intervention was associated with expansion of the intestinal epithelial stem cells pool (particularly of putative crypt base columnar cells); nevertheless, it was associated with a depletion of putative "position +4" stem cells in the peri-anastomotic segment after ileal resection.

Current results improve the understanding of the role of the intestinal epithelial stem cells dynamics in the intestinal repair. A better knowledge of intestinal epithelial stem cells modulation during the anastomotic healing might offer new insights into the development of perioperative adjuvant pharmacological interventions, including the use of growth factors such as teduglutide, and could be extrapolated also to other contexts. Additional studies are necessary to completely explain the observed putative epithelial stem cells behavior.

Chapter 4

Influence of teduglutide on the intestinal anastomosis outcome on an animal model

This chapter was partially published as:

Costa BP, Gonçalves AC, Abrantes AM, Matafome P, Seiça R, Sarmento-Ribeiro AB, Botelho MF, Castro-Sousa F: Effects of teduglutide on histological parameters of intestinal anastomotic healing. *Eur Surg.* 2017;49(5):218-227. Doi 10.1007/s10353-017-0478-9.

Beatriz P. Costa, Margarida Abrantes, Augusta Cipriano, Ângela Jesus, Mário Ruivo, Paulo Teixeira, Lígia Castro, Cristina Gonçalves, Ana Bela Sarmento Ribeiro, Maria Filomena Botelho, F. Castro Sousa: Avaliação dos efeitos da administração do *Glucagon-like Peptide 2* num modelo animal de anastomose intestinal - Análise preliminar. *Revista Portuguesa de Cirurgia.* 2015;32 (Supl março):93 (oral presentation at the XXXV Congresso Nacional de Cirurgia, Figueira da Foz, Portugal).

4.1. Abstract

Intestinal anastomotic failure continues to be one of the most relevant surgical incidents. Teduglutide is an enterotrophic long-acting equivalent of glucagon-like peptide 2. This study evaluated the effects of teduglutide short-term administration on the intestinal anastomosis outcome on an animal model. Wistar rats (n=31) were submitted to ileal resection and standard anastomosis, with or without postoperative teduglutide treatment, and sacrificed at the third or at the seventh day, with tissue sampling. Macroscopic outcome of the anastomosis was characterized according to the Anastomotic Complication Score. Histological parameters of anastomotic healing were assessed with the modified Houdart-Hutschenreiter's classification after hematoxylin and eosin staining. Collagen content and distribution were evaluated with the Gordon and Sweet's technique. Neoangiogenesis and epithelial proliferation indexes were determined with anti-CD31 and anti-Ki67 immunostaining, respectively. Paneth and goblet cells were studied with periodic acid shiff-alcian blue pH 2.5; subepithelial myofibroblasts and glial cells with anti-actin, smooth muscle and anti-S-100 immunostaning. Teduglutide administration had no apparent impact on the rate or severity of anastomotic leakage. Teduglutide was associated with higher levels of reepithelialization (p=0.022) and of neoangiogenesis (neovessels density=16.0±10.8/mm^2 *vs.* 5.3±3.4/mm^2, p=0.0001) at the seventh postoperative day. Lower expression of type I collagen (p=0.015) and higher content of type III collagen (p=0.007) in the submucosa were also documented, at the seventh day, in teduglutide-treated animals. This growth factor was also associated with an increase of subepithelial myofibroblasts density score at the seventh day, whereas no relevant influence was observed on Paneth, goblet and glial cells indexes. Those findings indicate a positive impact of teduglutide on the reepithelization and neoangiogenesis events of the proliferative phase of intestinal anastomotic repair. Additional studies are necessary to clarify its effects on the fibrogenesis process.

4.2. Introduction

Teduglutide is an enterotrophic long-acting equivalent of glucagon-like peptide 2 (GLP-2), which is a gastrointestinal growth factor with a relevant participation in the maintenance of intestinal mucosa integrity and function (Drucker and Yusta, 2014).

Intestinal anastomotic healing is a dynamic and highly regulated process of cellular, humoral and molecular mechanisms classically divided into three sequential overlapping stages (Thompson *et al.*, 2006; Rijcken *et al.*, 2014). In the exudative phase, during the first one to four days, coagulation process triggers the release of bioactive mediators that stimulate the recruitment of inflammatory cells. These cells participate in the wound debridement, extracellular matrix degradation, antigen presentation, and phagocytosis. The proliferative phase is characterized by reepithelialization, angiogenesis and fibroplasia and usually runs between the second and the fourteenth postoperative days. In the reparative phase, extracellular matrix remodeling lead to wound stabilization and contraction (Rijcken *et al.*, 2014).

Regardless of continuous improvements in surgical technique and care, intestinal anastomotic failure persists as a relevant surgical problem (Guyton *et al.*, 2016; Bosmans *et al.*, 2015).

Present investigation evaluated the influence of teduglutide administration on the intestinal anastomosis structural outcome, at the macroscopic and microscopic levels, on an animal model.

4.3. Methods

4.3.1. Ethical statement

Experiment was authorized by the Ethics Committee of the Faculty of Medicine, University of Coimbra, Coimbra, Portugal (License n° 32-06-2009) and conducted according to the institutional and national animals' defense recommendations.

4.3.2. Animals and experimental design

Adult male Wistar *albinus* rats weighting between 250 and 300g were housed in stainless steel cages under controlled temperature (22±1°C) and relative humidity (50±10%) conditions, with dark/light cycles of 12 hours. Animals were maintained on unrestricted access to standard rodent diet and tap water, except for two hours fasting before surgery (only with free access to water).

Animals were randomly allocated into two groups: "*Postoperative Teduglutide Administration*" ("*Ted +*") *versus* "*No Treatment*" ("*Ted -*"). Evaluation was performed at the time of the operation and at the time of sacrifice, on the third or seventh postoperative day (four subgroups), with ileal harvesting. Blinded assessment was guaranteed in the microscopic evaluation procedures.

4.3.3. Anesthesia and operative details

All surgical procedures were implemented by the same surgeon under clean conditions. Rats were anesthetized with an intraperitoneal injection of ketamine hydrochloride (75 mg/kg; Pfizer Inc., New York, USA) and chlorpromazine (3 mg/kg; Laboratórios Vitória, Amadora, Portugal).

After a 3-cm midline laparotomy, a 10-cm length ileal resection was undertaken, 5 cm upstream of ileocecal valve. An end-to-end anastomosis using eight full-thickness equidistant polydioxanone USP 6/0 stitches (PDS II, Ethicon, Johnson-Johnson Intl., Cincinnati, USA) restored the intestinal continuity. Abdomen was closed with two running sutures (muscle-aponeurotic and cutaneous) of braided coated polyglactin 910 USP 4/0 (Surgilactin, Sutures Limited, Wrexham, UK) and natural silk USP 4/0 (Surgisilk, Sutures Limited), respectively. On postoperative period, ingestion of 5% glucose in water (1:1) was consented in the first day, succeeded by *ad libitum* oral hydration and chow. Daily surveillance of the animals was undertaken and a health score was calculated as described previously by van Landeghem L *et al* (van Landeghem *et al.*, 2012a).

Surgical mortality and morbidity were recorded. At the third or seventh postoperative day, animals were sacrificed by cervical displacement and subjected to a relaparotomy with ileal resection (10-cm length, retaining distal 3 cm).

4.3.4. Teduglutide administration

In "*Ted* +" groups, teduglutide (American Peptide Company, Sunnyvale, California, USA) was administered subcutaneously in the postoperative period (from the operation day), 200 μg/kg body weight *per* day, diluted in 0.25 ml phosphate buffered saline pH 7.4 (PBS; Gibco, LifeTechnologies, Carlsbad, California, USA), after reconstitution in agreement with the manufacturer's instructions.

4.3.5. Tissue harvesting

One of three similar longitudinal strips of the most distal 4 cm of each ileal specimen (with the anastomosis in the middle), corresponding to one third of the circumference, was retrieved, after cautious washing with normal saline solution. One segment of ileum, immediately adjacent to the 4-cm ileal specimen previously described, 2-cm length, was also recovered. Samples were fixed in 10% formaldehyde, dehydrated and embedded in paraffin, and then 4 μm sections were prepared.

4.3.6. Macroscopic structural evaluation of the anastomosis

During relaparotomy, the peritoneal cavity was rigorously checked for anastomotic leakage, intra-abdominal abscess, peritonitis or intestinal obstruction. At the macroscopic examination, "*in situ*" normal anastomotic healing was considered as apparent anastomosis integrity, with no evidence of leakage or dehiscence, peri-anastomotic collections or obstruction. Anastomotic leakage was defined as a defect in the integrity of the surgical junction between two intestinal loops leading to a communication between the intra and extraluminal compartments (Chadi *et al.*, 2016; Shogan *et al.*, 2013). Macroscopic outcome of the anastomoses was characterized by

the Anastomotic Complication Score proposed by Bosmans JWAM *et al* (Bosmans *et al.*, 2016) for animal research, as follows: 0: No adhesions or abnormalities; 1: Adhesion to fat pad, clean anastomosis underneath; 2: Adhesion to intestinal loop, abdominal wall or other organ; 3: Anastomotic defect found underneath adhesion, no other abnormalities; 4: Signs of possible contamination; 5: Clear anastomotic complication; spread of pus, obstruction at the anastomosis, signs of peritonitis; 6: Fecal peritonitis; death due to peritonitis. Intra-abdominal adhesions are assessed and semiquantitatively graded using the standard Hulka scale (0 point: No adhesions; 1 point: Single, easily dissectible adhesion; 2 points: Multiple, easily dissectible adhesions; 3 points: Single, dense adhesion; 4 points: Multiple, dense adhesions) (Cakmak *et al.*, 2009).

4.3.7. Microscopic structural assessment of the anastomosis

Anastomotic samples were retrieved according to the former explanation and, for each one, at least two 4 μm sections were systematically analyzed, after having been staining with hematoxylin and eosin (H&E) or Gordon and Sweet's protocol or subjected to immunohistochemistry, following standard protocols.

Analysis was performed by an expert pathologist blinded to the experimental groups using a conventional binocular light microscope (Nikon Labophot, Nikon, Tokio, Japan). Photomicrographs were obtained on a light microscope (Nikon Eclipse 50i, Nikon Corporation) equipped with a digital camera (Nikon Digital Sight DS-Fi1, Nikon Corporation) and recorded with the integrated software.

4.3.7.1. Healing parameters according to the modified Houdart-Hutschenreiter's classification

Anastomotic healing was evaluated with an adaptation of the Houdart-Hutschenreiter's histopathological assessment scale (Cakmak *et al.*, 2009), which included the following criteria: mucosal reepithelialization, presence of inflammatory granulomas and formation of granulation tissue (infiltration of inflammatory cells,

neovascularization, presence of fibroblasts and development of fibrosis), muscle layer destruction (ischemic necrosis occurrence, continuity interruptions and inflammatory infiltration) and local inflammatory response (infiltration of neutrophils, lymphocytes, histiocytes and giants cells) (Table 4.1). Granulation tissue was morphologically identified as tissue containing numerous fibroblasts, inflammatory cells and microvessels within a loose matrix of collagen, at the center line of the anastomotic wound (Thompson *et al.*, 2006).

Table 4.1. Histological parameters of intestinal anastomotic healing (modified Houdart and Hutschenreiter's classification)[a]

1. Mucosal reepithelialization				
Grade 0	Absence of epithelialization on the anastomotic line			
Grade 1	Incomplete coating of the anastomotic wound with a single layer of cells			
Grade 2	Complete coating of the anastomotic wound with a single layer of cells			
Grade 3	Complete reepithelialization with glandular epithelium			
2. Inflammatory granuloma and formation of granulation tissue				
	Inflammatory cell presence	Neovascularization	Fibroblasts presence	Fibrosis development
Grade 0	Absence	Absence	Absence	Absence
Grade 1	Mild	Mild	Mild	Mild
Grade 2	Moderate	Moderate	Moderate	Moderate
Grade 3	Intense	Intense	Intense	Intense
3. Muscle layer destruction				
	Ischemic necrosis	Muscle layer continuity	Inflammatory infiltration	
Grade 0	Absence	Complete interruption	Absence	
Grade 1	Slight	Muscle synechia	Slight	
Grade 2	Mild	Complete restitution	Mild	
Grade 3	N.c.	N.c.	Intense	
4. Wound inflammatory infiltration				
	Neutrophils	Lymphocytes	Histiocytes	Giant cells
Grade 0	Absence	Absence	Absence	Absence
Grade 1	Mild	Mild	Mild	Mild
Grade 2	Moderate	Moderate	Moderate	Moderate
Grade 3	Intense	Intense	Intense	Intense

N.c., Not considered. [a] Adapted from reference Cakmak *et al.*, 2009

Five high-power fields (x400 magnification; 0.95 mm^2 area/field) from at least two 4-μm sections, stained with hematoxylin and eosin (H&E) following standard procedures, were evaluated *per* anastomosis.

4.3.7.2. Evaluation of collagen content and distribution

For each animal, at least three 4-μm cut sections of the anastomotic segment, obtained from the formalin-fixed and paraffin-embedded block, were stained with Gordon and Sweet's silver impregnation technique, according to standard protocol (Gordon and Sweets, 1936; Saxena, 2010), and systematically studied. Gordon and Sweet's staining is based on the argyrophilic properties of reticulin fibers. Reticulin fibers are thin fibers composed of type III collagen that form a delicate stromal network and acquire a black color against a gray to light pink background, while fibrous tissue composed of type I collagen appears brown (Gordon and Sweets, 1936; Saxena, 2010).

Succinctly, 4 μm sections were deparaffinized, hydrated and submitted to the Gordon and Sweet's protocol. Procedure included oxidation in 1% acidified potassium permanganate for five minutes ("oxidation"), discoloration with 2% oxalic acid for two minutes, treatment in 2.5% iron alum (ferric ammonium sulphate) for 15 to 30 minutes ("sensitization"), impregnation in ammoniacal silver solution for two minutes, reduction with 10% aqueous formalin for two minutes ("developing"), toning in 0.2% gold chloride (sodium tetrachloroaurate) for three minutes ("toning") and fixation in 5% aqueous sodium thiosulphate for three minutes; all those steps were always followed by rinsing with distilled water. After a new washing in distilled water, sections were counterstained with van Gieson's stain (mixture of picric acid and acid fuchsine) for two minutes, dehydrated, cleared and mounted.

For each sample, two standard regions from the *lamina propria*, submucosa and *muscularis propria* layers, and from the granulation tissue, were evaluated at 200x magnification. Thickness, orientation and distribution of collagen fibers were observed. A semiquantitative analysis was performed, based on the intensity of staining in the different layers or regions, using a visual analogue score: a score of "0" was considered as no staining, "1" as mild staining, "2" as moderate staining, and "3" as

intense staining. The mean value obtained for each bowel layer or region was considered.

4.3.7.3. Determination of the neoangiogenesis score

Angiogenesis was evaluated by the capillary density, using immunohistochemical staining of endothelial cells with the monoclonal antibody anti-CD31, as stated by Mall JW *et al* (Mall *et al.*, 2003).

Deparaffinized 4 μm sections of the anastomotic segment obtained according to previous description were treated with ultra-cell conditioning solution (Ultra CC1; Ventana Medical Systems, Inc., Tucson, Arizona, USA) and heated in a microwave oven (52 minutes at 96°C) for antigen retrieval. Thereafter, sections were incubated with anti-CD31 (Pecam-1) rat monoclonal antibody (Biocare Medical, Pacheco, California, USA), at 1:50 dilution, at 37°C for 44 minutes. Sections were treated with the amplification kit (Ventana Medical Systems, Inc.) and with the antibody diluent (Ventana Medical Systems, Inc.). Finally, they were counterstained with hematoxylin (Ventana Medical Systems, Inc), submitted to bluing reagent application (Ventana Medical Systems, Inc), dehydrated and mounted.

Two 4 μm sections of each sample were scanned systematically at 40x magnification to identify three areas with the highest microvessel density at the anastomosis site ("hot spots"). Microvessels were then counted in each vision field at 200x magnification (corresponding to an area of 3.8 mm^2). The angiogenesis score corresponded to the mean number of capillary vessels identified in the three 200x magnification vision fields.

4.3.7.4. Analysis of the epithelial proliferation index

Epithelial proliferation index was assessed using immunohistochemical staining with the monoclonal antibody anti-Ki67, a proliferation marker present during all active phases of the cell cycle (while absent in quiescent G0 cells) (Inglin *et al.*, 2008; Rekhtman and Bishop, 2011).

Deparaffinized 4 μm sections of the perianastomotic ileum were treated with ultra-cell conditioning solution (Ultra CC1; Ventana Medical Systems, Inc.) and heated in a microwave oven (36 minutes at 95°C). Sections were incubated with anti-Ki67 rabbit monoclonal primary antibody (Ventana Medical Systems, Inc.) at 37°C for 36 minutes. Sections were treated with antibody diluent (Ventana Medical Systems, Inc.), counterstained with hematoxylin (Ventana Medical Systems, Inc.), submitted to bluing reagent application (Ventana Medical Systems, Inc.), dehydrated and mounted.

A dark brown nuclear staining (of any intensity) was regarded as positive. The ratio between Ki67-labelled cells and the total number of cells *per* crypt was calculated after counting cells, at 400x magnification, in five contiguous and randomly selected longitudinal well-oriented sections of crypts (those in which it was possible to visually follow without interruption the continuation of a crypt into the villus).

4.3.8. Other histopathological analysis

Sections of 4 μm of the ileal perianastomotic specimens, recovered as previously stated, were stained with periodic acid schiff-alcian blue pH 2.5 (PAS-AB pH 2.5) or subjected to immunohistochemistry. Analysis was undertaken by a pathologist with the formerly reported equipment.

4.3.8.1. Estimation of the density of Paneth cells and goblet cells

For global assessment of the density of Paneth cells and goblet cells, a periodic acid schiff-alcian blue pH 2.5 (PAS-AB) staining protocol was used. PAS-AB pH 2.5 is a staining method used to detected polysaccharides (such as glycogen) and mucosubstances in tissues; acidic mucins appeared in blue, neutral mucins in magenta, mixtures of both in blue/purple and nuclei in deep blue (Rekhtman and Bishop, 2011; Ellis, 2014).

Briefly, slides were deparaffinized and hydrated, rinsed in distilled water, treated with 3% aqueous acetic acid for two minutes, stained with 1% alcian blue pH 2.5 (copper phthalocyanins solution in acetic acid and distilled water) for 30 minutes and washed well in running water for 10 minutes. Sections were then treated with 1% aqueous

periodic acid for 10 minutes, rinsed in distilled water, stained with Schiff's reagent (produced by treating basic fuchsine with sulfurous acid) for 15 minutes and washed well in running water for 10 minutes. Nuclei were stained with Mayer hematoxylin for 10 minutes and sections were washed in running water for 10 minutes. Sections were dehydrated, cleared and mounted.

For goblet cells evaluation and quantification, two contiguous well-oriented, full-length crypt-villus units *per* animal were randomly selected and scored, at 200x magnification. Mean number of identified goblet cells was considered.

Paneth cells are cells of the nonendocrine secretory lineage, with typical morphology (pyramidal-shaped) and secretory granules, localized at the bases of the crypts of Lieberkühn, interspersed with granule-free crypt base columnar cells (Roth *et al.*, 2012; Parry *et al.*, 2013). Paneth cells were counted in six contiguous and randomly selected longitudinal well-oriented sections of crypts, at 200x magnification, in ileal cross-sections. Mean value was considered.

4.3.8.2. Study of subepithelial myofibroblasts and enteric nervous system

Evaluation of subepithelial myofibroblasts in the lamina propria of the distal ileum was performed using immunohistochemical staining with the monoclonal antibody anti-actin, smooth muscle.

Subepithelial myofibroblasts were identified as α-smooth muscle actin-expressing stromal cells located in the lamina propria, under the epithelial layer and subjacent to the basement membrane, with characteristic morphology (spindle-shaped with slender cytoplasmic processes or with an enlarged cytoplasm), and forming a network around the crypts. Alfa(α)-smooth muscle actin remains the most typical intestinal myofibroblast marker, although not specific, also being expressed by pericytes, lymphatic lacteal smooth muscle cells, *muscularis mucosae* smooth muscle cells and bone marrow-derived mesenchymal stromal cells (Roulis *et al.*, 2016; Mifflin *et al.*, 2011).

Sections were deparaffinized with EZ Prep concentrate (10x) solution (Ventana Medical Systems, Inc., Tucson, Arizona, USA) and heating at 72°C. Deparaffinized sections were treated with ultra-cell conditioning solution (Ultra CC1; Ventana Medical Systems, Inc.) and heated in a microwave oven, 36 minutes at 95°C, for antigen retrieval. Then, sections were incubated with anti-actin, smooth muscle mouse monoclonal antibody (Cell Marque, Sigma-Aldrich, Rocklin, California, USA), at 1:100 dilution, at 37°C for 32 minutes. Sections were rinsed with reaction buffer concentrate (10x) (Ventana Medical Systems, Inc.), a Tris based buffer solution. Finally, they were counterstained with hematoxylin (Ventana Medical Systems, Inc), submitted to bluing reagent application (Ventana Medical Systems, Inc), dehydrated and mounted.

Assessment was performed in well-oriented crypt-villus axis of five randomly selected fields of vision, at 200x magnification (each field corresponding to 3.8 mm^2). A semiquantitative analysis of subepithelial myofibroblasts was performed considering: "1" as normal morphology, distribution and density, "2" as moderate increase of distribution and density and "3" as marked increase of distribution and density.

Enteric nervous system study was performed with immunohistochemistry through the expression of glial marker S-100 in the submucosal and myoenteric plexus of rats' ileum.

Sections were deparaffinized with high temperatures (72°C) and the EZ Prep concentrate (10x) solution (Ventana Medical Systems, Inc.). Deparaffinized sections were treated with ultra-cell conditioning solution (Ultra CC1; Ventana Medical Systems, Inc.) and heated in a microwave oven (eight minutes at 95°C) for antigen retrieval. Sections were submitted to enzymatic digestion with protease 3 (Ventana Medical Systems, Inc.) (one drop), an endopeptidase of the serine protease family, and were incubated with anti-S100 polyclonal rabbit antibody (Dako, Glostrup, Denmark), at 1:1000 dilution, at room temperature, for 24 minutes. Sections were treated with reaction buffer concentrate (10x) (Ventana Medical Systems, Inc.). Finally, they were counterstained with hematoxylin (Ventana Medical Systems, Inc.), submitted to bluing reagent application (Ventana Medical Systems, Inc.) for four minutes, dehydrated and mounted.

Expression of glial marker S-100 in the submucosal and myoenteric plexus was evaluated in four sections of rats' ileum, with light microscopy, at 100x magnification. Morphology, distribution and density of S-100 immunoreactive glial cells and nerve fibers were studied and a semiquantitative scoring was done as follows: "1" as few glial cells and fibers with a regular morphology and distribution; "2" as numerous glial cells and fibers; and "3" as dense networks of glial cells and fibers.

4.3.9. Statistical analysis

Statistical Package for Social Sciences (SPSS) for Windows, version 18 (SPSS, Chicago, Illinois, USA) was used for the statistical analysis. Testing for normality was performed with Shapiro Wilk and Kolmogorov-Smirnov-Lillifors tests. Non-parametric continuous variables were compared by Mann-Whitney U test and analysis of variance by ranks (Kruskall-Wallis test) with pairwise comparisons (for comparisons across multiple groups). Data were expressed as median and interquartile range (median ± IQR) or number (%). A $p<0.05$ was considered statistically significant.

4.4. Results

4.4.1. Macroscopic structural evaluation of the anastomosis

Thirty-one animals were studied: 16 were included into "*Ted* +" group (eight of them sacrificed on the third day) and 15 into the "*Ted* –" group (six killed at third day).

There were two cases of anastomotic leakage associated with mortality (in "*Res Ted* -" and "*Res Ted* +" groups, respectively), both with an Anastomotic Complication Score of "6" (Bosmans *et al.*, 2016). In a third case of mortality, there were no signs of anastomotic complication (death of unknown etiology) and the Anastomotic Complication Score was "1" (adhesion to fat pad and clean anastomosis underneath). These cases were omitted from additional analysis.

In the surviving animals, there was no evidence of anastomotic fistulae, intra-abdominal abscess, peritonitis or intestinal obstruction. Anastomotic Complication Score (Bosmans *et al.*, 2016) was lower or equal to "2" in all these animals. Semiquantitative

assessment of intra-abdominal adhesions did not exceed one point in the Hulka scale (single, easily dissectible adhesion) (Cakmak *et al.*, 2009) in any case. Morbidity included one case of small scurf at the teduglutide injection site.

Teduglutide was not associated with significant impact on the macroscopic outcome of the anastomosis, namely on the rate or severity of anastomotic leakage evaluated with the Anastomotic Complication Score (Bosmans *et al.*, 2016). Operative mortality and morbidity rates were not significantly different in animals with or without teduglutide treatment: 6.3 *vs.* 13.3%, *n.s.* and 6.3% *vs.* 0%, *n.s.*, respectively; as well as, the anastomotic complication score (Bosmans *et al.*, 2016) and the intra-abdominal adhesion index according to the Hulka scale (Cakmak *et al.*, 2009): 0±0 (0-6) *vs.* 1±2 (0-6), p=0.06 and 0±0 (0-1) *vs.* 0±1 (0-1), p=0.08, respectively.

4.4.2. Microscopic structural assessment of the anastomosis

4.4.2.1. Parameters of anastomotic repair in animals not submitted to teduglutide administration

In the animals not submitted to teduglutide treatment, histopathological assessment of the anastomotic repair according to the modified Hourdart-Hutschenreiter's classification revealed higher infiltration of inflammatory cells (p=0.012) and higher grade of fibrosis (p=0.003) in the granulation tissue at the seventh postoperative day, in comparison with the third day; higher number of giant cells in the wound was also observed at that time point (p=0.028) (Fig. 4.1; Table 4.2).

According to the Gordon and Sweet's silver staining, the anastomotic segment of animals not submitted to teduglutide demonstrated significantly higher global content of collagen at the seventh day than on the third day (types I and III; p=0.009), especially in the granulation tissue (p=0.008); and also, higher expression of type I collagen (p=0.002), particularly in the granulation tissue (p=0.003) and in the *muscularis propria* (p=0.018) (Table 4.3; Fig. 4.2). Type I/type III collagens ratio was higher at the seventh day, although not significantly [1.9±0.9 (1.1-2.3) *vs.* 1.0±0.8 (0.6-1.5), *n.s.*]. At the third day, granulation tissue did not express type I collagen, which was observed only in the submucosa.

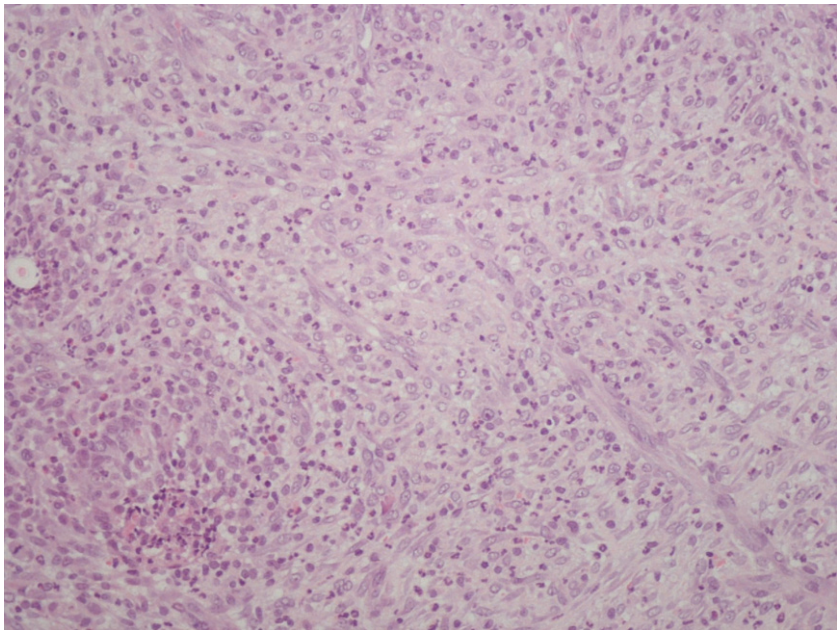

Figure 4.1. Histological section of the ileal anastomosis at the seventh postoperative day in an animal not submitted to teduglutide administration (hematoxylin-eosin staining; 200x). Moderate inflammatory cell infiltration was observed in the granulation tissue

4.4.2.2. Parameters of anastomotic repair in teduglutide-treated animals

Higher level of reepithelialization was documented at the seventh postoperative day in teduglutide-treated animals (p=0.022) according to the modified Hourdart-Hutschenreiter's scale (Table 4.2; Fig. 4.3). Furthermore, higher neoangiogenesis score (neovessels density=16.0±10.8/mm^2 *vs.* 5.3±3.4/mm^2, p=0.0001; Fig. 4.4 and 4.5) and enhanced epithelial proliferation index (81.0±11.0 *vs.* 74.8±19.0%, *n.s.*; Fig. 4.6 and 4.7) were verified, at the last moment of postoperative evaluation, in animals that underwent teduglutide treatment.

Teduglutide administration during seven postoperative days was associated with reduction of the global content of collagen (with a statistically not significant difference), as well as lower expression of type I collagen, without statistical significance in all the layers except in the submucosa [2.0±0.0 (1.0-3.0) *vs.* 3.0±0.0 (2.0-3.0) points, p=0.015]. Nevertheless, higher content of type III collagen in the submucosa [1.0±0.0 (1.0-1.0) *vs.* 0.0±0.0 (0.0-0.0) points, p=0.007] was observed in

teduglutide-treated animals at that moment (Table 4.3). At the seventh day, a not-significant reduction of the levels of type I collagen in the *lamina propria*, *muscularis propria* and granulation tissue, as well as of type III collagen in the *muscularis propria* and granulation tissue, were observed in animals treated with teduglutide (Fig. 4.8 and Fig. 4.9). No relevant effects of teduglutide on global type I/type III collagens ratio were evident.

Table 4.2. Intestinal anastomotic healing according to the modified Houdart-Hutschenreiter's classification*

Score	Study groups			
	Third postoperative day		Seventh postoperative day	
	Ted –	Ted +	Ted –	Ted +
1. Mucosal reepithelialization	1 ± 0 (1-1)	1 ± 1 (1-2)	1 ± 1 (1-3)	2 ± 1 (2-3)[b,e,f]
2. Granulation tissue formation				
Inflammatory cells presence	1 ± 0 (1-1)	1 ± 0 (1-1)	2 ± 0 (1-2)[a,d]	1 ± 1 (1-2)
Neovascularization	1 ± 0 (1-1)	1 ± 0 (1-1)	2 ± 0 (1-2)	2 ± 1 (1-3)[e,f]
Fibroblasts presence	1 ± 1 (1-2)	1 ± 0 (1-1)[d]	2 ± 1 (1-3)	1 ± 1 (1-2)
Fibrosis development	1 ± 0 (1-1)	0 ± 1 (0-1)[d]	1 ± 0 (1-1)[a]	1 ± 0 (1-1)[e,f]
3. Muscle layer destruction				
Ischemic necrosis	0 ± 1 (0-1)	1 ± 1 (0-1)	0 ± 1 (0-1)	0 ± 0 (0-0)
Muscle layer continuity	1 ± 0 (1-1)	1 ± 0 (1-1)	1 ± 0 (1-1)	1 ± 0 (1-1)
Inflammatory infiltration	2 ± 1 (1-3)	1 ± 2 (1-3)	1.5 ± 1 (1-3)	1 ± 1 (1-3)
4. Wound inflammatory infiltration				
Neutrophils	1 ± 0 (1-1)	1 ± 1 (1-2)	2 ± 1 (1-2)	2 ± 1 (1-2)
Lymphocytes	1 ± 1 (0-1)	1 ± 1 (0-2)	1 ± 1 (1-2)	1 ± 0 (1-1)
Histiocytes	0 ± 1 (0-1)	1 ± 1 (0-1)	1 ± 0 (1-2)	1 ± 0 (1-1)
Giant cells	0 ± 1 (0-1)	0 ± 1 (0-1)[d]	1 ± 0 (1-2)[a]	1 ± 1 (0-1)

Animals (n=28) were submitted to ileal resection and anastomosis and sacrificed on the third or seventh postoperative day. In "*Ted* +" groups, teduglutide was administered after the operation. For each sample, five high-power fields from at least two 4 μm sections stained with hematoxylin-eosin were evaluated *per* anastomosis. Parameters were graded into four categories (0: absent, 1: mild, 2: moderate, 3: intense). Data were presented as median±interquartile range (minimum-maximum). Kruskal-Wallis test was used. [a] "*Ted* -" (seventh day) *vs.* "*Ted* -" (third day), $p<0.05$; [b] "*Ted* +" (seventh day) *vs.* "*Ted* -" (seventh day), $p<0.05$; [c] "*Ted* +" (third day) *vs.* "*Ted* -" (third day), $p<0.05$; [d] "*Ted* +" (third day) *vs.* "*Ted* -" (seventh day), $p<0.05$; [e] "*Ted* +" (seventh day) *vs.* "*Ted* -" (third day), $p<0.05$; [f] "*Ted* +" (seventh day) *vs.* "*Ted* +" (third day), $p<0.05$. * Adapted from reference Cakmak *et al.*, 2009

Table 4.3. Collagen content and distribution in the ileal anastomotic segment

Score	Study groups			
	Third postoperative day		Seventh postoperative day	
	Ted –	Ted +	Ted –	Ted +
Total collagen	6 ± 3 (5-8)	5.5 ± 1 (5-7)[d]	11.5 ± 2 (9-15)[a]	10 ± 2 (8-11)[f]
Type I collagen	3 ± 0 (3-3)	3 ± 1 (2-3)[d]	7 ± 1 (6-8)[a]	5 ± 2 (4-7)[f]
Type III collagen	3 ± 3 (2-5)	3 ± 2 (2-4)	4 ± 3 (3-7)	4 ± 2 (4-6)[f]
Type I/type III collagens ratio	1 ± 0.8 (0.6-1.5)	1 ± 0.8 (0.5-1.5)	1.9 ± 0.9 (1.1-2.3)	1.2 ± 0.4 (0.7-1.8)
Total collagen in granulation tissue	1 ± 1 (0-1)	1 ± 1 (0-1)[d]	4.5 ± 2 (3-6)[a]	4 ± 1 (2-5)[f]
Type I collagen in *lamina propria*	0 ± 0 (0-0)	0 ± 0 (0-0)	1 ± 1 (0-1)	0 ± 0 (0-1)
Type I collagen in submucosa	3 ± 0 (3-3)	3 ± 1 (2-3)	3 ± 0 (2-3)	2 ± 0 (1-3)[b,e]
Type I collagen in *muscularis propria*	0 ± 0 (0-0)	0 ± 0 (0-0)[d]	1 ± 1 (0-2)[a]	1 ± 2 (0-2)
Type I collagen in granulation tissue	0 ± 0 (0-0)	0 ± 0 (0-0)[d]	3 ± 1 (2-3)[a]	2 ± 1 (1-3)[e,f]
Type III collagen in *lamina propria*	1 ± 0 (1-1)	1 ± 0 (1-1)	1 ± 0 (1-1)	1 ± 0 (1-1)
Type III collagen in submucosa	0 ± 2 (0-2)	0 ± 1 (0-1)	0 ± 0 (0-0)	1 ± 0 (1-1)[b]
Type III collagen in *muscularis propria*	1 ± 0 (1-1)	1 ± 0 (1-1)	1 ± 2 (1-3)	1 ± 1 (1-2)
Type III collagen in granulation tissue	1 ± 1 (0-1)	1 ± 1 (0-1)[d]	2 ± 1 (1-3)	1 ± 1 (1-3)

Animals (n=28) were submitted to ileal resection and anastomosis and sacrificed on the third or seventh postoperative day. In "*Ted*+" groups, teduglutide was administered after the operation. Collagen content and distribution were evaluated with the Gordon and Sweet's silver staining technique. Intensities of staining were graded in four categories (0: absent, 1: mild, 2: moderate, 3: intense) and total scores were the mean values obtained for each bowel layer or area. Data were presented as median±interquartile range (minimum-maximum). Kruskal-Wallis test was used. [a] "*Ted* -" (seventh day) *vs.* "*Ted* -" (third day), p<0.05; [b] "*Ted* +" (seventh day) *vs.* "*Ted* -" (seventh day), p<0.05; [c] "*Ted* +" (third day) *vs.* "*Ted* -" (third day), p<0.05; [d] "*Ted* +" (third day) *vs.* "*Ted* -" (seventh day), p<0.05; [e] "*Ted* +" (seventh day) *vs.* "*Ted* -" (third day), p<0.05; [f] "*Ted* +" (seventh day) *vs.* "*Ted* +" (third day), p<0.05

4.4.3. Density scores of Paneth cells, goblet cells, subepithelial myofibroblasts and glial cells

In animals not submitted to teduglutide administration, this study demonstrated, in comparison with baseline, lower number of Paneth cells *per* crypt in the perianastomotic tissue at the third and the seventh days [3±0.7 (2.3-3.2) *vs.* 5.3±1 (4-7), p=0.0001 and 4.1±1.2 (3.2-5) *vs.* 5.3±1 (4-7), p=0.007], lower number of goblet cells *per* crypt-villus unit at the seventh day [40±10 (31.5-47) *vs.* 53.3±10.5 (38.5-72), p=0.002]; higher expression of anti-actin, smooth muscle in subepithelial myofibroblasts at the third and the seventh days [2±0 (2-2) *vs.* 1±0 (1-1), p=0.0001 and 2±0 (2-2) *vs.* 1±0 (1-1), p=0.0001] and higher expression of glial marker S-100 in the submucosal and myoenteric plexus at the seventh postoperative day [2±0 (1-3) *vs.*

1±0 (1-1), *p*=0.0001 and 2±1 (1-3) *vs.* 1±0 (1-1), *p*=0.0001, respectively] (Fig. 4.10 to 4.13).

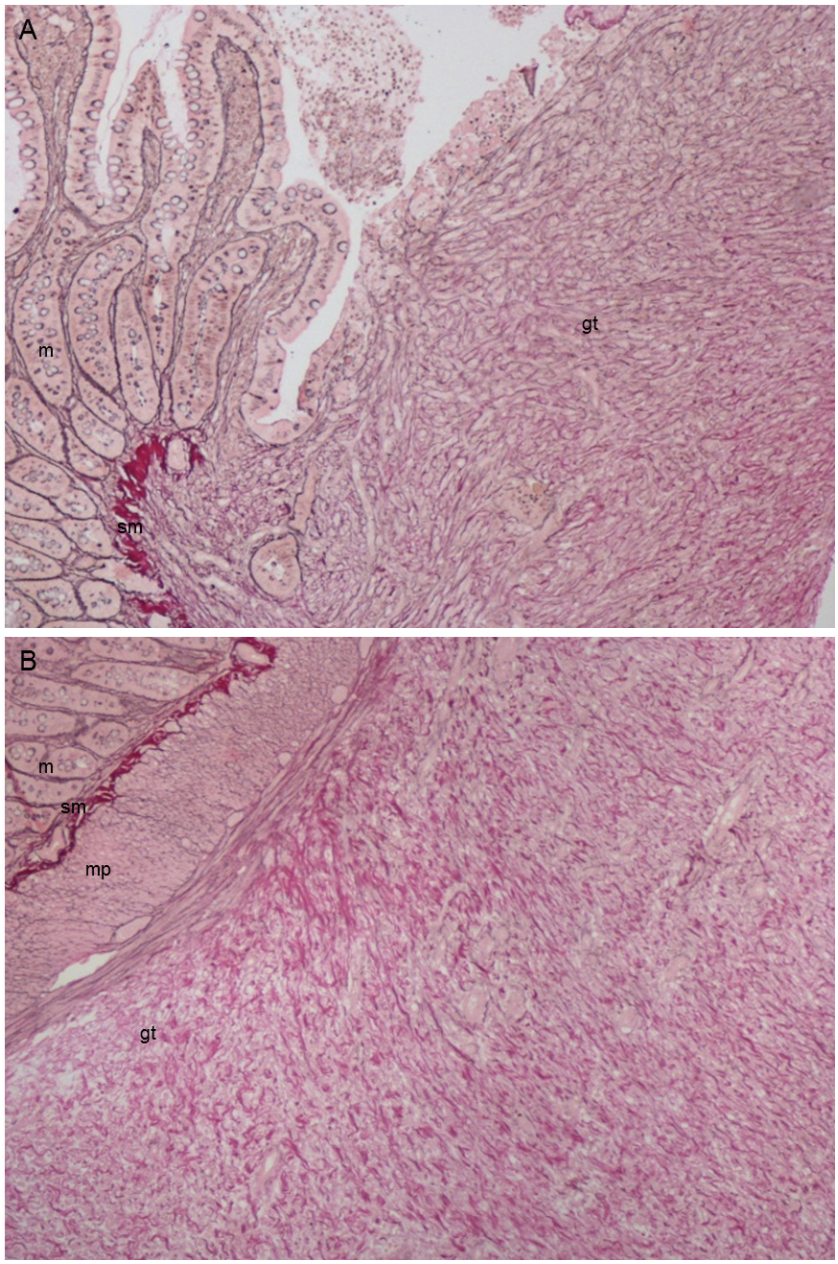

Figure 4.2. A and B. Ileal anastomosis at the seventh postoperative day, in an animal not submitted to teduglutide administration (Gordon and Sweet's staining; original magnification 100x). Anastomosis demonstrated high collagen content (especially type III). Type I collagen (light purplish brown) was observed mainly in submucosa and deep layers of granulation tissue, and also in *lamina propria* and *muscularis propria*. Dense deposition of type III collagen (bright black color) was observed in the granulation tissue and *muscularis propria*. * m, mucosa; sm, submucosa; mp, *muscularis propria*; gt, granulation tissue

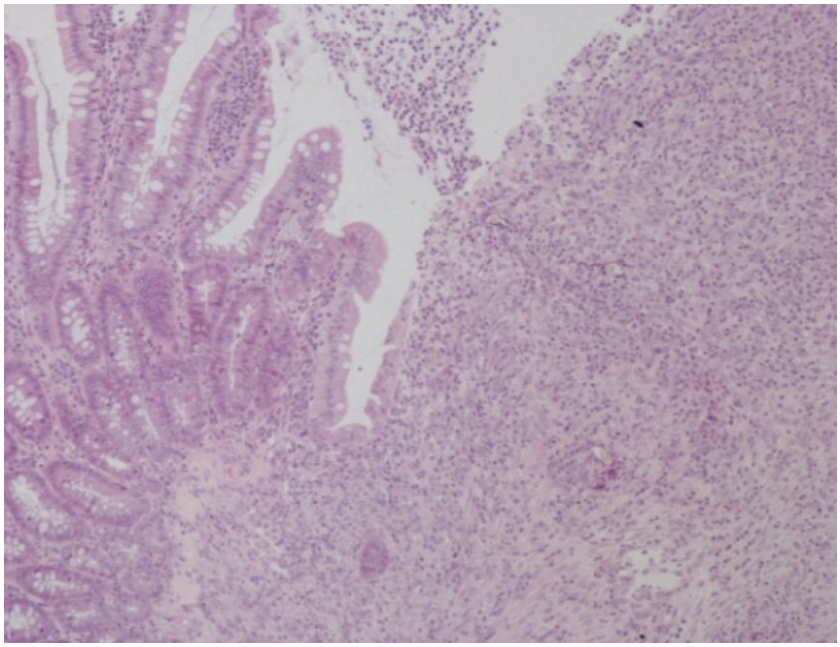

Figure 4.3. Ileal anastomosis at the seventh postoperative day, in a teduglutide-treated animal (hematoxylin-eosin staining; original magnification 100x). Slight reepithelialization, moderate neovascularization, abundant fibroblasts presence, and regular infiltration of inflammatory cells, mainly of polymorphonuclear neutrophils, were documented

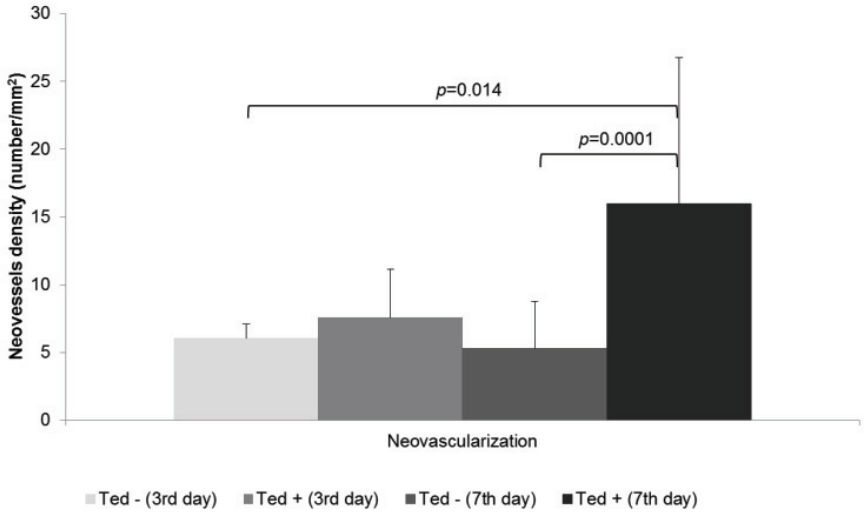

Figure 4.4. Neoangiogenesis in the anastomotic segments determined using immunohistochemical staining with the monoclonal antibody anti-CD31. Neoangiogenesis score corresponded to the mean number of capillary vessels identified in three 200x magnification vision fields (median±interquartile range). Animals (*n*=28) were submitted to ileal resection and anastomosis and sacrificed on the third or seventh postoperative day. In "*Ted+*" groups, teduglutide was administered after the operation. Kruskal-Wallis test with pairwise comparisons was used

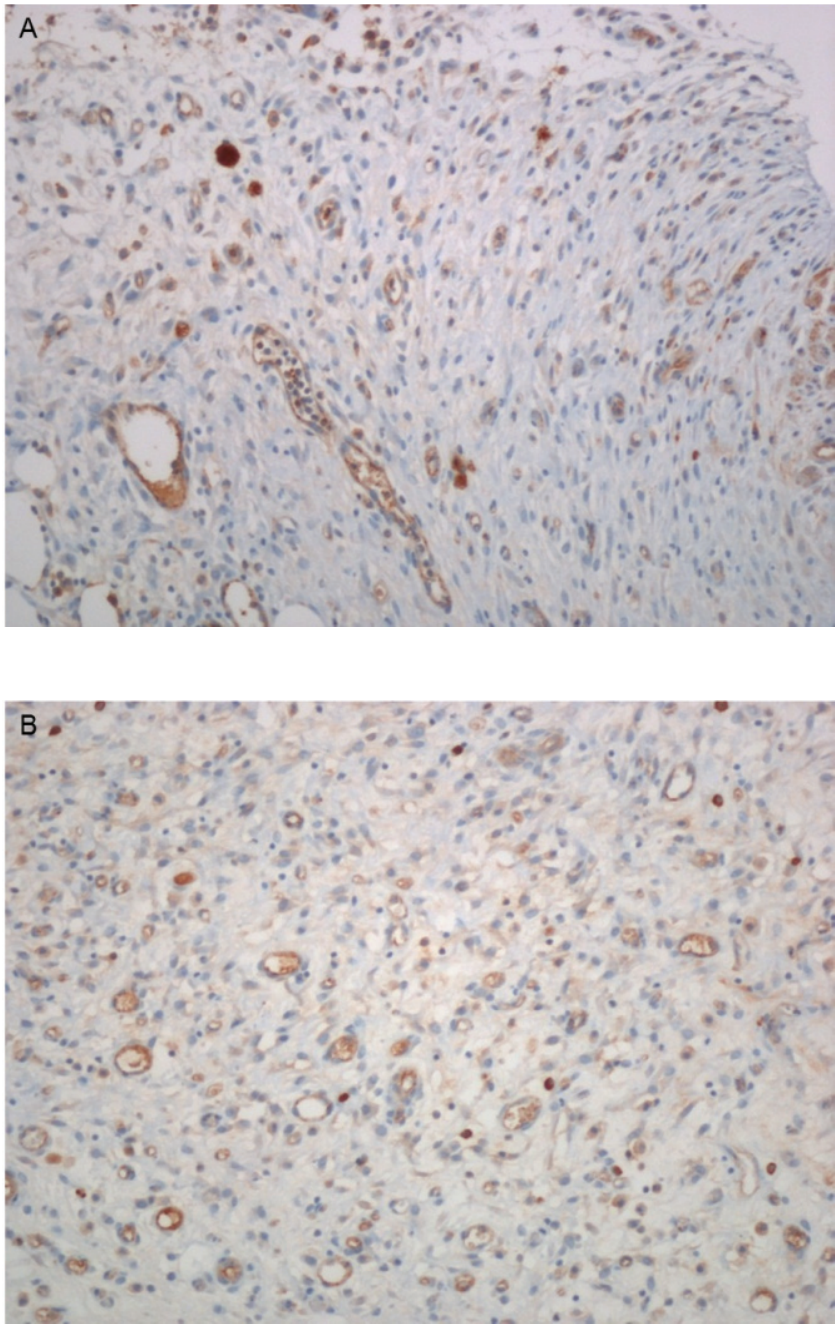

Figure 4.5. Neoangiogenesis in the anastomotic segment evaluated with immunohistochemical staining of the endothelial cells with the monoclonal antibody anti-CD31. A. Neoangiogenesis at the seventh day after ileal resection and anastomosis in a rat not submitted to teduglutide administration (CD31; original magnification 200x). **B.** Neoangiogenesis at the seventh day after ileal resection and anastomosis in a teduglutide-treated rat (CD31; original magnification 200x)

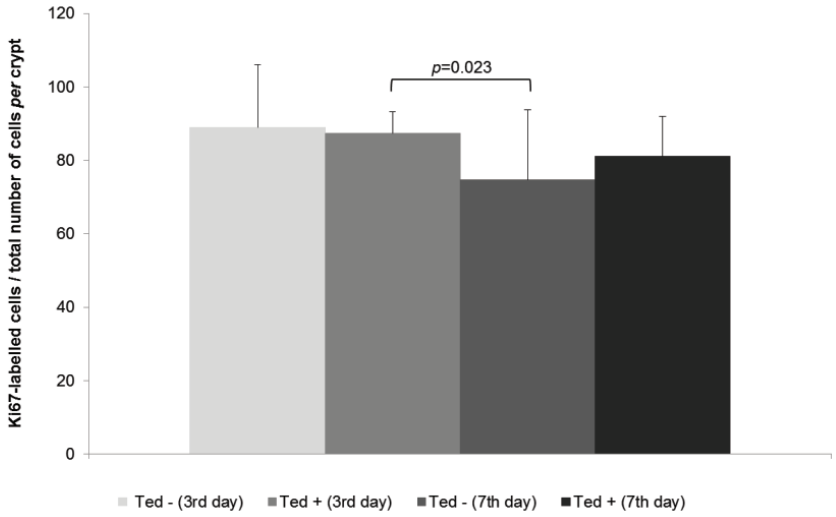

Figure 4.6. Epithelial proliferation evaluated in the rats' perianastomotic segment using immunohistochemical staining with the monoclonal antibody anti-Ki67. Proliferation index corresponded to the mean percentage of Ki67-labelled cells *per* crypt identified in five longitudinal sections of the crypts at 400x magnification (median±interquartile range). Animals (n=28) were submitted to ileal resection and anastomosis and sacrificed on the third or seventh postoperative day. In "*Ted*+" groups, teduglutide was administered after the operation. Kruskal-Wallis test with pairwise comparisons was used

Teduglutide administration was associated with an increase of the expression of anti-actin, smooth muscle in subepithelial myofibroblasts at the seventh day (Table 4.4; Fig. 4.14-4.15). No significant modifications of the goblet and Paneth cells densities nor of the expression of S-100 in the submucosal and myoenteric plexus were observed with teduglutide therapy (Table 4.4; Fig. 4.16-4.17).

4.5. Discussion

In this study, teduglutide had no apparent significant impact on the macroscopic outcome of the anastomosis evaluated by the Anastomotic Complication Score (Bosmans *et al.*, 2016). This fact may have been related with a probably underpowered study (type II statistical error originated by a small sample size).

Rats have been considered suitable animal models to analyze the intestinal anastomotic healing (Bosmans *et al.*, 2016) using histological, cellular, humoral or molecular parameters as primary outcomes, with clear advantages in the availability, costs, handling and housing requirements. However, the evaluation of clinical

outcomes may be influenced by rodents' strong resistance to infection and/or high efficient intra-abdominal immune system (Pommergaard *et al.*, 2011).

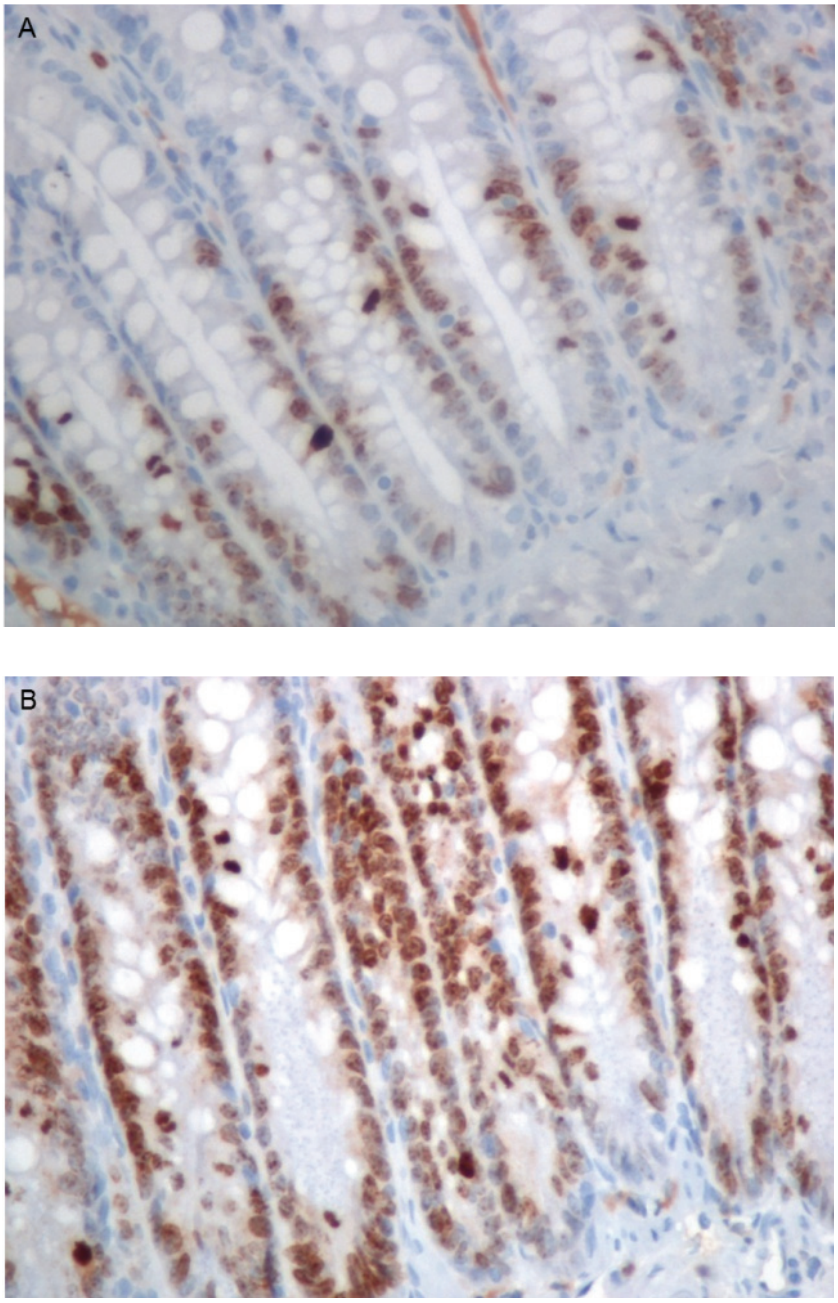

Figure 4.7. Epithelial proliferation evaluated in the perianastomotic segment using immunohistochemical staining with the monoclonal antibody anti-Ki67. A. Epithelial proliferative activity at the seventh day after ileal resection and anastomosis in a rat not submitted to teduglutide administration (Ki67; original magnification 400x). **B.** Epithelial proliferative activity at the seventh day after ileal resection and anastomosis in a teduglutide-treated rat (Ki67; original magnification 400x)

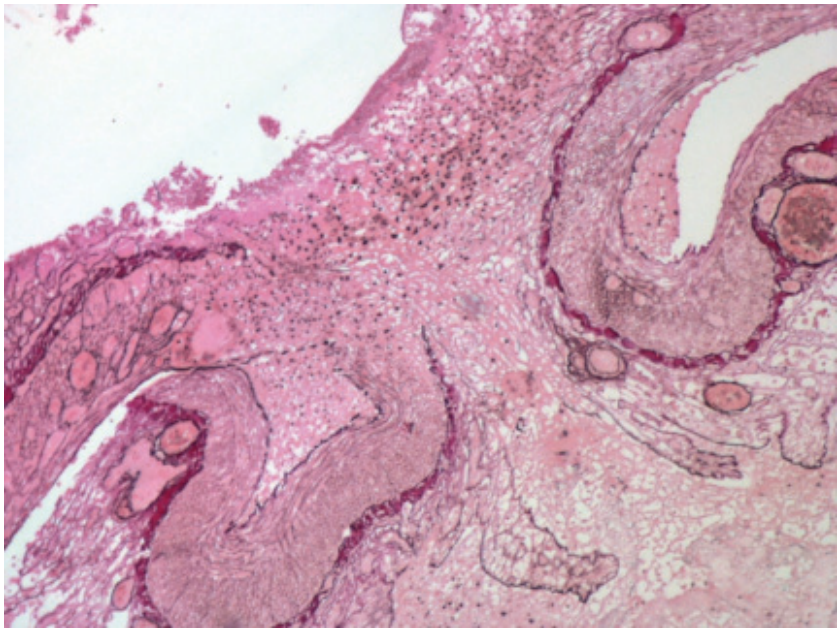

Figure 4.8. Ileal anastomosis at the third postoperative day in a teduglutide-treated animal, with Gordon and Sweet's staining (original magnification 100x). Anastomosis demonstrated low collagen content, mainly restricted to type III (bright black color). Granulation tissue did not express type I collagen (light purplish brown), which was observed only in the submucosa

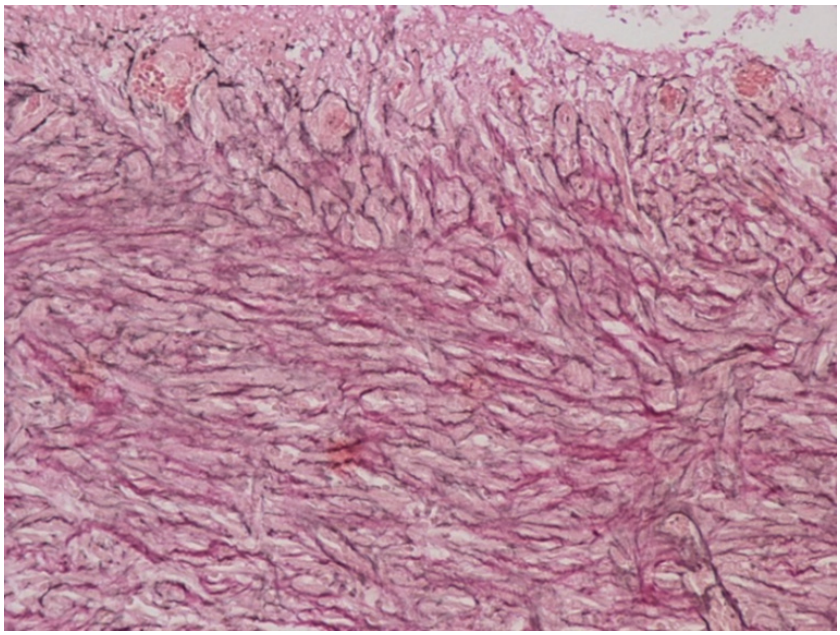

Figure 4.9. Ileal anastomosis at the seventh postoperative day in a teduglutide-treated animal, with Gordon and Sweet's staining (original magnification 200x). Granulation tissue demonstrates moderate content of type I and type III collagens (light purplish brown and bright black colors, respectively)

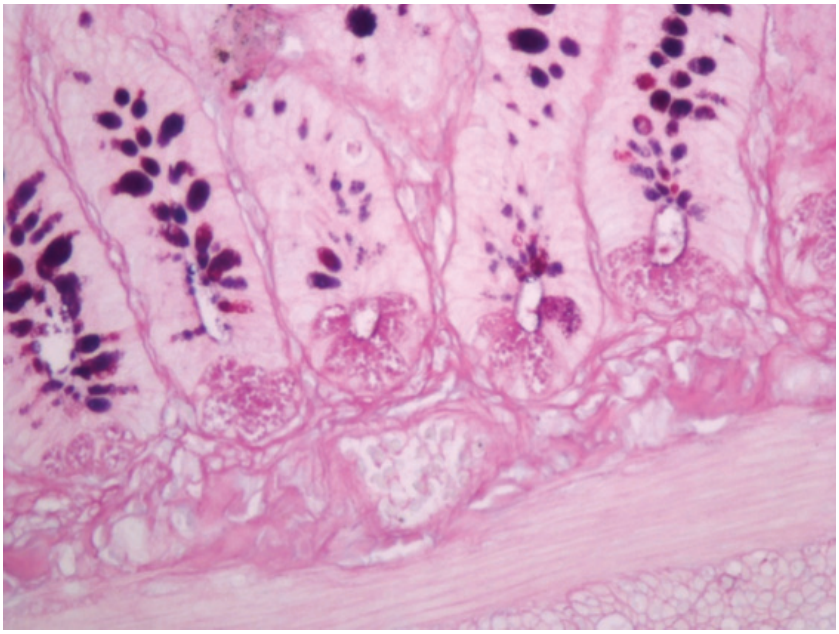

Figure 4.10. Paneth cells density at the seventh day after ileal resection and anastomosis in a rat not submitted to teduglutide treatment (periodic acid schiff-alcian blue pH 2.5 staining; original magnification 400x)

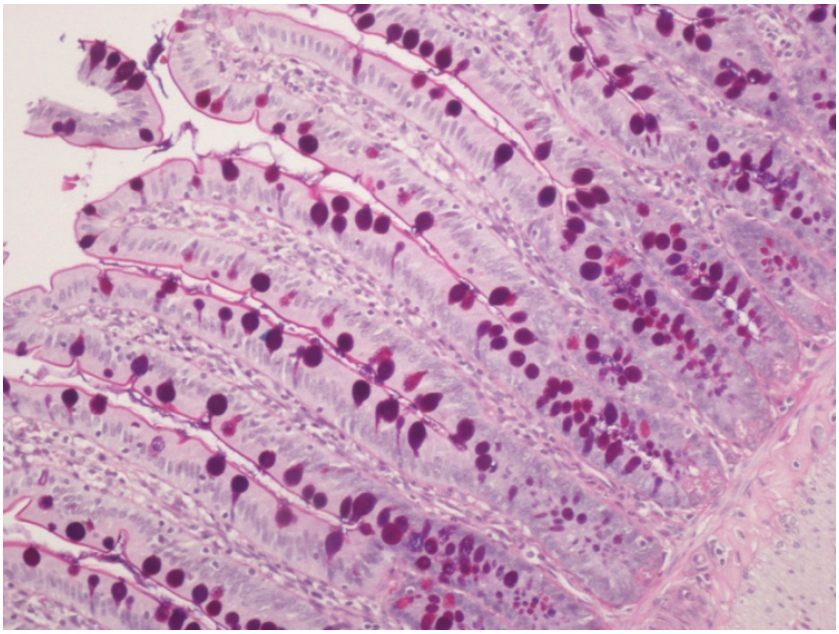

Figure 4.11. Goblet cells density at the seventh day after ileal resection and anastomosis in a rat not submitted to teduglutide treatment (periodic acid schiff-alcian blue pH 2.5 staining; original magnification 200x)

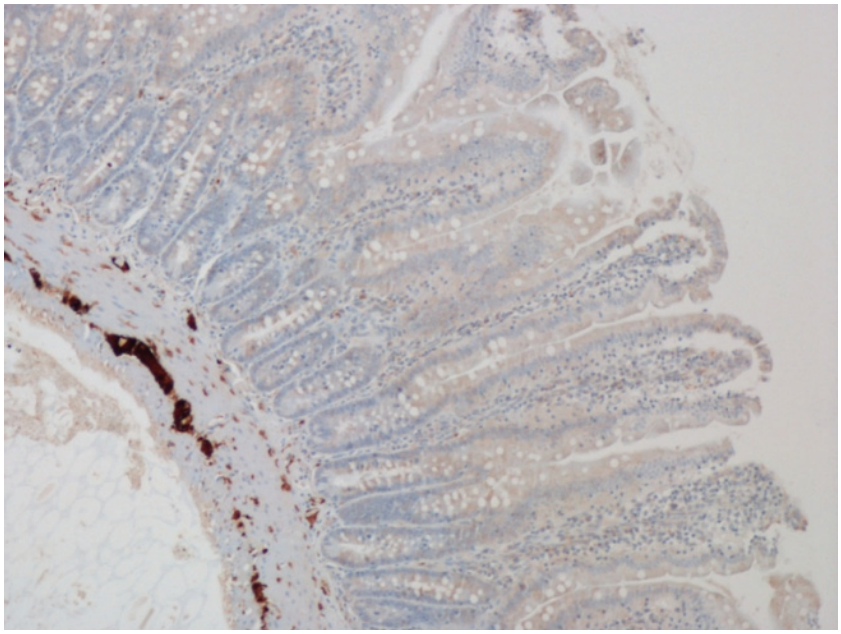

Figure 4.12. Expression of the glial marker S-100 in the submucosal and myoenteric plexus of the perianastomotic ileum, at the seventh day after ileal resection and anastomosis, in a rat not submitted to teduglutide administration (original magnification 100x)

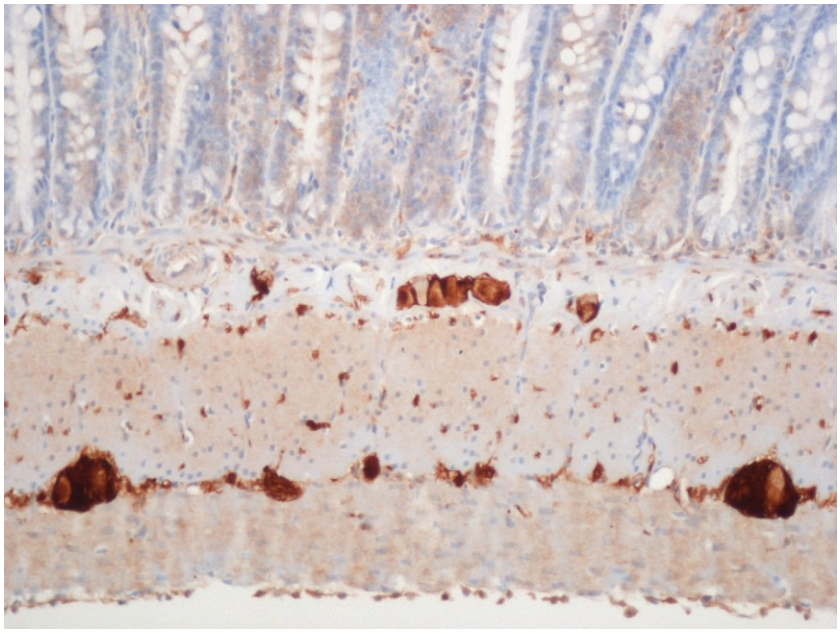

Figure 4.13. Glial cells and fibers of the submucosal and myoenteric plexus of the perianastomotic ileum, at the seventh day after ileal resection and anastomosis, in a rat not submitted to teduglutide administration (anti-S100 immunostaining; original magnification 200x)

Table 4.4. Subepithelial myofibroblasts, glial cells and nerve fibers in the perianastomotic segment

Score	Study groups			
	Third postoperative day		Seventh postoperative day	
	Ted –	Ted +	Ted –	Ted +
Subepithelial myofibroblasts (lamina propria)	2 ± 0 (2-2)	2.5 ± 1 (2-3)	2 ± 0 (2-2)	3 ± 1 (2-3)[a]
Glial cells and fibers (submucosal plexus)	2 ± 0 (2-2)	2 ± 0 (2-2)	2 ± 0 (1-3)	3 ± 1 (2-3)
Glial cells and fibers (myoenteric plexus)	2 ± 0 (2-2)	2 ± 0 (2-2)	2 ± 1 (1-3)	3 ± 1 (2-3)[b]

Subepithelial myofibroblasts of rats' ileum were evaluated with immunohistochemical staining with the monoclonal antibody anti-actin, smooth muscle. A semiquantitative assessment was performed in well-oriented crypt-villus axis of five randomly selected fields of vision, at 200x magnification, considering: "1" as normal morphology, distribution and density, "2" as moderate increase of distribution and density and "3" as marked increase of distribution and density. Glial cells and nerve fibers of rats' ileum were analyzed with immunohistochemistry through the expression of the glial marker S-100 in the submucosal and myoenteric plexus. A semiquantitative evaluation was undertaken in four sections of rats' ileum, at 100x magnification, considering: "1" as few glial cells and fibers with a regular morphology, distribution and density; "2" as numerous glial cells and fibers and "3" as dense networks of glial cells and fibers. Animals (n=28) were submitted to ileal resection and anastomosis and sacrificed on the third or seventh postoperative day. In "Ted+" groups, teduglutide was administered after the operation. Data were presented as median±interquartile range (minimum-maximum). Kruskal-Wallis test was used. [a] "*Ted* +" (seventh day) *vs.* "*Ted* -" (seventh day), $p<0.05$; [b] "*Ted* +" (seventh day) *vs.* "*Ted* +" (third day), $p<0.05$

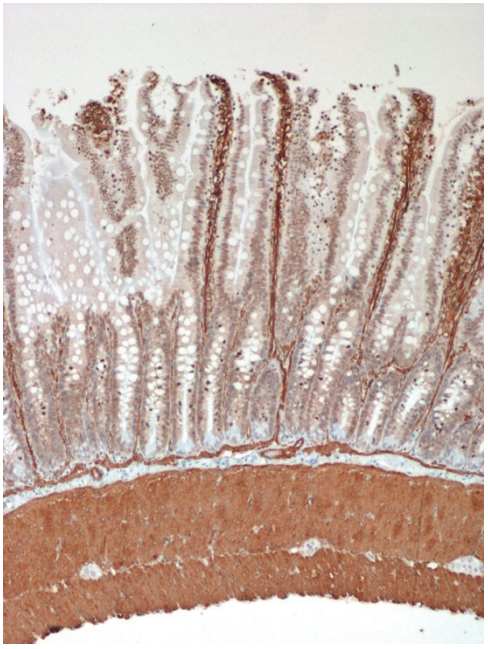

Figure 4.14. Cross-section of the perianastomotic ileum, at the seventh day after ileal resection and anastomosis, in a teduglutide-treated rat (anti-actin, smooth muscle; original magnification 100x)

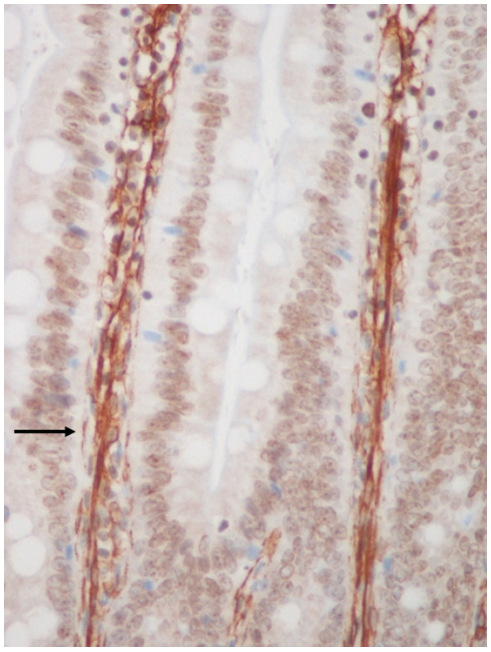

Figure 4.15. Subepithelial myofibroblasts *(arrow)* **in the lamina propria of the perianastomotic ileum, at the seventh day after ileal resection and anastomosis, in a teduglutide-treated rat** (anti-actin, smooth muscle; original magnification 400x)

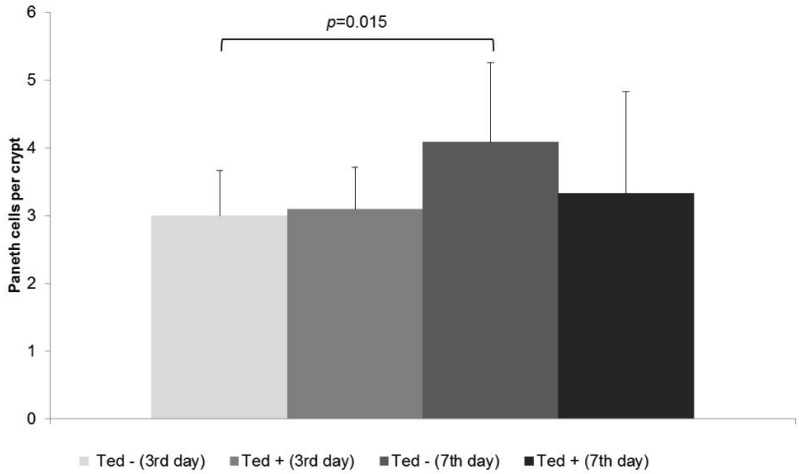

Figure 4.16. Paneth cells density in the rats' perianastomotic ileum using the periodic acid schiff-alcian blue pH 2.5 staining protocol. Paneth cells were counted in six contiguous and randomly selected longitudinal well-oriented sections of crypts, at 200x magnification (median±interquartile range). Animals (*n*=28) were submitted to ileal resection and anastomosis and sacrificed on the third or seventh postoperative day. In "*Ted+*" groups, teduglutide was administered after the operation. Kruskal-Wallis test with pairwise comparisons was used

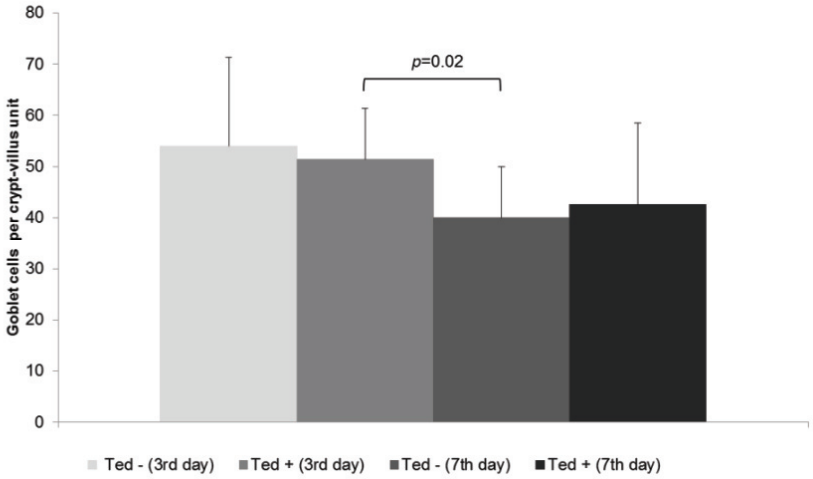

Figure 4.17. Goblet cells density in the rats' perianastomotic ileum using the periodic acid schiff-alcian blue pH 2.5 staining protocol. Goblet cells were counted in two randomly selected and contiguous, well-oriented, full-length crypt-villus units *per* animal, at 200x magnification (median±interquartile range). Animals (n=28) were submitted to ileal resection and anastomosis and sacrificed on the third or seventh postoperative day. In "*Ted+*" groups, teduglutide was administered after the operation. Kruskal-Wallis test with pairwise comparisons was used

Histological assessment has been considered an appropriate and very valuable outcome measure for the anastomotic healing study (Bosmans *et al.*, 2016).

The higher grade of fibrosis, the enhanced global collagen content in the wound, and the higher type I/type III collagens ratio (although not statistically significant) observed in this experiment at the seventh postoperative day were in accordance with the expected evolution of anastomotic healing (Rijcken *et al.*, 2014; Thompson *et al.*, 2006). In fact, an intensification of the fibrogenesis process occurs in the proliferation phase, when fibroblasts and myofibroblasts produce a more collagenous and less cellular matrix, increasing the tissue biomechanical resistence (Thompson *et al.*, 2006).

A significant increase of the neoangiogenesis index was observed in the perianastomotic segment of the teduglutide-treated animals, at the seventh day, confirming the proangiogenic effects of GLP-2 described in the literature (Dubé *et al.*, 2007).

Teduglutide administration during seven postoperative days was associated with a significantly more intense wound reepithelialization and an increase of the epithelial

proliferative activity (although not statistically significant). In fact, several studies demonstrated that exogenous GLP-2 prescription induces expansion of the intestinal epithelial surface, through stimulation of the epithelial cells proliferation in the crypts and inhibition of the apoptosis in crypts and villi (Drucker and Yusta, 2014; Janssen *et al.*, 2013; Dubé *et al.*, 2007).

Gordon and Sweet's impregnation technique suggested lower expression of type I collagen and higher content of type III collagen in the submucosa of teduglutide-treated animals at the seventh day. No statistically relevant effects on global type I/type III collagen ratio were evident in these animals. The interpretation of these results must consider the limitations of the Gordon and Sweet's staining method, which constitutes a semiquantitative morphometric assessment, although advantageous in allowing the evaluation of the content and topographic distribution of collagen in the different layers of ileum.

Majority of collagen, key component of extracellular matrix, is located at the submucosal layer, which ensures most of the biomechanical resistance of the anastomosis (Thompson *et al.*, 2006). In the intestine, types I and III collagens predomine and amount to 68% and 20%, respectively (Thompson *et al.*, 2006; Gelse *et al.*, 2003). Granulation tissue is characterized by an enhanced proportion of type III collagen (to approximately 30 to 40%) and a simultaneous decrease of type I collagen (Thompson, 2006). Anastomotic suture-holding capacity is transiently reduced in the first two or three days of the postoperative period, which is related to the increase of collagen degradation by matrix metalloproteinases; thereafter, in the proliferative phase of the healing process, strength increases due to enhanced *de novo* synthesis and deposition of collagen (Thompson, 2006).

Synthesis and deposition of collagens are complex processes (Gelse *et al.*, 2003). Fibrogenesis is completed only when collagen forms a stable, cross-linked and remodeled aggregation (Chen *et al.*, 2009; Gelse *et al.*, 2003). No necessary correlation exists between collagen content and mechanical strength of the anastomosis (Rijcken *et al.*, 2014; Hendriks *et al.*, 1990), and other factors, such as collagen subtypes and cross-linking, also appeared to be relevant (Rijcken *et al.*, 2014).

Paneth and goblet cells, subepithelial myofibroblasts and enteric nervous system have deserved less interest in the anastomotic healing research. Nevertheless, Paneth cells and goblet cells have an important influence in the microbiota-host interactions and in the intestinal repair (Bosmans *et al.*, 2017; Hou *et al.*, 2017). In fact, recent evidence points to a strong impact of gut microbiota on the intestinal anastomotic healing (Bachmann *et al.*, 2017). Previous studies suggested that teduglutide preferentially increase the proportion of enterocytes rather goblet cells (although this effect appears to be model specific), whereas others reported an increase of mucin-positive cells after chronic treatment (Rowland and Brubaker, 2011). Furthermore, teduglutide seems to induce wingless/β-catenin signaling pathway (Drucker and Yusta, 2014) that is involved the promotion of Paneth cells differentiation (Bloemendaal *et al.*, 2016). Additionally, GLP-2 receptors in subepithelial myofibroblasts and enteric neurons are thought to play a crucial role in the mediation of this growth factor effects (Drucker and Yusta, 2014; Janssen *et al.*, 2013; Rowland and Brubaker, 2011). Therefore, investigation of the response of those cells to teduglutide treatment in the perioperative context seems to be justified.

In this study, a significant reduction of the density of goblet and Paneth cells in the postoperative period was observed. Teduglutide had no relevant influence of on goblet and Paneth cells density indexes.

Goblet cell secretion exerts an important role in the regeneration of the functional epithelial mucous layer, a dynamic structure determinant in the maintenance of the intestinal defense barrier. A functional mucous layer influences positively the healing of colonic anastomosis (Bosmans *et al.*, 2017; Fay *et al.*, 2017). Mice deficient in the mucin 2 gene (*Muc2*) lack a functional mucous layer and demonstrated higher rate of leakage after proximal colonic anastomosis; as well as, higher plasma levels of intestinal fatty acid-binding protein (a marker of enterocyte damage); tendency for more intense leucocytes infiltration and less collagen deposition and neoangiogenesis; and a tendency towards higher systemic bacterial load at the third postoperative day (Bosmans *et al.*, 2017).

Paneth cells are highly specialized secretory cells, located at the base of the crypts and intercalated between crypt base epithelial stem cells. In addition to its role as key

mediators of host-microorganisms' interactions, through the production of cryptidins, defensins and lysozyme, Paneth cells are critical elements of epithelial stem cell niche, through the secretion of growth signaling factors crucial for the stem cells maintenance, including canonical wingless and notch ligands, epidermal growth factor and transforming growth factor β (Hou *et al.*, 2017; Tesori *et al.*, 2013; Smith *et al.*, 2012). Loss of Paneth cells *in vivo* origins the reduction of Lgr5-positive stem cells pool and the presence of Paneth cells in cultures *in vitro* increases the capacity of those cells to form multipotent and self-renewing organoids (Sato *et al.*, 2011). Recently, Parry L *et al* (Parry *et al.*, 2013) demonstrated the important participation of Paneth cells in the mediation of epithelial response to injury, in two mouse models of deletion of the transcription factor β-catenin within the crypt; Paneth cells were very sensitive to β-catenin loss and their absence compromised the recovery of the crypts from the damage (Parry *et al.*, 2013). In 2012, Yilmax OH *et al* (Yilmaz *et al.*, 2012) demonstrated that the stem cell niche regulates the size and activity of intestinal epithelial stem cells pool according to the nutrient availability, through repression of mammalian target of rapamycin complex 1 (mTORC1) signaling in Paneth cells. In their study, caloric restriction was associated with increase of proliferative Lgr5-positive cells and Paneth cells, mild mucosal atrophy and reduction of transit-amplifying proliferating cells (Yilmaz *et al.*, 2012).

Importance of biomechanical forces and mechanotransduction in the intestinal healing process has been documented (Kovalenco *et al.*, 2012). In present study, S-100 expression in glial cells and fibers increased at the seventh day (in relation with baseline), both on the submucosal and the myoenteric plexus. Recently, the regenerative potential of the enteric nervous system after ileal anastomosis was also suggested by Pfeifle VA *et al* (Pfeifle *et al.*, 2017), in a rat model, although with a faster recovery of the myoenteric plexus in comparison with the submucosal plexus.

In this analysis, subepithelial myofibroblasts were identified by α-smooth muscle actin expression, morphologic and location criteria, without recourse to other markers (such as vimentin or CD90/Thy1) or to ultrastructural characteristics (Roulis *et al.*, 2016; Mifflin *et al.*, 2011). Teduglutide was associated with an increase of subepithelial myofibroblasts density score at the seventh day. Subepithelial myofibroblasts seem to constitute relevant elements in the regeneration process. Previous studies suggest that

subepithelial myofibroblasts may regulate epithelial stem cell function, as constituents of the stem cell niche (Hou *et al.*, 2017; Roulis *et al.*, 2016); participate in extracellular matrix remodeling and mechanical regulation of the tissues; and be involved in antigen presentation and immunoregulation (Roulis *et al.*, 2016). Lamina propria mesenchymal cells, including subepithelial myofibroblasts, seem to express bone morphogenic protein signaling (bmp) antagonists (including noggin, gremlin1, gremlin2, and chordin-like1), non-canonical wingless (wnt) molecules (such as wnt 2b, wnt 4, wnt 5a, and wnt 5b) and the wnt/β-catenin agonists R-spondin 1 or 2. Therefore, they are considered to contribute for the maintenance of proliferating and non-differentiated epithelial stem cells and to the equilibrium between proliferation and differentiation. In fact, wnt signaling, transduced by β-catenin/transcription factor 4 (Tcf4) is fundamental for the maintenance of proliferating, non-differentiated status of stem cells in the crypts. Bmp signaling antagonizes wnt/β-catenin pathway, inhibiting self-renewal and promoting differentiation. Non-canonical wnt expression has been considered to participate in the control of wnt/β-catenin signaling in the stem cell niche, adjusting epithelial proliferation and differentiation. Subepithelial myofibroblasts are also considered to interact with immune cells types and to be able to sense inflammatory, bacterial and damage signals, activating tumor progression locus 2 (Tpl2)-cyclooxygenase 2 (Cox2)-prostagladin E2 (PGE2) pathway and promoting epithelial cells proliferation (Roulis *et al.*, 2016).

In current investigation, short extension of the ileal resections (10-cm lenght), lower than 20% of total small bowel length (Pénzes and Skála, 1977; Miller, 1971), allowed adequate tissue harvesting for baseline analysis without inducing a short-bowel syndrome. Extent of treatment (three or seven days) was chosen based on the expect course of the intestinal anastomotic healing, corresponding presumably to the predominantly inflammatory and proliferative phases (Rijcken *et al.*, 2014). Besides, the intestinotrophic effects of GLP-2 and its analogues have been demonstrated, in rat models, after treatment periods of three to ten days (Kaji *et al.*, 2008). Proliferative effects of GLP-2 or its long-acting analogues have been detected, indeed, as early as six hours after administration to mice (Austin *et al.*, 2016).

Present study did not include the mechanical evaluation of anastomotic repair, namely the determination of the bursting pressure, measure of anastomotic integrity, and of

the tensile strength, reflex of suture-holding capacity of the perianastomotic tissue (Pommergaard *et al.*, 2014; Thompson *et al.*, 2006). Although widely used, often as *major* end points, these parameters demonstrated relevant limitations related with the heterogeneity, reproducibility and accuracy of the determination methods, particularly in small animals (Pommergaard *et al.*, 2014; Vakalopoulos *et al.*, 2013), and may interfere with subsequent histological and biomolecular analysis. Furthermore, anastomotic bursting pressure may not correlate with the integrity of the anastomosis and the clinical outcome (Vakalopoulos *et al.*, 2013).

Despite several limitations (including the small number of cases and the semiquantitative analysis), results of present investigation denote a favoring impact of teduglutide short-term postoperative administration on the reepithelization and neoangiogenesis events of the proliferative phase of intestinal anastomotic repair. Effects of teduglutide on the fibrogenesis process deserve more investigation.

Additional studies are necessary to clarify the potential benefit of teduglutide in the high-risk context of intestinal anastomotic repair, including its efficacy, safety and applicability.

Chapter 5

Effects of the perioperative administration of teduglutide on the cellular viability and death, oxidative stress and inflammatory response

This chapter was partially published as:

Costa BP, Gonçalves AC, Abrantes AM, Matafome P, Seiça R, Sarmento-Ribeiro AB, Botelho MF, Castro-Sousa F: Intestinal inflammatory and redox responses to the perioperative administration of teduglutide in rats. *Acta Cir Bras*. 2017;32(8):648-661. Doi 10.1590/s0102-865020170080000007.

5.1. Abstract

Teduglutide is an intestinotrophic long-acting modified form of glucagon-like peptide 2, authorized for pharmacological rehabilitation of short-bowel syndrome. Present study intended to investigate the inflammatory and redox responses to teduglutide on an animal model of intestinal anastomosis and laparotomy. Wistar rats (*n*=62) were allocated into four groups: "*Ileal Resection and Anastomosis*" *versus* "*Laparotomy*", each one split into "*Postoperative Teduglutide Administration*" *versus* "*No Treatment*"; and euthanized at the third or the seventh day. Ileal and blood samples were recovered at the baseline and at the sacrifice. Flow cytometry was used to study the inflammatory response (IL-1α, MCP-1, TNF-α, IFN-γ and IL-4 concentrations), oxidative stress (cytosolic peroxides, mitochondrial reactive species, intracellular glutathione and mitochondrial membrane potential levels) and cellular viability and death (with annexin-V/propidium iodide double staining). Postoperative teduglutide treatment was associated with higher cellular viability index and lower early apoptosis ratio at the seventh day; higher cytosolic peroxides level at the third day and mitochondrial generation of reactive species at the seventh day; as well as higher tissue concentration of IL-4 and lower tissue pro-to-antiinflammatory cytokines ratio at the seventh day. Those findings suggested an intestinal prooxidative and antiinflammatory influence of teduglutide on the perioperative context with a potential interference in the intestinal anastomotic healing.

5.2. Introduction

Teduglutide is a long-acting recombinant analogue of human glucagon-like peptide 2 (GLP-2) authorized for the pharmacological rehabilitation of short-bowel syndrome (Drucker and Yusta, 2014). GLP-2 has been considered to have an important antiinflammatory activity, documented in animal models of chemically induced ileitis and colitis, promoting the reduction of local expression of interleukin (IL)-1β, interferon-γ (IFN-γ) and tumor necrosis factor-α (TNF-α) and the increase of IL-10 and IL-4 levels (Ivory *et al.*, 2008; Sigalet *et al.*, 2007). Similarly, other authors observed improvement of the damage score and decrease of tissue expression of IL-1, IL-7 and TNF-α, with polyethylene glycosylated porcine GLP-2, in a rodent model of ulcerative colitis (Qi *et al.*, 2017). Furthermore, the antiinflammatory effects of GLP-2 were also recently demonstrated on an experimental rat model of necrotizing enterocolitis, with the reduction of ileal interstitial TNF-α and IL-6 levels, and the improvement of clinical sickness score and survival rate (Nakame *et al.*, 2016).

Intestinal inflammatory and redox responses to the perioperative administration of teduglutide are not yet well understood. It may be hypothesized that teduglutide influences inflammatory and redox reactions with a potential interference in the intestinal anastomotic healing. Present study intended to investigate the inflammatory and redox responses to teduglutide short-term perioperative treatment on an animal model of intestinal anastomosis and laparotomy.

5.3. Methods

5.3.1. Study layout

Experiment was ratified by the Ethics Committee of the Faculty of Medicine, University of Coimbra, Coimbra, Portugal (Official Letter n° 32-06-2009) and implemented in consonance with the national recommendations for animals' safety.

Adult male Wistar *albinus* rats, weighting 250 to 300 g, were randomly allocated into four groups: "*Ileal Resection and Anastomosis*" ("*Res*") *versus* "*Laparotomy*" ("*Lap*"), each one split into "*Postoperative Teduglutide Administration*" ("*Ted +*") *versus* "*No Treatment*"

("*Ted* -"). Evaluation was accomplished at the operation and euthanasia, at the third or the seventh postoperative day [presumptively consonant with the inflammatory and proliferative stages of the intestinal anastomotic repair (Rijcken *et al.*, 2014)], with ileal harvesting and blood collection. Blinded assessment was guaranteed in all the laboratorial analysis. All the operative interventions were executed by the same surgeon, after two hours solid fasting, with clean surgical technique and under anaesthesia with an intraperitoneal injection of ketamine hydrochloride (75 mg/kg; Pfizer Inc., New York, USA) and chlorpromazine (3 mg/kg; Laboratórios Vitória, Amadora, Portugal).

In "*Res*" groups, a 10-cm length ileal resection was completed, retaining distal 5 cm, through a 3-cm midline laparotomy, and concluded with an end-to-end anastomosis with eight equidistant full-thickness polydioxanone USP 6/0 stitches (PDS II, Ethicon, Johnson-Johnson Intl., Cincinnati, USA); abdominal wall was closed with muscle-aponeurotic and cutaneous continuous sutures of braided coated polyglactin 910 USP 4/0 (Surgilactin, Sutures Limited, Wrexham, UK) and natural silk USP 4/0 (Surgisilk, Sutures Limited), respectively. In "*Lap*" groups, a 3-cm midline laparotomy was carried out with mild handling of the small bowel.

In the first postoperative day, 5% glucose in water at a 1:1 ratio was provided and, then, *ad libitum* rodent diet and hydration were restored. At the third or seventh postoperative day, animals were euthanized by cervical displacement and a relaparotomy with ileal resection was undertaken (10 cm length, conserving distal 3 cm). In "*Ted* +" groups, teduglutide (American Peptide Company, Sunnyvale, California, USA) was applied subcutaneously in the postoperative period (including on the day of the operation), 200 μg/kg/day, after preparation in agreement with the manufacturer's recommendations.

5.3.2. Tissue and blood sampling

Three similar longitudinal strips of the most distal 4-cm length of each ileal specimen, each one corresponding to one third of the circumference, were carefully retrieved for cell isolation procedure, homogenization and 10% formaldehyde fixation,

respectively. In "*Res*" groups, tissue samples obtained at the sacrifice corresponded to the anastomotic segment and included the anastomosis in the middle. Tissue baseline values of "*Res*" groups were considered for comparison with postoperative results of the "*Lap*" groups. Blood samples of 1 ml were collected before the operations, into ethylenediaminetetraacetic acid (EDTA)-containing tubes, stabilized with 0.1 mg/ml of aprotinin from bovine lung (Sigma-Aldrich, Sintra, Portugal) and 0.037 mg/ml of nicotinonitrile dihydrochloride hydrate (Sigma Aldrich), and centrifuged for 20 minutes at 1500x *g* and 4°C. Plasma aliquots were maintained at -80°C.

5.3.3. Intestinal tissue homogenization

Briefly, fragments from one ileal longitudinal strip, with approximately 1 mm, were rapidly introduced in a mixture of protease inhibitors (1 ml/100 mg) and submitted to mechanical homogenization using a little microstrainer. Inhibitors cocktail was previously prepared by adding aprotinin from bovine lung (Sigma-Aldrich), leupeptin hemisulfate salt (Sigma-Aldrich) and pepstatin A (Sigma-Aldrich) (1 μl of each, all diluted in a 10 mg/ml stock concentration) to 10 ml of phosphate buffered saline 7.4 (PBS 7.4, Gibco, Life Technologies, Carlsbad, California, USA) and stored on ice. Preparation was sonicated twice with one short pulse of ten seconds (50% amplitude modulation on vector rotation), cooled during ten seconds and distributed for two tubes of 1.5 ml. Sonication (one pulse of ten seconds) was repeated and centrifugation was undertaken, 14000x *g*, for ten minutes, at 4°C. Supernatant was removed to a new tube (pellet was preserved on ice for posterior RNA extraction in further studies). Centrifugation was repeated twice and supernatant was removed, aliquoted (100 μl) and stored at -80°C until further use.

5.3.4. Intestinal tissue dissociation and cell separation procedure

Cells were isolated from one ileal longitudinal strip, immediately after excision, by a standardized adaptation of the collagenase/dispase isolation technique proposed by

Evans GS *et al* (Evans *et al.*, 1992) and Dekaney CM *et al* (Dekaney *et al.*, 2007; Dekaney *et al.*, 2005), formely delineated in the Chapter 3, to produce a preparation mainly composed of epithelial and some mesenchymal cells.

5.3.5. Cellular viability and death study

Cell viability and death were analyzed by flow cytometry that is considered the most adequate method to study these processes on an individual cell basis, providing quantitative data with high efficiency and low operator-dependent interferences (Galluzzi *et al.*, 2012; Kroemer *et al.*, 2009).

Annexin-V (AV) is a 35 kDa calcium-dependent phospholipid-binding protein that adheres with high affinity to phosphatidylserine (Sgonc and Gruber, 1998). Phosphatidylserine, a phospholipid normally found at the inner surface of the plasma membrane of viable nucleated cells, is exposed at the surface of cells undergoing apoptosis, by translocation from the inner to the outer leaflet of the plasma membrane, and serves as a recognition signal for elimination of apoptotic cells by macrophages. Therefore, fluorescein-isothiocyanate-labeled annexin-V is a marker of phosphatidylserine extracellular exposure, an apoptotic signal on the cell surface, which occurs early in the apoptotic cycle (Galluzzi *et al.*, 2012; Kroemer *et al.*, 2009; Sgonc and Gruber, 1998).

Annexin-V assay is rapid, specific for an early event in the apoptotic process and does not require fixation. However, phosphatidylserine exposure is not exclusive of apoptotic cell death (it also constitutes an early characteristic of parthanatos and netosis); it may be reversible, independent from apoptosis (and even from cell death) and impaired in autophagy-deficient cells in apoptosis. Furthermore, Annexin-V may bind to intracellular phosphatidylserine when plasma membranes are ruptured (Kroemer *et al.*, 2009).

Propidium iodide (PI), a plasma membrane-impermeant fluorochrome in viable cells, binds stoichiometrically to deoxyribonucleic acid (DNA), intercalating between the bases, of the late apoptotic and necrotic cells (which are characterized by the loss of plasma membrane integrity and the disruption of nuclear membrane), causing red

fluorescence in the nucleus (Aubry *et al.*, 1999). Propidium iodide is used as exclusion vital chromatinophilic dye to quantify cells with sub-G1 DNA content in presence of plasma membrane permeabilization (Galluzzi *et al.*, 2012; Kroemer *et al.*, 2009).

In this experiment, annexin-V/propidium iodide double staining was used to evaluate viability and death in isolated cells, with the Annexin-V-FITC Apoptosis Detection Kit (Immunostep, Salamanca, Spain). Briefly, one million cells were washed once with 1 ml of phosphate buffered solution (PBS, pH 7.4, Gibco, Life Technologies, Carlsbad, California, USA) by centrifugation at 1000x *g* for five minutes and resuspended in 100 µl of cold binding buffer. Binding buffer was prepared with 10 mM 4-(2-hydroxyethyl)piperazine-1-ethanesulfonic acid solution (Hepes)/sodium hydroxide (pH 7.4), 140 mM sodium chloride, 2.5 mM calcium chloride. In this assay, one million cells were incubated in binding buffer with 5 µL of fluorescein-isothiocyanate-labeled annexin-V and 5 µl of propidium iodide, during 15 minutes, at room temperature, in the dark, following the manufacturer's recommended protocol. After incubation time, cells were diluted in 400 µL of ice-cold binding buffer, and analyzed by flow cytometry within one hour. Subsequently, cells were excited at a wavelength of 525 nm for annexin-V and 640 nm for propidium iodide. Fluorescent green staining of the plasma membrane indicated apoptosis by release of annexin-V to the outer leaflet of the plasma membrane; red staining of deoxyribonucleated acid with propidium iodide indicated the loss of plasma membrane integrity typical of late apoptotic and necrotic cells.

Analysis was accomplished using a FACSCalibur flow cytometer (Becton Dickinson, San Jose, California, USA). For each assay, $1x10^6$ cells were used. At least 10.000 events were collected by acquisition using CellQuest software (version 0.3, BD BioSciences, San Jose, California, USA) and analyzed using Paint-a-Gate 3.02 software (BD BioSciences). Cells were defined according to the positivity for annexin-V (AV) and/or propidium iodide (PI) labelling. Results were presented as percentage of early apoptotic (AV+/PI-), late apoptotic/necrotic (AV+/PI+), necrotic (AV-/PI+) and viable cells (AV-/PI-).

5.3.6. Oxidative stress study

Subsequent parameters were analysed in the isolated cells from rats' ileum by flow cytometry: peroxides levels in cytosol, with 2',7'-dichlorodihydrofluorescein diacetate ($DCFH_2$-DA) probe; reactive species production in the mitochondria, with dihydrorhodamine 123 (DHR 123) probe; intracellular reduced glutathione (GSH) content, with mercury orange staining; and mitochondrial membrane potential, with 5,5',6,6'-tethrachloro-1,1',3,3'-tethraethylbenzimidazolcarbocyanine iodide probe (JC-1). Analysis was fulfilled using the flow cytometer and software outlined above, conforming to formerly detailed techniques (Gonçalves *et al.*, 2013; Almeida *et al.*, 2008). For each assay, $1x10^6$ cells were used; at least 50.000 events were collected. Results were revealed as mean fluorescence intensity (MFI) values. Experiments were carried out in duplicate.

5.3.6.1. Monitoring reactive oxygen species generation in the cytosol

Intracellular reactive oxygen species production was measured with the fluorochrome 2',7'-dichlorodihydrofluorescein diacetate ($DCFH_2$-DA) probe, which is the most widely used fluorochrome for detection of intracellular oxidative stress (Dikalov *et al.*, 2014; Kalyanaraman *et al.*, 2012; Gomes *et al.*, 2005). $DCFH_2$-DA is a stable, non-fluorescent and cell permeable compound that is converted to 2',7'-dichlorodihydrofluorescein ($DCFH_2$) by intracellular esterases; when oxidized by reactive oxygen species, the deesterified product is converted to 2',7'-dichlorofluorescein (DCF), a fluorescent compound with excitation/emission wavelengths of 498/522 nm, respectively (Gomes *et al.*, 2005). Despite some limitations, $DCFH_2$-DA was considered a simple, rapid and sensible probe for intracellular reactive oxygen species detection, including hydrogen peroxide (H_2O_2; in presence of cellular peroxidase), peroxynitrite ($ONOO^-$) and hydroxyl radical ($HO^{\cdot}$) (Gomes *et al.*, 2005). $DCFH_2$-DA assay is also used to analyze cell death (Kroemer *et al.*, 2009). Overgeneration of intracellular radical oxygen species, whose levels $DCFH_2$-

DA was considered to reflect, precedes often the mitochondrial permeability transition occurring in intrinsic apoptosis and regulated necrosis.

The assay was performed according to a previously stated procedure (Almeida *et al.*, 2008; Halliwell and Whiteman, 2004) with the $DCFH_2$-DA probe (Molecular Probes, Life Technologies Corporation, Carlsbad, USA). A cell suspension of $1x10^6$ cells *per* milliliter was incubated with 5 μM of $DCFH_2$-DA dissolved in dimethylformamide 1 mM, to obtain a final concentration of 5 μM, for 45 minutes, at 37°C, in a humidified atmosphere of 5% carbon dioxide, in the dark. Cells were washed with phosphate buffered saline pH 7.4 (PBS 7.4; Gibco, Life Technologies Corporation) by centrifugation at 300x *g* for five minutes and resuspended in 400 μl of the same buffer solution. Analysis was performed with an excitation and emission wavelengths of 488 and 525 nm, respectively.

5.3.6.2. Monitoring reactive species production in the mitochondria

Mitochondria reactive species (RS) were detected with dihydrorhodamine 123 (DHR 123) probe (Cardoso *et al.*, 1998). DHR 123 is a probe widely used to detect several reactive species production in the mitochondria (including hypochlorous acid and peroxynitrite) (Gomes *et al.*, 2005). DHR 123 is a nonfluorescent, noncharged dye that easily penetrates cell membranes and is oxidized, by intracellular oxidants, to rhodamine 123, a fluorescent cationic and lipophilic compound, with excitation and emission wavelengths of 505 and 529 nm, respectively, which tends to accumulate in the mitochondria, held there by the membrane potential (Gomes *et al.*, 2005).

DHR123 (DHR123, Life Technologies Corporation, Carlsbad, USA) was added to one million cells *per* milliliter in phosphate buffered saline, at a final concentration of 5 μg/ml and incubated for 10 minutes in a shaking water bath, at 37°C, in the dark. Then, cells were washed, ressuspended in phosphate buffered saline, and kept on ice for immediate detection by flow cytometry using the previously described equipment.

5.3.6.3. Determination of total intracellular reduced glutathione content

Determination of the intracellular glutathione (GSH) expression, the most abundant nonprotein thiol in mammalian cells and an important antioxidant defense, was performed by flow cytometry using the fluorescent compound mercury orange [1-(4-chloromercuryphenoylazo)-2-napthol]. This compound binds stoichiometrically to mercurial sulfhydryl groups of intracellular nonprotein thiols with formation of fluorescent products. Restriction of staining time allows a selective marking, as this compound reacts faster with GSH than with the sulfhydryl groups of proteins (five minutes *versus* eight hours, approximately) and the reaction product emits an intense red fluorescence when excited with an argon laser at a wavelength of 488 nm (O'Connor *et al.*, 1988).

One million of cells were washed with phosphate buffered saline by centrifugation, 300x *g*, five minutes and resuspended in 1 ml of phosphate buffered saline. Cells suspension was incubated with 4 μL of mercury orange (MO; Sigma-Aldrich, Sintra, Portugal) in acetone (Sigma-Aldrich, Sintra, Portugal) 10 mM, at a final concentration of 40 μM, for 15 minutes, at room temperature, in the dark. After washing the cells twice with cold phosphate buffered saline by centrifugation at 300x *g* for five minutes, cells were resuspended in 400 μl of the same buffer solution and kept on ice. Analysis was performed at the excitation wavelength of 488 nm, by flow cytometry, using the aforementionated equipment.

5.3.6.4. Mitochondrial membrane potential measurement

Integrity of the inner mitochondrial membrane was evaluated by the gradient potential across this membrane, the mitochondrial membrane potential ($\Delta\psi$mt), using the fluorescent probe 5,5',6,6'-tethrachloro-1,1',3,3'-tethraethylbenzimidazolcarbocyanine iodide (JC-1) and flow cytometry, according to a previously outlined method (Martinou and Youle, 2011; Almeida *et al.*, 2008). This lipophilic cationic probe is a potentiometric dye able to selectively enter the mitochondria (Gomes *et al.*, 2005). JC-1 mitochondrial membrane potential-sensitive fluorochrome allows the

visualization of the energized mitochondria, monitorization of the mitochondrial membrane potential through the change of emission spectra and detection of the mitochondrial membrane permeabilization (Galluzzi *et al.*, 2012; Kroemer *et al.*, 2009). Mitochondrial membrane potential determines the selective uptake of JC-1 by mitochondria, emitting fluorescence at different wavelengths. When the membrane potential is high, aggregate formation in the mitochondria is predominant and red/greenish-orange fluorescence (590 nm) is emitted after excitation at 490 nm; on the contrary, as the mitochondrial membrane potential decreases, or if the membrane is depolarized, JC-1 forms monomers in the cytosol that emit green fluorescence (529 nm). Thus, the ratio of red/greenish-orange and green fluorescence determined by flow cytometry, which corresponds to aggregates/monomers quotient, provides an estimate of the mitochondrial membrane potential. An increase of the aggregates/monomers ratio indicates an increase in the mitochondrial membrane potential (Gomes *et al.*, 2005). Additionally, JC-1 constitutes a cytofluorometric method for cells viability and death analysis, contributing to the definition of cell death (through identification of irreversible mitochondrial transmembrane potential dissipation) and the characterization of death modality, as occurs in intrinsic apoptosis and parthanatos (Galluzzi *et al.*, 2012; Kroemer *et al.*, 2009).

Briefly, one million cells were washed with phosphate buffered saline through centrifugation at 300x *g* during five minutes, ressuspended in 1 ml of phosphate buffered saline and incubated with 1 μl of JC-1 dye (Molecular Probes, Life Technologies Corporation, Carlsbad, USA), in dimethyl sulfoxide (DMSO) (Sigma-Aldrich, Sintra, Portugal) at 5 mg/ml concentration, for 15 minutes, at 37°C, in the dark. At the end of the incubation period, cells were washed twice in cold phosphate buffered saline by centrifugation at 300x *g* for five minutes, ressuspended in 400 μl of same buffer solution and analyzed by flow cytometry. Results were presented as aggregates/monomers fluorescence intensities ratio, calculated through the quotient between mean fluorescence intensities (MFI) of aggregates and monomers.

5.3.7. Evaluation of tissue and systemic inflammatory response

A multiplex cytokine bead array approach was used to measure the expression of inflammatory cytokines, using the Rat Cytokine 5plex Kit FlowCytomix (eBioscience, Affymetrix, Vienna, Austria) produced for quantification of rats' homogenized tissue and plasma levels of interleukine-1α (IL-1α), macrophage chemo-attractant protein (MCP-1), tumour necrosis factor-α (TNF-α), interferon-γ (IFN-γ) and interleukine-4 (IL-4).

Flow cytometric multiplexed bead assay is characterized by high sensitivity, specificity, reproducibility and cost-efficiency (Tighe *et al.*, 2013). Succinctly, the biological test sample and a recombinant protein standard mixture are combined with a mixture of sets of micrometer scale beads, each impregnated with a fluorescent dye, stably coated with a capture antibody to the desired analyte (cytokine) to be detected. Beads can be differentiated by their sizes and by their distinct spectral addresses. After incubation and washing, a mixture of labeled detection antibodies (biotin-conjugated) specific for the desired cytokines and labeled with the same reporter dye (streptavidin-phycoerythrin) is added. After further washing, the detection antibody-cytokine-capture antibody-bead complex is analyzed through a flow cytometer. Each bead has the potential to have both the cytokine captured, and the specific detection antibody reporter-dye bound. Proportion of reporter bound depends upon cytokine concentration in the original biological solution allowing quantitative analysis of each bead. Calibration to bead sets incubated with dilution series of analytes allows quantitative interpretation (Tighe *et al.*, 2013).

In the Rat Cytokine 5plex Kit FlowCytomix, analyte sensitivity [defined as the concentration resulting in a fluorescent intensity significantly higher than that of the dilution medium (mean+2standard deviations)] was determined to be the following: IL-1α=8.5 pg/ml, MCP-1=0.8 pg/ml, TNF-α=4.3 pg/ml, IFN-γ=0.8 pg/ml and IL-4=0.3 pg/ml. Biological samples standardization was attentive to increase stability and representativeness of the cytokine measurement. Reagents were prepared following the manufacturer's recommendations (described in detail in Supplementary Data S1). Standard and test samples were analyzed using a FACSCalibur flow cytometer (Becton Dickinson, San Jose, California, USA) as stated in the producer's instructions. Mean

fluorescence intensities (MFIs) of the serially diluted standard samples were calculated and used to generate the standard curves of each cytokine that model protein concentration as a function of the MFI. Cytokine concentrations present in the test sample were calculated, using the corresponding standard curves and dilution factors. All the samples were run in duplicate. Results were presented in pg/ml. Tissue concentrations were normalized to the total protein content of the sample, estimated by the bicinchoninic acid protein assay (Smith *et al.*, 1985) recurring to bovine serum albumin as standard, and expressed as pg/μg protein. Pro-to-antiinflammatory cytokines ratio ([IL-1α]+[TNF-α]+[IFN-γ]/[IL-4]) and T-helper 1 lymphocytes (Th1)-to-T-helper 2 lymphocytes (Th2) cytokines quotient ([TNF-α]+[IFN-γ]/[IL-4]) were calculated (Ramirez *et al.*, 2013; Menger and Vollmar, 2004).

5.3.8. Bicinchoninic acid protein assay

Total protein content of the homogenate of each tissue specimen was determined by the bicinchoninic acid protein assay (Smith *et al.*, 1985) using bovine serum albumin as reference. Bicinchoninic acid is a stable water-soluble compound capable of origin an intense purple chromophore complex with cuprous ion in an alkaline milieu. Bicinchoninic acid allows monitoring cuprous ions (Cu^{+}) produced in the reaction of proteins with alkaline cupric ions (Cu^{2+}) (biuret reaction), creating chromophore complexes (that display a strong absorbance at 562 nm) proportional to a broad range of protein concentrations. Bicinchoninic acid protein assay is a simple, high sensitivity, one-step analysis, less susceptible to common interferences (like nonionic detergents and buffer salts) than the Lowry's technique (Reichelt *et al.*, 2016; Sapan *et al.*, 1999; Smith *et al.*, 1985).

In summary, protocol included the preparation of a working mixture of bicinchoninic acid solution (containing bicinchoninic acid, sodium carbonate, sodium tartrate and sodium bicarbonate in 0.1N sodium hydroxide, pH 11.25) and 4% copper sulphate [4% (w/v) $CuSO_4.5H_2O$], in a proportion of 50:1, and of calibration protein standards from bovine serum albumin (2000, 1500, 1000, 750, 500, 250, 125 and 25 μg/ml). All protein standards (25 μl of each) and the biological sample (5 μl of the homogenate in 20 μl of

water) were pipetted into a microwell plate, and 200 μl of the working mixture was added mixing thoroughly. Plate was covered, incubated at 37°C, for 30 minutes, in a water bath, and then, cooled to room temperature. Absorbance at 562 nm of all the samples was measured within ten minutes in an enzyme-linked immunosorbent assay (ELISA) equipment (Synergy™ HT Multi-Mode Microplate Reader, Biotek Instruments, Winooski, Vermont, USA). Protein concentration of the biological sample was calculated from the calibration plot constructed from protein standards and results were expressed in μg/ml.

5.3.9. Statistical analysis

Statistical analysis was completed using the SPSS Software version 18.0 (SPSS, Chicago, Illinois, USA). Testing for normality was performed with Shapiro Wilk and Kolmogorov-Smirnov-Lillifors tests. Data were indicated as median and interquartile range (median±IQR). Comparison of non-parametric continuous variables was undertaken with Mann-Whitney U test and analysis of variance by ranks (Kruskall-Wallis test) with pairwise comparisons. Correlations were determined by the Spearman's rank correlation coefficient (σ). A probability value of $p<0.05$ was considered to denote statistical significance.

5.4. Results

5.4.1. Postoperative outcome

Fifty-nine animals concluded the experiment and were comprised into the following groups: "*Res Ted* +" (15, eight of them sacrificed on the third day), "*Res Ted* –" (13, five sacrificed at third day), "*Lap Ted* +" (16, eight sacrificed on the third day) and "*Lap Ted* -" (15, seven sacrificed at third day).

5.4.2. Cellular viability and death

In animals not submitted to teduglutide treatment, ileal perianastomotic segments demonstrated a significant decrease of viable cells proportion between the third and seventh days (p=0.01) (Fig. 5.1).

Teduglutide administration was associated with an increase of viability index in the cells isolated from the perianastomotic segment at the seventh day (p=0.005) (Fig. 5.2).

Global evaluation of the effects of postoperative teduglutide treatment underscored the increase of cellular viability (p=0.0001) and decrease of early apoptosis occurrences at the seventh day (p=0.001) (Fig. 5.3).

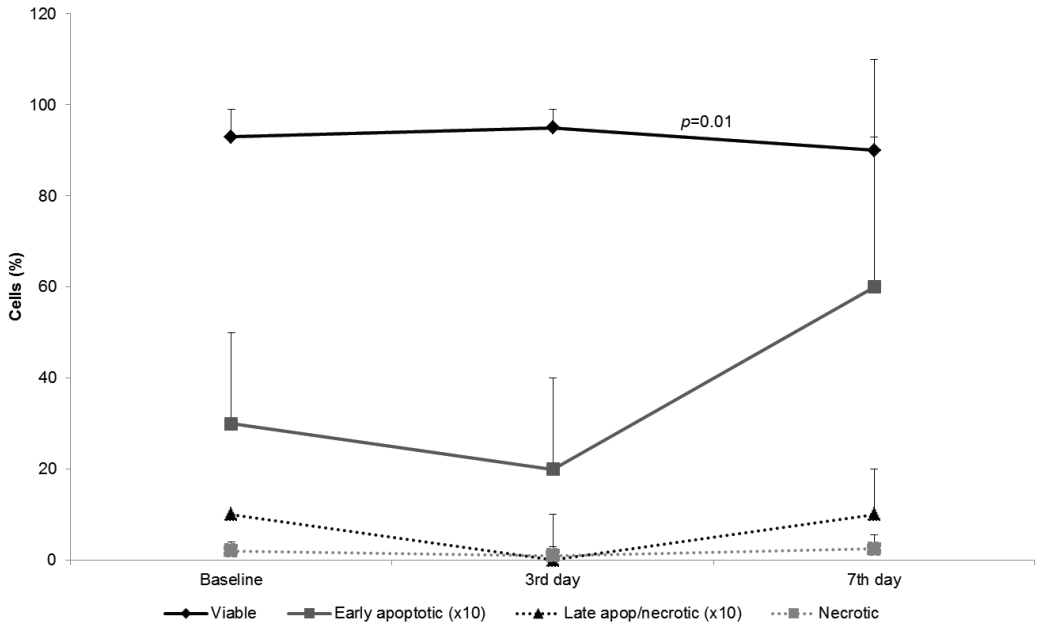

Figure 5.1. Viability and death in cells isolated from rats' ileum, at the third and seventh days after ileal resection and anastomosis, in animals not submitted to teduglutide treatment. Analysis was performed by flow cytometry using double staining with Annexin-V/Propidium iodide. Animals (n=13) were submitted to ileal resection and anastomosis and sacrificed on the third or seventh postoperative day. Samples recovered at sacrifice corresponded to the anastomotic segment. Baseline values were considered for comparison. Data were explicited as percentage (%) of viable, early apoptotic, late apoptotic/necrotic (*late apop/necrotic*) and necrotic cells (median±interquartile range). Kruskal-Wallis test with pairwise comparison was used

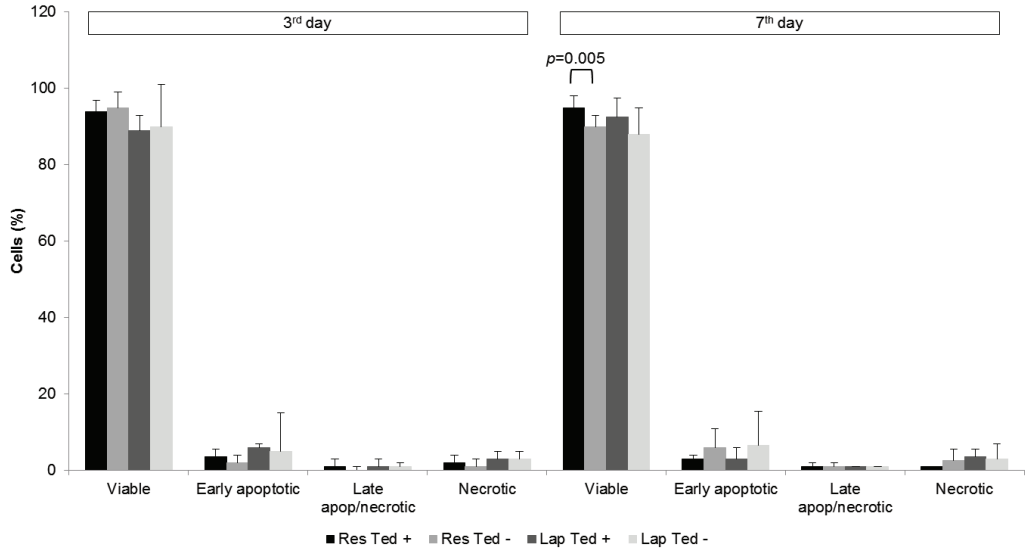

Figure 5.2. Viability and death in cells isolated from rats' ileum, at the third and seventh days after the operation, in the different groups of study. Analysis was performed by flow cytometry using double staining with Annexin-V/Propidium iodide. Animals (*n*=59) were submitted to ileal resection and anastomosis (*Res*) or laparotomy (*Lap*) and sacrificed on the third or seventh postoperative day. In groups "*Res Ted +*" and "*Lap Ted +*", teduglutide was administered after the operation. Samples recovered at sacrifice from rats submitted to ileal resection corresponded to the anastomotic segment. Data were explicited as percentage (%) of viable, early apoptotic, late apoptotic/necrotic (*late apop/necrotic*) and necrotic cells (median±interquartile range). Kruskal-Wallis test with pairwise comparison was used

5.4.3. Oxidative stress

Intestinal anastomotic healing induced a prooxidative influence, particularly evident at the third day, which was expressed by an increase of cytosolic peroxides level (p=0.0001) and reactive species generation in the mitochondria (p=0.005) and by a reduction of mitochondrial membrane potential (p=0.001) and cellular reduced glutathione content (p=0.001) until the seventh day (Fig. 5.4). Teduglutide treatment appeared to reinforce the prooxidative effects of anastomotic repair, although without reaching statistical significance (Fig. 5.5). When considering all the operated animals, postoperative teduglutide administration was significantly associated with an increase of the cytosolic peroxides level at the third day (p=0.042), as well as of the mitochondrial generation of reactive species at the seventh day (p=0.011) (Fig. 5.6). Teduglutide influence on the mitochondrial membrane potential appeared to be not relevant.

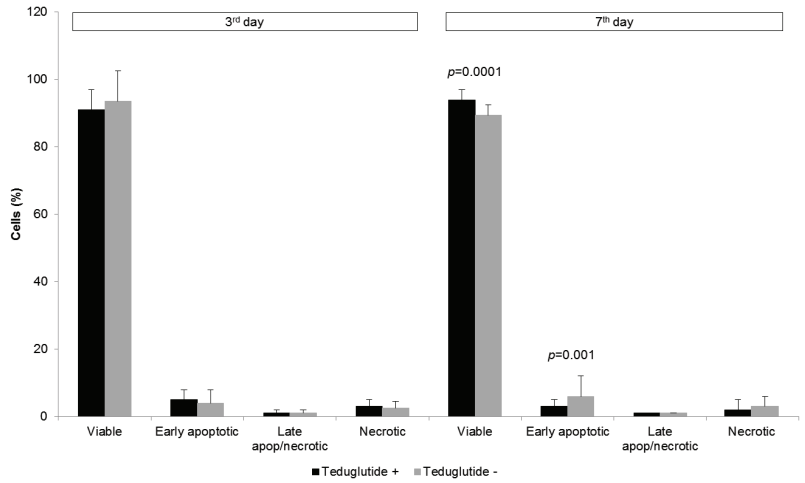

Figure 5.3. Viability and death in cells isolated from rats' ileum, at the third and seventh days after the operation, according to the teduglutide administration. Analysis was performed by flow cytometry using double staining with Annexin-V/Propidium iodide. Animals (*n*=59) were submitted to ileal resection and anastomosis (*Res*) or laparotomy (*Lap*) and sacrificed on the third or seventh postoperative day. In groups "*Teduglutide +*", teduglutide was administered after the operation. Samples recovered at sacrifice from rats submitted to ileal resection corresponded to the anastomotic segment. Data were explicited as percentage (%) of viable, early apoptotic, late apoptotic/necrotic (*late apop/necrotic*) and necrotic cells (median±interquartile range). Mann-Whitney U test was used

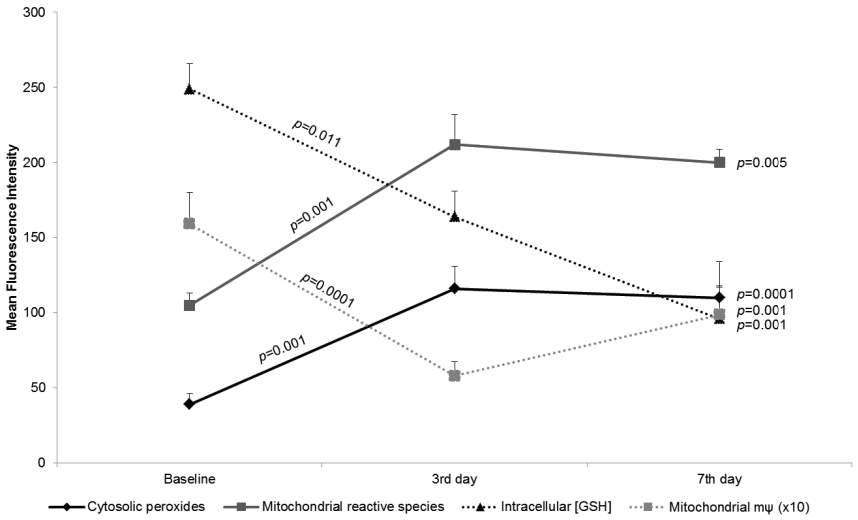

Figure 5.4. Oxidative stress evaluation in cells isolated from rats' ileum, at the third and seventh days after ileal resection and anastomosis, in animals not submitted to teduglutide treatment. Assessment was performed by flow cytometry using $DCFH_2$-DA, DHR123 and JC-1 fluorescent probes and mercury orange to determine cytosolic peroxides level, mitochondrial reactive species generation, mitochondrial membrane potential (mψ) and cellular reduced glutathione content ([GSH]), respectively. Animals (*n*=13) were submitted to ileal resection and anastomosis and sacrificed on the third or seventh postoperative day. Samples recovered at sacrifice corresponded to the anastomotic segment. Baseline values were considered for comparison. Data were presented as mean fluorescence intensity (MFI) values (median±interquartile range). Results of JC-1 probe were expressed as aggregates/monomers ratio. Kruskal-Wallis test with pairwise comparison was used

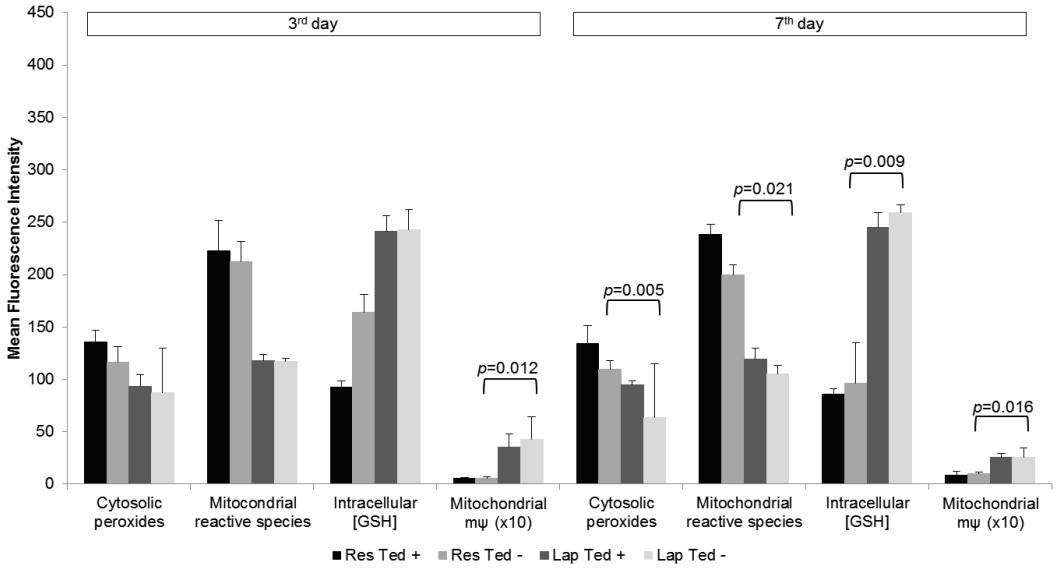

Figure 5.5. Oxidative stress evaluation in cells isolated from rats' ileum, at the third and seventh days after the operation, in the different groups of study. Assessment was performed by flow cytometry using $DCFH_2$-DA, DHR123 and JC-1 fluorescent probes and mercury orange to determine cytosolic peroxides level, mitochondrial reactive species generation, mitochondrial membrane potential (mψ) and cellular reduced glutathione content ([GSH]), respectively. Animals (n=59) were submitted to ileal resection and anastomosis (*Res*) or laparotomy (*Lap*) and sacrificed on the third or seventh postoperative day. In groups "*Res Ted +*" and "*Lap Ted +*", teduglutide was administered after the operation. Samples recovered at sacrifice from rats submitted to ileal resection corresponded to the anastomotic segment. Data were presented as mean fluorescence intensity (MFI) values (median±interquartile range). Results of JC-1 probe were expressed as aggregates/monomers ratio. Kruskal-Wallis test with pairwise comparison was used

5.4.4. Local inflammatory response

Anastomotic repair induced a significant upregulation of tissue IL-1α (p=0.0001), MCP-1 (p=0.026) and TNF-α (p=0.0001) until the third day, with a drop of TNF-α thereafter; as well as of IFN-γ between the third and seventh days (p=0.034) (Fig. 5.7). An increase of pro-to-antiinflammatory cytokines ratio until the seventh day (623.8±422.5 *vs.* 7098.5±7396.5, p=0.0001) and of Th1-to-Th2 cytokines ratio, especially until the third day (0.0±0.9 *vs.* 118.2±49.3, p=0.0001) were observed in the perianastomotic segment.

Teduglutide administration was associated with higher tissue levels of IL-4 at the seventh day after isolated laparotomy (p=0.036) (Fig. 5.8).

When considering all the studied animals, teduglutide treatment was associated with a higher expression of IL-4 at the seventh day after the operation (p=0.0001) (Fig. 5.9), concomitant with a lower pro-to-antiinflammatory and Th1-to-Th2 cytokines ratios (409.3±1768.1 *vs.* 2864.5±6613.6, p=0.012 and 0.0±2.2 *vs.* 3.0±7.3, p=0.017, respectively).

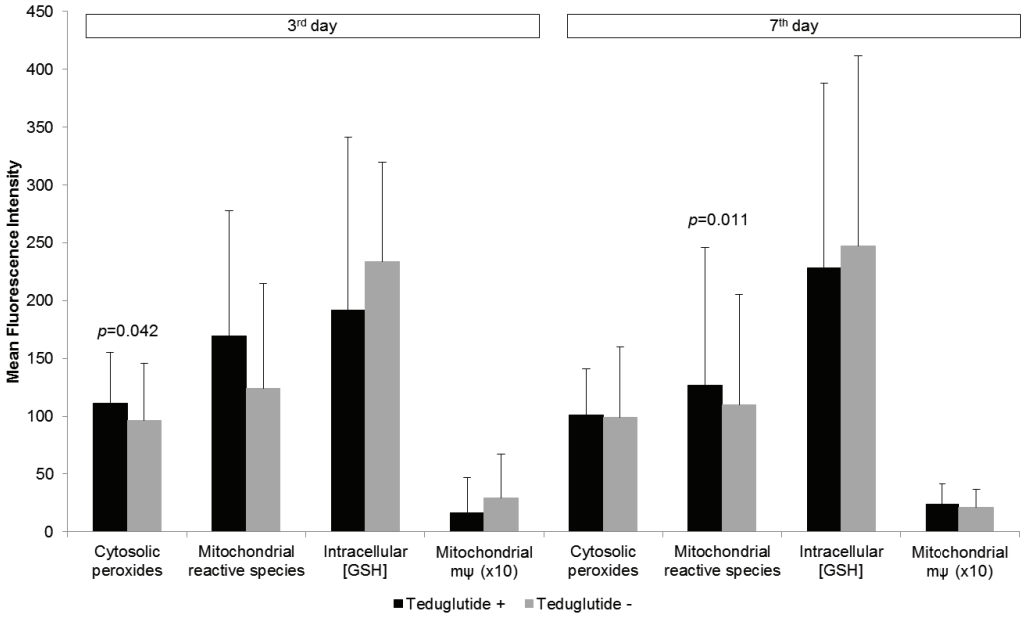

Figure 5.6. Oxidative stress evaluation in cells isolated from rats' ileum, at the third and seventh days after the operation, according to teduglutide administration. Assessment was performed by flow cytometry using DCFH2-DA, DHR123 and JC-1 fluorescent probes and mercury orange to determine cytosolic peroxides level, mitochondrial reactive species generation, mitochondrial membrane potential (mψ) and cellular reduced glutathione content ([GSH]), respectively. Animals (n=59) were submitted to ileal resection and anastomosis (*Res*) or laparotomy (*Lap*) and sacrificed on the third or seventh postoperative day. In groups "*Teduglutide* +", teduglutide was administered after the operation. Samples recovered at sacrifice from rats submitted to ileal resection corresponded to the anastomotic segment. Data were presented as mean fluorescence intensity (MFI) values (median±interquartile range). Results of JC-1 probe were expressed as aggregates/monomers ratio. Mann-Whitney U test was used

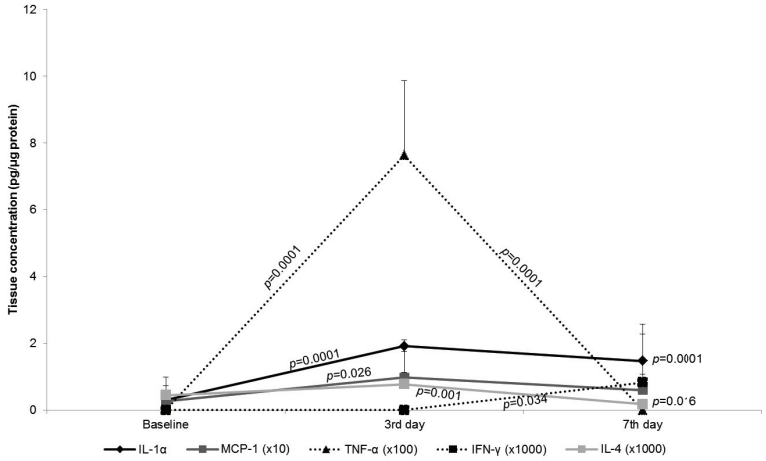

Figure 5.7. Analysis of tissue inflammatory response in rats' ileum by flow cytometric multiplexed bead assay, at the third and seventh days after ileal resection and anastomosis, in animals not submitted to teduglutide treatment. Animals (*n*=13) were submitted to ileal resection and anastomosis and sacrificed on the third or the seventh postoperative days. Samples recovered at sacrifice from rats submitted to ileal resection corresponded to the anastomotic segment. Baseline values were considered for comparison. Cytokines concentrations were determined as function of fluorescence intensities and normalized to the protein content of the sample. Data were expressed as pg/mg (median±interquartile range). Kruskal-Wallis test with pairwise comparison was used

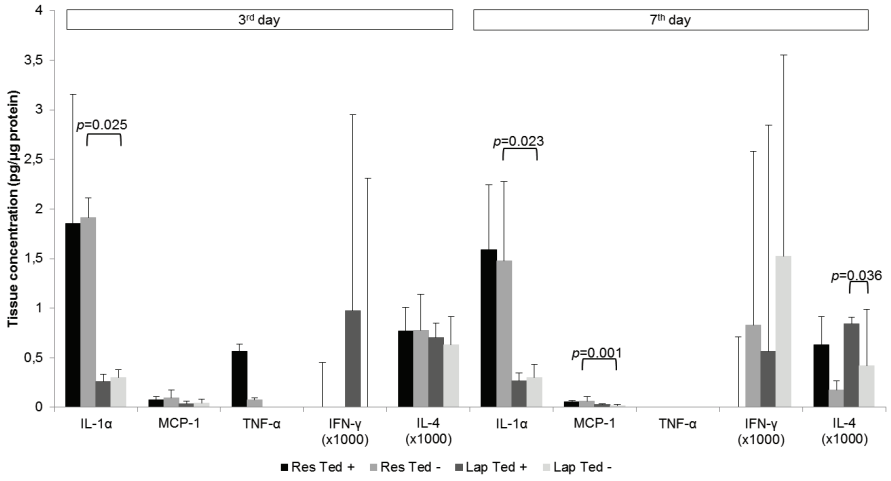

Figure 5.8. Analysis of tissue inflammatory response in rats' ileum by flow cytometric multiplexed bead assay, at the third and seventh days after the operation, in the different groups of study. Animals (*n*=59) were submitted to ileal resection and anastomosis (*Res*) or laparotomy (*Lap*) and sacrificed on the third or the seventh postoperative days. In groups "*Res Ted +*" and "*Lap Ted +*", teduglutide was administered after the operation. Samples recovered at sacrifice from rats submitted to ileal resection corresponded to the anastomotic segment. Cytokines concentrations were determined as function of fluorescence intensities and normalized to the protein content of the sample. Data were expressed as pg/mg (median±interquartile range). Kruskal-Wallis test with pairwise comparison was used

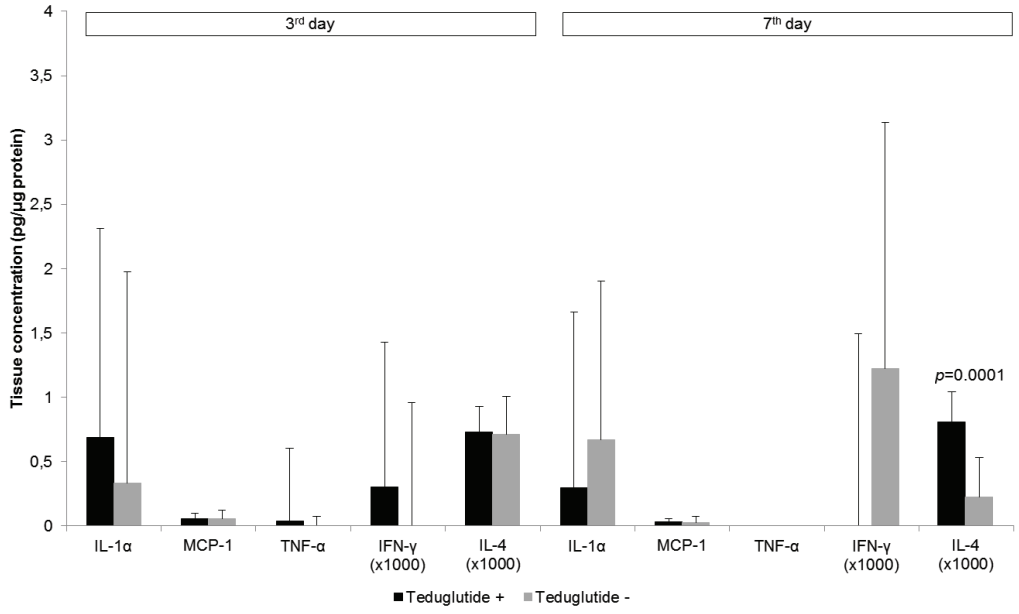

Figure 5.9. Analysis of tissue inflammatory response in rats' ileum by flow cytometric multiplexed bead assay, at the third and seventh days after the operation, according to the teduglutide administration. Animals (*n*=59) were submitted to ileal resection and anastomosis (*Res*) or laparotomy (*Lap*) and sacrificed on the third or the seventh postoperative days. In groups "*Teduglutide +*", teduglutide was administered after the operation. Samples recovered at sacrifice from rats submitted to ileal resection corresponded to the anastomotic segment. Cytokines concentrations were determined as function of fluorescence intensities and normalized to the protein content of the sample. Data were expressed as pg/mg (median±interquartile range). Mann-Whitney U test was used

5.4.5. Systemic inflammatory response

After ileal resection and anastomosis, an increase of plasma IFN-γ levels until the third day was documented; on the other hand, a decrease of IL-1α and TNF-α concentrations until the seventh day (p=0.0001 and p=0.0001, respectively) was also observed (Fig. 5.10).

Plasma pro-to-antiinflammatory and Th1-to-Th2 cytokines ratios increased until the third day after ileal resection and anastomosis (32.7±11.7 *vs.* 47.3±12.3, p=0.017 and 16.2±6.1 *vs.* 23.1±8.2, *n.s.*, respectively) and decreased thereafter (47.3±12.3 *vs.* 8.2±2.3, p=0.0001 and 23.1±8.2 *vs.* 8.2±2.3, p=0.0001, respectively).

Teduglutide administration was associated with lower plasma levels of IL-1α, IFN-γ and TNF-α at the seventh day after laparotomy (p=0.0001, respectively); lower levels of IL-4 at both moments of evaluation after laparotomy (p=0.013 and p=0.0001, respectively); as well as lower plasma concentrations of IFN-γ at the third day after ileal resection and anastomosis (p=0.004) (Fig. 5.11).

When analyzing all the animals, teduglutide administration was associated with lower plasma levels of IFN-γ at the third day (p=0.026) and of IL-1α (p=0.004), TNF-α (p=0.002), IFN-γ (p=0.0001) and IL-4 (p=0.0001) at the seventh day (Fig. 5.12). That growth factor was not associated with significant modifications of plasma pro-to-antiinflammatory or Th1-to-Th2 cytokine ratios.

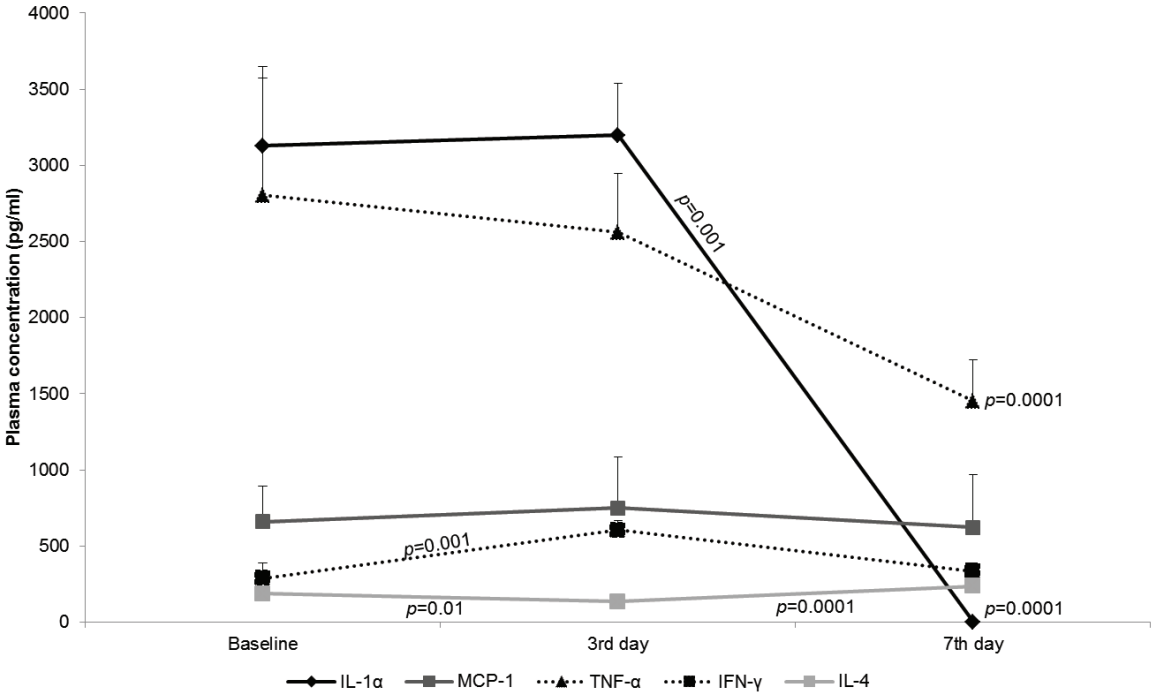

Figure 5.10. Analysis of systemic inflammatory response by flow cytometric multiplexed bead assay, at the third and seventh days after ileal resection and anastomosis, in animals not submitted to teduglutide treatment. Animals (n=13) were submitted to ileal resection and anastomosis and sacrificed on the third or seventh postoperative day. Baseline values were considered for comparison. Data were transmitted as plasma concentration (pg/ml) (median±interquartile range). Kruskal-Wallis test with pairwise comparison was used

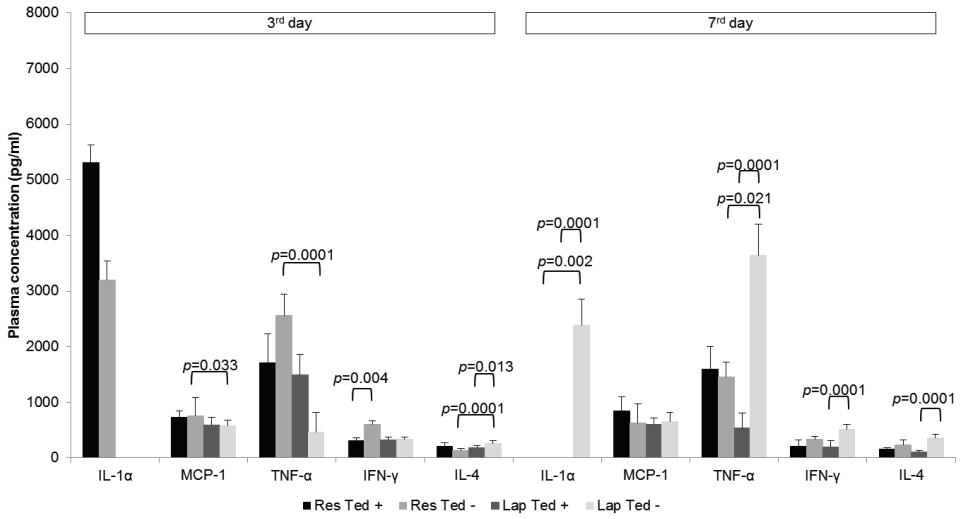

Figure 5.11. Analysis of systemic inflammatory response by flow cytometric multiplexed bead assay, at the third and seventh days after the operation, in the different groups of study. Animals (*n*=59) were submitted to ileal resection and anastomosis (*Res*) or laparotomy (*Lap*) and sacrificed on the third or seventh postoperative day. In groups "*Res Ted+*" and "*Lap Ted+*", teduglutide was administered after the operation. Data were transmitted as plasma concentration (pg/ml) (median±interquartile range). Kruskal-Wallis test with pairwise comparison was used

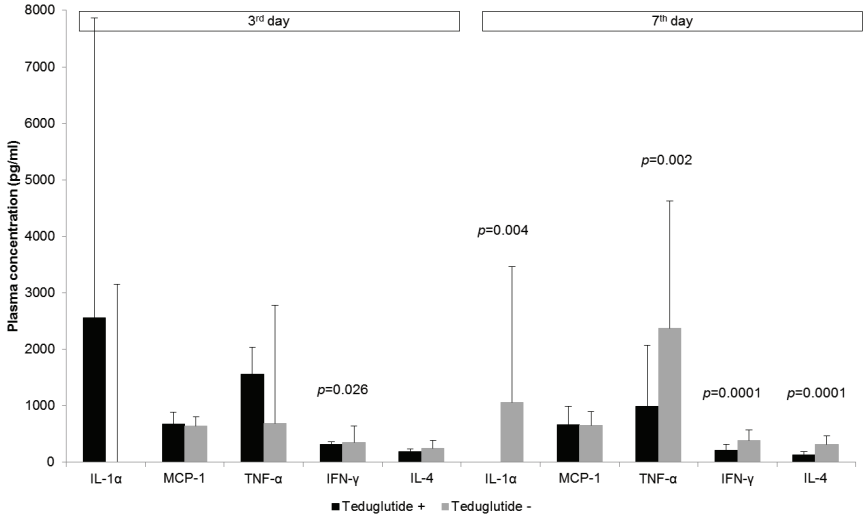

Figure 5.12. Analysis of systemic inflammatory response by flow cytometric multiplexed bead assay, at the third and seventh days after the operation, according to the teduglutide administration. Animals (*n*=59) were submitted to ileal resection and anastomosis (*Res*) or laparotomy (*Lap*) and sacrificed on the third or seventh postoperative day. In groups "*Teduglutide +*", teduglutide was administered after the operation. Data were transmitted as plasma concentration (pg/ml) (median±interquartile range). Mann-Whitney U test was used

5.4.6. Relevant correlations between cellular viability and death indexes, oxidative stress parameters and cytokines levels at the sacrifice

In the postoperative evaluation of cells isolated from the rats' ileum, cytosolic peroxides level, mitochondrial reactive species generation and mitochondrial membrane potential level correlated moderately and significantly with cellular viability (σ=50.4%, p=0.0001; σ=61.9%, p=0.0001 and σ=-49.8%, p=0.0001, respectively) (Table 5.1).

Table 5.1. Relevant correlations between cellular viability and death indexes, oxidative stress parameters and tissue levels of cytokines at the sacrifice (n=59)[a]

(σ / p)	Viability	Early ap	Late ap	Necrosis	Peroxides	Reac Sp	ic[GSH]	mψ	[IL-1α]	[MCP-1]	[TNF-α]	[IFN-γ]	[IL-4]
Viability		-76.6% p=0.0001		-69.1% p=0.0001	50.4% p=0.0001	61.9% p=0.0001	-50.6% p=0.0001	-49.8% p=0.0001	29.7% p=0.022	32.8% p=0.011	40.7% p=0.001	-28.6% p=0.028	
Early ap	-76.6% p=0.0001				-46.3% p=0.0001	-40.9% p=0.001	29.9% p=0.021	39.4% p=0.002	-27.5% p=0.035		-31.2% p=0.016		
Late ap	-58.5% p=0.0001			43.3% p=0.001		-27.4% p=0.036							
Necrosis	-69.1% p=0.0001		43.3% p=0.001		-41.4% p=0.001	-47.5% p=0.0001	45.8% p=0.0001	39.9% p=0.002	-25.9% p=0.048	-28.5% p=0.029			
Peroxides	50.4% p=0.0001	-46.3% p=0.0001		-41.4% p=0.001		78.8% p=0.0001	-72.4% p=0.0001	-74.7% p=0.0001	59.6% p=0.0001	55.5% p=0.0001	52.1% p=0.0001	-28.5% p=0.028	
Reac Sp	61.9% p=0.0001	-40.9% p=0.001	-27.4% p=0.036	-47.5% p=0.0001	78.8% p=0.0001		-86.5% p=0.0001	-73.9% p=0.0001	61.4% p=0.0001	63.1% p=0.0001	52.8% p=0.0001	-41.7% p=0.001	
ic[GSH]	-50.6% p=0.0001	29.9% p=0.021		45.8% p=0.0001	-72.4% p=0.0001	-86.5% p=0.0001		68.5% p=0.0001	-62.5% p=0.0001	-59.5% p=0.0001	-38% p=0.003		
mψ	-49.8% p=0.0001	39.4% p=0.002		39.9% p=0.002	-74.7% p=0.0001	-73.9% p=0.0001	68.5% p=0.0001		-70.8% p=0.0001	-54% p=0.0001	-71.4% p=0.0001	32.5% p=0.013	
[IL-1α]	29.7% p=0.022	-27.5% p=0.035		-25,9% p=0.048	59.6% p=0.0001	61.4% p=0.0001	-62.5% p=0.0001	-70.8% p=0.0001		59.7% p=0.0001	56.6% p=0.0001		
[MCP-1]	32.8% p=0.011			-28,5% p=0.029	55.5% p=0.0001	63.1% p=0.0001	-59.5% p=0.0001	-54% p=0.0001	59.7% p=0.0001		51.3% p=0.0001		
[TNF-α]	40,7% p=0,001	-31.2% p=0.016			52.1% p=0.0001	52.8% p=0.0001	-38% p=0.003	-71.4% p=0.0001	56.6% p=0.0001	51.3% p=0.0001		-36.6% p=0.004	30.5% p=0.019
[IFN-γ]	-28.6% p=0.028				-28,5% p=0,028	-41.7% p=0.001		32.5% p=0.013			-36.6% p=0.004		
[IL-4]											30.5% p=0.019		

[a] Analysis was performed by flow cytometry. Cellular viability and death indexes were determined using annexin-V/propidium iodide; cytosolic peroxides level (*Peroxides*), reactive species generation in the mitochondria (*Reac Sp*), mitochondrial membrane potential ($m\psi$) and cellular reduced glutathione content (*ic[GSH]*) with $DCFH_2$-DA, DHR123 and JC-1 fluorescent probes and mercury orange staining, respectively; and tissue levels of cytokines by flow cytometric multiplex bead assay. Spearman's correlation coefficient (σ) and value of significance (p) were presented. Early ap, Early apoptosis index; Late ap, Late apoptosis/necrosis index

Correlations between the levels of cytosolic peroxides and mitochondrial reactive species and tissue concentrations of IL-1α, MCP-1 and TNF-α were positive, while those of reduced gluthathione and mitochondrial membrane potential levels were inverse.

5.5. Discussion

Intestinal anastomotic healing is a complex process that progresses in three imbricated steps: inflammatory, proliferative and remodeling (Rijcken *et al.*, 2014; Thompson *et al.*, 2006). In this study, the repair process induced a significant decrease of the percentage of viable cells isolated from the perianastomotic segment between both postoperative moments of evaluation. Intestinal anastomotic healing was characterized by a relevant and sustained prooxidative influence, particularly evident at the third day, including an increase of the cellular oxidative burden and a decrease of the mechanisms of protection against the oxidative injury, as expected to occur during the infiltration of the wounded tissues by inflammatory cells (Rijcken *et al.*, 2014; Speca *et al.*, 2012).

Inflammatory response and balance between pro and antiinflammatory cytokines are important in determining the outcome of the wound healing process (Zubaidi *et al.*, 2015). Moreover, in a recently published meta-analysis, increased postoperative peritoneal levels of interleukine-6 (IL-6) (at the first, second and third days) and TNF-α (at the third, fourth and fifth days) were significantly associated with clinical relevant anastomotic leakage after colorectal surgery and were considered to contribute to its early detection (Sparreboon *et al.*, 2016b). Higher plasma levels of IL-6 at the first day were also significantly associated with anastomotic leakage after colorectal surgery, but with a poor predictive capacity (Sammour *et al.*, 2016). Nevertheless, in current context, local peritoneal cytokine levels appear to be of greater clinical relevance than systemic levels. Previous animal studies reported that systemic IL-6 administration exerts a negative effect on the healing of colonic anastomoses (Sammour *et al.*, 2016).

However, description of the cytokines profiles and their time course during the intestinal anastomotic healing has not always been consistent in the literature (Zubaidi *et al.*, 2015; Alzoghaibi and Zubaidi, 2014; Zubaidi *et al.*, 2010).

In this experiment, tissue and plasma levels of inflammatory cytokines were determined by flow cytometry using a multiplex bead array approach. This was a rapid and simple method that allowed simultaneous quantification of multiple cytokines in a small sample volume (Tighe *et al.*, 2013). The obtained results demonstrated high variability and, in some cases, did not reach the sensibility threshold of the assay (including some IL-1α and TNF-α determinations). Accurate measurement of cytokines expression is often hampered by stability and representativeness problems. In fact, cytokines have a short half-life and are susceptible to absorption, release from cells and degradation during sample collection and handling (Keutstermans *et al.*, 2013).

In the present study, anastomotic healing activated a predominant tissue proinflammatory and Th1 response. Repair process promoted a significant upregulation of IL-1α, MCP-1 and TNF-α until the third day; and of IFN-γ between the third and the seventh days. Similarly, Seifert GJ *et al* (Seifert *et al.*, 2014) demonstrated an upregulation of tissue IL-1α and IL-1β gene expressions on the second day and a downregulation in the later course until the eighth day, although without a consistent regulation of IFN-γ gene expression. Other authors described upregulation of IL-1β until the seventh day after an ileal anastomosis (Zubaidi *et al.*, 2015; Zubaidi *et al.*, 2010) and increase of IFN-γ expression between the third and seventh days (Zubaidi *et al.*, 2015); however, contrary to the present findings, they observed a decrease of TNF-α levels at the third postoperative day (Zubaidi *et al.*, 2015; Zubaidi *et al.*, 2010). In this investigation, downregulation of IL-4 at the seventh postoperative day was concordant with the literature (Zubaidi *et al.*, 2010) and the MCP-1 kinetic profile in the anastomotic segment was analogous to that previously demonstrated by Alzoghaibi MA and Zubaidi AM (Alzoghaibi and Zubaidi, 2014).

Current results revealed a predominant proinflammatory and Th1 systemic response at the third day after intestinal resection and anastomosis and a prevailing antiinflammatory and Th2 systemic reaction at the seventh day, in concordance with

the literature (Murakami *et al.*, 2007). As reported by previous experimental and clinical studies, the initial proinflammatory phase of the host response during the early postoperative period is followed by the antiinflammatory cytokines production by Th2 lymphocytes (Choileain and Redmond, 2006). Surgical stress induces a shift in the Th1/Th2 cell balance towards Th2 (Ramirez *et al.*, 2013; Murakami *et al.*, 2007; Decker *et al.*, 1996), suggesting downregulation of cell-mediated and upregulation of antibody-mediated immunity, proportional to the magnitude of injury (Ramirez *et al.*, 2013; Decker *et al.*, 1996).

This study demonstrated a favorable influence of teduglutide on intestinal cellular viability in the perioperative context, particularly after ileal resection and anastomosis, and confirms its anti-apoptotic effects. Previous studies demonstrated that GLP-2 increases the intestinal epithelial proliferation in the crypts and inhibits the apoptosis in the crypts and villi (Drucker and Yusta, 2014).

Furthermore, present findings suggested a prooxidative influence of teduglutide and did not corroborate other authors' conclusions pointing to an antioxidant effect (Arana *et al.*, 2017; Lei *et al.*, 2016; Drucker and Yusta, 2014; Janssen *et al.*, 2013; Arda-Pirincci *et al.*, 2011). In fact, Arda-Pirincci *et al* (Arda-Pirincci *et al.*, 2011) demonstrated that teduglutide pretreatment prevented tumor necrosis factor-alpha/actinomycin D-induced intestinal oxidative injury, in a mouse model, with reduction of lipid peroxidation (malondialdehyde levels) and glutathione levels, glutathione peroxidase and superoxide dismutase activities, and a marked increase in catalase activity. In 2016, Lei Q *et al* (Lei *et al.*, 2016) observed that exogeneous GLP-2 improves the intestinal antioxidant capacity, namely the tissue glutathione level, in a mouse model of total parenteral nutrition therapy. Dissimilar results of present study may be explained by the use of different models of intestinal injury (chemical/inflammatory *versus* surgical agression), materials used for oxidative stress analysis (homogenates of intestinal tissue instead of isolated cells' preparations) and teduglutide administration schedules (timing and posology).

In this investigation, postoperative prooxidative effect of teduglutide was expressed by an increase of peroxides level in the cytosol at the third day and of reactive species generation in the mitochondria at the seventh day. Those parameters of oxidative

stress correlated positively with cellular viability index suggesting absence of deleterious effects on cellular death promotion and, on the contrary, a favorable influence on viability; indeed, in present analysis, teduglutide was associated with proviability and antiapoptotic effects. Although excessive intestinal oxidative stress may negatively influence anastomotic repair through disruption of cell signaling (including of the redox modulation of effector cells proliferation and differentiation), irreversible oxidation of macromolecules and induction of cell death (Circu and Aw, 2012; Aw, 2012), as demonstrated by other authors (Teke et al., 2013; Poyrazoglu *et al.*, 2011), a certain level of redox stimulus is necessary to the normal course of the wound healing process (Rijcken *et al.*, 2014; Greaves *et al.*, 2013; Speca *et al.*, 2012).

In current experiment, teduglutide postoperative treatment was related with a significant upregulation of tissue IL-4 expression at the seventh postoperative day and a shift of the postoperative local balance towards an antiinflammatory and Th2 response at that time point, although those effects did not reach statistical significance when analyzing exclusively the anastomotic segments. Upregulation of IL-4 at the seventh day may promote the transition from a primarily inflammatory state to a more proliferative phase of healing. IL-4 has been associated with activation and differentiation of fibroblasts, production of collagens, upregulation of matrix metalloproteinase 2, matrix metalloproteinase 9 and tissue inhibitor of metalloproteinase 1, inhibition of the Th1 response and stimulation of Th2 cells (Speca *et al.*, 2012). Present results suggest that teduglutide may influence anastomotic healing through the interference in the pro and antiinflammatory pathways, with a prevailing antiinflammatory effect at the seventh postoperative day.

In conclusion, in present study, intestinal anastomotic healing was characterized by a local prooxidative and proinflammatory response. Surgical injury associated with intestinal resection and anastomosis induced a systemic predominantly proinflammatory and Th1 cytokines reaction at the third day and an antiinflammatory and Th2 response at the seventh day.

Postoperative teduglutide treatment was significantly associated with a tissue prooxidative and antiinflammatory influence, with potential interference in the inflammatory and proliferative phases of the intestinal anastomotic healing.

Chapter 6

Tissue growth factors profile after teduglutide administration on an animal model of intestinal anastomosis

This chapter was partially published as:

Costa BP, Gonçalves AC, Abrantes AM, Matafome P, Seiça R, Sarmento-Ribeiro AB, Botelho MF, Castro-Sousa F: Tissular growth factors profile after teduglutide administration on an animal model of intestinal anastomosis. *Nutr Hosp*. 2018;35(1):xxx-xxx. Doi 10.20960/nh1326 *(Accepted for publication in July 21, 2017).*

Costa BP, Sarmento-Ribeiro AB, Gonçalves AC, Botelho F, Abrantes M, F. Castro Sousa: Tissular growth factors profile after teduglutide administration on an animal model of intestinal anastomosis. *Clin Nutr.* 2015;34 (Supp1):S26 (outstanding abstract and poster at the 37th European Society for Clinical Nutrition and Metabolism Congress, Lisbon, 2015).

6.1. Abstract

Teduglutide is an enterotrophic analogue of glucagon-like peptide 2 (GLP-2) with an indirect and poorly known mechanism of action, approved for the rehabilitation of short-bowel syndrome. This study aimed to analyze the response of tissue growth factors to surgical injury and teduglutide administration on an animal model of intestinal anastomosis. Wistar rats (*n*=59) were distributed into four groups: "*Ileal Resection and Anastomosis*" or "*Laparotomy*", each one subdivided into "*Postoperative Teduglutide Administration*" or "*No Treatment*"; and sacrificed at the third or the seventh day, with ileal and blood harvesting. Gene expression of *insulin-like growth factor 1* (*Igf1*), *vascular endothelial growth factor a* (*Vegfa*), *transforming growth factor β1* (*Tgfβ1*), *connective tissue growth factor* (*Ctgf*), *fibroblast growth factor 2* (*Fgf2*), *fibroblast growth factor 7* (*Fgf7*), *epidermal growth factor* (*Egf*), *heparin-binding epidermal-like growth factor* (*Hbegf*), *platelet-derived growth factor b* (*Pdgfb*) and *glucagon-like peptide 2 receptor* (*Glp2r*) was studied by quantitative real-time reverse-transcription polymerase chain reaction. Plasma levels of Glp-2 were determined by competitive enzyme immunoassay. Upregulation of *Fgf7*, *Fgf2*, *Egf*, *Vegfa* and *Glp2r* at the third day, and of *Pdgfb* at the seventh day, was verified in the perianastomotic segments. Teduglutide administration was associated with higher fold-change of relative gene expression of *Vegfa* (3.6±1.3 *vs.* 1.9±2.0, *p*=0.0001), *Hbegf* (2.2±2.3 *vs.* 1.1±0.9, *p*=0.001), *Igf1* (1.6±7.6 *vs.* 0.9±0.7, *p*=0.002) and *Ctgf* (1.1±2.1 *vs.* 0.6±2.0, *p*=0.013); and lower fold-change of *Tgfβ1*, *Fgf7* and *Glp2r*. These results underscore the recognized role of *Igf1* and *Hbegf* as molecular mediators of the effects of teduglutide and suggest that other humoral factors, like *Vegf* and *Ctgf*, may also be relevant in the perioperative context. Induction of *Vegfa*, *Igf1* and *Ctgf* gene expressions might indicate a favorable influence of teduglutide on the intestinal anastomotic healing.

6.2. Introduction

Failure of intestinal anastomotic repair persists as a major source of morbidity and mortality in digestive surgery and one of the most feared postoperative complications (Guyton *et al.*, 2016; Bosmans *et al.*, 2015; Shogan *et al.*, 2013). Intestinal anastomotic healing is a multicellular multimolecular compelling process drived by the interplay of multiple signaling pathways and precisely controlled in terms of space and time (Rijcken *et al.*, 2014) (Table 6.1). Teduglutide is a long-acting modified form of glucagon-like peptide 2 (GLP-2), which is an intestinal growth-promoting factor with intestinotrophic, antisecretory, transit-modulating and antiinflammatory effects. GLP-2 demonstrates a complex, indirect and poorly understood mechanism of action that appears to be mediated, at least partially, by insulin-like growth factor 1, ErbB superfamily of ligands, fibroblast growth factor 7, and vascular endothelial growth factor (Drucker and Yusta B, 2014). Response of tissue growth factors, key mediators of the anastomotic repair, to teduglutide administration in the perioperative context of intestinal anastomosis is still to be defined.

This study intended to analyze the response of tissue growth factors to surgical injury and teduglutide short-term administration on an animal model of intestinal anastomosis.

Table 6.1. Simplified overview of the intestinal anastomotic healing

Phase	Timing	Predominant cell types	Relevant mediators	Process
Inflammation	1 to 4 days	Platelets, neutrophils, M1 macrophages, fibroblasts	PDGF, TGF-β, VEGF, IGF-1, cytokines, chemokines, coagulation factors, plasma proteases, arachidonic acid metabolites, vasoactive amines, ROS	Coagulation, inflammation, debridement, ECM degradation, protection, provisional wound closure
Proliferation	2 to 14 days	Fibroblasts, myofibroblasts, smooth muscle cells, M2 macrophages, lymphocytes, epithelial cells, endothelial cells	PDGF, TGF-β, FGF-2, IGF-1, VEGF, EGF, HB-EGF, cytokines, chemokines	Reepithelialization, neoangiogenesis, fibroplasia, definitive wound closure
Remodeling	14 to 180 days	Fibroblasts, lymphocytes	PDGF, TGF-β	Collagen cross-link, maturation of the wound

ECM, extracellular matrix; EGF, Epidermal growth factor; FGF-2, Fibroblast growth factor 2; HB-EGF, heparin-binding epidermal growth factor; IGF-1, Insulin-like growth factor 1; PDGF, Platelet-derived growth factor; ROS, Reactive oxygen species; TGF-β, Transforming growth factor β; VEGF, Vascular endothelial growth factor. Adapted from Rijcken E *et al.*, 2014

6.3. Methods

6.3.1. Study protocol and surgical procedures

Experiment was approved by the Ethics Committee of the Faculty of Medine, University of Coimbra, Coimbra, Portugal (Official Letter nº 32-06-2009) and performed according to the institutional and national animals' protection guidelines.

Adult male Wistar *albinus* rats were randomly allocated into four groups: "*Ileal Resection and Anastomosis*" ("*Res*") or "*Laparotomy*" ("*Lap*"), each one subdivided into "*Postoperative Teduglutide Administration*" ("*Ted* +") or "*No Treatment*" ("*Ted* -"). Assessment was performed at the operation and sacrifice moments, at the third or the seventh postoperative day (eight subgroups), with ileal segment harvesting and blood collection. Blinded evaluation was accomplished in the laboratorial analysis. Animals weighting 250 to 300 g were harboured in ventilated cages with a controlled environment of temperature (22±1°C), relative humidity (50±10%), and light-dark cycles of 12 hours; and with free access to water and standard rodent diet.

All the surgical interventions were performed by the same surgeon after two hours solid fasting, with clean surgical technique and under anaesthesia with intraperitoneal ketamine hydrochloride (75 mg/kg; Pfizer Inc., New York, USA) and chlorpromazine (3 mg/kg; Laboratórios Vitória, Amadora, Portugal). In "*Res*" groups, a 10-cm length ileal resection was undertaken, 5 cm upstream of ileocecal valve, after a 3-cm abdominal wall midline incision. A standard end-to-end anastomosis was constructed with eight equidistant full-thickness polydioxanone USP 6/0 stitches (PDS II, Ethicon, Johnson-Johnson Intl., Cincinnati, USA). Abdominal wall was closed with muscle-aponeurotic and cutaneous running sutures of braided coated polyglactin 910 USP 4/0 (Surgilactin, Sutures Limited, Wrexham, UK) and natural silk USP 4/0 (Surgisilk, Sutures Limited), respectively. In "*Lap*" groups, animals were subjected to a 3-cm midline laparotomy (without resection) with gentle manipulation of the small bowel.

In "*Ted* +" groups, teduglutide (American Peptide Company, Sunnyvale, California, USA) was administered in the postoperative period (from the operation day), 200 μg/kg/day, subcutaneously, dissolved in 0.25 ml phosphate buffered saline pH 7.4 (PBS, pH 7.4, Gibco, Life Technologies, Carlsbad, California, USA), after preparation

according to the manufacturer's recommendations. In the first postoperative day, ingestion of water with 5% glucose at a 1:1 ratio was allowed and then unrestricted oral hydration and chow were reassumed. Daily surveillance was performed and operative mortality and morbidity were registered. At the third or seventh postoperative day, animals were sacrificed by cervical displacement and a relaparotomy with ileal resection was performed (10-cm length, preserving distal 3 cm).

6.3.2. Tissue and blood collection

Three similar longitudinal strips of the most distal 4-cm length of each ileal operative specimen, each one corresponding to one third of the circumference, were carefully recovered, after gentle washing with normal saline solution, for homogenization and additional procedures, respectively. Tissue baseline values of *"Ileal Resection and Anastomosis*" groups were considered for comparison with postoperative results of the "*Laparotomy*" groups; tissue samples recovered at the sacrifice in those animals corresponded to the perianastomotic segments.

Blood samples of 1 ml were drawn in the morning, before the operations, from the tail vein, into polyethylene therephthalate K3 ethylenediaminetetraacetic acid (K3EDTA) vacutainers. Samples were stabilized immediately with 0.1 mg/ml of aprotinin from bovine lung (Sigma-Aldrich, Sintra, Portugal) and 0.037 mg/ml of dipeptidylpeptidase IV competitive inhibitor nicotinonitrile dihydrochloride hydrate (Sigma-Aldrich) and centrifuged for 20 minutes at 1500x *g* and 4°C. Plasma aliquots were stored at -80°C.

6.3.3. Intestinal tissue homogenization

As mentioned in the Chapter 5, pieces from one ileal longitudinal strip recovered in consonance with precedent report, with approximately 1 mm, were promptly added to a mixture of protease inhibitors in a proportion of 1 ml/100 mg and underwent mechanical homogenization. Inhibitors preparation was formerly prepared by

misturing aprotinin from bovine lung (Sigma-Aldrich), leupeptin hemisulfate salt (Sigma-Aldrich) and pepstatin A (Sigma-Aldrich) (1 μl of each, all diluted in a 10 mg/ml stock concentration) with 10 ml of phosphate buffered saline (PBS, pH 7.4, Gibco, Life Technologies) and stored on ice. Misture was sonicated twice with one short pulse of ten seconds, cooled during ten seconds and distributed into two tubes of 1.5 ml. Sonication (one pulse of ten seconds) was repeated and centrifugation was undertaken, 14000x *g*, for 10 minutes, at 4°C. Supernatant was removed to a new tube and pellet was preserved on ice for posterior ribonucleic acid (RNA) extraction.

6.3.4. Analysis of gene expression levels of growth factors and glucagon-like peptide 2 receptor

Quantitative real-time reverse-transcription polymerase chain reaction (qRT-PCR) was used to characterize the messenger ribonucleic acid (mRNA) expression profile of genes of growth factors potentially involved in the anastomotic healing: *Insulin-like growth factor 1, transcript variant: Igf1; Vascular endothelial growth factor A, transcript variant 2: Vegfa; Transforming growth factor, beta 1: Tgfb1; Connective tissue growth factor: Ctgf; Fibroblast growth factor 2: Fgf2; Fibroblast growth factor 7: Fgf7; Epidermal growth factor: Egf; Heparin-binding EGF-like growth factor: Hbegf; Platelet-derived growth factor beta polypeptide: Pdgfb; Glucagon-like peptide 2 receptor: Glp2r*. Quantitative RT-PCR multistep protocol required high-quality RNA purification, optimal conversion of RNA to complementary deoxyribonucleic acid (cDNA) (reverse-transcription), amplification of the cDNA using polymerase chain reaction (PCR); and sensitive and accurate real-time detection of amplification products (Fraga *et al.*, 2008; Nolan *et al.*, 2006).

Total RNA was extracted from the homogenates of the longitudinal strips of ileum using the Isolate II RNA Mini Kit (Bioline, London, UK). One microgram of isolated total RNA was used for reverse-transcription, which was accomplished with the Tetro cDNA Synthesis Kit (Bioline) and using random hexamers. Real-time PCR primers were designed with the Beacon Designer (Premier Biosoft, Palo Alto, USA) and obtained from Sigma-Aldrich (Sintra, Portugal). All the genes included in this study were described in the National Center for Biotechnology Information (NCBI) Gene

database (http://www.ncbi.nlm.nih.gov/) as indicated in Supplementary Table S5. Quantitative RT-PCR was performed on a Bio-Rad iQ5 real-time PCR instrument (BioRad, Hercules, California, USA) using the SensiFAST SYBR & Fluorescein Kit (Bioline). Detailed description of the qRT-PCR protocol was included in Supplementary Data S2.

Data were analyzed by relative mRNA quantification (Pfaffl, 2004) using *Hypoxanthine phosphoribosyltransferase 1* (*Hprt1*) as housekeeping gene internal control. All normalized values of samples corresponding to the moment of sacrifice were divided by the normalized value of the baseline (that is arbitrarily set to one), and expressed as fold variations. In rats that underwent laparotomy without resection, relative quantification was performed using mean ΔC_T (threshold cycle) at baseline value of rats submitted to ileal resection.

RNA extraction

Succinctly, biological samples were first lysed and homogenized in the presence of guanidinium thiocyanate, a chaotropic salt that immediately deactivated endogenous RNases to ensure purification of intact RNA. After homogenization, ethanol was added to the sample. Lysate was filtered and the RNA adjusted to RNA binding conditions. Sample was then processed through a spin column containing a silica membrane to which the RNA binds. Genomic DNA contamination was removed by a DNase I digestion during the preparation. Any impurities such salts, metabolites and cellular components were removed by simple washing steps of the silica membrane with two different buffers. High-quality purified total RNA was then eluted in RNase-free water and stored at -80°C.

Reverse-transcription (conversion of RNA to cDNA)

The Tetro cDNA Synthesis Kit (Bioline) was used, which contains moloney strain of murine leukemia virus (MMLV) reverse transcriptase and is suitable for the production of templates for RT-PCR amplification.

Real-time polymerase chain reaction

In real-time PCR, the amount of product formed was monitored by the proportional fluorescence of the dye (fluorescein) introduced into the reaction, and the number of amplification cycles required to obtain a particular amount of DNA molecules was registered. Assuming a certain amplification efficiency between 90-105%, which usually is close to a doubling of the number of molecules *per* amplification cycle, it was possible to calculate the number of DNA molecules of the amplified sequence that were initially present in the sample (Fraga *et al.*, 2008; Nolan *et al.*, 2006; Pfaffl, 2004).

Each sample was monitored for fluorescein and signals were regarded as significant if the fluorescence intensity exceeded 10-fold of the standard deviation of the baseline fluorescence, defined as threshold cycles (C_T). C_T were selected in the line in which all samples were in the logarithmic phase. For each sample, PCR was performed in duplicate.

6.3.5. Determination of glucagon-like peptide 2 plasma concentrations

Plasma levels of glucagon-like peptide 2 (Glp-2) were determined by competitive enzyme immunoassay (EIA) using the Glp-2 EIA Kit 96-Well Plate (Phoenix Europe GmbH, Karlsuhe, Germany), designed for quantification of rat total [Arg34]Glp2 in plasma, in accordance to the manufacturer's recommended protocol (described in detail in Supplementary Data S3). Threshold of sensitivity of the assay was 0.16 ng/ml and typical range was 0-100 ng/ml. Cross-reactivity with rat and human GLP-2 was 100% and with rat and human GLP-1/[92-128]proglucagon was 5%. All determinations were done in duplicate.

Enzyme-linked immunosorbent assay (ELISA) protocol is characterized by high specificity and sensitivity, as well as broad analytical range and reproducibility. However, disadvantages of this procedure include the inability to distinguish between bioactive and inactive compounds, different binding affinity of the antibodies, narrow dynamic range, auto-antibody interference, high costs, requirement of large sample

volumes, and feasibility of the measurement of only one analyte at a time on a given sample volume (Tighe *et al.*, 2013).

According to the basic principles, key event of the competitive immunoassay was the process of competitive reaction between the sample targeted peptide (or a standard peptide) and the biotinylated peptide with the primary antibody bound to the secondary antibody that coats the wells of a microtiter plate (Gan and Patel, 2013). Briefly, a secondary antibody, with nonspecific binding sites blocked, was immobilized on a solid phase, a 96 wells microtiter plate. The crystallizable fragment (Fc) of a capture primary antibody, with specificity for the peptide molecules, binded to the secondary antibody that coated the immunoplate. Biological sample peptide and standard peptide (containing a known concentration of recombinant Glp-2) competed with a biotinylated peptide for the antigen-binding fragment (Fab) of the primary antibody. Unbound protein was removed through extensive washing. Then, a streptavidin conjugated with the enzyme horseradish peroxidase (streptavidin-horseradish peroxidase complex) was added, which interacted with the biotinylated peptide. Excess of free enzyme conjugates was removed by washing. A chromogenic substrate (3,3',5,5'-tetramethylbenzidine) was added, which was chemically converted by the activity of the enzyme horseradish peroxidase coupled to the primary antibody, resulting in a color change. The intensity of the yellow color (that corresponded to the enzyme activity) was inversely proportional to the amount of peptide bound to the primary antibody in biological sample and standard solutions and directly proportional to the amount of biotinylated peptide-streptavidin-horseradish peroxidase complex. Finally, the optical density of the reaction was measured with a spectrophotometer (by the increased absorbance at 450 nm) and compared with the optical density of the known standard samples to determine peptide concentrations. Since the increase in absorbance was inversely proportional to the amount of captured peptide in the biological sample, the latter could be derived by interpolation from a reference curve generated in the same assay with reference standards of known concentrations of peptide (Phoenix Europe GmbH, 2017). Glp-2 plasma concentrations were calculated using the corresponding standard curve and the microplate reader with Gen5 software (Synergy HT, Biotek, Winooski, Vermont, USA), and expressed in ng/ml.

6.3.6. Statistical analysis

Results were analysed with Statistical Package for Social Sciences (SPSS) version 18 software package (SPSS, Chicago, Illinois, USA). Shapiro-Wilk and Kolmogorov-Smirnov-Lillifors normality tests were used. Data were indicated as medians and interquartile ranges (median ± IQR) or numbers (%). Non-parametric continuous variables were compared by Mann-Whitney U test and analysis of variance by ranks (Kruskall-Wallis test) with pairwise comparisons. Correlations were calculated by the Spearman's rank correlation coefficient (σ). Categorical variables were compared by Qui-square test. The established threshold for statistical significance was 95% ($p<0.05$).

6.4. Results

6.4.1. Postoperative outcome

Fifty-nine animals finished the protocol and were comprised into the groups: "*Res Ted* +" (15, eight of them sacrificed on the third day), "*Res Ted* –" (13, five sacrificed at third day), "*Lap Ted* +" (16, eight sacrificed on the third day) and "*Lap Ted* -" (15, seven sacrificed at third day).

6.4.2. Response of tissue growth factors gene expression to ileal resection and anastomosis

In the perianastomotic segments, upregulation of gene expression of *Fgf7* (fold-change: 12.6±2.8), *Fgf2* (fold-change: 6.1±2.2), *Egf* (fold-change: 2.7±2.2), *Vegfa* (fold-change: 2.7±1.0) and *Glp2r* (fold-change: 2.3±2.1) at the third postoperative day (Fig. 6.1 A); as well as of *Pdgfb* (fold-change: 2.0±1.5), *Igf1*, *Egf*, *Hbegf*, *Vegfa* and *Glp2r* at the seventh day was verified (Fig. 6.1 B). Moreover, downregulation of *Igf1* (fold-change: 0.2±0.3), *Hbegf* (fold-change: 0.4±0.5), *Tgfβ1* (fold-change: 0.4±0.3) and *Ctgf* at the third day (Fig. 6.1 A); as well as of *Tgfβ1* (fold-change: 0.5±0.3), *Fgf7* (fold-change: 0.5±0.4), *Ctgf* (fold-change: 0.5±0.3) and *Fgf2* at the seventh day was also observed (Fig. 6.1 B).

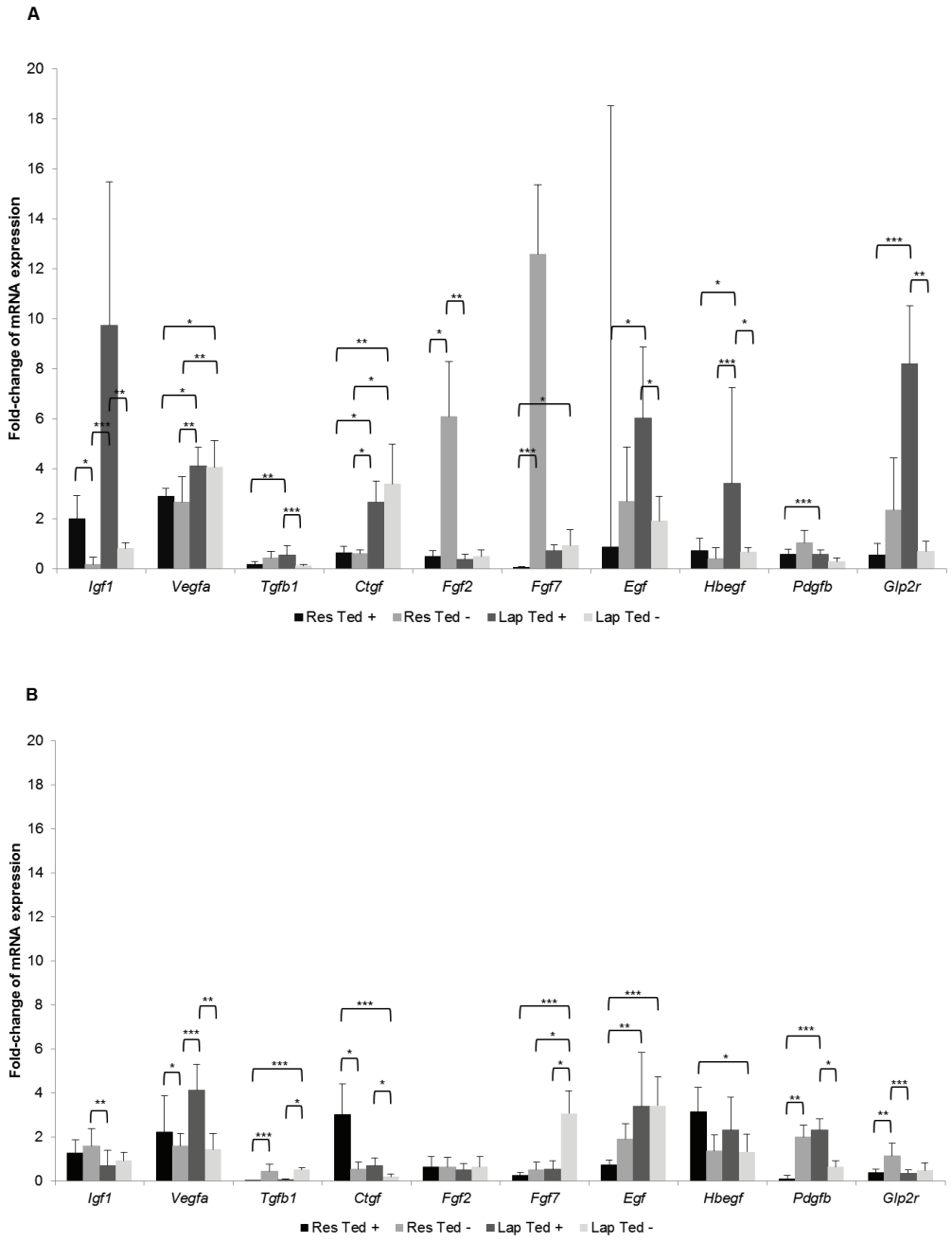

Figure 6.1. Fold-changes of relative gene expression of growth factors and *Glp2 receptor* in the rats' ileum, at the third (A) and the seventh (B) days after operation, determined by qRT-PCR. Animals (*n*=59) were submitted to ileal resection and anastomosis ("*Res*") or laparotomy ("*Lap*") and sacrificed on the third or seventh postoperative day. In groups "*Res Ted +*" and "*Lap Ted +*", teduglutide was administered after the operation. Samples recovered at the sacrifice from rats that underwent ileal resection corresponded to the anastomotic segment. Values were normalized to *Hprt* gene and fold-changes were generated by comparison with baseline values of rats submitted to ileal resection (*n*=28). Results were expressed as median±interquartile range. Kruskal-Wallis test with pairwise comparisons was used. * $p<0.05$; ** $p<0.01$; *** $p<0.001$

Glp2r expression was upregulated after ileal resection and anastomosis, particularly at the third postoperative day, while it was downregulated after isolated laparotomy.

In the perianastomotic segments, lower fold-change of relative gene expression of *Vegfa* and *Ctgf* at the third day, and of *Fgf7* at the seventh day, was observed in comparison with the ileal samples recovered after isolated laparotomy (Fig. 6.1).

6.4.3. Response of tissue growth factors gene expression to isolated laparotomy

In the ileal samples recovered after isolated laparotomy, upregulation of gene expression of *Vegfa* (fold-change: 4.1±1.1), *Ctgf* (fold-change: 3.4±1.6) and *Egf* at the third postoperative day; and of *Egf* (fold-change: 3.4±1.3), *Fgf7* (fold-change: 3.1±1.0), *Vegfa* and *Hbegf* at the seventh day was documented (Fig. 6.1). Furthermore, downregulation of *Tgfβ1* (fold-change: 0.1±0.1), *Pdgfb* (fold-change: 0.3±0.1), *Fgf2* (fold-change: 0.5±0.3), *Igf1*, *Fgf7*, *Hbegf* and *Glp2*, at the third day after the operation; as well as of *Ctgf* (fold-change: 0.2±0.1), *Glp2r* (fold-change: 0.5±0.4), *Tgfβ1* (fold-change: 0.5±0.1), *Fgf2* and *Pdgfb* at the seventh day, was also evident.

6.4.4. Response of tissue growth factors gene expression to teduglutide postoperative administration

In the anastomotic segments, teduglutide was significantly associated with upmodulation of gene expression of *Igf1* (2.0±0.9 *vs.* 0.3±0.3, p=0.028), and downmodulation of *Fgf2* (0.5±0.3 *vs.* 6.1±2.2, p=0.028) and *Fgf7* (0.1±0.0 *vs.* 12.6±2.8, p=0.0001) at the third day; as well as upregulation of *Vegfa* (2.2±1.7 *vs.* 1.6±0.6, p=0.045) and *Ctfg* (3.0±1.4 *vs.* 0.5±0.3, p=0.014), and downregulation of *Tgfβ1* (0.0±0.0 *vs.* 0.5±0.3, p=0.0001), *Pdgfb* (0.0±0.1 *vs.* 2.0±0.5, p=0.001) and *Glp2r* (0.4±0.2 *vs.* 1.1±0.6, p=0.002) at the seventh day (Fig. 6.1).

When considering all the animals (those submitted to ileal resection or isolated laparotomy), at the third postoperative day, teduglutide was significantly associated

with a higher fold-change of relative gene expression of *Igf1* (5.6±8.0 *vs.* 0.7±0.7, *p*=0.0001) and *Hbegf* (1.5±2.8 *vs.* 0.6±0.4, *p*=0.001); and lower fold-change of *Fgf2* (0.5±0.2 *vs.* 0.8±5.5, *p*=0.002) and *Fgf7* (0.2±0.7 *vs.* 1.3±11.4, *p*=0.0001) (Fig. 6.2). At the seventh postoperative day, teduglutide was significantly associated with higher fold-change of relative gene expression of *Vegfa* (3.6±2.0 *vs.* 1.5±0.6, *p*=0.0001), *Ctgf* (1.1±2.4 *vs.* 0.3±0.4, *p*=0.0001) and *Hbegf* (3.0±1.6 *vs.* 1.3±0.7, *p*=0.004); and lower fold-change of *Tgfβ1* (0.02±0.04 *vs.* 0.5±0.5, *p*=0.0001), *Fgf7* (0.4±0.4 *vs.* 0.9±2.6, *p*=0.007) and *Glp2r* (0.4±0.2 *vs.* 1.0±0.7, *p*=0.0001) (Fig. 6.2).

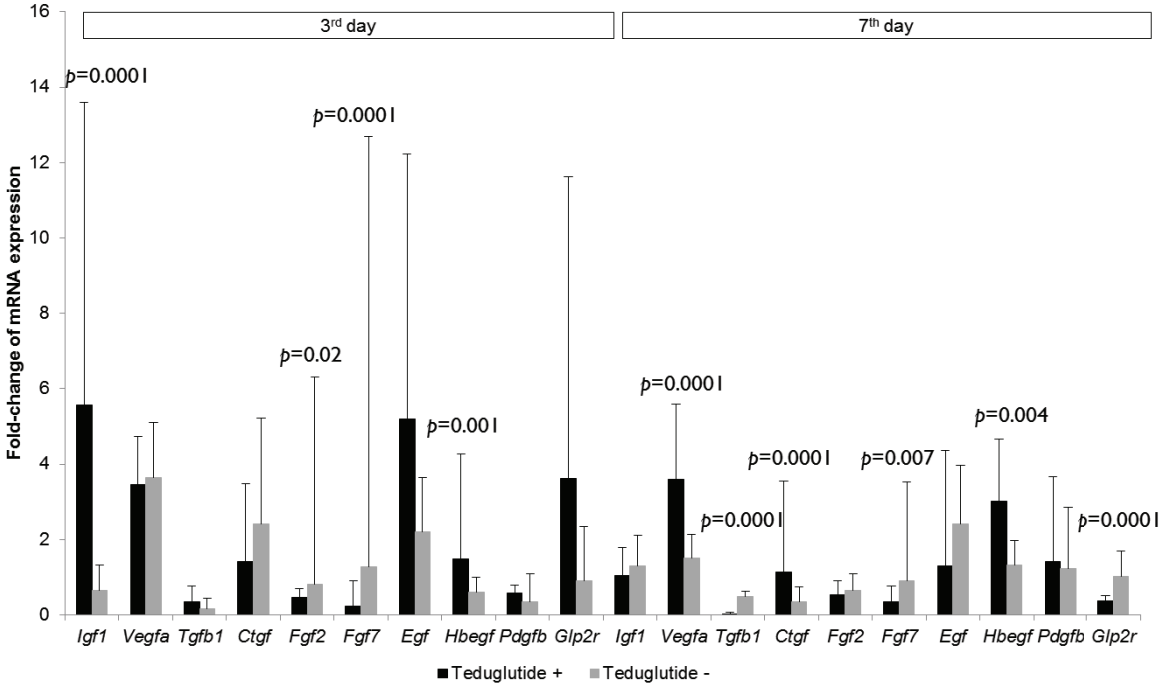

Figure 6.2. Fold-change of relative gene expression of growth factors and *Glp2 receptor*, in the ileum of rats from all groups (*n*=59), according to the teduglutide administration. Relative gene expression was determined at the moment of sacrifice (third or seventh day, after ileal resection and anastomosis or after laparotomy) by qRT-PCR. Samples recovered at the sacrifice from rats submitted to ileal resection corresponded to the anastomotic segment. Values were normalized to *Hprt* gene and fold-changes were generated by comparison with baseline values of rats submitted to ileal resection (*n*=28). Results were expressed as median±interquartile range. Mann-Whitney U test was used. *Teduglutide* +, Postoperative teduglutide administration; *Teduglutide* -,Without teduglutide administration

In all the animals (*n*=59), at the sacrifice, teduglutide was significantly associated with higher fold-change of relative gene expression of *Vegfa* (3.6±1.3 *vs.* 1.9±2.0, *p*=0.0001), *Hbegf* (2.2±2.3 *vs.* 1.1±0.9, *p*=0.001), *Igf1* (1.6±7.6 *vs.* 0.9±0.7, *p*=0.002) and *Ctgf* (1.1±2.1 *vs.* 0.6±2, *p*=0.013); and lower fold-change of *Tgfβ1* (0.1±0.4 *vs.* 0.4±0.4, *p*=0.002), *Fgf7* (0.4±0.6 *vs.* 1.2±3.0, *p*=0.0001) and *Glp2r* (0.5±6.1 *vs.* 1.0±0.9, *p*=0.042) (Fig. 6.3).

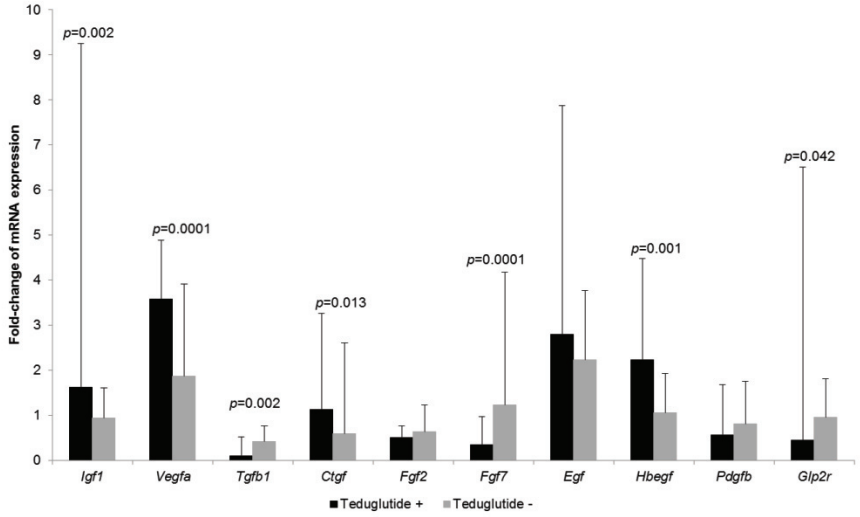

Figure 6.3. Fold-change of relative gene expression of growth factors and *Glp2 receptor*, in the ileum of rats from all groups (*n*=59) at the moment of sacrifice, according to the teduglutide administration. Relative gene expression was determined at the moment of sacrifice (third or seventh day, after ileal resection and anastomosis or after laparotomy) by qRT-PCR. Samples recovered at the sacrifice from rats submitted to ileal resection corresponded to the anastomotic segment. Values were normalized to *Hprt* gene and fold-changes were generated by comparison with baseline values of rats submitted to ileal resection (*n*=28). Results were expressed as median±interquartile range. Mann-Whitney U test was used. *Teduglutide +*, Postoperative teduglutide administration; *Teduglutide -*, Without teduglutide administration

6.4.5. Glucagon-like peptide 2 plasma concentrations

Median baseline levels of plasma Glp-2 were 0.906±0.578 (0.385-4.140) ng/ml. In animals not submitted to teduglutide treatment, plasma levels of Glp-2 suffered a relevant increase between the third and the seventh days after ileal resection (0.798±0.312 *vs.* 2.549±4.007 ng/ml, *p*=0.0001) and after laparotomy (0.836±0.766 *vs.*

1.239±0.549 ng/ml, *p*=0.03) (Fig. 6.4 A). At the seventh postoperative day, Glp-2 plasma levels were higher after ileal resection than after laparotomy (2.549±4.007 *vs.* 1.239±0.549 ng/ml, *n.s.*) (Fig. 4B).

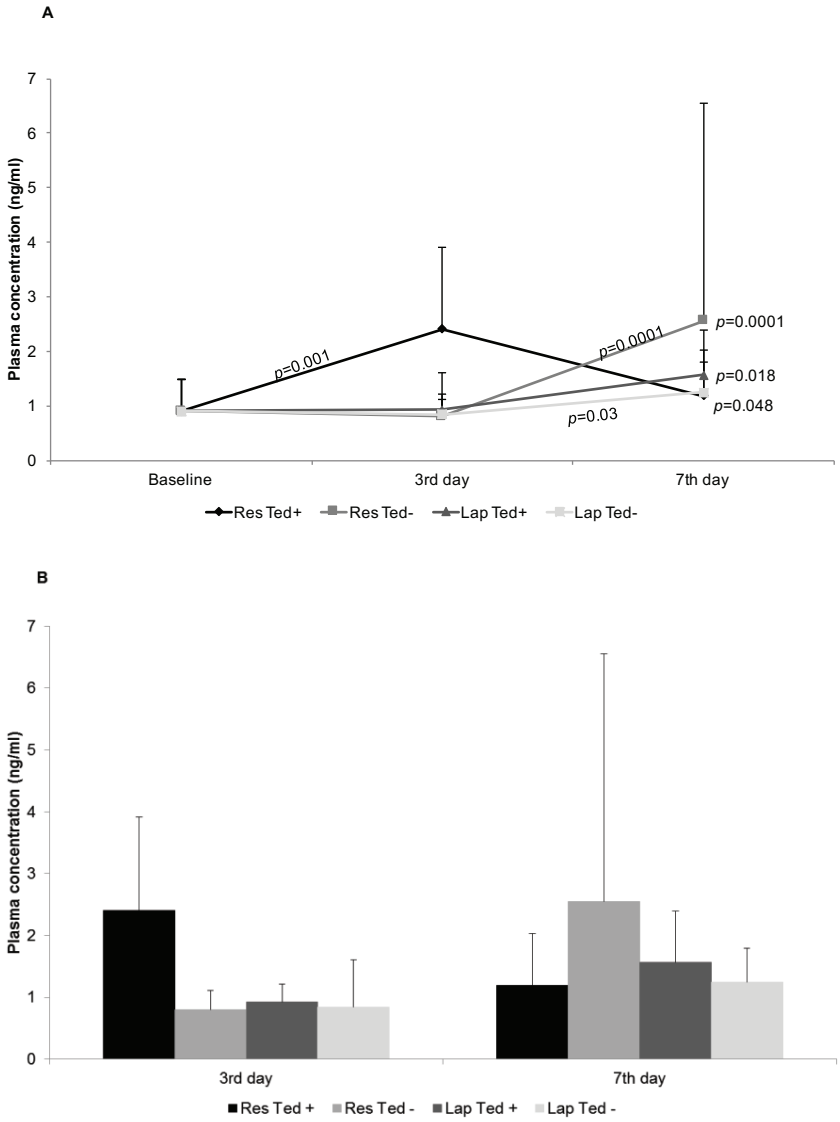

Figure 6.4. Glp-2 plasma levels as determined by competitive enzyme immunoassay at the third and seventh days after the operation in animals not submitted to teduglutide treatment (A) and in the different groups of study (B). Animals (*n*=59) underwent ileal resection and anastomosis (*Res*) or laparotomy (*Lap*) and were sacrificed at the third or at the seventh postoperative days. In groups "*Res Ted+*" and "*Lap Ted+*", teduglutide was administered after the operation. Baseline values were considered for comparison. Data were presented ng/ml (median±interquartile range). Kruskal-Wallis test with pairwise comparison was used

Teduglutide-treated animals demonstrated higher Glp-2 plasma levels at the third day after ileal resection and anastomosis (2.407±1.507 *vs.* 0.798±0.312 ng/ml, *n.s.*) and lower concentrations at the seventh day (1.187±0.845 *vs.* 2.549±4.007 ng/ml, *n.s.*), although without achievement of the statistical significance threshold (Fig. 6.4 B).

When analyzing all operated animals (submitted to ileal resection or laparotomy), teduglutide administration was associated with higher levels of Glp-2 at the third day (1.354±1.703 *vs.* 0.836±0.364 ng/ml, p=0.011) and at the seventh day (1.5±0.819 *vs.* 1.392±1.192 ng/ml, *n.s.*); no significant differences were observed when considering simultaneously both moments of sacrifice (1.5±1.039 *vs.* 1.234±0.786 ng/ml, *n.s.*).

6.4.6. Correlations between gene expressions of growth factors and Glp2 receptor at the sacrifice

At the sacrifice, *Glp2r* relative gene expression correlated directly with *Egf*, *Hbegf*, *Ctgf, Fgf7, Tgfβ1* and *Igf1* gene expressions and inversely with Glp2 plasma levels (Table 6.2).

Plasma levels of Glp-2 at the moment of sacrifice correlated significantly and negatively with relative gene expression of *Glp2r*, *Ctgf*, *Fgf7* and *Egf*; no significant correlations with *Igf1*, *Vegfa* and *Hbegf* mRNA expressions were observed.

5.5. Discussion

Present findings, namely the upregulation of *Fgf7, Fgf*2, *Egf* and *Vegfa* gene expression levels at the third postoperative day, and of *Pdgfb*, *Vegfa*, *Egf* and *Igf1* at the seventh day, in the perianastomotic segments, reenforce the recognized participation of these growth factors in the wound healing process (Rijcken *et al.*, 2014; Greaves *et al.*, 2013). Upregulation of *Pdgfb* and *Igf1* gene expression occurred in the predominantly proliferative phase, whereas that of *Vegfa* was verified in both inflammatory and proliferative stages, as predicted (Rijcken *et al.*, 2014; Greaves *et al.*, 2013). However, downregulation of *Tgfβ1* and *Ctgf* gene expressions observed in the anastomotic segment at the third and at the seventh postoperative days was unexpected, giving the

relevant participation of those growth factors in the anastomotic repair (Rijcken *et al.*, 2014; Seifert *et al.*, 2014).

Table 6.2. **Correlations between relative gene expressions of growth factors and Glp2 receptor in rats' small intestine and plasma levels of Glp2 at the moment of sacrifice (*n*=59)**[a]

σ / p	*Igf1*	*Vegfa*	*Tgfβ1*	*Ctgf*	*Fgf2*	*Fgf7*	*Egf*	*Hbegf*	*Pdgfb*	*Glp2r*	Plasma [Glp2]
Igf1			34.2% *p*=0.009		-27.7% *p*=0.036	-31.4% *p*=0.016				30.4% *p*=0.02	
Vegfa			-28.6% *p*=0.029			-41.3% *p*=0.001					
Tgfβ1	34.2% *p*=0.009	-28.6% *p*=0.029		-28.2% *p*=0.032		34% *p*=0.009	36.7% *p*=0.005		29,6% *p*=0,024	48.2% *p*=0.0001	
Ctgf			-28.2% *p*=0.032				27.3% *p*=0.038		-52,6% *p*=0,0001	37% *p*=0.004	-40.7% *p*=0.002
Fgf2	-27.7% *p*=0.036					30.3% *p*=0.021	53.2% *p*=0.0001	31.8% *p*=0.015			
Fgf7	-31.4% *p*=0.016	-41.3% *p*=0.001	34% *p*=0.009		30.3% *p*=0.021		44.4% *p*=0.0001			37.6% *p*=0.004	-40.5% *p*=0.002
Egf			36.7% *p*=0.005	27.3% *p*=0.038	53.2% *p*=0.0001	44.4% *p*=0.0001		44.3% *p*=0.001		52.7% *p*=0.0001	-31.9% *p*=0.016
Hbegf					31.8% *p*=0.015		44.3 % *p*=0.001			39.9% *p*=0.002	
Pdgfb			29.6% *p*=0.024	-52.6% *p*=0.0001							
Glp2r	30.4% *p*=0.02		48.2% *p*=0.0001	37% *p*=0.004		37.6% *p*=0.004	52.7% *p*=0.0001	39.9% *p*=0.002			-30.6% *p*=0.022
Plasma [Glp2]				-40.7% *p*=0.002		-40.5% *p*=0.002	-31.9% *p*=0.016			-30.6% *p*=0.022	

[a] Relative gene expressions of growth factors and *Glp2 receptor* and postoperative plasma levels of Glp2 ([Glp2]) were determined by qRT-PCR and competitive enzyme immunoassay, respectively. Spearman's rank correlation coefficient (σ) and level of significance (*p*) were presented. *Igf1: insulin-like growth factor 1, transcript variant 1, mRNA; Vegfa: vascular endothelial growth factor A, transcript variant 2, mRNA; Tgfb1: transforming growth factor, beta 1, mRNA; Ctgf: connective tissue growth factor, mRNA; Fgf2: fibroblast growth factor 2, mRNA; Fgf7: fibroblast growth factor 7, mRNA; Egf: epidermal growth factor, mRNA; Hbegf: heparin-binding epidermal-like growth factor, mRNA; Pdgfb: platelet-derived growth factor beta polypeptide, mRNA; Glp2r: glucagon-like peptide 2 receptor, mRNA*

In fact, Seigert GJ *et al* (Seifert *et al.*, 2014) demonstrated, recently, a consistent upregulation of tissue *Tgfβ*, *Ctgf* and *Igf1* gene expressions after ileoileal anastomosis. Epigenetic modifications triggered by environmental factors, including DNA methylation, histone modifications of DNA and RNA interference by regulatory noncoding RNA (such as microRNAs) (Mann and Mann, 2013) may have contributed to these results.

In this experiment, teduglutide administration was significantly associated with higher fold-change of relative gene expression of *Igf1*, *Hbegf*, *Vegfa* and *Ctgf*, as well as with lower fold-change of *Tgfβ1* and *Fgf7*, in the postoperative period.

Induction of *Igf1* messenger RNA expression in teduglutide-treated animals documented in this study was according to the literature (Drucker and Yusta, 2014) and was observed at the third day, both in the anastomotic segments and in the ileal samples recovered after isolated laparotomy. Igf1 is considered a critical mediator of the enterotrophic effects of Glp-2 (Bortvedt *et al.*, 2012), although not systematically required (Drucker and Yusta, 2014). Igf1 promotes growth of small intestinal epithelium and participates in the fibroplasia, modulating the proliferation of fibroblasts and myofibroblasts and the synthesis of collagen (Latella *et al.*, 2013; Bortvedt *et al.*, 2012). Several studies demonstrated that this growth factor administration improves the healing parameters, on animal models of colonic anastomosis, in standard and high-risk contexts (Rijcken *et al.*, 2014; Oines *et al.*, 2014).

An increase of *Hbegf* messenger RNA expression levels in teduglutide-treated animals was verified in current study, at both postoperative time points (although statistically significant only at the seventh day after isolated laparotomy). Involvement of the ErbB ligant-ErbB signaling pathway in the proliferative actions of Glp-2 was suggested in previous experiments (Drucker and Yusta, 2014). Studies about the refeeding-induced mucosal proliferation revealed also the importance of ErbB signaling for the actions of endogenous Glp-2 (Drucker and Yusta, 2014).

Hbegf has mitogenic and chemotactic effects on epithelial cells, fibroblasts and smooth muscle cells; promotes extracellular matrix synthesis and angiogenesis; modulates vasodilatation and preserves microcirculatory blood flow; improves intestinal motility; and demonstrates antiinflammatory effects (Rijcken *et al.*, 2014; Yang *et al.*, 2014; Radulescu *et al.*, 2011). Moreover, this growth factor seems to preserve the intestinal mucosa and to restore gut barrier function after intestinal injury (Yang *et al.*, 2014). Indeed, a potent intestinal cytoprotective effect of Hbegf on intestinal epithelial cells (including stem cells), endothelial cells, pericytes, immunocytes and neuronal cells has been demonstrated in animal models of necrotizing enterocolitis, ischemia/reperfusion injury, and hemorrhagic shock and resuscitation (Yang *et al.*, 2014). Furthermore, in

2011, Radulescu A *et al* (Radulescu *et al.*, 2011) demonstrated, on an animal model, that exogenous Hbegf promoted intestinal anastomotic repair, and that the *Hbegf* (-/-) knockout mice had worse healing scores and higher morbidity and mortality rates after intestinal anastomosis.

Induction of *Vegfa* and *Ctgf* gene expression levels observed in this study in teduglutide-treated animals at the seventh day suggest that these growth factors may be also relevant as downstream mediators of Glp-2 effects in the perioperative context.

Vegfa has an important participation in wound healing, as it promotes the early events of angiogenesis (namely endothelial cell migration, proliferation and differentiation) and lymphangiogenesis (Rijcken *et al.*, 2014; Barrientos *et al.*, 2008). In 2011, Adas G *et al* (Adas *et al.*, 2011) demonstrated a favorable impact of *Vegfa* plasmid delivery on the healing of ischemic colonic anastomosis on an animal model, including enhanced fibroblast activity, collagen deposition, angiogenesis, hydroxyproline levels and bursting pressure. After intraoperative local Vegfa administration in a rabbit model of colonic anastomoses, Ishii M *et al* (Ishii *et al.*, 2009) found improved bursting pressure, increased hydroxyproline levels and, also, significantly enhanced submucosal capillary vascular counts.

Ctgf is considered a key determinant in the formation and maintenance of connective tissues and in the wound repair process (Speca *et al.*, 2012; Jacobson and Cunningham, 2012; Barrientos *et al.*, 2008). In fact, this growth factor promotes the proliferation, differentiation and chemotaxis of fibroblasts, the epithelial-mesenchymal transition, the extracellular matrix formation and remodeling, the reepithelialization (by stimulation of cell migration) and the angiogenesis (Speca *et al.*, 2012; Jacobson and Cunningham, 2012; Barrientos *et al.*, 2008). Discrepant responses of *Ctgf* and *Tgfβ1* gene expressions to teduglutide administration, observed in this study, were surprising because Ctgf is controlled by Tgfβ1 in a Smad-dependent way and acts as a downstream mediator of Tgfβ action on connective tissue cells (Speca *et al.*, 2012; Barrientos *et al.*, 2008).

Present data indicated that the teduglutide administration was associated with downregulation of *Tgfβ1* gene expression in the anastomotic segments at both

moments of evaluation. This fact raises concern about a potential negative impact on the anastomotic healing, since Tgfβ participates in all phases of this process (Rijcken *et al.*, 2014; Barrientos *et al.*, 2008).

Tgfβ is a pleiotropic polypeptide hormone that modulates the mucosal immune response and the tissue remodeling in the gut. In fact, Tgfβ downregulates the production of proinflammatory cytokines, promotes the differentiation of regulatory T-cells and induces the production of secretory immunoglobulin A (Biancheri *et al.*, 2014; Speca *et al.*, 2012). This growth factor also regulates extracellular matrix turnover and exerts an important role in tissue physiologic remodeling and wound repair in the intestine. Indeed, Tgfβ promotes the recruitment, proliferation, differentiation and activation of extracellular matrix-producting cells (Biancheri *et al.*, 2014; Latella *et al.*, 2013; Speca *et al.*, 2012; Barrientos *et al.*, 2008) and the epithelial and endothelial-mesenchymal transition (Speca *et al.*, 2012). It also stimulates extracellular matrix production and deposition (enclosing types I and III collagens, fibronectin and proteoglycans) and inhibits its degradation (including through the inhibition of matrix metalloproteinases 1, 3 and 9) (Latella *et al.*, 2013; Barrientos *et al.*, 2008; Speca *et al.*, 2012). Tgfβ promotes epithelial restitution inducing the migration of epithelial cells across the wound margin (Biancheri *et al.*, 2014; Speca *et al.*, 2012), stimulates the recruitment of inflammatory cells and macrophage-mediated tissue debridement (Barrientos *et al.*, 2008), promotes angiogenesis (thought upregulation of Vegf) (Speca *et al.*, 2012; Barrientos *et al.*, 2008) and participates in wound contraction (Barrientos *et al.*, 2008). Several cell types can produce and respond to TGF-β, including epithelial cells, macrophages, regulatory T-cells, myofibroblasts, and dendritic cells (Biancheri *et al*, 2014). Adenoviral-mediated transfer of *Tgfβ1* on an animal model of colonic anastomoses, through intraluminal local administration, was associated with a significant increase of the anastomotic bursting pressure (Migaly *et al.*, 2004).

The downregulation of *Fgf7* gene in animals submitted to teduglutide treatment documented in the present study (statistically significant only in the anastomotic segments at the third day and in the ileal samples recovered after isolated laparotomy at the seventh day) was also unexpected, because this growth factor has been proposed as one of the mediators of Glp-2 action, particularly on the colonic mucosa

(Drucker and Yusta B, 2014). Fgf7 (also known as keratinocyte growth factor 1, Kgf1) is a mitogenic growth factor with an important role in the intestinal epithelial growth, maintenance and repair and in the preservation of the barrier function (Rijcken *et al.*, 2014; Cai *et al.*, 2012; Barrientos *et al.*, 2008). A favorable effect of this growth factor on the intestinal mucosal protection has been demonstrated, on experimental studies, in the context of chemically-induced inflammatory bowel disease, chemotherapy and radiation mucositis, ischemia/reperfusion syndrome, short-bowel syndrome and total parenteral nutrition (Cai *et al.*, 2012). Intraperitoneal administration of truncated Kgf on an animal model of colonic anastomosis was associated with enhanced anastomotic bursting pressure, lower inflammatory activity on histological examination and higher crypt cell proliferation rates (Egger *et al.*, 2001).

In present study, an increase of Glp-2 plasma levels after ileal resection was documented in the postoperative period and was congruent with the literature. In fact, several animal experiments demonstrated an increase of plasma Glp-2 concentrations following intestinal resections, with a positive correlation with its magnitude (Tappenden, 2014; Muto *et al.*, 2013; Garrison *et al.*, 2009; Koopmann *et al.*, 2009; Martin *et al.*, 2005).

Posology of teduglutide in our experiment was based on previous published experimental and clinical studies on the intestinotrophic properties and pharmacodynamic characteristics of GLP-2 and its analogues (Qi *et al.*, 2017; Burness and McCormak, 2013; Arda-Pirincci *et al.*, 2012; Alters *et al.*, 2012; Kaji *et al.*, 2009; Kaji *et al.*, 2008; Martin *et al.*, 2004).

As outlined above, most of the Glp-2 effects are indirect and secondary to endocrine, paracrine, autocrine and neural signaling activated by the Glp2r (Drucker and Yusta, 2014). In present study, higher correlation coefficients were presupposed between relative mRNA expressions of *Glp2r* and *Igf1*, *Hbegf* and *Fgf7* gene expression levels, because these growth factors have been recognized as molecular downstream mediators of the Glp2r signaling in gastrointestinal tract (Drucker and Yusta, 2014). Gene expressions of *Fgf2* and *Vegfa*, two of the most important mediators of neoangiogenesis (Greaves *et al.*, 2013), did not correlated significantly as awaited. In

relation to the Glp-2/Glp2r axis, current investigation indicated that tissue *Glp2r* expression may be negatively affected by increased Glp-2 plasma concentrations.

In conclusion, results of present study underscore the recognized role of Igf1 and Hbegf as molecular mediators of the effects of teduglutide and suggest that other humoral factors, like Vegfa and Ctgf may be also relevant in the perioperative context of intestinal anastomosis. A negative influence of teduglutide on postoperative Tgfβ1 relative gene expression was also indicated.

Albeit the negative impact on postoperative tissue Tgfβ1, induction of Vegfa, Igf1 and Ctgf gene expressions might indicate a favorable influence of teduglutide on the intestinal anastomotic healing.

Chapter 7

Teduglutide effects on gene modulation of fibrogenesis on an animal model of intestinal anastomosis

This chapter was partially published as:

Costa BP, Gonçalves AC, Abrantes AM, Alves R, Matafome P, Seiça R, Sarmento-Ribeiro AB, Botelho MF, Castro-Sousa F: Teduglutide effects on gene regulation of fibrogenesis on an animal model of intestinal anastomosis. *J Surg Res.* 2017;216:87-98. Doi 10.1016/j.jss.2017.04.022.

7.1. Abstract

Teduglutide is an enterotrophic analogue of glucagon-like peptide 2 approved for the rehabilitation of short-bowel syndrome. This study purposed to analyze the effects of teduglutide administration on the gene regulation of fibrogenesis during the intestinal anastomotic healing on an animal model. Wistar rats (*n*=62) were assigned into four groups: "*Ileal Resection and Anastomosis*" or "*Laparotomy*", each one subdivided into "*Postoperative Teduglutide Administration*" or "*No Treatment*"; and sacrificed at the third or at the seventh days, with ileal sample harvesting. Gene expression of matrix components and remodeling factors [matrix metalloproteinases (*Mmp*) and tissue inhibitors of metalloproteinases (*Timp*)], and growth factors was studied by quantitative real-time reverse-transcription polymerase chain reaction. Net collagen deposition was assessed through the *Collagen*-to-*Mmp*-to-*Timp* ratio of fold-change of relative gene expression. Gene expression profiles revealed a balance towards net degradation of collagen at the third day of the intestinal anastomotic healing. Teduglutide appeared to be associated with an overall accumulation of collagen at the third day of the anastomotic repair, attributable to the upregulation of *Timp1* and *Timp2 and Collagen type IV alpha 1* and downregulation of *Mmp3 and Mmp12*; and to a net degradation of collagen at the seventh day, derived from repression of *Collagen type III alpha 1*, *Collagen type V alpha 1, Collagen type IV alpha 1* and *Timp1* expression. Teduglutide seemed to be associated with a favorable influence on fibrogenesis at the third day of the intestinal anastomotic repair and to a trend to fibrolysis at the seventh day.

7.2. Introduction

Extracellular matrix is a dynamic non-cellular three-dimensional network of macromolecules with particular physical, biochemical and biomechanical properties that confers structural stability to the tissues and supports organ function and repair (Gattazzo *et al.*, 2014). In the intestine, extracellular matrix constitutes a key element of the epithelial stem cell niche (Gattazzo *et al.*, 2014; Speca *et al.*, 2012). Extracellular matrix is constituted by collagen (the most important structural component), proteoglycans, hyaluronan, elastin and elastin-associated proteins, fibronectin, laminins, and matricellular proteins (Theocharis *et al.*, 2016). Remodeling was accomplished by extracellular matrix modifying-proteins that include proteases, such as the matrix metalloproteases [matrix metalloproteinases (mmps), a disintegrins and metalloproteases (adams), adams with thrombospondin motifs (adamts)], the plasminogen/plasmin system and the cathepsin proteases, and tissue inhibitors of metalloproteinases (timps) (Cui *et al.*, 2017; Amar *et al.*, 2017; Theocharis *et al.*, 2016; Speca *et al.*, 2012). Matrix macromolecules are synthesized and secreted by several cell types, including fibroblasts and epithelial, endothelial and immune cells. Extracellular matrix modulates cellular growth, migration, differentiation and survival, preserves homeostasis, and drives morphogenesis, through the interaction with surface receptors, such as integrins, discoidin domain receptors (DDR), CD44, syndecans and glypicans (Theocharis *et al.*, 2016).

In the gut, majority of collagen is contained within the submucosal layer, which is the main responsible for the biomechanical resistence of the anastomosis, particularly during the inflammatory phase of wound healing (Thompson *et al.*, 2006). Fibrogenesis derives from the activation of mesenchymal cells, mainly fibroblasts and myofibroblasts, which produce a collagen-rich extracellular matrix that gradually replace temporary fibrin matrix (Speca *et al.*, 2012; Thompson *et al.*, 2006). Collagen content in the perianastomotic tissues results from a precisely controlled equilibrium between synthesis and catabolism (Ågren *et al.*, 2011).

Collagens are trimeric molecules formed by three polypeptide α chains, which contain the sequence repeat (glycine–X–Y)*n* (X being usually proline and Y 4-hydroxyproline). These repeats allow the formation of a triple helical conformation, which is the

structural feature characteristic of the collagen superfamily (Theocharis *et al.*, 2016; Gelse *et al.*, 2003). Most abundant collagen types in the intestine (I, III and V) belong to the fibrillar group (Gelse *et al.*, 2003). Type I collagen predominates (approximately 68%), followed by type III (20%) and type V (12%) (Thompson *et al.*, 2006). Those collagens are characterized by the aggregation into supramolecular structures with a typical quarter-staggered fibril-array (Gelse *et al.*, 2003) (Table 7.1; Fig. 7.1A).

Table 7.1. Classification and chain composition of the most abundant collagens in the intestine[a]

Collagen group	Collagen type	Composition
Fibrillar collagens		
	I	$\alpha1[I]_2\ \alpha2[I]$
	III	$\alpha1[III]_3$
	V	$\alpha1[V]_3$ $\alpha1[V]_2\ \alpha2[V]$ $\alpha1[V]\ \ \alpha2[V]\ \alpha3[V]$
Network-forming collagens		
	IV	$\alpha1[IV]_2\ \alpha2[IV]$ $\alpha3[IV]\ \alpha4[IV]\ \alpha5[IV]$ $\alpha5[IV]_2\ \alpha6[IV]$

[a] Adapted from Theocharis *et al.*, 2016

All fibril-forming collagens are composed of a large continuous triple helix bordered by the amino and carboxyl-propeptides, respectively, and are synthesized as precursors, the procollagens, which are secreted in the extracellular space (Ricard-Blum and Ruggiero, 2005). Tropocollagen triple helices suffer self-assembly and regular staggering to form fibrils that are stabilized by cross-links and packed together into large fibers (Theocharis *et al.*, 2016). Type I collagen triple helixes are generally constituted by a heterotrimer with two identical $\alpha1$(I)-chains and one $\alpha2$(I)-chain and are usually incorporated into aggregates containing either type III or type V collagens. Type III collagen is a homotrimer of three $\alpha1$(III) chains frequently integrated in mixed fibrils (with type I collagen). Type V collagen is heterotrimer of three different α-chains ($\alpha1$, $\alpha2$ and $\alpha3$) and generally forms heterofibrils with types I and III collagens in interstitial matrixes (Gelse K *et al.*, 2003).

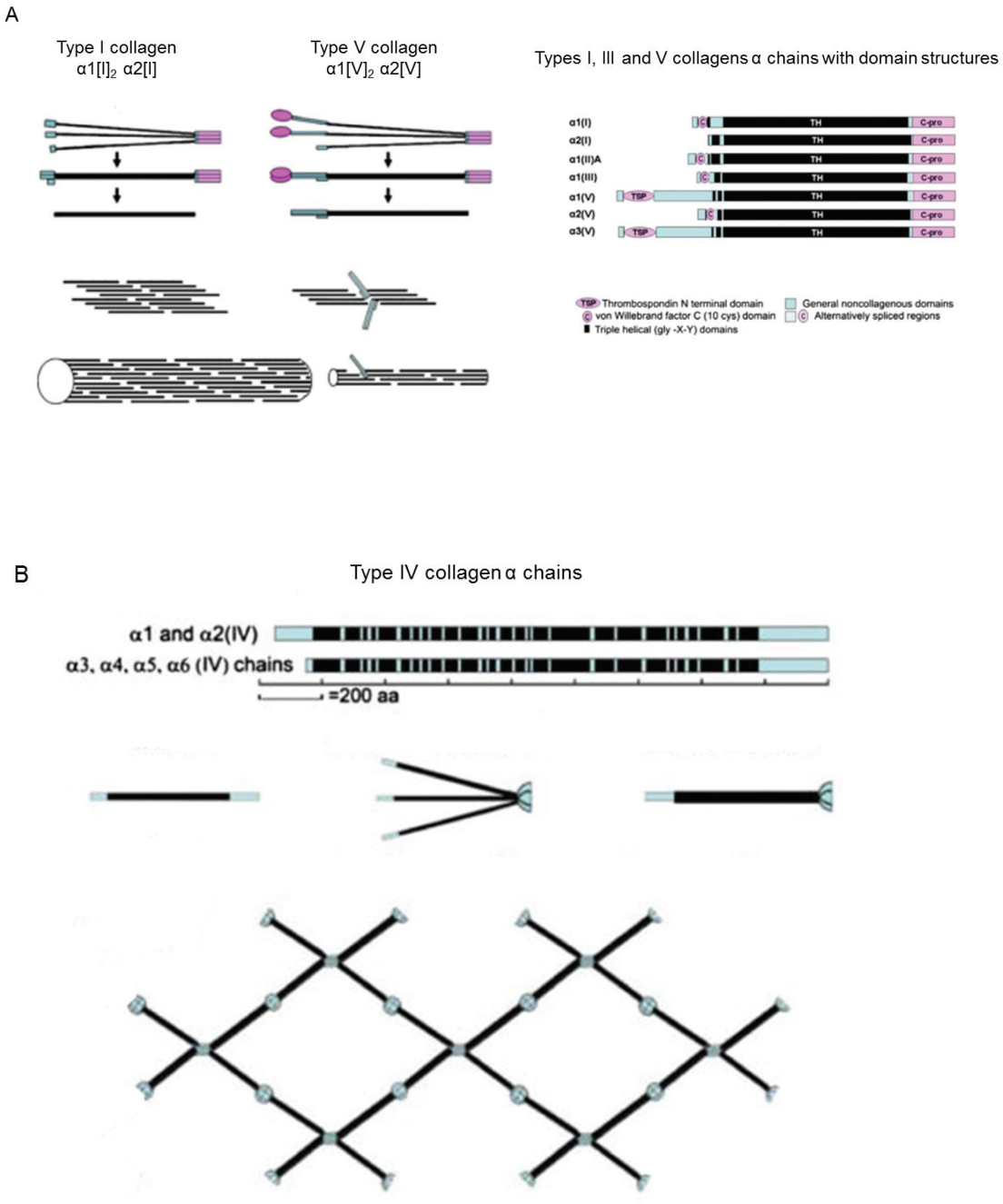

Figure 7.1. Structural features of the most abundant collagens in the intestine. Types I, III and V collagens are fibrillar collagens (**A**), which are characterized by the aggregation into supramolecular structures with a quarter-staggered fibril-array. Type IV collagen (**B**), a network-forming collagen, is the most important component of basement membranes and forms a more flexible triple helix conjunct organized into a meshwork (Theocharis *et al.*, 2016; Gelse *et al.*, 2003). Adapted from Gordon MK and Hahn RA, 2010

Collagen V is the most heterogeneous among the fibrillar collagens; in addition to the heterotrimer $[\alpha1(V)]_2\alpha2(V)$ found in most tissues, several other chain associations exist, including hybrid molecules (Ricard-Blum and Ruggiero, 2005). Type IV collagen, a network-forming collagen, is the most proeminent structural component of basement membranes, where it forms a stable two-dimensional supramolecular aggregate (Gelse *et al.*, 2003). There are six α-chains that can constitute type IV collagen trimmers but the most frequent chain composition is $[\alpha1(IV)]_2\alpha2(IV)$ (Gordon and Hahn, 2010) (Table 7.1; Fig. 7.1B).

Extracellular matrix-degrading enzymes play critical roles in the tissue remodeling and repair (Theocharis *et al.*, 2016). Mmps, also designed matrixins, are a group of at least 28 calcium-activated zinc-dependent endopeptidases (23 in humans), collectively capable of degrading all extracellular matrix components. Moreover, mmps participate in the inflammatory and immune responses, angiogenesis, reepithelialization and proteolytic activation or degradation of chemokines, cytokines, cell-surface molecules and growth factors (such as insulin-like growth factor, transforming growth factor β and fibroblast growth factors) (Levin *et al.*, 2017; Cui *et al.*, 2017; Biancheri *et al.*, 2014; Speca *et al.*, 2012; Ravi *et al.*, 2007). Main characteristics of some relevant mmps potentially involved in the intestinal anastomotic repair are listed in Table 7.2.

Control of the extracellular matrix turnover during the anastomotic wound healing process depends on a rigorous balance between synthesis and degradation, and involves interactions between extracellular matrix components, proteases (including mmps) and proteases inhibitors (comprising timps) (Ågren *et al.*, 2011; Baker EA, 2003). Failure to maintain the homeostasis of the extracellular matrix, with disturbances in the balance between synthesis and degradation of its components, seems to constitute an important factor in the pathogenesis of intestinal anastomotic failure (dehiscence or stenosis) (Ågren *et al.*, 2011; Pasternak *et al.*, 2010; Ågren *et al.,* 2006; Stumpf *et al.*, 2005) (Fig. 7.2).

Table 7.2. Relevant members of the metalloproteinases family, their substrates and role in physiological processes

MMP	Collagen substrates	Non-collagen ECM substrates	Other targets	Physiological processes
MMP1	I, II, III,VII, VIII, X, gelatin	Aggrecan, nidogen, perlecan, proteoglycan link protein, serpins, tenascin-C, versican	Casein, α1-antichymotrypsin, α1-antitrypsin, α1-proteinase inhibitor, IGF-BP-3 and -5, IL-1β, L-selectin, ovostatin, pro-TNF-α, SDF-1	Wound healing Immune response
MMP13	I, II, III, IV, gelatin	Aggrecan, fibronectin, laminin, perlecan, tenascin	Casein, plasminogen activator 2, pro-MMP9 and 13, SDF-1	Tissue remodeling Immune response
MMP2	I, II, III, IV, V, VII, X, XI, gelatin	Aggrecan, elastin, fibronectin, laminin, nidogen, proteoglycan link protein, versican	Active MMP9 and 13, FGF-R1, IGF-BP-3 and 5, IL-1β, pro-TNF-α, TGF-β	Angiogenesis
MMP9	IV, V, VII, X, XIV, gelatin	Aggrecan, elastin, fibronectin, laminin, nidogen, proteoglycan link protein, versican	CXCL5, IL-1β, IL2-R, plasminogen, pro-TNF-α, SDF-1, TGF-β	Cellular apoptosis
MMP3	II, III, IV, IX, X, XI, gelatin	Aggrecan, decorin, elastin, fibronectin, laminin, nidogen, perlecan, proteoglycan, proteoglycan link protein, versican	Casein, α1-antichymotrypsin, α1-proteinase inhibitor, antithrombin III, E-cadherin, fibrinogen, IGF-BP-3, L-selectin, ovostatin, pro-HB-EGF, pro-IL-1β, pro-MMP-1, -8, and -9, pro-TNF-α, SDF-1	Tissue remodeling
MMP12	IV, gelatin	Elastin, fibronectin, laminin	Casein, plasminogen	Immune response
MMP14	I, II, III, gelatin	Aggrecan, elastin, fibrin, fibronectin, laminin, nidogen, perlecan, proteoglycan, tenascin, vitronectin	αvβ3 integrin, CD44, pro-MMP2 and 13, pro-TNF-α, SDF-1, α1-proteinase inhibitor, tissue transglutaminase	Tissue remodeling Immune response Morphogenesis Cellular apoptosis

CD44, Cluster of differentiation 44; CXCL5, C-X-C motif chemokine ligand 5; ECM, Extracellular matrix; IGF-BP, Insulin-like growth factor binding protein; IL, Interleukin; IL-2R, Interleukin 2 receptor; FGF-R1, Fibroblast growth factor receptor 1; MMP, Metalloproteinase; Pro-HB-EGF, Pro-heparin-binding epidermal-like growth factor; Pro-MMP, Pro-metalloproteinase; Pro-TNF-α, Pro-tumor necrosis factor alpha; SDF-1, Stromal cell-derived factor-1; TGF-β,Transforming growth factor beta. Adapted from Cui N *et al.*, 2017

Overexpression of MMP1, MMP2 and MMP9 in biopsies obtained perioperatively from patients' colon was associated with an increased risk of subsequent anastomotic leakage (Stumpf *et al.*, 2005). In previous clinical studies, MMP2, MMP8 and MMP9 were found to be significantly elevated in the abdominal fluid drainage of patients with anastomotic leakage after colorectal surgery. Indeed, the peritoneal fluid level of MMP9 was considered a potential early marker to diagnose colorectal anastomotic leakage at a preclinical stage (Cini *et al.*, 2013). Additionally, the treatment with Mmp inhibitors has been shown to improve the biomechanical properties in animal models

of colonic anastomotic healing (Krarup *et al.*, 2017; Krarup *et al.*, 2013; Ågren *et al.*, 2011).

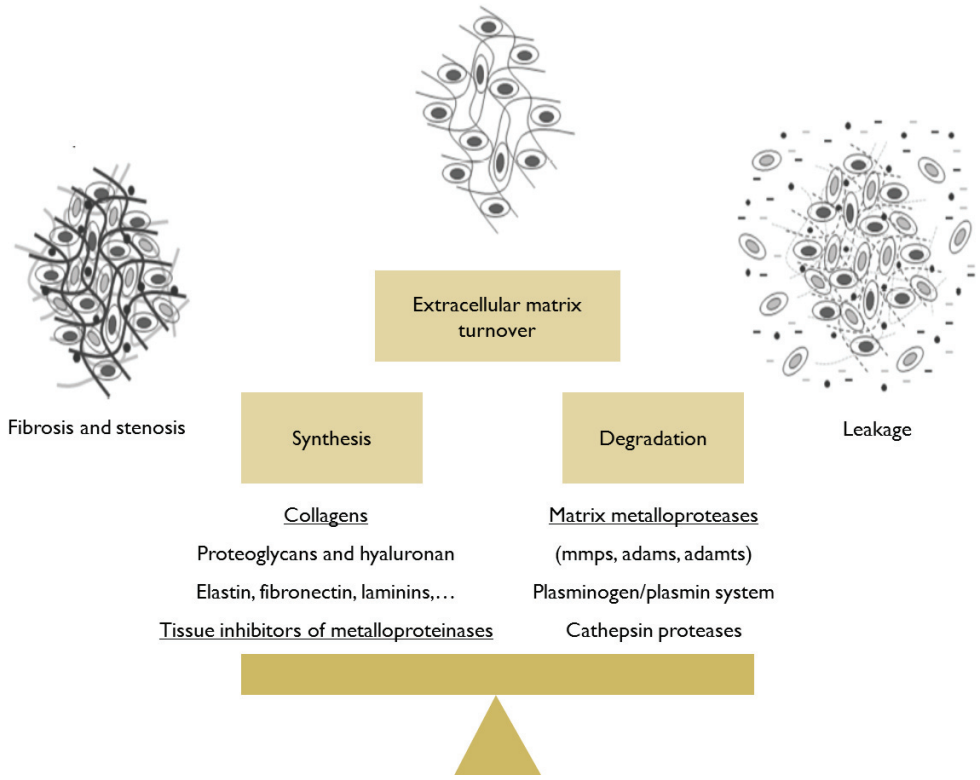

Figure 7.2. Simplified schematic representation of the extracellular matrix turnover. Extracellular matrix (ECM) homeostasis is maintained by a delicate equilibrium between continuous synthesis and degradation. Synthesis of ECM components, mainly collagens, by fibroblasts and myofibroblasts, is balanced with the activity of the ECM-degrading enzymes and its inhibitors, such as tissue inhibitors of metalloproteinases. During the intestinal anastomotic healing, abnormal ECM degradation may contribute to the development of leakage, while excessive deposition may conduct to fibrosis and stenosis (Theocharis *et al.*, 2016; Agren *et al.*, 2011). Adams, A disintegrins and metalloproteases; Adamts, Adams with thrombospondin motifs; Mmps, matrix metalloproteinases

Teduglutide is an enterotrophic analogue of glucagon-like peptide 2 approved for the rehabilitation of short-bowel syndrome (Drucker and Yusta B, 2014).

At present, response of the intestinal fibrogenesis to teduglutide administration in the perioperative context of intestinal anastomosis is not well understood. This study proposed to analyze the effects of teduglutide short-term treatment on the gene

modulation of fibrogenesis during the intestinal anastomotic healing, on an animal model, including the gene expression levels of the main extracellular matrix components and remodeling factors, mmps and timps.

7.3. Methods

7.3.1. Study protocol

Adult male Wistar *albinus* rats were randomly assigned into four groups: "*Ileal Resection and Anastomosis*" ("*Res*") or "*Laparotomy*" ("*Lap*"), each one subdivided into "*Postoperative Teduglutide Administration*" ("*Ted* +") or "*No Treatment*" ("*Ted* -"). Evaluation was conducted at the moments of the operation and sacrifice, at the third or the seventh postoperative day (eight subgroups), with recovering of ileal segments (except during isolated laparotomy). All the laboratorial analyses were performed in a blinded manner for the experimental groups.

Study was approved by the Ethics Committee of the Faculty of Medicine, University of Coimbra, Coimbra, Portugal and undertaken in consonance with institutional and national animals' protection guidelines.

7.3.2. Animals

Animals weighting 250 to 300 g were acclimatized to the laboratory environment for five days before experimental study; kept in temperature (22±1°C) and humidity (50±10%) controlled ventilated cages, with light/dark cycles of 12 hours; and maintained on water and standard rodent diet *ad libitum*.

7.3.3. Surgical interventions

All the operative procedures were executed by the same surgeon after a period of two hours fasting (water was never restricted) and determination of the preoperative

weight, with clean surgical technique and under anesthesia with an intraperitoneal injection of ketamine hydrochloride (75 mg/kg, Pfizer Inc., New York, USA) and chlorpromazine (3 mg/kg, Laboratórios Vitória, Amadora, Portugal).

In "*Ileal Resection and Anastomosis*" ("*Res*") groups, a 10-cm length ileal resection was performed, preserving distal 5 cm, after a 3-cm midline laparotomy. Continuity was restored by a standard end-to-end anastomosis with an interrupted single-layer full-thickness suture of eight equidistant polydioxanone USP 6/0 stitches (PDS II, Ethicon, Johnson-Johnson Intl., Cincinnati, USA). Abdominal wall was closed in two layers (muscle-aponeurotic and cutaneous) of continuous sutures, with braided coated poliglactin 910 USP 4/0 (Surgilactin, Sutures Limited, Wrexham, UK) and natural silk USP 4/0 (Surgisilk, Sutures Limited), respectively. In "*Laparotomy*" ("*Lap*") groups, a 3-cm midline laparotomy (without resection) was performed with gentle manipulation of the small bowel.

In the first postoperative day, ingestion of water with 5% glucose at a 1:1 ratio was allowed and, then, *ad libitum* oral hydration and chow were reassumed. Rats were monitored on a daily basis during the entire extent of the experiment. Operative morbidity and mortality were recorded. At the end of study, at the third or seventh postoperative day, animals were sacrificed by cervical displacement and a relaparotomy with ileal resection was performed (10-cm length, preserving distal 3 cm). During relaparotomy, peritoneal cavity was carefully inspected for anastomotic leakage, intra-abdominal abscess, peritonitis or intestinal obstruction; intra-abdominal adhesions were semiquantitatively graded using the Hulka scale (Cakmak *et al.*, 2009).

7.3.4. Teduglutide administration

In "*Ted +*" groups, teduglutide (American Peptide Company, Sunnyvale, California, USA) was prepared following the manufacturer's recommendations and administered subcutaneously in the postoperative period (starting on the day of the operation), 200 μg/kg per day, dissolved in 0.25 ml phosphate buffered saline pH 7.4 (PBS 7.4, Gibco, LifeTechnologies, Carlsbad, California, USA).

7.3.5. Tissue harvesting

Most distal segment, with 4-cm length, was carefully removed from each ileal operative specimen. Sample was opened at the mesenteric side, washed in normal saline solution and divided into three similar longitudinal strips, each one corresponding to one third of the circumference. These three longitudinal samples were prepared for quantitative real-time reverse-transcription polymerase chain reaction (qRT-PCR) after tissue homogenization, and additional studies, respectively, as mentionated in previous chapters.

In "*Ileal Resection and Anastomosis*" ("*Res*") groups, distal samples recovered at sacrifice corresponded to the anastomotic segment and included the anastomosis in the middle; tissue baseline values of these animals were considered for comparison with postoperative results of the "*Laparotomy*" ("*Lap*") groups.

7.3.6. Intestinal tissue homogenization

Intestinal tissue homogenization procedure was previously detailed in Chapter 5. Succintly, fragments from one ileal longitudinal strip recovered as previous depiction were immediately introduced in a mixture of protease inhibitors in a proportion of 1 ml/100 mg and submitted to mechanical homogenization. Inhibitors cocktail was formerly prepared by adding aprotinin from bovine lung (Sigma Aldrich, Sintra, Portugal), leupeptin hemisulfate salt (Sigma Aldrich) and pepstatin A (Sigma Aldrich) (1 μl of each, all diluted in a 10 mg/ml stock concentration) to 10 ml of phosphate buffered saline pH 7.4 (PBS pH 7.4, Gibco, LifeTechnologies) and stored on ice. Preparation was sonicated twice with one short pulse of ten seconds, cooled during ten seconds and distributed into two tubes of 1.5 ml. Sonication (one pulse of ten seconds) was repeated and centrifugation was undertaken, 14,000x *g*, for ten minutes, at 4°C. Supernatant was removed to a new tube and pellet was preserved on ice for posterior ribonucleic acid extraction.

7.3.7. Analysis of gene expression levels of extracellular matrix components and remodeling factors

Quantitative real-time RT-PCR (qRT-PCR) was used to characterize the messenger ribonucleic acid (mRNA) expression profile of extracellular matrix-related genes in rats' ileum. Gene expression of main extracellular matrix components (*Collagen, type I, alpha 1: Col1a1; Collagen, type III, alpha 1: Col3a1; Collagen, type IV, alpha 1: Col4a1; Collagen, type V, alpha 1: Col5a1*) was studied simultaneously with that of genes involved in extracellular matrix remodeling, matrix metalloproteinases (collagenases *Mmp1* and *Mmp13*, gelatinases *Mmp2* and *Mmp9*, stromelysin *Mmp3*, elastase *Mmp12* and membrane-type *Mmp14*) and tissue inhibitors of metalloproteinases 1 and 2 (*Timp1* and *Timp2*).

Total RNA was obtained from the homogenate of the longitudinal strip of ileum with the Isolate II RNA Mini Kit (Bioline, London, UK). One microgram of isolated total RNA was used for reverse-transcription, which was executed with the Tetro cDNA Synthesis Kit (Bioline) and using random hexamers. Real-time PCR primers were designed with the Beacon Designer (Premier Biosoft, PA, USA) and were obtained from Sigma-Aldrich (Sintra, Portugal). All the genes included in this study were described in the National Center for Biotechnology Information (NCBI) Gene database (http://www.ncbi.nlm.nih.gov/) as shown in Supplementary Table S6. Quantitative RT-PCR was accomplished on a Bio-Rad iQ5 real-time PCR instrument (BioRad, Hercules, California, USA) using the SensiFAST™ SYBR & Fluorescein Kit (Bioline). For each sample, PCR was performed in duplicate. Data were interpreted by relative mRNA quantification (Pfaffl, 2004) using *Hypoxanthine phosphoribosyltransferase 1* (*Hprt1*) as housekeeping gene internal control. All normalized values of samples corresponding to the moment of sacrifice were divided by the normalized value of the baseline (that was arbitrarily set to one) and expressed as fold variations. In rats that underwent laparotomy without resection, relative quantification was performed using mean ΔC_T (threshold cycle) at baseline value of rats submitted to ileal resection. Genes were considered upregulated when the fold-change of relative expression was higher than "1.5" and downregulated when it was lower than "0.5".

Net collagen deposition in rats' small bowel at the moment of sacrifice was assessed using the method proposed by Sandler *et al* (Strup-Perrot *et al.*, 2004; Sandler *et al.*, 2003). It was assumed that no net collagen deposition or degradation occurred in control baseline samples. Thus, the *Collagen*-to-*Mmp*-to-*Timp* value of fold-change of relative expression was set to "1" for baseline controls and used as a reference. Briefly, relative change of gene expression of *Mmp* was calculated by determining the fold-change of the *Mmp* mRNA expression relative to the *Timp*; fold-change for *collagen* mRNA was then divided by the fold-change value for the *Mmp*/*Timp* quotient to yield the fold-change in the ratio of collagen deposition to collagen degradation compared with the baseline. Values obtained reflected a tendency toward "collagen deposition" relatively to the steady state when above one and toward matrix "degradation" when inferior to one. "Net collagen deposition" or "degradation" were considered to exist when at least 70% of the studied ratios, an arbitrary cut-off, were higher or lower than one, respectively.

7.3.8. Statistical analysis

Statistical analysis was carried out using the Statistical Package for Social Sciences (SPSS) version 18 software (SPSS, Chicago, Illinois, USA). Shapiro-Wilk and Kolmogorov-Smirnov-Lillifors tests were used to assess the type of distribution of variables. Data were indicated as medians and interquartile ranges (median ± IQR). Comparison of non-parametric continuous variables was performed with Mann-Whitney U test and analysis of variance by ranks (Kruskall-Wallis test) with pairwise comparisons. Correlations were determined by the Spearman's rank correlation coefficient (σ). A $p<0.05$ was considered statistically significant.

7.4. Results

7.4.1. Postoperative course

Fifty-nine animals completed the study and were included into the groups: "*Res Ted* +" (15, eight of them sacrificed on the third day), "*Res Ted* –" (13, five sacrificed at third

day), "*Lap Ted* +" (16, eight sacrificed on the third day) and "*Lap Ted* -" (15, seven sacrificed at third day).

7.4.2. Relative gene expression levels of extracellular matrix components in the postoperative period

Analysis of relative gene expression in the perianastomotic ileal segments, on animals not submitted to teduglutide treatment, at the third day, revealed upregulation of *Col1a1*, reflected on the respective fold-change of expression between baseline and that time point (2.08±1.27), as well as, of *Mmp2* (2.32±1.15), *Mmp3* (7.90±1.00), *Mmp13* (2.29±0.82) and *Mmp14* (8.13±5.03); downregulation of *Col4a1* (0.47±0.25), *Timp1* (0.33±0.41), *Timp2* (0.04±0.07) and *Mmp1* (0.46±1.40) also occurred (Fig. 7.3 A). At the seventh day, upregulation of *Col1a1* (3.44±1.99), *Col3a1* (2.76±1.16), *Col5a1* (3.68±2.43), *Timp1* (2.26±1.23), *Mmp3* (6.28±6.87), *Mmp12* (2.30±2.63), *Mmp13* (12.46±7.18) and *Mmp14* (1.86±1.69) and downregulation of *Col4a1* (0.80±0.38), *Mmp1* (0.93±0.75), *Mmp2* (0.88±0.27) and *Mmp9* (0.56±0.36) were also verified (Fig. 7.3 B).

In animals not submitted to teduglutide administration, "net degradation" of collagen was observed at the third postoperative day, in the perianastomotic segments and in the ileal samples recovered after isolated laparotomy, as demonstrated in 95% and 70% of the 56 analyzed *Collagen*-to-*Mmp*-to-*Timp* ratios of fold-change of relative gene expression, respectively; "net deposition" was documented in the perianastomotic ileum at the seventh day (in 70% of the ratios) and "net degradation" was evident after isolated laparotomy at the same moment (in 73% of the ratios).

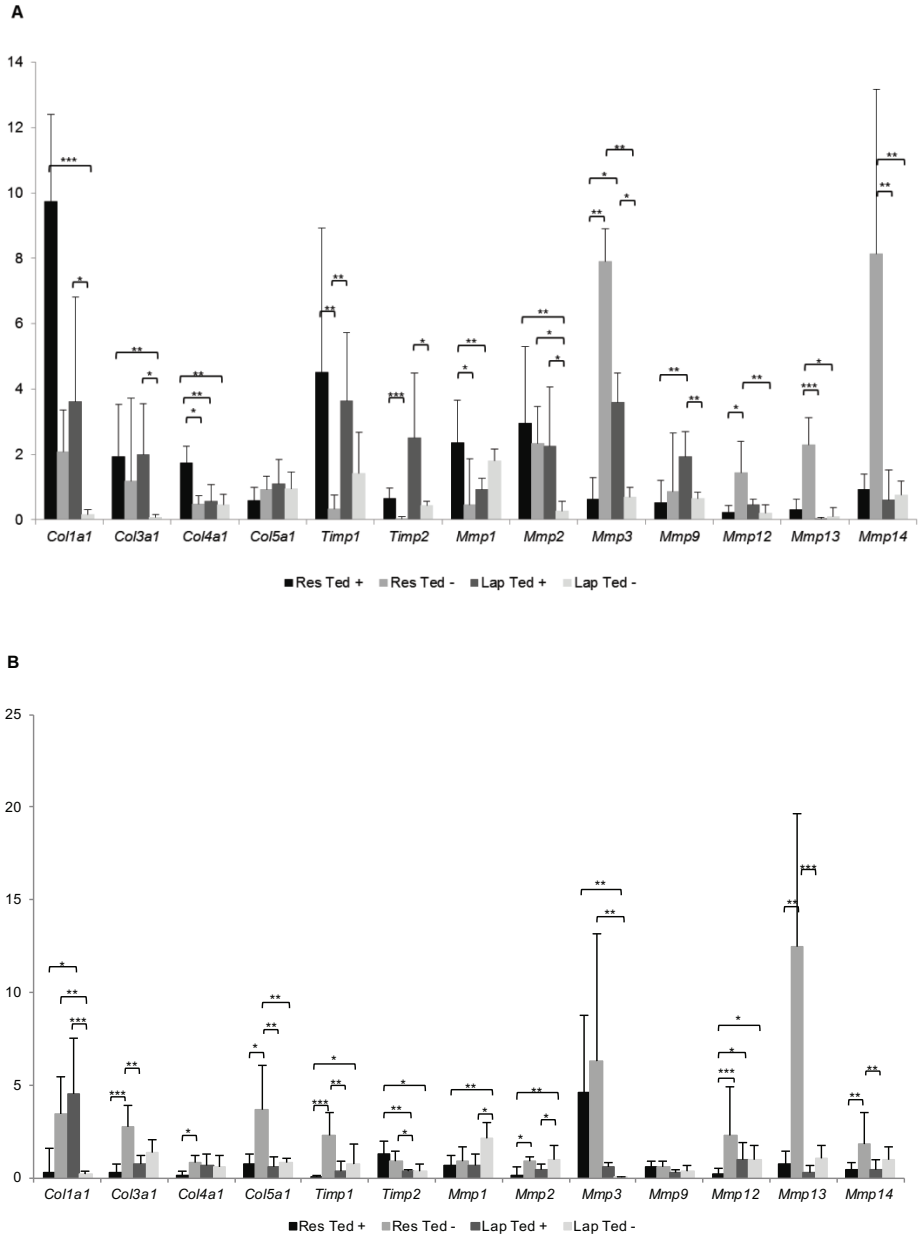

Figure 7.3. Fold-changes of relative gene expression of collagens, matrix metalloproteinases (Mmps) and tissue inhibitors of metalloproteinases (Timps) in cells isolated from rats' ileum, at third (A) and at seventh days (B) after operation, determined by qRT-PCR. Wistar rats (*n*=59) were assigned into four groups: "*Ileal resection and anastomosis*" ("*Res*") or "*Laparotomy*" ("*Lap*"), each one subdivided into "*Postoperative Teduglutide Administration*" ("*Ted+*") or "*No Treatment*" ("*Ted-*"), and sacrificed at third or at seventh days, with ileal sample harvesting. Samples recovered at the sacrifice in rats that underwent ileal resection corresponded to the anastomotic segment. Values were normalized to *Hypoxanthine phosphoribosyltransferase 1* gene and fold-changes were generated by comparison with baseline values of rats submitted to ileal resection (*n*=28). Results were expressed as median±interquartile range. Kruskal-Wallis test with pairwise comparisons was used. * $p<0.05$; ** $p<0.01$; *** $p<0.001$

7.4.3. Relative gene expression of extracellular matrix components after teduglutide administration

At the third day of the anastomotic healing, teduglutide treatment was associated with higher fold-change of expression of *Col4a1* (1.73±0.52 *vs.* 0.47±0.25, *p*=0.023), *Timp1* (4.51±4.41 *vs.* 0.33±0.41, *p*=0.004), *Mmp1* (2.35±1.32 *vs.* 0.46±1.40, *p*=0.021), *Timp2* (0.65±0.31 *vs.* 0.04±0.07, *p*=0.0001), and lower fold-change of *Mmp3* (0.62±0.67 *vs.* 7.90±1.00, *p*=0.002) and *Mmp12* (0.22±0.20 *vs.* 1.44±0.95, *p*=0.01), in comparison with controls ("*Res Ted -*" group rats) (Fig. 7.3 A).

At the seventh day of the anastomotic repair, teduglutide administration was associated with lower fold-change of expression of *Col3a1* (0.28±0.49 *vs.* 2.76±1.16, *p*=0.0001), *Col4a1* (0.16±0.19 *vs.* 0.80±0.38, *p*=0.01), *Col5a1* (0.74±0.57 *vs.* 3.68±2.43, *p*=0.025), *Timp1* (0.04±0.07 *vs.* 2.26±1.23, *p*=0.0001), *Mmp2* (0.15±0.44 *vs.* 0.88±0.27, *p*=0.013), *Mmp12* (0.24±0.25 *vs.* 2.30±2.63, *p*=0.0001), *Mmp13* (0.76±0.67 *vs.* 12.46±7.18, *p*=0.002) and *Mmp14* (0.45±0.40 *vs.* 1.86±1.69, *p*=0.002) (Fig. 7.3 B).

In animals submitted to teduglutide treatment, "net deposition" of collagen was observed in the perianastomotic segments at the third day, as demonstrated in 80% of the 56 studied *Collagen*-to-*Mmp*-to-*Timp* ratios of fold-change of relative gene expression, while "net degradation" was evident at the seventh day in 75% of the studied quotients (Fig. 7.4-7.7).

In animals submitted to teduglutide administration after isolated laparotomy, "net deposition" of collagen was documented in the ileal segments at the third day (as demonstrated in 91% of the studied *Collagen*-to-*Mmp*-to-*Timp* ratios) and "net degradation" at the seventh day (evident in 71% of the studied parameters).

Globally, at the third postoperative day (after ileal resection or isolated laparotomy), teduglutide administration was associated with higher fold-change of *Col1a1* (5.15±7.27 *vs.* 0.23±1.87, *p*=0.0001), *Col3a1* (1.92±1.46 *vs.* 0.14±1.04, *p*=0.001), *Col4a1* (1.36±1.22 *vs.* 0.47±0.18, *p*=0.005), *Timp1* (3.77±2.68 *vs.* 0.83±1.23, *p*=0.0001), *Timp2* (2.14±1.98 *vs.* 0.41±0.41, *p*=0.0001) and *Mmp2* (2.65±1.96 *vs.* 0.54±2.11, *p*=0.01) (Fig. 7.8).

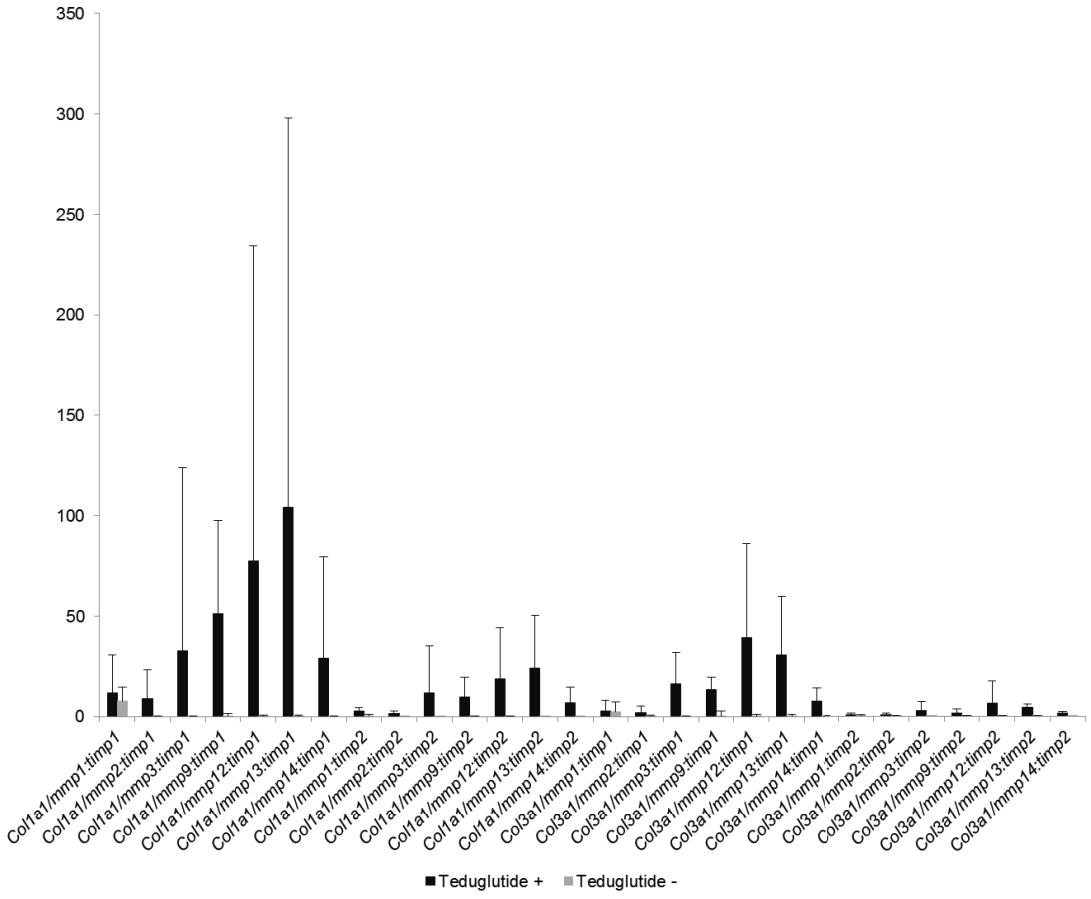

Figure 7.4. *Collagen (1a1/3a1)*-to-*Mmp*-to-*Timp* ratio of fold-change of relative gene expression in rats' perianastomotic segments (*n*=28), at the third postoperative day, according to the teduglutide administration*. Relative expression of *Mmp* was calculated by determining the fold-change of the *Mmp* mRNA expression relative to its relevant inhibitor *Timp*; fold change for *collagen* mRNA was then divided by the fold-change value for the relevant *Mmp*/*Timp* to yield the fold-change in the ratio of collagen deposition to collagen degradation compared with the baseline. Relative expressions were normalized to *Hypoxanthine phosphoribosyltransferase 1* gene and fold-changes were generated by comparison with baseline values. Results were expressed as median±interquartile range. Mann-Whitney U test was used. *Teduglutide* +, Postoperative teduglutide administration; *Teduglutide* -, Without teduglutide administration. *All the differences were statistically significant except: *Col3a1/mmp1:timp1* and *Col3a1/mmp1:timp2*

At the seventh postoperative day, teduglutide administration was associated with lower fold-change of *Col3a1* (0.59±0.58 *vs.* 1.96±1.46, *p*=0.0001), *Col5a1* (0.69±0.39 *vs.* 1.53±3.05, *p*=0.008), *Timp1* (0.07±0.40 *vs.* 1.73±1.90, *p*=0.0001), *Mmp1* (0.64±0.58 *vs.* 1.30±1.22, *p*=0.002), *Mmp2* (0.33±0.40 *vs.* 0.95±0.54, *p*=0.0001), *Mmp12* (0.49±1.10

vs. 1.19±2.34, *p*=0.02), *Mmp13* (0.33±0.65 *vs.* 5.67±11.73, *p*=0.0001) and *Mmp14* (0.45±0.39 *vs.* 1.30±1.17, *p*=0.0001) (Fig. 7.8).

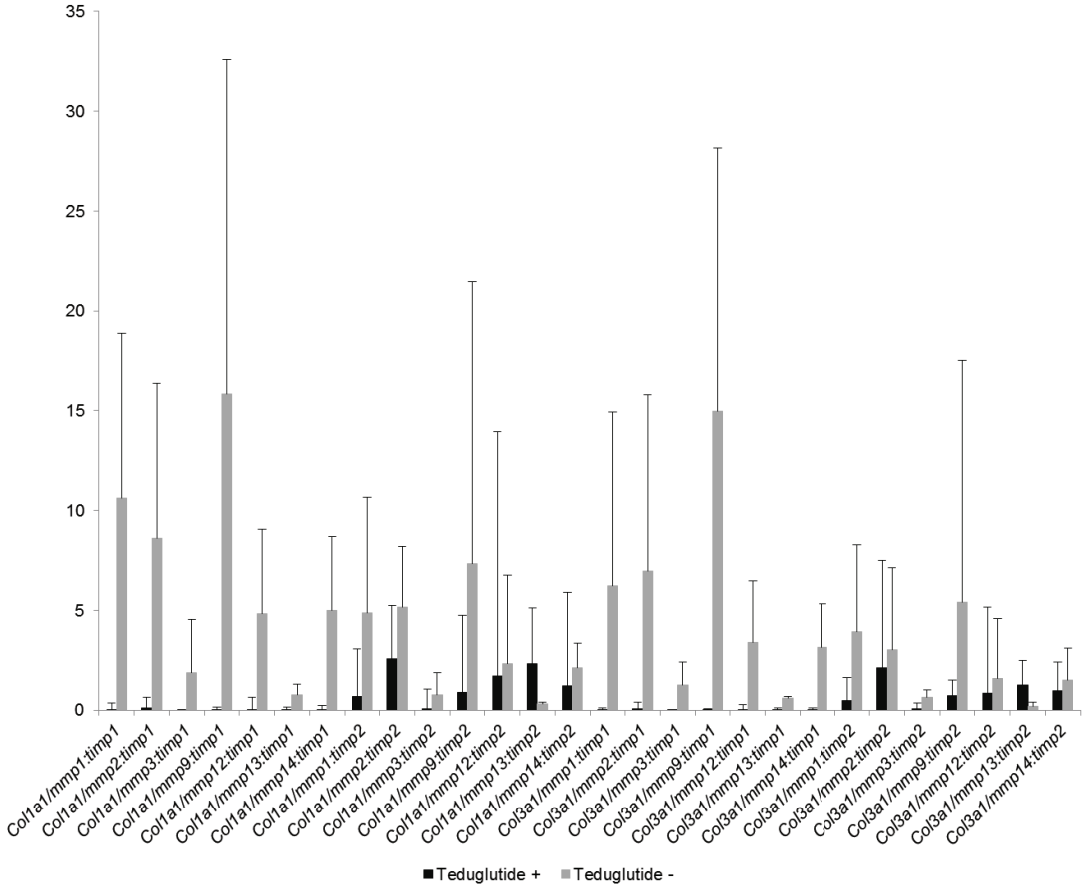

Figure 7.5. *Collagen (1a1/3a1)*-to-*Mmp*-to-*Timp* ratio of fold-change of relative gene expression in rats' perianastomotic segments (*n*=28), at the seventh postoperative day, according to the teduglutide administration*. Relative expression of *Mmp* was calculated by determining the fold-change of the *Mmp* mRNA expression relative to its relevant inhibitor *Timp*; fold change for *collagen* mRNA was then divided by the fold-change value for the relevant *Mmp*/*Timp* to yield the fold-change in the ratio of collagen deposition to collagen degradation compared with the baseline. Relative expressions were normalized to *Hypoxanthine phosphoribosyltransferase 1* gene and fold-changes were generated by comparison with baseline values. Results were expressed as median±interquartile range. Mann-Whitney U test was used. *Teduglutide* +, Postoperative teduglutide administration; *Teduglutide* -, Without teduglutide administration. * All the differences were statistically significant except: *Col1a1/mmp2:timp2, Col1a1/mmp3:timp2, Col1a1/mmp12:timp2, Col1a1/mmp14:timp2; Col3a1/mmp2:timp2, Col3a1/mmp9:timp2* and *Col3a1/mmp14:timp2*

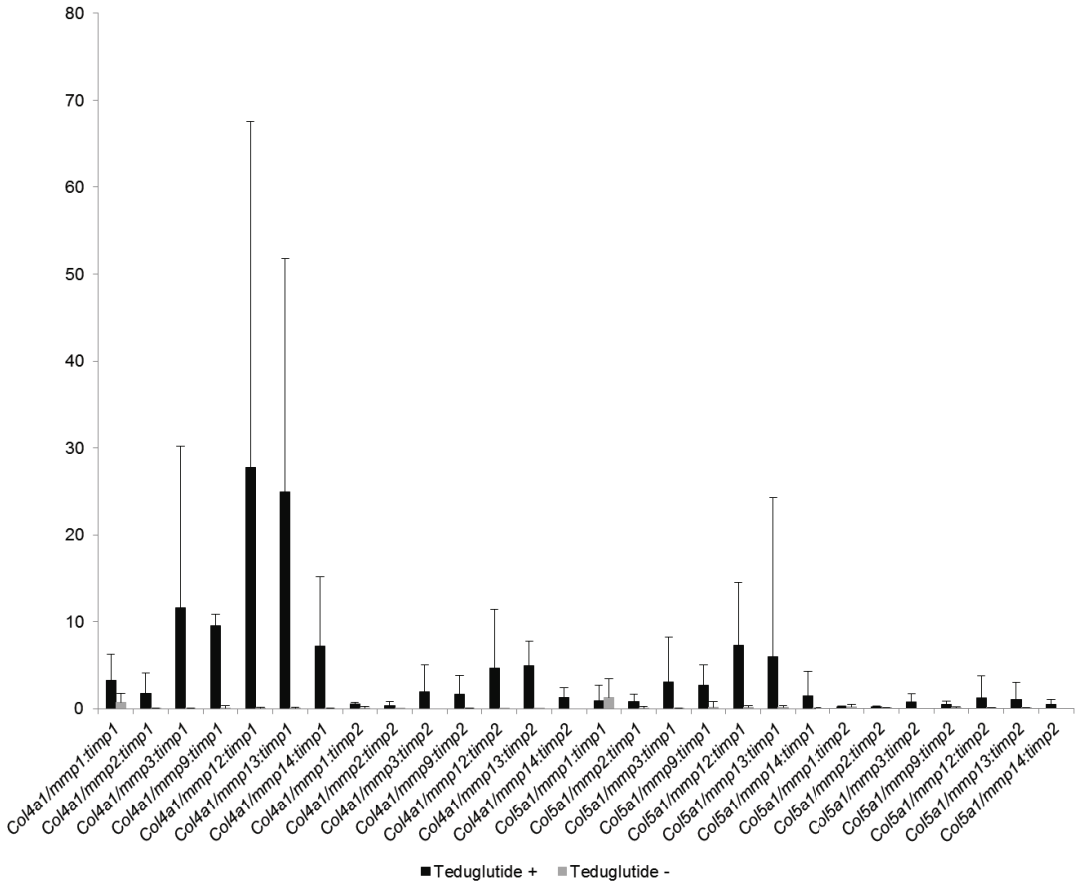

Figure 7.6. *Collagen (4a1/5a1)*-to-*Mmp*-to-*Timp* ratio of fold-change of relative gene expression in rats' perianastomotic segments (*n*=28), at the third postoperative day, according to the teduglutide administration*. Relative expression of *Mmp* was calculated by determining the fold-change of the *Mmp* mRNA expression relative to its relevant inhibitor *Timp*; fold change for *collagen* mRNA was then divided by the fold-change value for the relevant *Mmp*/*Timp* to yield the fold-change in the ratio of collagen deposition to collagen degradation compared with the baseline. Relative expressions were normalized to *Hypoxanthine phosphoribosyltransferase 1* gene and fold-changes were generated by comparison with baseline values. Results were expressed as median±interquartile range. Mann-Whitney U test was used. *Teduglutide* +, Postoperative teduglutide administration; *Teduglutide* -, Without teduglutide administration. *All the differences were statistically significant except: Col5a1/mmp1:timp1, *Col5a1/mmp2:timp1, Col5a1/mmp3:timp1, Col5a1/mmp13:timp1, Col5a1/mmp1:timp2, Col5a1/mmp2:timp2, Col5a1/mmp3:timp2, Col5a1/mmp9:timp2, Col5a1/mmp12:timp2, Col5a1/mmp13:timp2, Col5a1/mmp14:timp2*

When considered all the animals (submitted to ileal resection or isolated laparotomy), at the moment of sacrifice (at the third or the seventh day), teduglutide treatment was associated with higher fold-change of *Col1a1* (3.79±5.04 *vs.* 0.33±2.64, *p*=0.0001) and *Timp2* (0.90±1.71 *vs.* 0.44±0.64, *p*=0.003) (similar to the verified at the third day); and

lower fold-change of *Col5a1* (0.70±0.47 *vs.* 0.95±1.42, *p*=0.005), *Mmp12* (0.43±0.40 *vs.* 0.98±1.17, *p*=0.004), *Mmp13* (0.17±0.41 *vs.* 1.57±8.34, *p*=0.0001) and *Mmp14* (0.58±0.58 *vs.* 1.30±2.38, *p*=0.001) (Fig. 7.9).

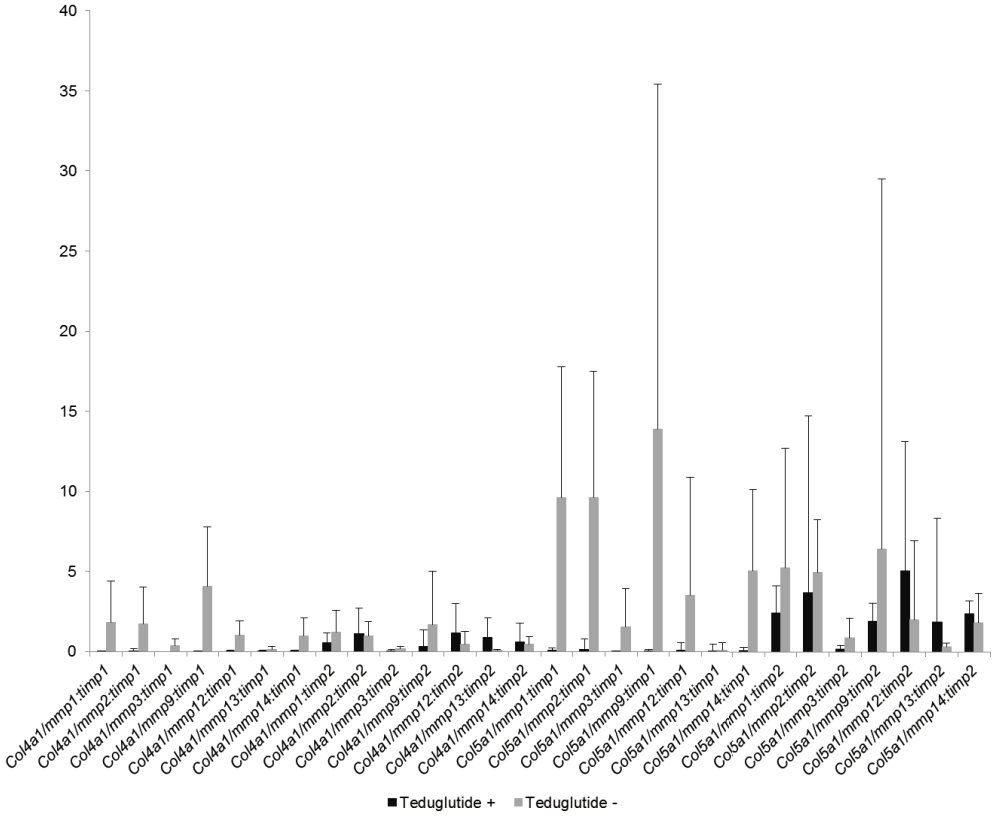

Figure 7.7. *Collagen (4a1/5a1)*-to-*Mmp*-to-*Timp* ratio of fold-change of relative gene expression in rats' perianastomotic segments (n=28), at the seventh postoperative day, according to the teduglutide administration*. Relative expression of *Mmp* was calculated by determining the fold-change of the *Mmp* mRNA expression relative to its relevant inhibitor *Timp*; fold change for *collagen* mRNA was then divided by the fold-change value for the relevant *Mmp*/*Timp* to yield the fold-change in the ratio of collagen deposition to collagen degradation compared with the baseline. Relative expressions were normalized to *Hypoxanthine phosphoribosyltransferase 1* gene and fold-changes were generated by comparison with baseline values. Results were expressed as median±interquartile range. Mann-Whitney U test was used. *Teduglutide* +, Postoperative teduglutide administration; *Teduglutide* -, Without teduglutide administration. *All the differences were statistically significant except: *Col4a1/mmp1:timp2, Col4a1/mmp2:timp2, Col4a1/mmp12:timp2, Col4a1/mmp14:timp2, Col5a1/mmp1:timp2, Col5a1/mmp2:timp2, Col5a1/mmp12:timp2* and *Col5a1/mmp14:timp2*

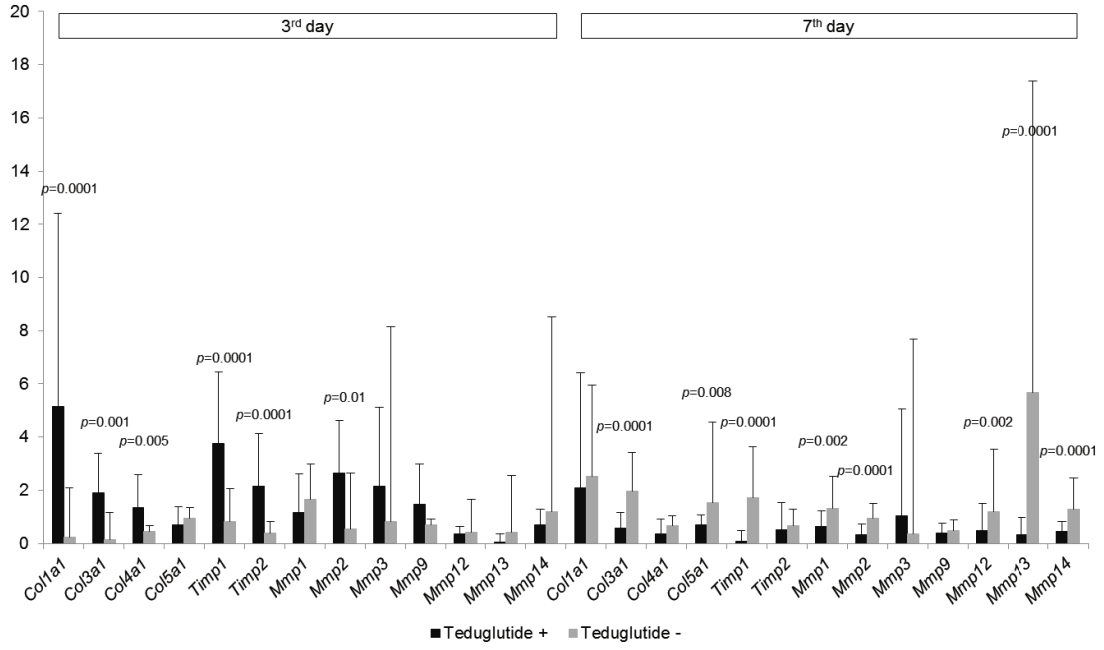

Figure 7.8. Fold-changes of relative gene expression of collagens, matrix metalloproteinases (Mmps) and tissue inhibitors of metalloproteinases (Timps), determined by qRT-PCR, in rats' ileum at the moment of sacrifice (after ileal resection and anastomosis or isolated laparotomy), according to the teduglutide administration (*n*=59). Samples recovered at the sacrifice in rats submitted to ileal resection corresponded to the anastomotic segment. Values were normalized to *Hypoxanthine phosphoribosyltransferase 1* gene and fold-changes were generated by comparison with baseline values of rats submitted to ileal resection (*n*=28). Results were expressed as median±interquartile range of fold-change. Mann-Whitney U test was used. *Teduglutide* +, Postoperative teduglutide administration; *Teduglutide* -, Without teduglutide administration

Globally, teduglutide administration favored "net collagen deposition" (evident in 75% of the 56 analyzed *Collagen*-to-*Mmp*-to-*Timp* ratios), while "net collagen degradation" was observed in not treated animals (evident in 77% of the ratios). In teduglutide-treated animals, significantly higher values were observed in 43% of the *Collagen*-to-*Mmp*-to-*Timp* ratios, while lower values were presented in only 5% (Fig. 7.10 and 7.11).

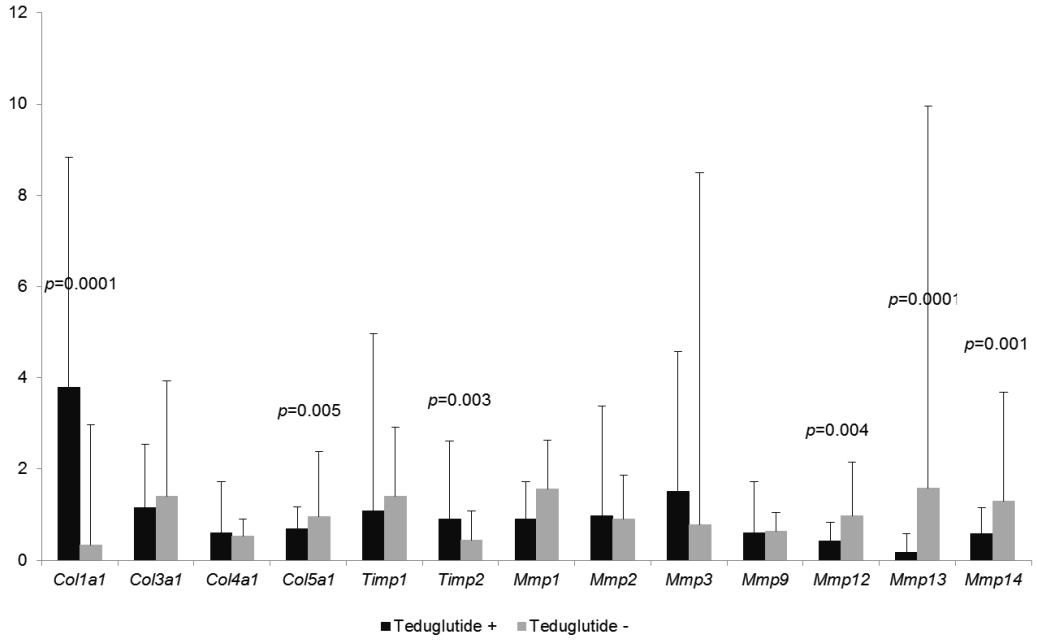

Figure 7.9. Fold-changes of relative gene expression of collagens, matrix metalloproteinases (*Mmps*) and tissue inhibitors of metalloproteinases (*Timps*), determined by qRT-PCR, in rats' ileum of all groups (*n*=59) at the moment of sacrifice (third or seventh day; after ileal resection and anastomosis or isolated laparotomy), according to teduglutide administration. Samples recovered at the sacrifice in rats submitted to ileal resection corresponded to the anastomotic segment. Values were normalized to *Hypoxanthine phosphoribosyltransferase 1* gene and fold-changes were generated by comparison with baseline values of rats submitted to ileal resection (*n*=28). Results were expressed as median±interquartile range of fold-change. Mann-Whitney U test was used. *Teduglutide* +, Postoperative teduglutide administration; *Teduglutide* -, Without teduglutide administration

7.5. Discussion

In present study, global gene expression profiles revealed, a balance towards fibrolysis (net degradation of collagen) at third day of intestinal anastomotic healing, associated with upregulation of *Mmp2*, *Mmp3*, *Mmp13* and *Mmp14* expression and downregulation of *Timp1* and *Timp2*; and towards fibrogenesis (deposition of collagen) at seventh day, associated with upregulation of *Col1a1, Col3a1, Col5a1* and *Timp1* expression and downregulation of *Mmp1*, *Mmp2* and *Mmp9*. Upmodulation of stromelysin *Mmp3*, collagenase *Mmp13*, membrane-type *Mmp14* and *Col1a1* was

observed consistently throughout the repair, as well as, downregulation of *Col4a1* and collagenase *Mmp1*.

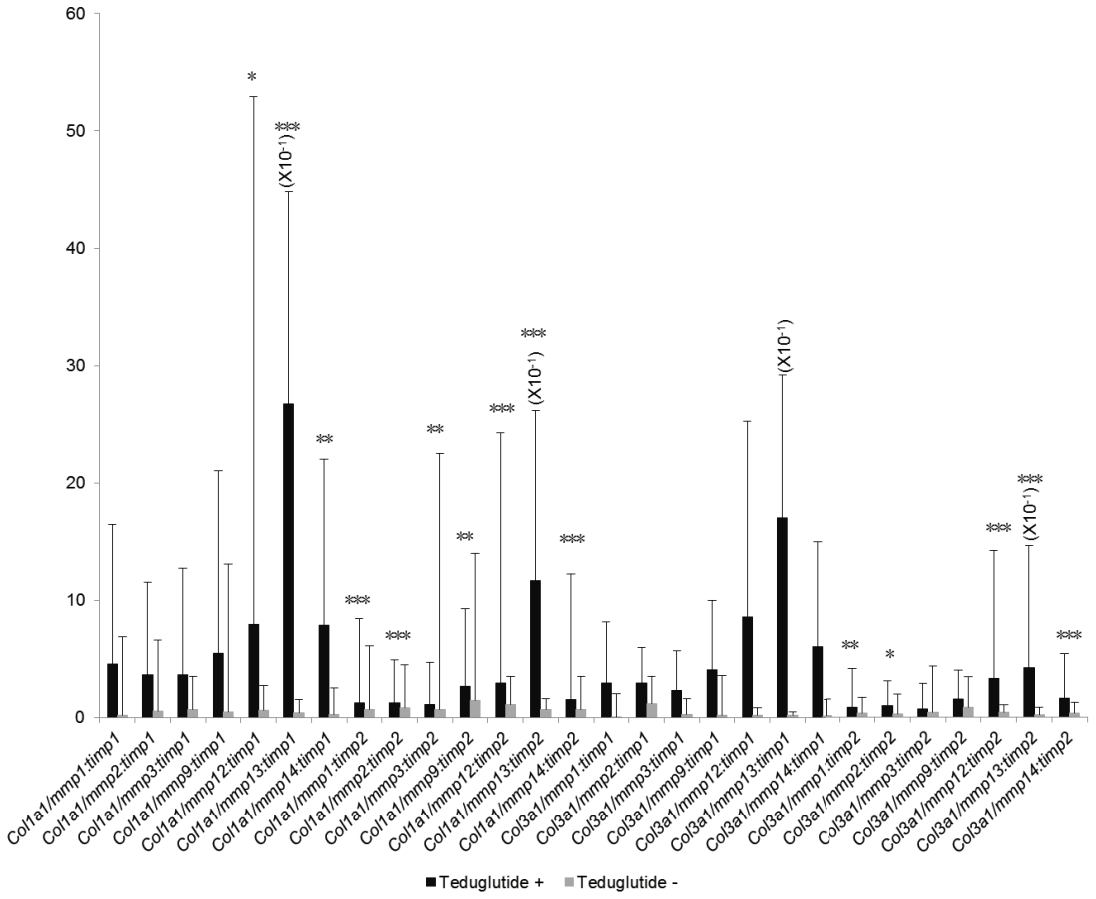

Figure 7.10. *Collagen (1a1/3a1)*-to-*Mmp*-to-*Timp* ratio of fold-change of relative gene expression in rats' ileum of all groups (*n*=59), at the moment of sacrifice (third or seventh day; after ileal resection and anastomosis or isolated laparotomy), according to the teduglutide administration. Relative expression of *Mmp* was calculated by determining the fold-change of the *Mmp* mRNA expression relative to its relevant inhibitor *Timp*; fold-change for *collagen* mRNA was then divided by the fold-change value for the relevant *Mmp*/*Timp* to yield the fold-change in the ratio of collagen deposition to collagen degradation compared with the baseline. Relative expressions were normalized to *Hypoxanthine Phosphoribosyltransferase 1* gene and fold-changes were generated by comparing with baseline values of rats submitted to ileal resection (*n*=28). Samples from rats that underwent ileal resection corresponded to the anastomotic segment. Results were expressed as median±interquartile range. Mann-Whitney U test was used. *Teduglutide* +, Postoperative teduglutide administration; *Teduglutide* -, Without teduglutide administration. * $p<0.05$; ** $p<0.01$, *** $p<0.001$

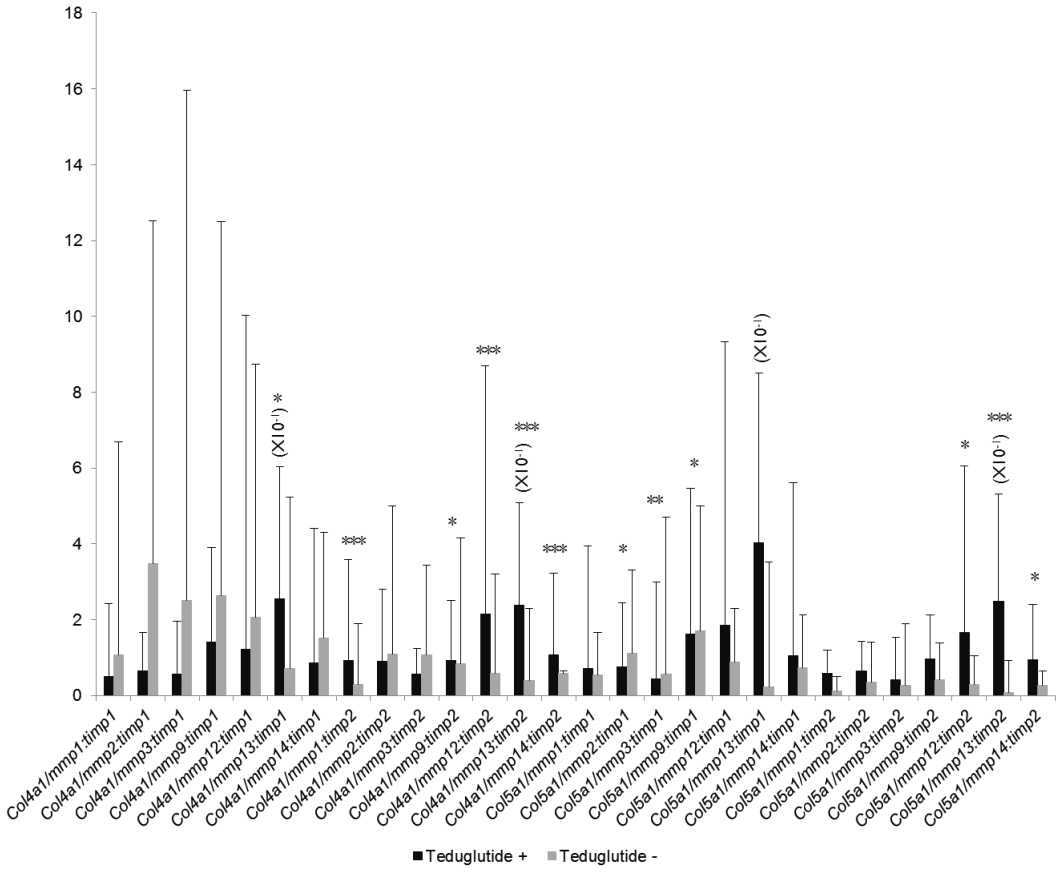

Figure 7.11. *Collagen (4a1/5a1)*-to-*Mmp*-to-*Timp* ratio of fold-change of relative gene expression in rats' ileum of all groups (*n*=59), at the moment of sacrifice (third or seventh day; after ileal resection and anastomosis or isolated laparotomy), according to the teduglutide administration. Relative expression of *Mmp* was calculated by determining the fold-change of the *Mmp* mRNA expression relative to its relevant inhibitor *Timp*; fold-change for *collagen* mRNA was then divided by the fold-change value for the relevant *Mmp*/*Timp* to yield the fold-change in the ratio of collagen deposition to collagen degradation compared with the baseline. Relative expressions were normalized to *Hypoxanthine Phosphoribosyltransferase 1* gene and fold-changes were generated by comparing with baseline values of rats submitted to ileal resection (*n*=28). Samples from rats that underwent ileal resection corresponded to the anastomotic segment. Results were expressed as median±interquartile range. Mann-Whitney U test was used. *Teduglutide* +, Postoperative teduglutide administration; *Teduglutide* -, Without teduglutide administration. * $p<0.05$; ** $p<0.01$, *** $p<0.001$

Recently, Seifert GT *et al* demonstrated upregulation of *Mmp2*, *Mmp3*, *Mmp9*, *Mmp12*, *Mmp13* and *Mmp14* during ileal anastomotic healing (Seifert *et al.*, 2014). Similarly, Krarup PM *et al* (Krarup *et al.*, 2013) found a profund increase of Mmp8, Mmp9 and Mmp12 gene and protein expressions, a modest enhancement of *Mmp13*

gene expression and of Mmp2 gene and protein expressions, in colon anastomosis, at the third day of the healing process, comparing with non-injured adjacent colon; *Mmp3* was not significantly upmodulated. In 2006, Ågren MS *et al* showed, in a rat model, that hydroxyproline concentration of a colonic anastomosis decreased to 43% at third postoperative day, more intensely in the suture-holding zone, and returned to the baseline levels at the seventh day (restoring a similar content in suture and suture-free areas) (Ågren *et al.*, 2006).

According to the gene expression analysis, teduglutide appeared to be associated with a trend to increase the overall deposition of collagen at the predominantly inflammatory phase of the anastomotic healing (third postoperative day), as suggested by the *Collagen*-to-*Mmp*-to-*Timp* ratios of relative mRNA expression. This effect was attributable to the reduction of fibrolysis, related with the induction of gene expression of *Timp1* and *Timp2* and downmodulation of *Mmp3* and *Mmp12* (as well as, of *Mmp9*, *Mmp13* and *Mmp14*, although not significant); furthermore, an upregulation of *Col4a1* was also observed.

On the contrary, at the proliferative phase of anastomotic repair (seventh day), teduglutide was associated with a trend to decrease collagen deposition, possibly due to the reduction of fibrogenesis explained by the downmodulation of *Timp1*, *Col3a1*, *Col4a1* and *Col5a1*, and *Col1a1* (not significant).

Nevertheless, globally, teduglutide seemed to be associated with a predominantly profibrogenic effect, mainly derived from the downregulation of elastase *Mmp12*, collagenase *Mmp13* and membrane-type *Mmp14*.

Downregulation of *Mmp13* and *Mmp14* was the most consistent effect of teduglutide, observed simultaneously in the anastomotic segments and in the ileal samples recovered after isolated laparotomy, both at third and at seventh day. Mmp14 is a membrane-type Mmp that potentiates other Mmps, degrades types I and III collagens and other extracellular matrix molecules, participates on the myofibroblasts migration and promotes wound healing (Ravi *et al.*, 2007). Mmp13 is a collagenase with a large substrate specificity, able to cleave fibrillar collagens (including types I and III) and gelatin and to potentiate the inflammatory response (Cui *et al.*, 2017; Ravi *et al.*, 2007).

Interferences with the number, activation and secretion of extracellular matrix-producing cells, as well as with the inflammatory response, oxidative stress and growth factors profile may be involved on the teduglutide effects on fibrogenesis. In fact, fibrogenesis involves complex interactions between cells, extracellular matrix, cytokines, chemokines and growth factors (Latella *et al.*, 2013; Speca *et al.*, 2012). Activated myofibroblasts, the extracellular matrix-producing cells, are derived from resident mesenchymal cells (fibroblasts, subepithelial myofibroblasts and smooth muscle cells), epithelial and endothelial cells, stellate cells, pericytes and bone marrow stem cells (Latella *et al.*, 2013; Speca *et al.*, 2012). Relevant molecular mediators of extracellular matrix production include transforming growth factor β, connective tissue growth factor, platelet-derived growth factor, insulin-like growth factors 1 and 2, epidermal growth factor, vascular endothelial growth factor, fibroblast growth factors, cytokines, chemokines and products of oxidative stress, among others (Latella *et al.*, 2015; Latella *et al.*, 2013; Speca *et al.*, 2012).

In previous chapter of this thesis, it was demonstrated that teduglutide postoperative administration (after ileal resection or isolated laparotomy) was associated, at third day, with higher fold-change of relative gene expression of *insulin-like growth factor 1* and *heparin-binding epidermal-like growth factor* and lower fold-change of *fibroblast growth factor 2* and *fibroblast growth factor 7*; while, at seventh day, it was related with higher fold-change of relative gene expression of *vascular endothelial growth factor a*, *connective tissue growth factor* and *heparin-binding epidermal-like growth factor* and lower fold-change of *transforming growth factor β1*, *fibroblast growth factor 7* and *glucagon-like peptide 2 receptor*.

In present study, promotion of fibrogenesis at third postoperative day might have result from teduglutide upregulation of *insulin-like growth factor 1* expression, while tendency to collagenolysis at seventh day might have derived from the inhibition of *transforming growth factor β1* signaling. Insulin-like growth factor 1 is a recognized critical mediator of the enterotrophic effects of glucagon-like peptide 2 (Drucker and Yusta, 2014; Bortvedt *et al.*, 2012) that plays an important role on the modulation of the proliferation of fibroblasts/myofibroblasts and on the deposition of collagen (Latella *et al.*, 2013; Bortvedt *et al.*, 2012). Transforming growth factor β is a

pleiotropic cytokine that regulates extracellular matrix turnover (Biancheri *et al.*, 2014), induces mesenchymal cells activation and differentiation into myofibroblasts, and stimulates extracellular matrix synthesis (Latella *et al.*, 2013). Both transforming growth factor β (and its receptors) and insulin-like growth factor 1 are overexpressed in fibrostenotic Crohn's disease and in animal models of intestinal fibrosis (Latella *et al.*, 2015; Latella *et al.*, 2013). Furthermore, a recent systematic review and meta-analysis on pharmaceutical interventions for the improvement of colonic anastomotic healing, demonstrated that insulin-like growth factor 1 improved anastomosis stability on experimental models (Oines *et al.*, 2014).

Main limitations of present investigation must be considered in the interpretation of the results, namely the small number of studied animals in each group and the lack of protein expression analysis. The first shortcoming may have contributed to increase the dispersion of the results and, in some cases, to the difficulty to reach statistical significance. Regarding to the methodology, quantitative RT-PCR allowed a relative quantification of mRNA transcript content, but the presence of RNA does not always reflect the protein levels. Potential interferences in collagen synthesis and deposition at posttranscriptional, posttranslational and postsecretional levels may not have been detected (Chen *et al.*, 2009; Gelse *et al.*, 2003), such as disruption of the formation and stabilization of collagen triple helices, assembly into fibrils, or cross-linking (Chen *et al.*, 2009). Accordingly, any therapeutic implications of this study require further investigation.

Favorable influence of teduglutide treatment on the overall deposition of collagen observed at the third day of the intestinal anastomotic healing, demonstrated in gene expression analysis, might reduce the probability of anastomotic failure, in the period of higher risk. In fact, in the first two to three days of postoperative period, a transient reduction of the anastomotic strength occurs, associated to the degradation of extracellular matrix proteins (especially preexisting mature collagen) by the proteinase activity in the wound. Thereafter, strength increases by *de novo* synthesis and deposition of collagen, in the predominantly proliferative phase of the healing process (Thompson *et al.*, 2006). Burst pressure of a small intestine anastomosis is approximately 50% of normal at the second and third postoperative days, whilst a

tensile strength similar to the unwounded tissue is only reached four weeks after surgery (Thompson *et al.*, 2006). Seifert GT *et al* (Seifert *et al.*, 2014) observed that the number of genes consistently up or downregulated peaked at the second postoperative day and decreases until the eighth day, reflecting, according to those authors, the clinically most important phase of intestinal anastomotic healing.

Although the decrease of collagen deposition at the seventh day of the anastomotic repair might raise apprehension about the susceptibility to dehiscence, the limited temporal extent of the potential profibrogenic effect of teduglutide might reduce the risk of anastomotic stenosis and peritoneal adhesions, while protecting against fistulization during the higher risk period.

Results of present study might also be relevant to indicate potential effects of teduglutide on the progression of intestinal fibrotic diseases, increasingly recognized as major causes of morbidity and mortality (Latella *et al.*, 2015), such as inflammatory bowel diseases, radiation enteropathy, postsurgical intestinal adhesions, and others. Teduglutide was indeed considered a promising therapeutic strategy in Crohn's disease, targeting the intestinal barrier function (Blonski *et al.*, 2013; Buchman *et al.*, 2010).

In conclusion, in present study, gene expression profiles revealed a balance towards net degradation of collagen at third day of the intestinal anastomotic healing and towards net deposition at seventh day. Teduglutide appeared to be associated with a favorable influence on fibrogenesis at the third day of the intestinal anastomotic repair, considered the period of higher risk of failure, and to a trend to fibrolysis at the seventh day.

Further research is necessary to confirm those results and to determine the cellular and molecular mechanisms underlying to the teduglutide effects on fibrogenesis.

Chapter 8

General discussion and concluding remarks

Regardless of progresses in surgical technique and perioperative care, failure of intestinal anastomotic healing remains one of the most feared complications in digestive surgery (Guyton *et al.*, 2016; Bosmans *et al.*, 2015). Indeed, intestinal anastomotic leakage has a profound adverse impact on the operative morbidity and mortality rates, oncologic and functional outcomes, patients' quality of life and socioeconomic costs (Gessler *et al.*, 2017; Chadi *et al.*, 2016; Midura *et al.*, 2015; Shogan *et al.*, 2013; Luján *et al.*, 2011). An early detection and a timely integrated therapeutic intervention are critical for the successful management of the anastomosis complications (Chadi *et al.*, 2016). Nevertheless, accurate risk stratification and control of relevant susceptibility factors are of upmost clinical and socioeconomic relevance.

Anastomotic healing is a complex multicellular and multimolecular process susceptible to innumerous interferences and its pathophysiology remains to be completely elucidated (Guyton *et al.*, 2016).

Numerous experimental studies have been undertaken on the role of adjuvants of intestinal anastomosis healing. However, many of those studies were characterized by low internal validity and reporting quality and, also, by significant heterogeneity. Furthermore, efficacy and safety issues, as well as clinical applicability and economic constraints were frequent limitations. Until now, no clear evidences were documented to support the implementation of any of those strategies for the routine clinical use (Nerstrom *et al.*, 2016; Yauw *et al.*, 2015; Rijcken *et al.*, 2014; Oines *et al.*, 2014).

Teduglutide is a long-acting analogue of glucagon-like peptide 2 (GLP-2) with enterotrophic properties, approved for the pharmacological rehabilitation of short-bowel syndrome (Drucker and Yusta, 2014), and considered safe and well tolerated (Kim and Keam *et al.*, 2017; Billiauws *et al.*, 2017; Naberhuis *et al.*, 2016; Austin *et al.*, 2016).

Present study evaluated the influence of teduglutide short-term administration on the cellular, humoral and molecular mediators of intestinal anastomotic healing on an animal model. The ultimate goal of this investigation was to clarify the potential of teduglutide as a promoting strategy for improvement of intestinal anastomotic healing. In order to achieve that goal, several aspects were addressed, including the influence

of teduglutide on the intestinal anastomosis clinical and structural outcome; the response of putative intestinal epithelial stem cells to teduglutide in the context of anastomosis repair; the effects of teduglutide on the cellular viability and death processes, oxidative stress, and tissue and systemic inflammatory response; perioperative tissue growth factors profiles after teduglutide administration; and the effects of teduglutide on the gene regulation of fibrogenesis during anastomosis repair.

Intestinal anastomosis healing process

Relevant aspects of the intestinal anastomosis healing were analyzed in this investigation. The role of the intestinal epithelial stem cells modulation in intestinal repair was analysed by multiparameter flow cytometry cellular phenotyping. Present findings corroborated the existence of two functional, interconvertible, putative epithelial stem cells subpopulations with distinct behavior after surgical injury and teduglutide administration and also with different correlation profiles with redox, inflammatory and growth factors signaling parameters (additional data on Supplementary Tables S7 and S8). A significant and high positive correlation was documented between putative crypt base columnar subpopulation proportion and parameters suggesting a local prooxidative influence, albeit accompanied by a positive correlation with cellular viability index; the opposite behavior was observed with the putative "position +4" stem cells fraction. Redox biology seems to play an important role in the intestinal epithelium homeostasis and repairing efficiency (Circu and Aw, 2012). The referred subpopulations of stem cells correlated in opposite direction with tissue proinflammatory interleukin 1α (IL-1α) and plasma macrophage chemo-attractant protein 1 (MCP-1) levels, and *fibroblast growth factor 7* gene expression levels. IL-1 cytokine family is involved in the preservation of gut mucosal homeostasis, including the integrity of epithelial barrier and the promotion of epithelial repair (Lopetuso *et al.*, 2013). Fibroblast growth factor 7 is a potent mitogenic growth factor with a relevant role in intestinal growth, maintenance and repair (Cai *et al.*, 2012). This study allowed a better insight on the role of the intestinal epithelial stem cells modulation in intestinal repair.

Infiltration of the anastomotic wound by inflammatory cells and fibroblasts, and development of reepithelialization, neoangiogenesis and fibroplasia were observed by histological and immunohistochemical analysis. Anastomosis repair induced a relevant and sustained prooxidative influence (including an increase of the levels of cytosolic peroxides and mitochondrial reactive species and a reduction of the mitochondrial membrane potential and intracellular reduced glutathione content); a proinflammatory/T-helper 1 lymphocytes tissue response; an initial proinflammatory/T-helper 1 lymphocytes and a late antiinflammatory/T-helper 2 lymphocytes systemic reaction. During anastomotic repair, upregulation of gene expression of *fibroblast growth factor 2*, *fibroblast growth factor 7*, *epidermal growth factor*, *vascular endothelial growth factor a*, at the third day, as well as of *platelet-derived growth factor b*, at the seventh day, was observed. Gene expression profiles of extracellular matrix components and remodeling factors revealed a balance towards fibrolysis at the third day of the intestinal anastomotic healing, associated with upregulation gene expression of *matrix metalloproteinase* (*Mmp*) *2*, *Mmp3*, *Mmp13* and *Mmp14*; and downregulation of *collagen type IV alpha 1* and *tissue inhibitors of metalloproteinase* (*Timp*) *1* and *Timp2*; and towards fibrogenesis at the seventh day, attributable to the upregulation of *Collagens type I alpha 1*, *Collagen type III alpha 1* and *Collagen type V alpha 1* and *Timp 1*.

Teduglutide effects on intestinal anastomosis healing

In this study, teduglutide was not associated with apparent relevant impact on the rate or the severity of anastomotic leakage. This fact may have been related with the probably low statistical power of the study and, also, with the high efficiency of intra-abdominal immune system of rodents (Pommergaard *et al.*, 2011).

Nevertheless, present findings suggest potential effects of teduglutide on the reepithelialization, neoangiogenesis and fibroplasia events of the intestinal anastomotic healing (Fig. 8.1). Impact of this growth factor exogenous administration on the cellular, humoral and molecular mediators of the anastomosis repair was summarized in Figures 8.2 and 8.3.

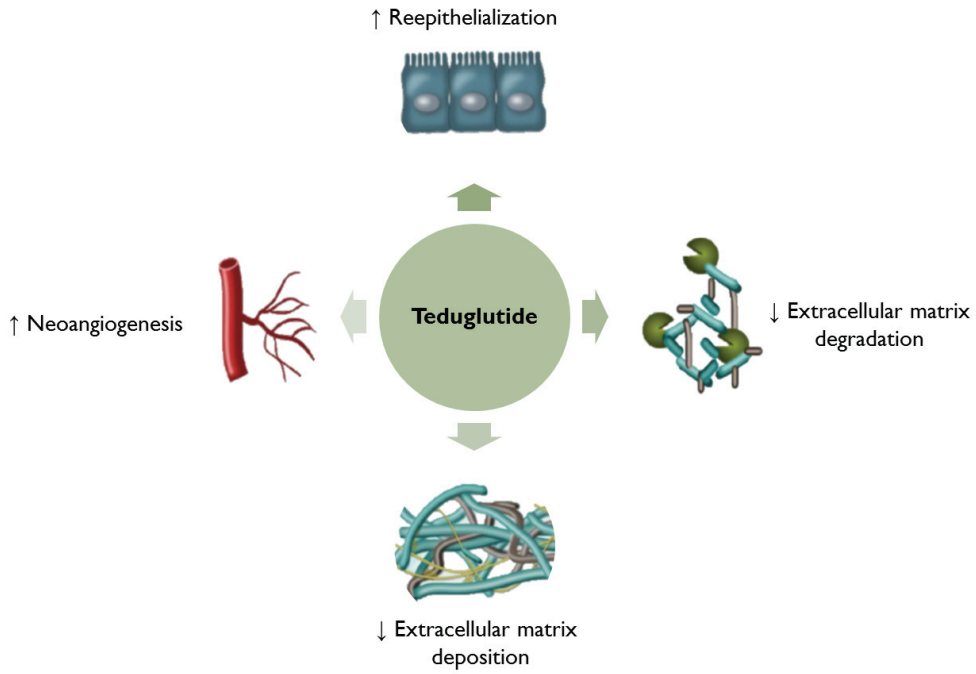

Figure 8.1. Illustration depicting the main potential effects of teduglutide on the intestinal anastomotic healing, in a rodent model, suggested by the present investigation. The inhibition of extracellular matrix degradation (at gene expression level) was observed at the third day. The promotion of reepithelialization and neoangiogenesis, and the trend towards the reduction of extracellular matrix deposition (at gene expression level) were documented at the seventh day

In this study, teduglutide appeared to be characterized by a context and time-dependent response.

A favorable effect of teduglutide on the reepithelialization and neoangiogenesis events of the proliferative phase of anastomotic repair was documented in histological and immunohistochemical analysis.

Teduglutide appeared to promote the reepithelialization in the predominantly proliferative phase of anastomotic healing, as demonstrated by histological examination. This effect may have be related with the expansion of the putative crypt base columnar stem cells pool and the concomitant reduction of the putative "+4 position" stem cells fraction, observed in teduglutide-treated animals. Therefore, the mechanism underlying the promotion of epithelialization may have involved the proliferation of putative crypt base columnar stem cells, and/or the conversion of

putative "+4 position" stem cells to crypt base columnar cells and/or to transit-amplifying progenitors that differentiated into mature epithelial cells.

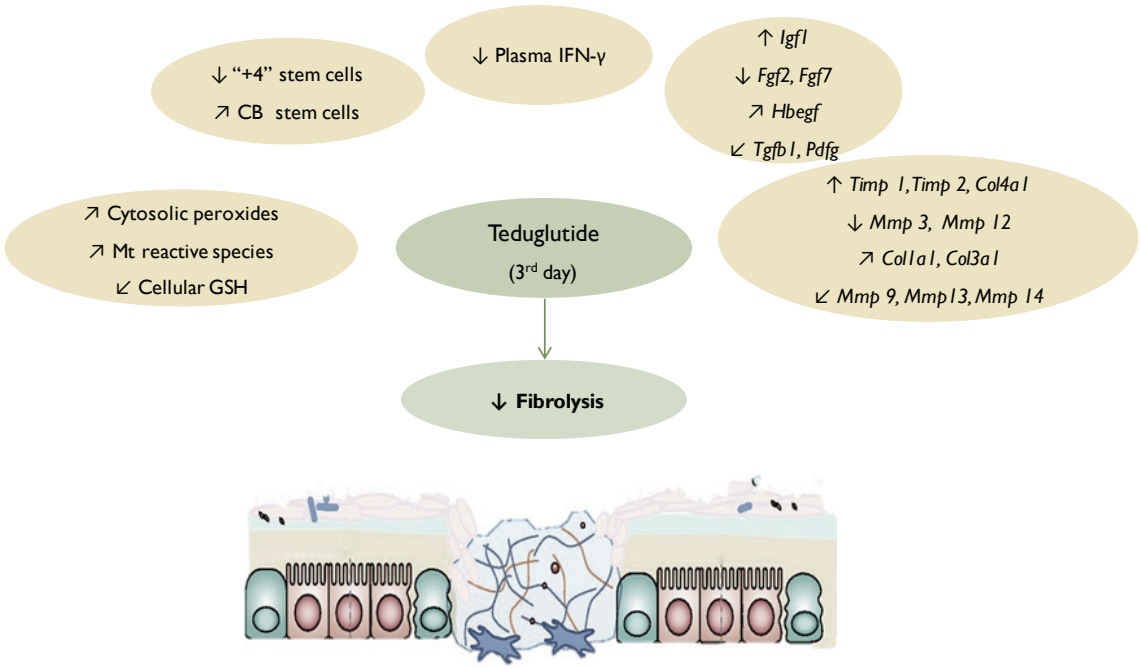

Figure 8.2. Schematic overview of the influence of teduglutide on the cellular, humoral and molecular mediators of the intestinal anastomotic repair at the third day, suggested by the present study. "4" stem cells, Putative "+4 position" epithelial stem cells; CB stem cells, Putative crypt base columnar epithelial stem cells; Cellular GSH, Cellular reduced glutathione; *Col1a1, Collagen, type I, alpha 1, mRNA; Col3a1, Collagen, type III, alpha 1, mRNA; Col4a1, Collagen, type IV, alpha 1, mRNA; Col5a1, Collagen, type V, alpha 1, mRNA; Ctgf, Connective tissue growth factor;* IFN-γ, Interferon-γ; *Igf1, Insulin-like growth factor 1, transcript variant 1, mRNA;* IL-4, Interleukin 4; *Fgf2, Fibroblast growth factor 2, mRNA; Fgf7, Fibroblast growth factor 7, mRNA; Hbegf: Heparin-binding epidermal-like growth factor, mRNA; Mmp3, Matrix metallopeptidase 3, mRNA; Mmp 9, Matrix metallopeptidase 9, mRNA; Mmp12, Matrix metallopeptidase 12, mRNA; Mmp13, Matrix metallopeptidase 13, mRNA; Mmp14, Matrix metallopeptidase 14, mRNA;* Mt reactive species, Mitochondrial reactive species; *Pdgfb: Platelet-derived growth factor beta polypeptide, mRNA; Timp1, TIMP metallopeptidase inhibitor 1, mRNA (coding for metalloproteinase inhibitor 1); Timp2, TIMP metallopeptidase inhibitor 2, mRNA; Tgfb1, Transforming growth factor, beta 1, mRNA; Vegfa, Vascular endothelial growth factor A, transcript variant 2, mRNA.* ↗ Trend to increase or upmodulation (not statistically significant); ↙ Trend to decrease or downmodulation (not statistically significant)

The promotion of the epithelialization was associated with an increase of cellular viability index and a trend (not statistically significant) to higher epithelial proliferation index, higher tissue concentrations of interleukin 4 (IL-4), lower tissue concentrations of interferon γ (IFN-γ), and higher levels of oxidative stress parameters, such as

cytosolic peroxides and mitochondrial reactive species. This was congruent with the important role of the redox biology in the regenerative potential of the intestinal epithelium, namely in cell signaling, modulation of proliferation and differentiation and regulation of death (Circu *et al.*, 2012). The trend to a prooxidative influence may favor the intestinal epithelial stem cells progression from a proliferative to a differentiated state (Circu *et al.*, 2012).

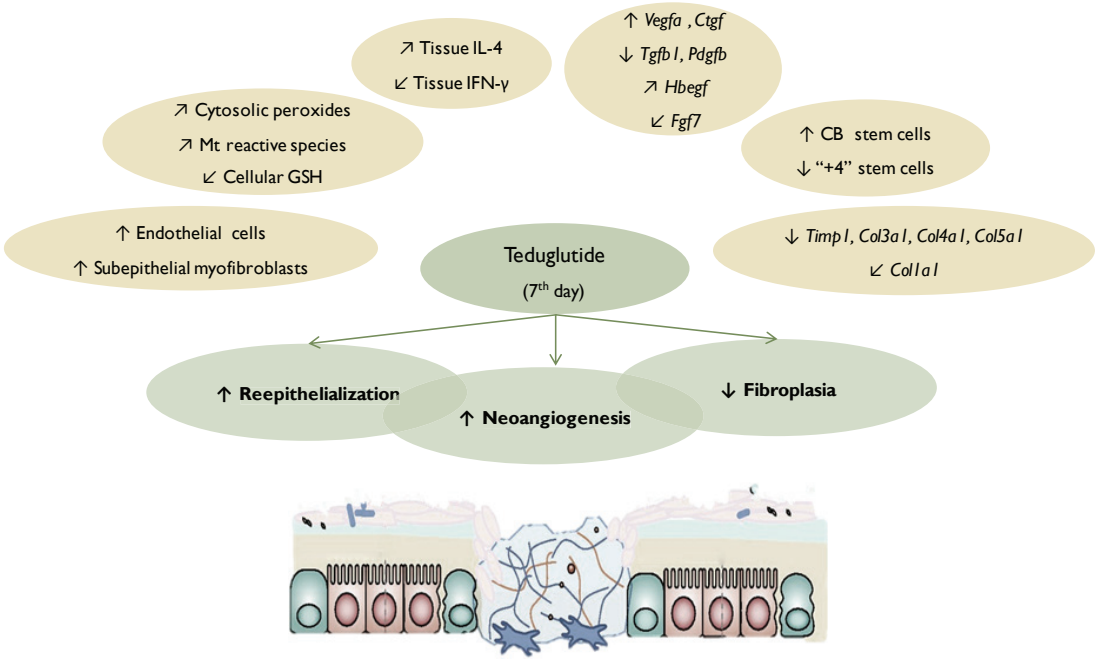

Figure 8.3. Schematic overview of the influence of teduglutide on the cellular, humoral and molecular mediators of the intestinal anastomotic repair, at the seventh day, suggested by the present study. "4" stem cells, Putative "+4 position" epithelial stem cells; CB stem cells, Putative crypt base columnar epithelial stem cells; Cellular GSH, Cellular reduced glutathione; *Col1a1, Collagen, type I, alpha 1, mRNA; Col3a1, Collagen, type III, alpha 1, mRNA; Col4a1, Collagen, type IV, alpha 1, mRNA; Col5a1, Collagen, type V, alpha 1, mRNA; Ctgf, Connective tissue growth factor;* IFN-γ, Interferon-γ; *Igf1, Insulin-like growth factor 1, transcript variant 1, mRNA;* IL-4, Interleukin 4; *Fgf2, Fibroblast growth factor 2, mRNA; Fgf7, Fibroblast growth factor 7, mRNA; Hbegf: Heparin-binding epidermal-like growth factor, mRNA; Mmp3, Matrix metallopeptidase 3, mRNA; Mmp 9, Matrix metallopeptidase 9, mRNA; Mmp12, Matrix metallopeptidase 12, mRNA; Mmp13, Matrix metallopeptidase 13, mRNA; Mmp14, Matrix metallopeptidase 14, mRNA;* Mt reactive species, Mitochondrial reactive species; *Pdgfb: Platelet-derived growth factor beta polypeptide, mRNA; Timp1, TIMP metallopeptidase inhibitor 1, mRNA (coding for metalloproteinase inhibitor 1); Timp2, TIMP metallopeptidase inhibitor 2, mRNA; Tgfb1, Transforming growth factor, beta 1, mRNA; Vegfa, Vascular endothelial growth factor A, transcript variant 2, mRNA.* ↗ Trend to increase or upmodulation (not statistically significant); ↙ Trend to decrease or downmodulation (not statistically significant)

The favorable effect of teduglutide on reepithelialization may have be related with the upregulation of gene expression of *insulin-like growth factor 1* at the third day and of *connective tissue growth factor* at the seventh day (Latella *et al.*, 2013; Speca *et al.*, 2012; Bortvedt *et al.*, 2012). Increase of subepithelial myofibroblasts density evidenced in teduglutide-treated animals may have been relevant because they are important constituents of the stem cells niche, participating in the regulation of epithelial stem cells behavior in the regeneration process (Smith *et al.*, 2012), and are considered cellular mediators of the GLP-2 and teduglutide effects, through the release of insulin-like growth factor 1 and likely other growth factors (Drucker and Yusta, 2014; Rowland and Brubaker, 2011). Teduglutide treatment was not associated with relevant modifications of the number of Paneth cells *per* crypt, which also represent a critical element of the epithelial stem cells niche, nor of the number of goblet cells *per* crypt-villus unit.

Teduglutide administration was associated with an induction of the neovessels development in the perianastomotic tissue at the seventh day, as evaluated by anti-CD31 immunostaining of endothelial cells. This effect may have resulted from the upmodulation of the gene expression of the *vascular endothelial growth factor a*, promoter of endothelial cells migration and proliferation (Greaves *et al.*, 2013), as well of the *connective tissue growth factor*, at the seventh day, and of *insulin-like growth factor 1*, at the third day. Nevertheless, teduglutide was associated with downregulation of the gene expression of *fibroblast growth factor 2* at the third day, considered the most important proangiogenic factor in the early phase after injury (Greaves *et al.*, 2013).

In relation to the fibrogenesis process, teduglutide was not associated with significant differences on the global collagen content of the perianastomotic tissue nor on the type I to type III collagens ratio, as indicated by the semiquantitative assessment with the morphometric method of Gordon-Sweet's histological staining.

Neverthless, a trend to the repression of fibrolysis was observed, at gene expression level, at the predominantly inflammatory phase of anastomotic repair (third day), counteracting the trend to extracellular matrix degradation induced by the surgical injury. In fact, upmodulation of gene expression of *Timp1*, *Timp2* and *Collagen type IV alpha 1*, and downregulation of gene expression of *Mmp3* and *Mmp12* (and of *Mmp9*,

Mmp13 and *Mmp14,* albeit not statistically significant) was verified at that time point. Expression of the genes coding alpha 1 chains of types I and III collagens was also induced, although without reaching the threshold of statistical significance. Inhibition of fibrolysis at the third day may have been related with the upregulation of gene expression of *insulin-like growth factor 1*, and of *heparin-binding epidermal-like growth factor* (not significant).

On the contrary, at the predominantly proliferative phase of the reparative process (seventh day), gene expression of extracellular matrix components and remodeling factors suggested an inhibition of fibrogenesis. This effect may have been related with the downregulation of gene expression of *Timp1* and genes coding types III, IV and V collagens alpha chains. Repression of *Collagen type I alpha 1* expression (not significant) was also observed. These events were concordant with a trend (albeit not significant) to the reduction of global collagen content of the perianastomotic tissues (at the expense of type I collagen) on the semiquantitative evaluation with the Gordon-Sweet's method; nevertheless, a significant increase of type III collagen content in the submucosa was documented with this technique. A plausible simultaneous reduction (not significant) of fibroblasts infiltration of the anastomosis was revealed by the histological analysis. Gene downmodulation of fibrogenesis at the seventh day may be explained by the inhibition of gene expression of *transforming growth factor $\beta 1$*, a powerful profibrogenic growth factor (Biancheri P *et al.*, 2014; Latella *et al.*, 2013).

The trend to the inhibition of fibrolysis demonstrated at the third day by gene expression analysis suggests that teduglutide may protect against anastomotic failure in the period of lower biomechanical resistance and, therefore, of higher risk (Bosmans *et al.*, 2015; Thompson *et al.*, 2006). Nevertheless, the decrease of collagen deposition and the downmodulation of the relative gene expression of *transforming growth factor $\beta 1$* at the seventh day, suggested by the gene expression analysis, causes uncertainty about the increase of dehiscence susceptibility.

Transforming growth factor β has a relevant participation in the tissue remodeling and in the modulation of the mucosal immune response (Biancheri *et al.*, 2014), and interfere in the all the phases of anastomosis healing (Rijcken *et al.*, 2014). Transforming growth factor β signaling is characterized by tissue and context-

specificity of cell responses (Zhang, 2018; Budi *et al.*, 2017). The composition and compartmentalization of the receptor complexes define the activation of signaling pathways and the interactions with Smad-interacting transcription factors and co-regulators determine the cell-type specificity of the transcription responses to the ligands (Budi *et al.*, 2017). Regulation of the production of this pleiotropic cytokine is particularly complex and occurred at several levels, including transcription, translation, secretion and activation (Cebinelli *et al.,* 2016). Several cell types can both produce and respond to transforming growth factor β, including epithelial cells, monocytes/macrophages, regulatory T-cell and myofibroblasts (Biancheri *et al.*, 2014). Genetic polymorphisms (Cebinelli *et al.,* 2016) and epigenetic modifications triggered by environmental factors, including deoxyribonucleic acid (DNA) methylation, histone modifications of DNA and ribonucleic acid (RNA) interference by regulatory noncoding RNA may have interfered with present results (Mann and Mann, 2013).

Despite of the intestinal transit-modulating properties attributed to the exogenous administration of GLP-2 (Drucker and Yusta, 2014), no significant impact of teduglutide on glial cells and fibers density was testified in present analysis.

Most of the teduglutide effects were observed after seven days of treatment, with exception of the promising increase of the fibrogenesis (documented at the third day). Although the short-term extent of perioperative treatment may minimize the risk for undesired tumor promoting effects, the potential use of teduglutide as adjuvant of the intestinal anastomotic healing should exclude, until further information, individuals with active or suspected malignancy.

At present, the study of the pathophysiology of the intestinal anastomosis healing is hampered by the complexity (that hinders a holistic approach) and the absence of objective methodological resources for *in vivo* dynamic evaluation and monitoring of the repair progression. The currently used animal models, mainly rodent, are not completely representative of the pathophysiology of the anastomotic failure in the human patients.

Main limitations of this investigation must be considered in the interpretation of the results and may reduce the translational impact of present findings.

Unfortunately, the small sample size may have introduced a statistical type II error.

Present study did not include the functional assessment of anastomosis, namely the determination of the bursting pressure and the tensile strength (Pommergaard *et al.*, 2014; Thompson *et al.*, 2006). Nevertheless, regardless the widespread use, these parameters have demonstrated relevant limitations related with the heterogeneity, reproducibility and accuracy of the methodology (especially in small animals), and also with the lack of reliable correlations with the structural integrity of the anastomosis and the clinical outcome (Pommergaard *et al.*, 2014; Vakalopoulos *et al.*, 2013).

Regarding to the specific methodology, study of growth factors and extracellular matrix remodeling factors was implemented at gene expression level, which does not always reflect tissue protein expression and activity levels, as posttranscriptional, posttranslational and postsecretional interferences may occur. Moreover, overall collagen content on the perianastomotic tissue may not correlate with the functional outcome. A complex biosynthetic and depositional pathway leads to the formation of the insoluble collagen matrix but the fibrogenesis is completed only when collagens formed a cross-linked and remodeled matrix (Chen *et al.*, 2009).

An analysis of the teduglutide influence on the early small-bowel anastomotic healing in standard context was performed. Notwithstanding, extend the study to high-risk conditions (such as ischemia), to other segments of intestinal tract (including colon and colorectal anastomosis) and to the predominant remodeling phase could be also relevant.

A systemic therapy, through subcutaneous administration, was undertaken, based on previous experimental studies (Qi *et al.*, 2017; Burness and McCormak, 2013; Arda-Pirincci *et al.*, 2012; Alters *et al.*, 2012; Kaji *et al.*, 2009; Kaji *et al.*, 2008; Martin *et al.*, 2004) and no direct dose-effect assessment was accomplished. Previous studies suggest different effects according to the variations of GLP-2 dose and delivery method (Kaji *et al.*, 2008). Other administration schedules could be studied in future studies. Local therapy, through direct perianastomotic injection, use of coated sutures, concomitant sealing with adhesives or impregnated matrixes, may be more advantageous and to allow a sustained but low-dosage release of the growth factor at the anastomotic site, reducing the potential undesired side-effects.

New methodological resources for the evaluation of intestinal anastomotic healing might be used in further investigations, such as the high-resolution probe-based confocal laser endomicroscopy and the spectral domain polarization-sensitive optical coherence tomography (De Palma *et al.*, 2014; Son *et al.*, 2014).

Notwithstanding the aforementioned limitations, present study contributed to improve the knowledge of the potential impact of teduglutide on the intestinal anastomotic repair (Fig. 8.4). This insight is relevant to explore its potential role as a perioperative healing-adjuvant strategy, but also for the patients with short-bowel syndrome undergoing intestinal anastomotic procedures in the course of this growth factor therapy.

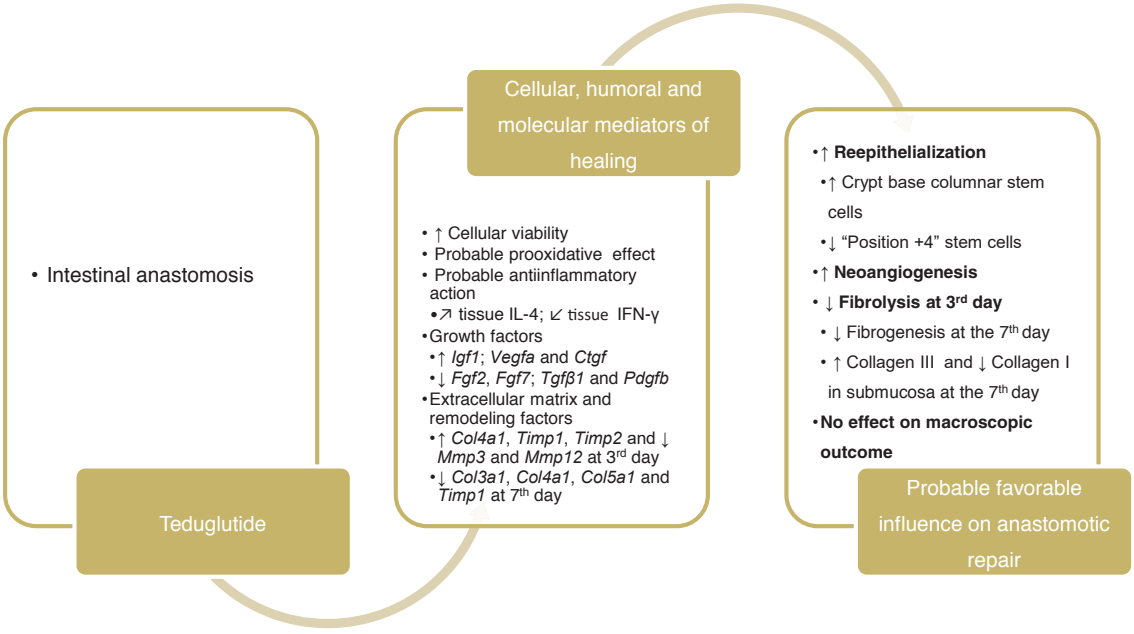

Figure 8.4. Schematic representation of the influence of teduglutide administration on the intestinal anastomotic repair process. *Col3a1, Collagen, type III, alpha 1, mRNA; Col4a1, Collagen, type IV, alpha 1, mRNA; Col5a1, Collagen, type V, alpha 1, mRNA; Ctgf, Connective tissue growth factor;* IFN-γ, Interferon-γ; *Igf1, Insulin-like growth factor 1, transcript variant 1, mRNA;* IL-4, Interleukin 4; *Fgf2, Fibroblast growth factor 2, mRNA; Fgf7, Fibroblast growth factor 7, mRNA; Mmp3, Matrix metallopeptidase 3, mRNA; Mmp12, Matrix metallopeptidase 12, mRNA; Pdgfb: Platelet-derived growth factor beta polypeptide, mRNA; Timp1, TIMP metallopeptidase inhibitor 1, mRNA (coding for metalloproteinase inhibitor 1); Timp2, TIMP metallopeptidase inhibitor 2, mRNA; Tgfb1, Transforming growth factor, beta 1, mRNA; Vegfa, Vascular endothelial growth factor A, transcript variant 2, mRNA.*
↗ Trend to increase or upmodulation (not statistically significant); ↙ Trend to decrease or downmodulation (not statistically significant)

Further research should address the impact of the teduglutide on gut microbiome, which emerged as an important determinant of the anastomosis outcome, and to explore the influence of genetic polymorphisms in the susceptibility of anastomotic dehiscence.

Teduglutide therapeutic potential, demonstrated in this study, could be explored in other contexts, including in the reestablishment of the gut homeostasis in the intestinal dysfunction of the critically ill patients. Previous studies, including of Costa BP (Costa *et al.*, 2017), suggested that biomarkers of intestinal dysfunction, such as citrullinemia, were associated with disease severity and mortality in intensive care units, namely in severe trauma patients. Intestinal dysfunction, with autodigestion and release of bacterial and toxic intestine-derived mediators, has been hypothesized to play a central role in the pathophysiology of systemic inflammatory response syndrome, multiple organ failure, sepsis and death in the critical illness.

To conclude, the present study reflects the complexity of the anastomotic repair and points to a favorable influence of teduglutide on the intestinal anastomotic healing that deserves additional investigation.

Chapter 9

References

Adas M, Kemik O, Adas G, Arikan S, Kuntsal L, Kapran Y, Toklu AS (2013) Is combined therapy more effective than growth hormone or hyperbaric oxygen alone in the healing of left ischemic and non-ischemic colonic anastomoses? Clinics (Sao Paulo). 68:1440–1445.

Adas G, Percem A, Adas M, Kemik O, Arikan S, Ustek D, Cakiris A, Abaci N, Kemik AS, Kamali G, Karahan S, Akcakaya A, Karatepe O: VEGF-A and FGF gene therapy accelerate healing of ischemic colonic anastomoses (experimental study) (2011) Int J Surg. 9:467-471.

Ågren MS, Andersen TL, Andersen L, Schiødt CB, Surve V, Andreassen TT, Risteli J, Franzén LE, Delaissé J, Heegaard AM, Jorgensen LN (2011) Nonselective matrix metalloproteinase but not tumor necrosis factor-α inhibition effectively preserves the early critical colon anastomotic integrity. Int J Colorectal Dis. 26:329–337.

Ågren MS, Andersen TL, Mirastschijski U, Syk I, Schiødt CB, Surv V, Lindebjerg J, Delaissé JM (2006) Action of matrix metalloproteinases at restricted sites in colon anastomosis repair: an immunohistochemical and biochemical study. Surgery. 140(1):72-82.

Almeida S, Sarmento-Ribeiro AB, Januário C, Rego AC, Oliveira CR (2008) Evidence of apoptosis and mitochondrial abnormalities in peripheral blood cells of Huntington's disease patients. Biochem Biophys Res Commun. 374(4):599-603.

Alters SE, McLaughlin B, Spink B, Lachinyan T, Wang CW, Podust V, Schellenberger V, Stemmer WP (2012) GLP2-2G-XTEN: a pharmaceutical protein with improved serum half-life and efficacy in a rat Crohn's disease model. PLoS One. 7(11):e50630. doi: 10.1371/journal.pone.0050630

Alzoghaibi MA, Zubaidi AM (2014) Upregulation of the proinflammatory cytokine-induced neutrophil chemoattractant-1 and monocyte chemoattractant protein-1 in rats' intestinal anastomotic wound healing - does it matter? Asian J Surg. 37(2):86-92.

Alzoghaibi MA: Concepts of oxidative stress and antioxidant defense in Crohn's disease (2013) World J Gastroenterol. 19(39):6540-6547.

Amar S, Minond D, Fields GB (2017) Clinical implications of compounds designed to inhibit ECM-modifying metalloproteinases. Proteomics. doi: 10.1002/pmic.201600389.

Arana MR, Tocchetti GN, Zecchinati F, Londero AS, Dominguez C, Perdomo V, Rigalli JP, Maris Villanueva SS, Mottino AD (2017) Glucagon-like peptide 2 prevents down-regulation of intestinal multidrug resistance-associated protein 2 and P-glycoprotein in

endotoxemic rats. Toxicology. Aug 22. pii: S0300-483X(17)30233-0. doi: 10.1016/j.tox.2017.08.007.

Arda-Pirincci P, Bolkent S (2011) The role of glucagon-like peptide-2 on apoptosis, cell proliferation, and oxidant-antioxidant system at a mouse model of intestinal injury induced by tumor necrosis factor-alpha/actinomycin D. Mol Cell Biochem. 350(1-2):13-27.

Arda-Pirincci P, Oztay F, Bayrak BB, Yanardag R, Bolkent S (2012) Teduglutide, a glucagon-like peptide 2 analogue: a novel protective agent with anti-apoptotic and anti-oxidant properties in mice with lung injury. Peptides. 38(2):238-247.

Ashburn JH, Stocchi L, Kiran RP, Dietz DW, Remzi FH (2013) Consequences of anastomotic leak after restorative proctectomy for cancer: effect on long-term function and quality of life. Dis Colon Rectum. 56(3):275-80.

Aubry JP, Blaecke A, Lecoanet-Henchoz S, Jeannin P, Herbault N, Caron G, Moine V, Bonnefoy JY (1999) Annexin V used for measuring apoptosis in the early events of cellular cytotoxicity. Cytometry. 37(3):197-204.

Austin K, Markovic MA, Brubaker PL (2016) Current and potential therapeutic targets of glucagon-like peptide-2. Curr Opin Pharmacol. 1:13-18.

Aw TY (2012) Tissue oxidative stress revisited: significance of ROS and redox signaling. Semin Cell Dev Biol. 23(7):721.

Aznan MI, Khan OH, Unar AO, Tuan Sharif SE, Khan AH, Syed Abd Aziz SH, Zakaria AD (2016) Effect of Tualang honey on the anastomotic wound healing in large bowel anastomosis in rats-A randomized controlled trial. BMC Complement Altern Med. 16:28.

Bachmann R, Leonard D, Delzenne N, Kartheuser A, Cani PD (2017) Novel insight into the role of microbiota in colorectal surgery. Gut. 66:738–749.

Baker EA, Leaper DJ (2003) Profiles of matrix metalloproteinases and their tissue inhibitors in peritoneal drainage fluid: relationship to wound healing. Wound Rep Reg. 11:268-274.

Bakker IS, Morks AN, Ten Cate Hoedemaker HO, Burgerhof JGM, Leuvenink HG, van Praagh JB, Ploeg RJ, Havenga K; Collaborative C-seal Study Group (2017) Randomized clinical trial of biodegradeable intraluminal sheath to prevent anastomotic leak after stapled colorectal anastomosis. Br J Surg. 104(8):1010-1019.

Baldassano S, Amato A, Cappello F, Rappa F, Mulè F (2013) Glucagon-like peptide-2 and mouse intestinal adaptation to a high-fat diet. J Endocrinol. 217(1):11-20.

Barker N, van Es JH, Kuipers J, Kujala P, van den Born M, Cozijnsen M, Haegebarth A, Korving J, Begthel H, Peters PJ, Clevers H (2007) Identification of stem cells in small intestine and colon by marker gene Lgr5. Nature. 449(7165):1003-7.

Barker N, Clevers H (2010) Leucine-rich repeat-containing G-protein-coupled receptors as markers of adult stem cells. Gastroenterology. 138(5):1681-1696.

Barker N, van Oudenaarden A, Clevers H (2012) Identifying the stem cell of the intestinal crypt: Strategies and pitfalls. Cell Stem Cell. 11(4):452-60.

Barker N (2014) Adult intestinal stem cells: Critical drivers of epithelial homeostasis and regeneration. Nat Rev Mol Cell Biol. 15:20-33.

Barrientos S, Brem H, Stojadinovic O, Tomic-Canic M (2014) Clinical application of growth factors and cytokines in wound healing. Wound Repair Regen. 22(5):569-78.

Barrientos S, Stojadinovic O, Golinko, MS, Brem H, Tomic-Canic M (2008) Growth factors and cytokines in wound healing. Wound Rep Reg. 2008;16:585–601.

Berg JK, Kim EH, Li B, Joelsson B, Youssef NN (2014) A randomized, double-blind, placebo-controlled, multiple-dose, parallel-group clinical trial to assess the effects of teduglutide on gastric emptying of liquids in healthy subjects. BMC Gastroenterology. 14:25.

Biancheri P, Giuffrida P, Docena GH, MacDonald TT, Corazza GR, Sabatino AD (2014) The role of transforming growth factor (TGF)-β in modulation the immune response and fibrogenesis in the gut. Cytokine & Growth Factor Reviews. 25:45-55.

Billiauws L, Bataille J, Boehm V, Corcos O, Joly F (2017) Teduglutide for treatment of adult patients with short bowel syndrome. Expert Opin Biol Ther. 17:623-632.

Bloemendaal AL, Buchs NC, George BD, Guy RJ (2016) Intestinal stem cells and intestinal homeostasis in health and in inflammation: A review. Surgery. 159(5):1237-48.

Blonski W, Buchner AM, Aberra F, Lichtenstein G (2013) Teduglutide in Crohn's disease. Expert Opin Biol Ther. 13(8):1207-1214.

Bobkiewicz A, Studniarek A, Krokowicz L, Szmyt K, Borejsza-Wysocki M, Szmeja J, Marciniak R, Drews M, Banasiewicz T (2017) Gastrointestinal tract anastomoses with the biofragmentable anastomosis ring: is it still a valid technique for bowel anastomosis? Analysis of 203 cases and review of the literature. Int J Colorectal Dis. 32(1):107-111.

Boersema GS, Wu Z, Kroese LF, Vennix S, Bastiaansen-Jenniskens YM, van Neck JW, Lam KH, Kleinrensink GJ, Jeekel J, Lange JF (2016) Hyperbaric oxygen therapy improves colorectal anastomotic healing. Int J Colorectal Dis. 31(5):1031-8.

Boersema GSA, Vennix S, Wu Z, Te Lintel Hekkert M, Duncker DGM, Lam KH, Menon AG, Kleinrensink GJ, Lange JF (2017) Reinforcement of the colon anastomosis with cyanoacrylate glue: a porcine model. J Surg Res. May 10. pii: S0022-4804(17)30254-8.

Boesen AK, Maeda Y, Madsen MR (2013) Perioperative fluid infusion and its influence on anastomotic leakage after rectal cancer surgery: implications for prevention strategies. Colorectal Disease. 15:e522–e527.

Bortvedt SF, Lund PK (2012) Insulin-like growth factor 1: common mediator of multiple enterotrophic hormones and growth factors. Curr Opin Gastroenterol. 28(2):89-98.

Bosmans JW, Jongen AC, Birchenough GM, Nyström EE, Gijbels MJ, Derikx JP, Bouvy ND, Hansson GC (2017) Functional mucous layer and healing of proximal colonic anastomoses in an experimental model. Br J Surg. 104(5):619-630.

Bosmans JWAM, Jongen ACHM, Bouvy ND, Derikx JPM (2015) Colorectal anastomotic healing: Why the biological processes that lead to anastomotic leakage should be revealed prior to conduction intervention studies. BMC Gastroenterology. 15:180-186

Bosmans JWAM, Moossdorff M, Al-Taher M, van Beek L, Derikx JPM, Bouby ND (2016) International consensus statement regarding the use of animal models for research on anastomoses in the lower gastrointestinal tract. Int J Colorectal Dis. 31:1021-1030.

Brinkman AS, Murali SG, Hitt S, Solverson PM, Holst JJ, Ney DM (2012) Enteral nutrients potentiate glucagon-like peptide 2 action and reduce dependence on parenteral nutrition in a rat model of human intestinal failure. Am J Physiol Gastrointest Liver Physiol. 303(5):G610-22.

Brown SR, Mathew R, Keding A, MarshallHC, Brown JM, Jayne DG (2014) The impact of postoperative complications on long-term quality of like after curative colorectal cancer surgery. Ann Surg. 259(5):916-923.

Buchman AL, Katz S, Fang JC, Bernstein CN, Abou-Assi SG; Teduglutide Study Group (2010) Teduglutide, a novel mucosally active analog of glucagon-like peptide-2 (GLP-2) for the treatment of moderate to severe Crohn's disease. Inflamm Bowel Dis. 16(6):962-973.

Buczacki SJ, Zecchini HI, Nicholson AM, Russell R, Vermeulen L, Kemp R, Winton DJ (2013) Intestinal label-retaining cells are secretory precursors expressing Lgr5. Nature. 495: 65-69.

Budi EH, Duan D, Derynck (2017) Transforming growth factor-β receptors and Smads: Regulatory complexity and functional versatility. Trends Cell Biol. 27:658-672.

Bulut K, Pennartz C, Felderbauer P, Meier JJ, Banasch M, Bulut D, Schmitz F, Schmidt WE, Hoffman P (2008) Glucagon like peptide-2 induces intestinal restitution through VEGF release from subepithelial myofibroblasts. Eur J Pharmacol. 578:279-285.

Burness CB, McCormack PL (2008) Teduglutide: a review of its use in the treatment of patients with short bowel syndrome. Drugs. 73(9):935-947.

Cabrera-Perez J, Badovinac VP, Griffith TS (2017) Enteric immunity, the gut microbiome, and sepsis: Rethinking the germ theory of disease. Experimental Biology and Medicine. 242:127-139.

Cağlikülekçi M, Ozçay N, Oruğ T, Aydoğ G, Renda N, Atalay F (2002) The effect of recombinant growth hormone on intestinal anastomotic wound healing in rats with obstructive jaundice. Turk J Gastroenterol. 13:17-23.

Cai Y, Wang W, Liang H, Sun L, Teitelbaum DH, Yang H (2012) Keratinocyte growth factor improves epithelial structure and function in a mouse model of intestinal ischemia/reperfusion. PLoS One. 7(9):e44772.

Cakmak G, Irkorucu O, Ucan B, Emre A, Bahadir B, Demirtas C, Tascilar O, Karakaya K, Acikgoz S, Kertis G, Ankarali H, Pasaoglu H, Comert M (2009) Simvastatin improves wound strength after intestinal anastomosis in the rat. J Gastrointest Surg. 13:1707-1716

Cardoso SM, Pereira C, Oliveira CR (1998) The protective effect of vitamin E, idebenone and reduced glutathione on free radical mediated injury in rat brain synaptosomes. Biochem Biophys Res Commun. 246(3):703-710

Cebinelli GCM, Trugilo KP, Garcia SB, Oliveira KB (2016) TGB-β1 functional polymorphisms: A review. Eur Cytokine Netw. 27:81-89.

Cetinkaya K, Dinc S, Gulcelik MA, Renda N, Ustun H, Caydere M, Alagol H (2005) Granulocyte macrophage-colony stimulating factor improves impaired anastomotic wound healing in rats treated with intraperitoneal mitomycin-C. Surg Today. 35:290-294.

Chadi SA, Fingerhut A, Berho M, DeMeester SR, Fleshman8 JW, Hyman NH, Margolin DA, Joseph E. Martz JE, McLemore EC, Molena D, Newman MI, Rafferty JF, Safar B, Senagore

AJ, Zmora O, Wexner SD (2016) Emerging Trends in the Etiology, Prevention, and Treatment of Gastrointestinal Anastomotic Leakage. J Gastrointest Surg. 20:2035-2051.

Chen CZ, Raghunath M (2009) Focus on collagen: In vitro systems to study fibrogenesis and antifibrosis – State of the art. Fibrogenesis Tissue Repair. 2:7.

Choileain N, Redmond HP (2006) Cell response to surgery. Arch Surg. 141(11):1132-40.

Choy PY, Bissett IP, Docherty JG, Parry BR, Merrie A, Fitzgerald A (2011) Stapled versus handsewn methods for ileocolic anastomoses. Cochrane Database Syst Rev. Sep 7;(9):CD004320.

Cini C, Wolthuis A, D'Hoore A (2013) Peritoneal fluid cytokines and matrix metalloproteinases as early markers of anastomotic leakage in colorectal anastomosis: a literature review and meta-analysis. Colorectal Disease. 15:1070-1077.

Circu ML, Aw TY (2012) Intestinal redox biology and oxidative stress. Semin Cell Dev Biol. 23(7):729-737.

Clevers H (2013) The intestinal crypt, a prototype stem cell compartment. Cell. 154(2):274-84.

Colak T, Dag A, Turkmenoglu O, Polat A, Comelekoglu U, Bagdatoglu O, Polat G, Akca T, Sucullu I, Aydin S (2007) The effect of octreotide on healing of injured colonic anastomosis with immediate postoperative intraperitoneal administration of 5-Fluorouracil. Dis Colon Rectum. 50:660-669.

Costa BP, Martins P, Verissimo C, Simões M, Tome M, Grazina M, Pimentel J, Castro-Sousa F (2017) Intestinal dysfunction in the critical trauma patients – An early and frequent event. Nutr Hosp 34(2):284-289.

Cueto J, Barrientos T, Rodriguez E, Espinosa L, Palma J, Cojab J, Orozco T, Haro A, Del Moral P (2014) Further experimental studies on a biodegradable adhesive for protection of colorectal anastomosis. Arch Med Res. 45(4):331-6.

Cui N, Hu M, Khalil RA (2014) Biochemical and biological attributes of matrix metalloproteinases. Prog Mol Biol Transl Sci. 147:1-73

De la Portilla F, García-Cabrera AM, Pereira S, de Marco F, Molero M, Muntane J, Padillo FJ (2016) An experimental study on the use of calcium alginate to heal colonic anastomoses. J Invest Surg. 29(1):32-9.

De Palma GD, Luglio G, Staibano S, Bucci L, Esposito D, Maione F, Mascolo M, Ilardi G, Forestieri P (2014) Perioperative characterization of anastomotic doughnuts with high-resolution probe-based confocal laser endomicroscopy in colorectal cancer surgery: a feasibility study. Surg Endosc. 28(7):2072-7.

Decker D, Schondorf M, Bidlingmaier F, Hirner A, von Ruecker AA (1996) Surgical stress induces a shift in the type-1/type-2 T-helper cell balance, suggesting down-regulation of cell-mediated and up-regulation of antibody-mediated immunity commensurate to the trauma. Surgery. 119(3):316-325.

Dekaney CM, Fong JJ, Rigby RJ, Lund PK, Henning SJ, Helmrath MA (2007) Expansion of intestinal stem cells associated with long-term adaptation following ileocecal resection in mice. Am J Physiol Gastrointest Liver Physiol. 293(5):G1013-22.

Dekaney CM, Rodriguez JM, Graul MC, Henning SJ (2005) Isolation and characterization of a putative intestinal stem cell fraction from mouse jejunum. Gastroenterology. 129(5):1567–1580.

Delavary BM, van der Veer WM,van Egmond M, Niessen FG, Beelen RHJ (2011) Macrophages in skin injury and repair. Immunobiology. 216:753–762.

Demetriades H, Kanellos I, Mantzoros I, Kalfadis S, Galovatsea K, Zaraboukas T, Betsis D (2002) Effects of lanreotide on the healing of small bowel anastomoses following obstructive ileus in rats. Colorectal Dis. 4(1):23-27.

Demirer S, Sengül N, Inan A, Eroğlu A, Bumin C, Kuterdem E (2001) Effect of recombinant human granulocyte/macrophage colony-stimulating factor on the healing of colonic anastomosis in rats. J Invest Surg. 14:221-225.

D'Hoore A, Albert MR, Cohen SM, Herbst F, Matter I, Van Der Speeten K, Dominguez J, Rutten H, Muldoon JP, Bardakcioglu O, Senagore AJ,Ruppert R, Mills S, Stamos MJ, Påhlman L, Choman E, Wexner SD; COMPRES collaborative study group (2015) COMPRES: A prospective postmarketing evaluation of the compression anastomosis ring CAR 27(™) /ColonRing(™).Colorectal Dis. 17(6):522-9.

Di Cristofaro L, Ruffolo C, Pinto E, Massa M, Antoniutti M, Cagol M, Massani M, Alfieri R, Costa A, Bassi N, Castoro C, ScarpaM (2014) Complications after surgery for colorectal cancer affect quality of life and surgeon-patient relationship. Colorectal Dis. 16(12):O407–O419.

Dikalov SI, Harrison DG (2014) Methods for detection of mitochondrial and cellular reactive oxygen species. Antioxid Redox Signal. 20(2):372-382.

Dinc S, Alagol H, Gulcelik MA, Ozbirecikli B, Kuru B, Renda N, Ustun H (2002) Locally applied granulocyte-macrophage colony-stimulating factor improves the impaired bowel anastomoses in rats with long-term corticosteroid treatment. World J Surg. 26:1208-1213.

Dinc S, Ozbirecikli B, Gulcelik MA, Ergeneci D, Kuru B, Erdem E, Caydere M, Alagol H (2004a) The effects of locally injected granulocyte macrophage-colony stimulating factor on the healing of intraoperatively irradiated intestinal anastomoses in rats. J Exp Clin Cancer Res. 23:77-82.

Dinc S, Gulcelik MA, Kuru B, Ergeneci D, Camlibel M, Caydere M, Alagol H (2004b) Effects of locally applied recombinant human granulocyte-macrophage colony-stimulating factor on ischemic bowel anastomoses in rat. Eur Surg Res. 36:59-63.

Drucker DJ (2002) Gut adaptation and the glucagon-like peptides. Gut. 50(3):428-435.

Drucker DJ, Yusta B (2014) Physiology and pharmacology of the enteroendocrine hormone glucagon-like peptide-2. Annu Rev Physiol. 76:561-583.

Dubé PE, Brubaker PL (2007) Frontiers in glucagon-like peptide-2: multiple actions, multiple mediators. Am J Physiol Endocrinol Metab. 293:E460-5.

Egger B, Inglin R, Zeeh J, Dirsch O, Huang Y, Büchler MW (2001) Insulin-like growth factor I and truncated keratinocyte growth factor accelerate healing of left-sided colonic anastomoses. Br J Surg. 88(1):90-98.

El-Jamal N, Erdual E, Neunlist M, Koriche D, Dubuquoy C, Maggiotto F, Chevalier J, Berrebi D, Dubuquoy L, Boulanger E, Cortot A, Desreumaux P (2014) Glugacon-like peptide-2: broad receptor expression, limited therapeutic effect on intestinal inflammation and novel role in liver regeneration. Am J Physiol Gastrointest Liver Physiol. 307(3):G274-85.

Ellebæk MB, Baatrup G, Gjedsted J, Fristrup C, Qvist N (2014) Cytokine response in peripheral blood indicates different pathophysiological mechanisms behind anastomotic leakage after low anterior resection: a pilot study. Tech Coloproctol. 18:1067–1074.

Ellis Roy (2017) Alcian blue and PAS staining protocol: http://www.ihcworld.com/_protocols/special_stains/alcian_blue_pas_ellis.htm. Assessed in May 13th, 2017.

Erdem E, Dinç S, Erdem D, Ustün H, Caydere M, Alagöl H (2002) Effects of intraperitoneal chemotherapy and GM-CSF on anastomotic healing: an experimental study in rats. J Surg Res. 108:1-6.

European Commission (2010) Directive 2010/63/EU on protection of animals used for scientific purposes. http://ec.europa.eu/environment/chemicals/lab_animals/pdf/guidance/directive/en.pdf. Assessed in 25 August 2017.

Evans GS, Flint N, Somers AS, Eyden B, Potten CS (1992) The development of a method for the preparation of rat intestinal epithelial cell primary cultures. J Cell Sci. 101(Pt1):219-231.

Faruquzzaman SK (2009) The healing role of erythropoietin in the obstructive vs nonobstructive left colonic anastomosis. Bratisl Lek Listy. 110:530–535.

Fay KT, Ford ML, Coopersmith CM (2017) The intestinal microenvironment in sepsis. Biochim Biophys Acta. Mar 7. pii:S0925-4439(17)30081-9.

Fraga D, Meulia T, Fenster S (2008) Real-Time PCR. In Current Protocols Essential Laboratory Techniques 10.3.1-10.3.34. 2008; John Wiley and Sons, Inc. Published Online: 1 October 2008. Doi: 10.1002/9780470089941.et1003s00.

Francisco-Cruz A, Aguilar-Santelises M, Ramos-Espinosa O, Mata-Espinosa D, Marquina-Castillo B, Barrios-Payan J, Hernandez-Pando R (2014) Granulocyte-macrophage colony-stimulating factor: Not just another haematopoietic growth factor. Med Oncol. 31(1):774.

Frasson M, Flor-Lorente B, Rodriguez JL Granero-Castro P, Hervás D, Alvarez Rico MA, Brao MJ, Sánchez González JM, Garcia-Granero E; ANACO Study Group (2015) Risk factors for anastomotic leak after colon resection for cancer: Multivariate analysis and nomogram from a multicentric, prospective, national study with 3193 patients. Ann Surg. 262:321–330.

Fresno L, Fondevila D, Bambo O, Chacaltana A, García F, Andaluz A (2010) Effects of platelet-rich plasma on intestinal wound healing in pigs. Vet J. 185:322-327.

Frysak Z, Schovanek J, Iacobone M, Karasek D (2015) Insulin-like Growth Factors in a clinical setting: Review of IGF-I. Biomed Pap Med Fac Univ Palacky Olomouc Czech Repub. 159(3):347-51.

Fuchs TF, Surke C, Stange R, Quandte S, Wildemann B, Raschke MJ, Schmidmaier G (2012) Local delivery of growth factors using coated suture material. ScientificWorldJournal. 2012:109216.

Futier E, Constantin JM, Petit A, Chanques G, Kwiatkowski F, Flamein R, Slim K, Sapin V, Jaber S, Bazin JE: Conservative vs restrictive individualized goal-directed fluid replacement strategy in major abdominal surgery: A prospective randomized trial. Arch Surg. 2010;145(12):1193-200.

Galanopoulos G, Pramateftakis MG, Raptis D, Mantzoros I, Kanellos D, Angelopoulos S, Koliakos G, Zaraboukas T, Lazaridis C (2011) The effects of iloprost on colonic anastomotic healing in rats. Tech Coloproctol. 15 (Suppl 1):S117–S120.

Galluzzi L, Vitale I, Abrams JM, Alnemri ES, Baehrecke EH, Blagosklonny MV, Dawson TM, Dawson VL, El-Deiry WS, Fulda S, Gottlieb E, Green DR, Hengartner MO, Kepp O, Knight RA, Kumar S, Lipton SA, Lu X, Madeo F, Malorni W, Mehlen P, Nuñez G, Peter ME, Piacentini M, Rubinsztein DC, Shi Y, Simon HU, Vandenabeele P, White E, Yuan J, Zhivotovsky B, Melino G, Kroemer G (2012) Molecular definitions of cell death subroutines: Recommendations of the Nomenclature Committee on Cell Death 2012. Cell Death Differ. 19(1):107-120.

Gan SD, Patel KR (2013) Enzyme immunoassay and enzyme-linked immunosorbent assay. J Invest Dermatol. 133(9):e12.

García de Lorenzo y Mateos A, Acosta Escribano J, Rodríguez Montes JA (2007) Clinical importance of bacterial translocation. Nutr Hosp. 22 Suppl 2:50-55.

Garfinkle R, Abou-Khalil J, Morin N, Ghitulescu G, Vasilevsky CA, Gordon P, Demian M, Boutros M (2017) Is there a role for oral antibiotic preparation alone before colorectal surgery? ACS-NSQIP analysis by coarsened exact matching. Dis Colon Rectum. 60(7):729-737.

Garrison AP, Dekaney CM, von Allmen DC, Lund PK, Henning SJ, Helmrath MA (2009) Early but not late administration of glucagon-like peptide-2 following ileo-cecal resection augments putative intestinal stem cell expansion. Am J Physiol Gastrointest Liver Physiol. 296(3):G643-50.

Gattazzo F, Urciuolo A, Bonaldo P (2014) Extracellular matrix: A dynamic microenvironment for stem cell niche. Biochim Biophys Acta. 1840(8):2506-2519.

Gelse K, Pöschl E, Aigner T (2003) Collagens - structure, function, and biosynthesis. Adv Drug Deliv Rev. 55(12):1531-1546.

Gessler B, Eriksson O, Angenete E (2017) Diagnosis, treatment, and consequences of anastomotic leakage in colorectal surgery. Int J Colorectal Dis. 32(4):549-556.

Giaccaglia V, Salvi PF, Antonelli MS, Nigri G, Pirozzi F, Casagranda B, Giacca M, Corcione F, de Manzini N, Balducci G, Ramacciato G (2016) Procalcitonin reveals early dehiscence in colorectal surgery: The PREDICS study. Ann Surg. 263(5):967-972.

Giusto G, Vercelli C, Iussich S, Tursi M, Perona G, Gandini M: Comparison of the effects of platelet-rich or growth factor-rich plasma on intestinal anastomosishealing in pigs. BMC Vet Res. 2017;13:188.

Gomes A, Fernandes E, Lima JLFC (2005) Fluorescence probes used for detection of reactive oxygen species. J. Biochem. Biophys. Methods 65:45–80.

Gordon H, Sweets HH (1936) A simple method for the silver impregnation of reticulum. Am J Pathol. 12(4):545-552.

Gordon MK, Hahn RA (2010) Collagens. Cell Tissue Res. 339(1): 247–257

Gracz AD, Puthoff BJ, Magness ST (2012) Identification, isolation, and culture of intestinal epithelial stem cells from murine intestine. Methods Mol Biol. 2012;879:89-107.

Gracz AD, Magness ST (2014) Defining hierarchies of stemness in the intestine: evidence from biomarkers and regulatory pathways. Am J Physiol Gastrointest Liver Physiol. 307(3):G260-73.

Graves CE, Co C, Hsi RS, Kwiat D, Imamura-Ching J, Harrison MR, Stoller ML (2017) Magnetic compression anastomosis (Magnamosis): First-in-human trial. J Am Coll Surg. 225(5):676-681.

Greaves NS, Ashcroft KJ, Baguneid M, Bayat A (2013) Current understanding of molecular and cellular mechanisms in fibroplasia and angiogenesis during acute wound healing. J Dermatol Sci. 72(3):206-217.

Gulcelik MA, Dinc S, Bir F, Elitok O, Alagol H, Oz M (2005) Locally applied molgramostim improves wound healing at colonic anastomoses in rats after ligation of the common bile duct. Can J Surg. 48:213-218.

Günes HV, Demirer S, Aydinuraz K, Kepenekci I, Kuterdem E, Aribal D (2006) Effects of basic fibroblast growth factor and phenytoin on healing of abdominal wall fascia and colonic anastomoses. Int Surg. 91:151-156.

Gustafsson P, Jestin P, Gunnarsson U, Lindforss U (2015) Higher frequency of anastomotic leakage with stapled compared to hand-sewn ileocolic anastomosis in a large population-based study. World J Surg. 39(7):1834-1839.

Guyton KL, Hyman NH, Alverdy JC (2016) Prevention of perioperative anastomotic healing complications: Anastomotic stricture and anastomotic leak. Adv Surg. 50(1):129-41.

Ha GW, Kim JH, Lee MR (2017) Oncologic impact of anastomotic leakage following colorectal cancer surgery: A systematic review and meta-analysis. Ann Surg Oncol Doi 10.1245/s10434-017-5881-8.

Halliwell B, Whiteman M (2004) Measuring reactive species and oxidative damage in vivo and in cell culture: how should you do it and what do the results mean? Br J Pharmacol. 142:231–255.

Hammond J, Lim S, Wan Y, Gao X, Patkar A (2014) The burden of gastrointestinal anastomotic leaks: An evaluation of clinical and economic outcomes. J Gastrointest Surg. 18:1176-1185.

Hao XY, Yang KHGuo TK, Ma B, Tian JH, Li HL (2008) Omentoplasty in the prevention of anastomotic leakage after colorectal resection: a meta-analysis. Int J Colorect Dis. 23:1159–1165.

Heijmans J, de Jeude JFVL, Koo B, Rosekrans SL, Wielenga MCB, van de Wetering M, Ferrante M, Lee AS, Onderwater JJM, Paton JC, Paton AW, Mommaas AM, Kodach LL, Hardwick JC, Hommes DIW, Clevers H, Muncan V (2013) ER stress causes rapid loss of intestinal epithelial stemness through activation of the unfolded protein response. Cell Reports. 3:1128-1139.

Hendriks T, Mastboom WJ (1990) Healing of experimental intestinal anastomoses. Parameters for repair. Dis Colon Rectum. 33(10):891-901.

Herrle F, Diener MK, Freudenberg S, Willeke F, Kienle P, Boenninghoff R, Weiss C, Partecke LI, Schuld J, Post S (2016) Single-layer continuous versus double-layer continuous suture in colonic anastomoses - a randomized multicentre trial (ANATECH trial). J Gastrointest Surg. 20(2):421-30.

Heyboer M 3rd, Shrama D, Santiago W, McCulloch N (2017) Hyperbaric oxygen therapy: Side effects defined and quatified. Adv Wound Care (New Rochelle). 6(6):210-224.

Hirai K, Tabata Y, Hasegawa S, Sakai Y (2016) Enhanced intestinal anastomotic healing with gelatin hydrogel incorporating basic fibroblast growth factor. J Tissue Eng Regen Med. 10:E433-E442.

Hirst NA, Tiernan JP, Millner PA, Jayne DG (2014) Systematic review of methods to predict and detect anastomotic leakage in colorectal surgery. Colorectal Dis. 16: 95-109.

Hou Q, Ye L, Huang L, Yu Q (2017) The research progress on intestinal stem cells and its relationship with intestinal microbiota. Front Immunol. 8:599.

Hyman NH (2009) Managing anastomotic leaks from intestinal anastomoses. Surgeon. 7(1):31-35.

Hyoju SK, Klabbers RE, Aaron M, Krezalek MA, Zaborin A, Wiegerinck M, Hyman NH, Zaborina O, Van Goor H, Alverdy JC (2017) Oral polyphosphate suppresses bacterial collagenase production and prevents anastomotic leak due to Serratia marcescens and Pseudomonas aeruginosa. Ann Surg. Feb 3. Doi: 10.1097/SLA.0000000000002167.

Iakoubov R, Lauffer LM, Trivedi S, Kim YI, Brubaker PL (2009) Carcinogenic effects of exogenous and endogenous glucagon-like peptide-2 in azoxymethane-treated mice. Endocrinology. 150:4033-4043.

Iizuka M, Konno S (2011) Wound healing of intestinal epithelial cells. World J Gastroenterol. 17(17):2161-71.

Inglin RA, Baumann G, Wagner OJ, Candinas D, Egger B (2008) Insulin-like growth factor I improves aspects of mycophenolate mofetil-impaired anastomotic healing in an experimental model. Br J Surg. 95(6):793-798.

Ishii M, Tanaka E, Imaizumi T, Sugio Y, Sekka T, Tanaka M, Yasuda M, Fukuyama N, Shinozaki Y, Hyodo K, Tanioka K, Mochizuki R, Kawai T, Mori H, Makuuchi H (2009) Local VEGF administration enhances healing of colonic anastomoses in a rabbit model. Eur Surg Res. 42(4):249-257.

Ivory CP, Wallace LE, McCafferty DM, Sigalet DL (2008) Interleukin-10-independent anti-inflammatory actions of glucagon-like peptide 2. Am J Physiol Gastrointest Liver Physiol. 295:G1202-G1210.

Jacobson A, Cunningham JL (2012) Connective tissue growth factor in tumor pathogenesis. Fibrogenesis Tissue Repair. 5(Suppl 1 Proceedings of Fibroproliferative disorders: from biochemical analysis to targeted therapies Petro E Petrides and David Brenner):S8. eCollection 2012.

Jafari MD, Wexner SD, Martz JE, McLemore EC, Margolin DA, Sherwinter DA, Lee SW, Senagore AJ, Phelan MJ, Stamos MJ (2015) Perfusion assessment in laparoscopic left-sided/anterior resection (PILLAR II): A Multi-Institutional Study. J Am Coll Surg. 220:82-92.

Janssen P, Rotondo A, Mulé F, Tack J (2013) Review article: a comparison of glucagon-like peptides 1 and 2. Aliment Pharmacol Ther. 37:18–36.

Jongen AC, Bosmans JW, Kartal S, Lubbers T, Sosef M, Slooter GD, Stoot JH, van Schooten FJ, Bouvy ND, Derikx JP (2016) Predictive factors for anastomotic leakage after colorectal surgery: Study protocol for a prospective observational study (REVEAL Study). JMIR Res Protoc. 5(2):e90.

Juo Y-Y, Hyder O, Haider AH, Camp M, Lidor A, Ahuja N (2014) Is minimally invasive colon resection better than traditional approaches?: First comprehensive national examination with propensity score matching. JAMA Surg. 149(2):177-184.

Kaemmer DA, Otto J, Binneboesel M, Klink C, Krones C, Jansen M, Cloer C, Oettinger A, Schumpelick V, Klinge U (2010) Erythropoietin (EPO) influences colonic anastomotic healing in a rat model by modulating collagen metabolism. J Surg Res. 163:e67–e72.

Kaji T, Tanaka H, Holst JJ, Redstone H, Wallace L, de Heuval E, Sigalet DL (2008)The effects of variations in dose and method of administration on glucagon like pepti de-2 activity in the rat. Eur J Pharmacol. 596(1-3):138-45.

Kaji T, Tanaka H, Redstone H, Wallace LE, Holst JJ, Sigalet DL (2009) Temporal changes in the intestinal growth promoting effects of glucagon-like peptide 2 following intestinal resection. J Surg Res. 152(2):271-80

Kalyanaraman B, Darley-Usmar V, Davies KJA, Dennery PA, Forman HJ, Grisham MB, Mann GE, Moore K, Jackson Roberts II L, Ischiropoulos H (2012) Measuring reactive oxygen and nitrogen species with fluorescent probes: challenges and limitations. Free Radic Biol Med. 52(1):1-6.

Kannen V, Garcia SB, Stopper H, Waaga-Gasser AM (2013) Glucagon-like peptide 2 in colon carcinogenesis: possible target for anti-cancer therapy? Pharmacol Ther. 139:87-94.

Kar S, Mohapatra V, Singh S, Rath PK, Behera TR (2017) Single layered versus double layered intestinal anastomosis: A randomized controlled trial. J Clin Diagn Res. 11(6):PC01-PC04.

Karaman K, Bostanci EB, Dincer N, Ulas M, Ozer I, Dalgic T, Ercin U, Bilgihan A, Ginis Z, Akoglu M (2012) Effects of thyroid hormone supplementation on anastomotic healing after segmental colonic resection. J Surg Res. 176:460–467.

Karatepe O, Kurtulus I, Yalcin O, Battal M, Kamali G, Aydin T (2011) Adrenomedulline improves ischemic left colonic anastomotic healing in an experimental rodent model. Clinics (Sao Paulo). 66:1805-1810.

Karliczek A, Harlaar NJ, Zeebregts CJ, Wiggers T, Baas PC, van Dam GM (2009) Surgeons lack predictive accuracy for anastomotic leakage in gastrointestinal surgery. Int J Colorectal Dis. 24(5):569-76.

Kaux JF, Emonds-Alt T (2017) The use of platelet-rich plasma to treat chronic tendinopathies: A technical analysis. Platelets. Jul 31:1-15. doi: 10.1080/09537104.2017.1336211.

Kemper K, Prasetyanti PR, De Lau W, Rodermond H, Clevers H, Medema JP (2012) Monoclonal antibodies against Lgr5 identify human colorectal cancer stem cells. Stem Cells 30(11):2378-2386.

Keustermans GCE, Hoeks SBE, Meerding JM, Prakken BJ, Jager W (2013) Cytokine assays: An assessment of the preparation and treatment of blood and tissue samples. Methods. 61:10-17.

Kilkenny D, Browne WJ, Cuthill IC, Emerson M, Altman DG (2010a) Improving bioscience research reporting: the ARRIVE guidelines for reporting animal research. PLoS Biol. 8:e1000412.

Kilkenny C, Browne WJ, Emerson M, Altman DG (2010b) Animal research: Reporting in vivo experiments: The ARRIVE guidelines. Br J Pharmacol. 160:1577-1579.

Kim ES, Keam SJ (2017) Teduglutide: A Review in Short Bowel Syndrome. Drugs. 77:345-352.

Kim TH, Saadatpour A, Guo G, Saxena M, Cavazza A, Desai N, Jadhav U, Jiang L, Rivera MN, Orkin SH, Yuan GC, Shivdasani RA (2016) Single-cell transcript profiles reveal multilineage priming in early progenitors derived from Lgr5(+) intestinal stem cells. Cell Rep. 16(8):2053-60.

Kim WT, Ryu CJ (2017) Cancer stem cell surface markers on normal stem cells. BMB Rep. 50(6):285-298.

Kiran RP, Murray ACA, Chiuzan C, Estrada D, Forde K (2015) Combined preoperative mechanical bowel preparation with oral antibiotics significantly reduces surgical site

infection, anastomotic leak, and ileus after colorectal surgery. Ann Surg. 262(3): 416-25; discussion 423-5.

Kiziltan R, Yılmaz Ö, Çelik S, Yıldırm S, Alp HH, Aras A, Kotan Ç (2016) Effect of thymoquinone on the healing of left colon anastomosis: an experimental study. Springerplus. 2016;5(1):956.

Koehler JA, Harper W, Barnard M, Yusta B, Drucker DJ (2008) Glucagon-like peptide-2 does not modify the growth or survival of murine or human intestinal tumor cells. Cancer Res. 68:7897-7904.

Koller SE, Bauer KW, Egleston BL, Smith R, Philp MM, Ross HM, Esnaola NF (2017) Comparative Effectiveness and Risks of Bowel Preparation Before Elective Colorectal Surgery. Ann Surg. Feb 1. doi: 10.1097/SLA.0000000000002159.

Koo BK, Clevers H (2014) Stem cells marked by the R-spondin receptor LGR5. Gastroenterology. 147(2):289-302.

Koopmann MC, Liu X, Boehler CJ, Murali SG, Holst JJ, Ney DM (2009) Colonic GLP-2 is not sufficient to promote jejunal adaptation in a pn-dependent rat model of human short bowel syndrome. JPEN J Parenter Enteral Nutr. 33:629–639.

Kornmann V, van Ramshorst B, van Dieren S, van Geloven N, Boermeester M, Boerma D (2016) Early complication detection after colorectal surgery (CONDOR): study protocol for a prospective clinical diagnostic study. Int J Colorectal Dis. 31(2):459-64.

Kovalenko PL, Flanigan TL, Chaturvedi L, Basson MD (2012) Influence of defunctionalization and mechanical forces on intestinal epithelial wound healing. Am J Physiol Gastrointest Liver Physiol. 303(10):G1134-43.

Krarup PM, Eld M, Heinemeier K, Jorgensen LN, Hansen MB, Ågren MS (2013) Expression and inhibition of matrix metalloproteinase (MMP)-8, MMP-9 and MMP-12 in early colonic anastomotic repair. Int J Colorectal Dis. 28:1151–1159.

Krarup PM, Eld M, Jorgensen LN, Hansen MB, Ågren MS (2017) Selective matrix metalloproteinase inhibition increases breaking strength and reduces anastomotic leakage in experimentally obstructed colon. Int J Colorectal Dis. Jul 17. doi: 10.1007/s00384-017-2857-x.

Kroemer G, Galluzzi L, Vandenabeele P, Abrams J, Alnemri ES, Baehrecke EH, Blagosklonny MV, El-Deiry WS, Golstein P, Green DR, Hengartner M, Knight RA, Kumar S, Lipton SA, Malorni W, Nuñez G, Peter ME, Tschopp J, Yuan J, Piacentini M, Zhivotovsky B, Melino G;

Nomenclature Committee on Cell Death 2009 (2009) Classification of cell death: Recommendations of the Nomenclature Committee on Cell Death 2009. Cell Death Differ. 16(1):3-11.

Küper MA, Trütschel S, Weinreich J, Königsrainer A, Beckert S (2016) Growth hormone abolishes the negative effects of everolimus on intestinal wound healing. World J Gastroenterol. 22:4321-4329.

Latella G, Sferra R, Speca S, Vetuschi A, Gaudio E (2013) Can we prevent, reduce or reverse intestinal fibrosis in IBD? Eur Rev Med Pharmacol Sci. 17(10):1283-1304.

Lee SY, Kim CH, Kim YJ, Kim HR (2015) Impact of anal decompression on anastomotic leakage after low anterior resection for rectal cancer: a propensity score matching analysis. Langenbecks Arch Surg. 400(7):791-6.

Lei Q, Bi J, Wang X, Jiang T, Wu C, Tian F, Gao X, Wan X, Zheng H (2016) GLP-2 prevents intestinal mucosal atrophy and improves tissue antioxidant capacity in a mouse model of total parenteral nutrition. Nutrients. 8(1). pii: E33. doi: 10.3390/nu8010033.

Levin M, Udi Y, Solomonov I, Sagi I (2017) Next generation matrix metalloproteinase inhibitors - Novel strategies bring new prospects. Biochim Biophys Acta. Jun 19. pii: S0167-4889(17)30161-1. doi: 10.1016/j.bbamcr.2017.06.009.

Levin TG, Powell AE, Davies PS, Silk AD, Dismuke AD, Anderson EC, Swain JR, Wong MH (2010) Characterization of the intestinal cancer stem cell marker CD166 in the human and mouse gastrointestinal tract. Gastroenterology. 139(6):2072-2082.e5.

Li NN, Zhao WT, Wu XT (2016) Can a nickel-titanium memory-shape device serve as a substitute for the stapler in gastrointestinal anastomosis? A systematic review and meta-analysis. J Surg Res. 201(1):82-93.

Li P, Fang F, Cai J, Tang D, Li Q, Wang D (2013) Fast-track rehabilitation vs conventional care in laparoscopic colorectal resection for colorectal malignancy: A meta-analysis. World J Gastroenterol. 19(47): 9119-9126.

Lindberg G (2008) Basic physiology of motility, absorption and secretion. In: Langnas AN, Goulet O, Quiley EMM, Tappenden KA, editors. Intestinal failure: Diagnosis, management and transplantation. Oxford, UK: Blackwell Publishing, Ltd. pp. 20-32.

Liu J, Khalil RA (2017) Matrix metalloproteinase inhibitors as investigational and therapeutic tools in unrestrained tissue remodeling and pathological disorders. Prog Mol Biol Transl Sci. 148;355-420.

Liu Y, Yang Y, Liu H, Song Y, Jia X, Zhang X, Guo J (2012) [Preliminary study on mechanisms of granulocyte macrophage-colony stimulating factor in enhancing impaired colonic anastomotic healing in rats treated with intraperitoneal oxaliplatin]. Zhongguo Xiu Fu Chong Jian Wai Ke Za Zhi. 26:1232-1236.

Lloyd DAJ, Gabe SM (2008) Intestinal morphology, intestinal regeneration and the promise of tissue engineering. Pp 13-19. In Intestinal failure: Diagnosis, management and transplantation. Edited by Langnas AN, Goulet O, Quiley EMM, Tappenden KA; Blackwell Publishing, Ltd, Oxford, UK; ISBN 978-1-4051-4637-1.

Lopetuso LR, Chowdhry S, Pizarro TT (2013) Opposing functions of classic and novel IL-1 family members in gut health and disease. Front Immunol. 4:181.

Lu P, Struijs M-C, Mei J, Witte-Bouma J, Korteland-van Male AM, de Bruijn ACJM, van Goudoever JB, Renes IB (2013) Endoplasmic reticulum stress, unfolded protein response and altered T cell differentiation in necrotizing enterocolitis. PLoS ONE. 8(10): e78491.

Luján JJ, Németh ZH, Barratt-Stopper PA, Bustami R, Koshenkov VP, Rolandelli RH (2011) Factors influencing the outcome of intestinal anastomosis. Am Surg. 77(9):1169-1175.

Mall JW, Schwenk W, Philipp AW, Büttemeyer R, Pollmann C (2003) Intraperitoneal administration of the angiogenesis inhibitor thalidomide does not impair anastomotic healing following large bowel resection in a rabbit model. World J Surg. 27(10):1119-1123.

Mann A, Niekisch K, Schirmacher P, Blessing M (2006) Granulocyte-macrophage colony-stimulating factor is essential for normal wound healing. Journal of Investigative Dermatology Symposium Proceedings. 11:87-92.

Mann J, Mann DA (2013) Epigenetic regulation of wound healing and fibrosis. Curr Opin Rheumatol. 25:101-107.

Mantzoros I, Kanellos I, Angelopoulos S, Koliakos G, Pramateftakis MG, Kanellos D, Zacharakis E, Zaraboukas T, Betsis D (2006) The effect of insulin-like growth factor I on healing of colonic anastomoses in cortisone-treated rats. Dis Colon Rectum. 49:1431-1438.

Marathe CS, Rayner CK, Jones K, Horowitz M (2013) Glucagon-like peptides 1 and 2 in health and disease: A review. Peptides. 44:75-86.

Marinatou A, Theodoropoulos GE, Karanika S, Karantanos T, Siakavellas S, Spyropoulos BG, Toutouzas K, Zografos G (2014) Do anastomotic leaks impair postoperative health-related quality of life after rectal cancer surgery? A case-matched study. Dis Colon Rectum. 57(2):158-166.

Martí-Carvajal AJ, Gluud C, Nicola S, Simancas-Racines D, Reveiz L, Oliva P, Cedeño-Taborda J (2015) Growth factors for treating diabetic foot ulcers. Cochrane Database Syst Rev. Oct 28;(10):CD008548. doi: 10.1002/14651858.CD008548.pub2.

Martin GR, Wallace LE, Hartmann B, Holst JJ, Demchyshyn L, Toney K, Sigalet DL (2005) Nutrient-stimulated GLP-2 release and crypt cell proliferation in experimental short bowel syndrome. Am J Physiol Gastrointest Liver Physiol. 288:G431–G438.

Martin GR, Wallace LE, Sigalet DL (2004) Glucagon-like peptide-2 induces intestinal adaptation in parenterally fed rats with short bowel syndrome. Am J Physiol Gastrointest Liver Physiol. 286(6):G964-72.

Martinou JC, Youle RJ (2011) Mitochondria in apoptosis: bcl-2 family members and mitochondrial dynamics. Dev Cell. 21(1):92-101.

Masoomi H, Luo R, Mills S, Carmichael JC, Senagore AJ, Stamos MJ (2013) Compression anastomosis ring device in colorectal anastomosis: a review of 1,180 patients. Am J Surg. 205(4):447-451.

McDermott FD, Heeney A, Kelly ME, Steele RJ, Carlson GL, Winter DC (2015) Systematic review of pre-operative, intraoperative and postoperative risk factors for colorectal anastomotic leaks. Br J Surg. 102:462–479.

McGrath J, Drummond G, McLachlan E, Kilkenny C, Wainwright C (2010) Guidelines for reporting experiments involving animals: the ARRIVE guidelines. Br J Pharmacol. 160:1573–1576.

Menger MD, Vollmar B (2004) Surgical trauma: hyperinflammation versus immunosuppression? Langenbecks Arch Surg. 389(6):475-484.

Midura EF, Hanseman D, Davis BR, Atkinson SJ, Abbott DE, Shah SA, Paquette IM (2015) Risk factors and consequences of anastomotic leak after colectomy: a national analysis. Dis Colon Rectum. 58:333-338.

Mifflin RC, Pinchuk IV, Saada JI, Powell DW (2011) Intestinal myofibroblasts: targets for stem cell therapy. Am J Physiol Gastrointest Liver Physiol. 300(5):G684-96.

Migaly J, Lieberman J, Long W, Fisher C, Rolandelli RH (2004) Effect of adenoviral-mediated transfer of transforming growth factor-beta1 on colonic anastomotic healing. Dis Colon Rectum. 2004;47(10):1699-705.

Miller DL (1971) Rat small intestine: Development, composition and effects of perfusion. Digestive Diseases. 16:247-253.

Mizrahi I, Wexner SD (2017) Clinical role of fluorescence imaging in colorectal surgery - a review. Expert Rev Med Devices. 14(1):75-82.

Moraes VY, Lenza M, Tamaoki MJ, Faloppa F, Belloti JC (2014) Platelet-rich therapies for musculoskeletal soft tissue injuries. Cochrane Database Syst Rev. Apr 29;(4):CD010071. doi: 10.1002/14651858.CD010071.pub3.

Moran M, Ozmen MM, Duzgun AP, Gok R, Renda N, Seckin S, Coskun F (2007) The effect of erythropoietin on healing of obstructive vs nonobstructive left colonic anastomosis: an experimental study. World J Emerg Surg. 2007;2:13.

Morks AN, Havenga K, Ploeg RJ (2011) Can intraluminal devices prevent or reduce colorectal anastomotic leakage: A review. World J Gastroenterol. 17(40): 4461-4469.

Murakami M, Sato N, Sato N, Nakamura T, Masunaga H (2007) Changes in lymphocyte phenotypes and cytokine production by surgical stress in a rat small intestinal resection model. J Clin Biochem Nutr. 40:216–220.

Muto M, Kaji T, Mukai M, Nakame K, Yoshioka T, Tanimoto A, Matsufuji H (2013) Ghrelin and glucagon-like peptide-2 increase immediately following massive small bowel resection. Peptides. 43:160–166.

Naberhuis JK, Tappenden KA (2016) Teduglutide for safe reduction of parenteral nutrient and/or fluid requirements in adults: A systematic review. JPEN J Parenter Enteral Nutr. 40:1096-1105.

Nachiappan S, Askari A, Malietzis G, Giacometti M, White I, Jenkins JT, Kennedy RH, Faiz O (2015) The impact of anastomotic leak and its treatment on cancer recurrence and survival following elective colorectal cancer resection. World J Surg. 39(4): 1052–1058.

Naimi RM, Madsen KB, Askov-Hansen C, Brandt CF, Hartmann B, Holst JJ, Mortensen PB, Jeppesen PB (2013) A dose-equivalent comparison of the effects of continuous subcutaneous glucagon-like peptide 2 (GLP-2) infusions versus meal related GLP-2 injections in the treatment of short bowel syndrome (SBS) patients. Regulatory Peptides. 184:47–53.

Nakame K, Kaji T, Mukai M, Shinyama S, Matsufuji H (2016) The protective and anti-inflammatory effects of glucagon-like peptide-2 in an experimental rat model of necrotizing enterocolitis. Peptides. 75:1-7.

Nefzger CM, Jardé T, Rosselo FJ, Horvay K, Knaupp AS, Powel DR, Chen J, Abud HE, Polo JM (2016) A versatile strategy for isolation a highly enriched population of intestinal stem cells. Stem Cell Reports. 6:321-329.

Nasiri S, Mirminachi B, Taherimehr R, Shadbakhsh R, Hojat M (2017) The effect of omentoplasty on the rate of anastomotic leakage after intestinal resection: A randomized controlled trial. Am Surg. 83(2):157-161.

Nerstrøm M, Krarup PM, Jorgensen LN, Ågren MS (2016) Therapeutic improvement of colonic anastomotic healing under complicated conditions: A systematic review. World J Gastrointest Surg. 8:389-401.

Neutzling CB, Lustosa SA, Proenca IM, da Silva EM, Matos D (2012) Stapled versus handsewn methods for colorectal anastomosis surgery. Cochrane Database Syst Rev. Feb 15;(2):CD003144.

Nikolian VC, Kamdar NS, Regenbogen SE, Morris AM, Byrn JC, Suwanabol PA, Campbell DA, Hendren S (2017) Anastomotic leak after colorectal resection: A population-based study of risk factors and hospital variation. Surgery 161:1619-27.

Nolan T, Hands RE, Bustin SA (2006) Quantification of mRNA using real-time RT-PCR. Nat Protoc. 1(3):1559-82.

Nordentoft T, Pommergaard HC, Rosenberg J, Achiam MP (2015) Fibrin glue does not improve healing of gastrointestinal anastomoses: A systematic review. Eur Surg Res. 54:1–13.

O'Connor JE, Kimler BF, Morgan MC, Tempas KJ (1988) A flow cytometric assay for intracellular nonprotein thiols using mercury orange. Cytometry. 9(6):529–532.

O'Mahony L (2008) Immunology of the small intestine. In: Langnas AN, Goulet O, Quiley EMM, Tappenden KA, editors. Intestinal failure: Diagnosis, management and transplantation. Oxford, UK: Blackwell Publishing, Ltd; pp. 33-44.

Oines MN, Krarup P, Jorgensen LN, Agren MS (2014) Pharmacological interventions for improved colonic anastomotic healing: A meta-analysis. World J Gastroenterol 20(35):12637-12648.

Ozdogan M, Oruk I, Renda N, Kaynaroglu V, Baykal A (2005) The effect of exogenous melatonin on experimental colonic anastomosis. Acta Chir Belg. 105:302–305.

Ozel Turkcu U, Cakmak GK, Demir EO, Bakkal H, Oner MO, Okyay RD, Bassorgun IC, Ciftcioglu MA (2012) The effect of erythropoietin on anastomotic healing of irradiated rats. J Invest Surg. 25:127-135.

Ozen IO, Ekingen G, Taşlipinar MY, Bukan N, Demiroğullari B, Karabulut R, Sönmez K, Başaklar AC, Kale N (2007) Effect of melatonin on healing of colonic anastomosis in a rat model of peritonitis. Eur Surg Res. 39:122-127.

Palmer SC, Saglimbene V, Mavridis D, Salanti G, Craig JC, Tonelli M, Wiebe N, Strippoli GF (2014) Erythropoiesis-stimulating agents for anaemia in adults with chronic kidney disease: a network meta-analysis. Cochrane Database Syst Rev. Dec 8;(12):CD010590. doi: 10.1002/14651858.CD010590.pub2.

Parry L, Young M, El Marjou F, Clarke AR (2013) Evidence for a crucial role of paneth cells in mediating the intestinal response to injury. Stem Cells. 31(4):776-785.

Parthasarathy M, Greensmith M, Bowers D, Groot-Wassink T (2016) Risk factors for anastomotic leakage after colorectal resection: a retrospective analysis of 17 518 patients. Colorectal Disease. 19:288-298.

Pasternak B, Matthiessen P, Jansson K, Andersson M, Aspenberg P (2010) Elevated intraperitoneal matrix metalloproteinases-8 and -9 in patients who develop anastomotic leakage after rectal cancer surgery: a pilot study. Colorectal Dis. 12(7 Online):e93-8.

Pavlovic V, Ciric M, Jovanovic V, Stojanovic P (2016) Platelet Rich Plasma: a short overview of certain bioactive components. Open Med (Wars). 11:242-247.

Pénzes L, Skála I (1977) Changes in the mucosal surface area of small gut of rats of different ages. J Anat. 124(Pt 1):217-222.

Pfaffl MW (2004) Quantification strategies in real-time PCR. In A-Z of quantitative PCR (Editor: S.A. Bustin); International University Line (IUL); La Jolla, CA, USA; 87-112

Pfeifle VA, Gros SJ, Frongia G, Schäfer KH, Holland-Cunz S (2017) Regenerative capacity of the enteric nervous system after ileoileal anastomoses in a rat model. Eur J Pediatr Surg. 27(2):200-205.

Phoenix Europe GmbH (2017) Protocol for Catalog #EK-028-14 [Arg34]-GLP-2 (human, rat) EIA Kit. www.phoenixbiotech.net/catalog/repository/EIA/EK_028_14.pdf. Assessed in May 13th, 2017.

Pironi L, Arends J, Bozzetti F, Cuerda C, Lyn Gillanders L, Jeppesen PB, Joly F, Kelly D, Lal S, Staun M, Szczepanek K, van Gossun A, Wanten G, Schneider SM; Home Artificial Nutrition

& Chronic Intestinal Failure Special Interest Group of ESPEN (2016) ESPEN guidelines on chronic intestinal failure in adults. Clin Nutr. 35:247-307.

Piscaglia AC (2014) Intestinal stem cells and celiac disease. World J Stem Cells. 6(2):213-229.

Pommergaard HC, Gessler B, Burcharth J, Angenete E, Haglind E, Rosenberg J (2014) Preoperative risk factors for anastomotic leakage after resection for colorectal cancer: a systematic review and metaanalysis. Colorectal Dis. 16(9):662-671.

Pommergaard HC, Achiam MP, Rosenberg J (2012) External coating of colonic anastomoses: a systematic review. Int J Colorectal Dis. 27(10):1247-1258.

Pommergaard HC, Rosenberg J, Schumacher-Petersen C, Achiam MP (2011) Choosing the best animal species to mimic clinical colon anastomotic leakage in humans: a qualitative systematic review. Eur Surg Res. 47(3):173-81.

Poyrazoglu Y, Yigit T, Harlak A, Mentes O, Gorgulu S, Uzar AI, Kozak O (2011) Effects of prevention of oxidative and nitro-oxidative stress on experimental rat colon anastomosis using acetylcysteine, ebselen and 1400w. Acta Chir Belg. 111(1):26-31.

Qi KK, Lv JJ, Wu J, Xu ZW (2017) Therapeutic effects of different doses of polyethylene glycosylated porcine glucagon-like peptide-2 on ulcerative colitis in male rats. BMC Gastroenterol. 17(1):34.

Qu H, Liu Y, Bi DS (2015) Clinical risk factors for anastomotic leakage after laparoscopic anterior resection for rectal cancer: a systematic review and meta-analysis. Surg Endosc. 29(12):3608-3617.

Radulescu A, Zhang HY, Chen CL, Chen Y, Zhou Y, Yu X, Otabor I, Olson JK, Besner GE (2011) Heparin-binding EGF-like growth factor promotes intestinal anastomotic healing. J Surg Res. 171(2):540-550.

Rajasekhar VK, Begemann M (2007) Concise review: Roles of polycomb group proteins in development and disease: A stem cell perspective. Stem Cells. 25:2498-2510.

Ramirez MF, Huitink JM, Cata JP (2013) Perioperative Clinical Interventions That Modify the Immune Response in Cancer Patients. Open Journal of Anesthesiology. 3:133-139.

Ravi A, Garg P, Sitaraman SV (2007) Matrix metalloproteinases in inflammatory bowel disease: boon or a bane? Inflamm Bowel Dis. 13(1):97-107.

Redstone HA, Buie WD, Hart DA, Wallace L, Hornby PJ, Sague S, Holst JJ, Sigalet DL (2010) The effect of glucagon-like Peptide-2 receptor agonists on colonic anastomotic wound healing. Gastroenterol Res Pract. 2010. pii:672453. doi: 10.1155/2010/672453.

Rehn M, Krarup PM, Christensen LH, Seidelin JB, Ågren MS, Syk I (2015) GM6001 increases anastomotic leakage following colonic obstruction possibly by impeding epithelialization. Surg Infect (Larchmt). 16(6):702-8.

Reichelt WN, Waldschitz D, Herwig C, Neutsch L (2016) Bioprocess monitoring: minimizing sample matrix effects for total protein quantification with bicinchoninic acid assay. J Ind Microbiol Biotechnol 2016;43:1271–1280.

Reisinger KW, Poeze M, Hulsewé KW, van Acker BA, van Bijnen AA, Hoofwijk AG, Stoot JH, Derikx JP (2014) Accurate prediction of anastomotic leakage after colorectal surgery using plasma markers for intestinal damage and inflammation. J Am Coll Surg. 219(4):744-51.

Rekhtman N, Bishop JA (2011) Quick reference handbook for surgical pathologists. Berlin Heidelberg: Springer-Verlag; 2011.

Rencuzogullari A, Benlice C, Valente M, Abbas MA, Remzi FH, Gorgun E (2017) Predictors of anastomotic leak in elderly patients after colectomy: Nomogram-based assessment from the american college of surgeons national surgical quality program procedure-targeted cohort. Dis Colon Rectum. 60(5):527-536.

Rho CR, Park MY, Kang S (2015) Effects of granulocyte-macrophage colony-stimulating (GM-CSF) factor on corneal epithelial cells in corneal wound healing model. PLoS One. 10:e0138020.

Ricard-Blum S, Ruggiero F (2005) The collagen superfamily: from the extracellular matrix to the cell membrane. Pathol Biol (Paris). 2005;53(7):430-442.

Rijcken E, Sachs L, Fuchs T, Spiegel HU, Neumann PA (2014) Growth factors and gastrointestinal anastomotic healing. J Surg Res. 187(1):202-210.

Rijcken E, Fuchs T, Sachs L, Kersting CM, Bruewer M, Krieglstein CF (2010) Insulin-like growth factor 1-coated sutures improve anastomotic healing in an experimental model of colitis. Br J Surg. 97(2):258-65.

Rizk P, Barker N (2012) Gut stem cells in tissue renewal and disease: methods, markers, and myths. Wiley Interdiscip Rev Syst Biol Med. 4(5):475-496.

Rojas-Machado SA, Romero-Simó M, Arroyo A, Rojas-Machado A, López J, Calpena R (2012) Prediction of anastomotic leak in colorectal cancer surgery based on a new prognostic index PROCOLE (prognostic colorectal leakage) developed from the meta-analysis of observational studies of risk factors. Int J Colorectal Dis. 31:197-210.

Roos D, Dijksman LM, Tijssen JG, Gouma DJ, Gerhards MF, Oudemans-van Straaten HM (2013) Systematic review of perioperative selective decontamination of the digestive tract in elective gastrointestinal surgery. Br J Surg. 100(12):1579–88.

Rosenbloom AL (2009) Mecasermin (recombinant human insulin-like growth factor I). Adv Ther. 26(1):40-54.

Roth S, Franken P, Sacchetti A, Kremer A, Anderson K, Sansom O, Fodde R (2012) Paneth cells in intestinal homeostasis and tissue injury. PLoS One. 7(6):e38965.

Roulis M, Flavell RA (2016) Fibroblasts and myofibroblasts of the intestinal lamina propria in physiology and disease. Differentiation. 92(3):116-131.

Rowland KJ, Brubaker PL: The "cryptic" mechanism of action of glucagon-like peptide-2. Am J Physiol Gastrointest Liver Physiol. 2011;301(1):G1-8. doi: 10.1152/ajpgi.00039.2011.

Sakallioglu AE, Yagmurlu A, Dindar H, Hasirci N, Renda N, Deveci MS (2004) Sustained local application of low-dose epidermal growth factor on steroid-inhibited colonic wound healing. J Pediatr Surg. 39(4):591-595.

Sammour T, Lewis M, Thomas ML, Lawrence MJ, Hunter A, Moore JW (2017) A simple web-based risk calculator (www.anastomoticleak.com) is superior to the surgeon's estimate of anastomotic leak after colon cancer resection. Tech Coloproctol. 21:35–41.

Sammour T, Singh PP, Zargar-Shoshtari K, Su'a B, Hill AG (2016) peritoneal cytokine levels can predict anastomotic leak on the first postoperative day. Dis Colon Rectum. 59(6):551-6.

Sandler NG, Mentink-Kane MM, Cheever AW, Wynn TA (2003) Global gene expression profiles during acute pathogen-induced pulmonary inflammation reveal divergent roles for Th1 and Th2 responses in tissue repair. J Immunol. 171:3655–3667.

Sangiorgi E, Capecchi MR (2008) Bmi1 is expressed in vivo in intestinal stem cells. Nat Genet. 40(7):915-20.

Sapan CV, Lundblad RL, Price NC (1999) Colorimetric protein assay techniques. Biotechnol Appl Biochem. 29 (Pt 2):99-108.

Saribeyoğlu K, Baca B, Hamzaoğlu I, Pekmezci S, Karahasanoğlu T, Hamzaoğlu H (2003) Does becaplermin (platelet-derived growth factor-BB) reverse detrimental effects of ischemia on colonic anastomosis? Dis Colon Rectum. 46:516–520.

Sato T, van Es JH, Snippert HJ, Stange DE, Vries RG, van den Born M, Barker N, Shroyer NF, van de Wetering M, Clevers H (2011) Paneth cells constitute the niche for Lgr5 stem cells in intestinal crypts. Nature. 469(7330):415-418.

Sato T, Vries RG, Snippert HJ, van de Wetering M, Barker N, Stange DE, van Es JH, Abo A, Kujala P, Peters PJ, Clevers H (2009) Single Lgr5 stem cells build crypt-villus structures in vitro without a mesenchymal niche. Nature. 459(7244):262-5.

Saxena R (2010) Special stains in interpretation of liver biopsies. Technical Articles. Connection:92–103. https://pt.scribd.com/document/171923166/28829-2010-Conn14-Special-Stains-Interpretation-Liver-Biopsies-Saxena. Assessed in 6 April 2017.

Scarborough JE, Mantyh CR, Sun Z, Migaly J (2015) Combined mechanical and oral antibiotic bowel preparation reduces incisional surgical site infection and anastomotic leak rates after elective colorectal resection. Ann Surg. 262(2):331-337.

Scarborough JE, Schumacher J, Kent KC, Heise CP, Greenberg CC (2017) Associations of specific postoperative complications with outcomes after elective colon resection: A procedure-targeted approach toward surgical quality improvement. JAMA Surg. 152(2):e164681.

Schwartz LK, O'Keefe SJD, Fujioka K, Gabe SM, Lamprecht G, Pape UF, Li B, Youssef NN, Jeppesen PB (2016) Long-term teduglutide for the treatment of patients with intestinal failure associated with short bowel syndrome. Clin Transl Gastroenterol. 7:e142.

Seifert GS, Seifert M, Kulemann B, Holzner PA, Glatz T, Timme S, Sick O, Höppner J, Hopt UT, Marjanovic G (2014) Searching for the molecular benchmark of physiological intestinal anastomotic healing in rats: An experimental study. Eur Surg Res. 53:73-85.

Şenocak R, Özer MT, Kaymak Ş, Kılbaş Z, Günal A, Uyanık M, Kozak O (2017) Can human recombinant epidermal growth factor improve ischemia and induce healing of anastomosis in an experimental study in a rabbit model? J Invest Surg. 30:101-109.

Sgonc R, Gruber J (1998) Apoptosis detection: an overview. Experimental Gerontology. 33(6):525–533.

Shakhsheer BA, Lec B, Zaborin A, Guyton K, Defnet AM, Bagrodia N, Kandel JJ, Zaborina O, Hernandez SL, Alverdy J: Lack of evidence for tissue hypoxia as a contributing factor in

anastomotic leak following colon anastomosis and segmental devascularization in rats. Int J Colorectal Dis. 2017;32:539–547.

Shogan BD, Smith DP, Christley S, Gilbert JA, Zaborina O, Alverdy JC (2014) Intestinal anastomotic injury alters spatially defined microbiome composition and function. Microbiome. 2:35-45.

Shogan BD, Carlisle EM, Alverdy JC, Umanskiy K (2013) Do we really know why colorectal anastomoses leak? J Gastrointest Surg. 17(9):1698-1707.

Sigalet DL, Wallace LE, Holst JJ, Martin GR, Kaji T, Tanaka H, Sharkey KA (2007) Enteric neural pathways mediate the anti-inflammatory actions of glucagon-like peptide 2. Am J Physiol Gastrointest Liver Physiol. 293(1):G211–21.

Silva SM, Jerônimo MS, Silva-Pereira I, Bocca AL, Sousa JB (2014) Effects of bromopride on expression of metalloproteinases and interleukins in left colonic anastomoses: an experimental study. Braz J Med Biol Res. 2014;47(10):911-6.

Singh PP, Zeng IS, Srinivasa S, Lemanu DP, Connolly AB, Hill AG (2014) Systematic review and meta-analysis of use of serum C-reactive protein levels to predict anastomotic leak after colorectal surgery. Br J Surg. 2014;101(4):339-346.

Sipahi M, Zengin K, Tanik S, Arslan E, Çubukçu A (2014) Effects of circadian rhythm disorders on wound healing and strength of bowel anastomosis in rats. Wounds. 26(11):317-22.

Sipos F, Muzes G (2017) Teduglutide-induced stem cell function in intestinal repair. J Invest Surg. 0:1-3.

Slesser AA, Pellino G, Shariq O, Cocker D, Kontovounisios C, Rasheed S, Tekkis PP (2016) Compression versus hand-sewn and stapled anastomosis in colorectal surgery: a systematic review and meta-analysis of randomized controlled trials. Tech Coloproctol. 20(10):667-676.

Slieker JC, Daams F, Mulder IM, Jeekel J, Lange JF (2013) Systematic review of the technique of colorectal anastomosis. JAMA Surg. 148(2):190-201.

Smith NR, Davies PS, Silk AD, Wong MH (2012) Epithelial and mesenchymal contribution to the niche: a safeguard for intestinal stem cell homeostasis. Gastroenterology. 143(6):1426-1430.

Smith PK, Krohn RI, Hermanson GT, Mallia AK, Gartner FH, Provenzano MD, Fujimoto EK, Goeke NM, Olson BJ, Klenk DC (1985) Measurement of protein using bicinchoninic acid. Anal Biochem. 150(1):76-85.

Smith SA, Roberts DJ, Lipson ME, Buie WD, MacLean AR (2016) Postoperative nonsteroidal anti-inflammatory drug use and intestinal anastomotic dehiscence: A systematic review and meta-analysis. Dis Colon Rectum. 59(11):1087-1097.

Smith RJ, Rao-Bhatia A, Kim TH (2017) Signaling and epigenetic mechanisms of intestinal stem cells and progenitors: insight into crypt homeostasis, plasticity, and niches. Wiley Interdiscip Rev Dev Biol. 6(5). doi: 10.1002/wdev.281.

Son KH, Jeong HW, Jung WW, Kim HS, Lee SK, Kim KT, Ahn CB, Park KY, Kim BM, Lee SH (2014) The use of collagen content as determined by spectral domain polarization-sensitive optical coherence tomography to assess colon anastomosis healing in a rat model. Eur Surg Res. 52(1-2):32-40.

Sozutek A, Colak T, Cetinkunar S, Reyhan E, Irkorucu O, Polat G, Cennet A (2016) The Effect of Platelet-Rich-Plasma on the Healing of Left Colonic Anastomosis in a Rat Model of Intra-Abdominal Sepsis. J Invest Surg. 29:294-301.

Sparreboom CL, Wu ZQ, Ji JF, Lange JF (2016a) Integrated approach to colorectal anastomotic leakage: Communication, infection and healing disturbances. World J Gastroenterol. 22(32):7226-7235.

Sparreboom CL, Wu Z, Dereci A, Boersema GS, Menon AG, Ji J, Kleinrensink GJ, Lange JF (2016b) Cytokines as Early Markers of Colorectal Anastomotic Leakage: A Systematic review and Meta-Analysis. Gastroenterol Res Pract. 2016;2016:3786418. doi: 10.1155/2016/3786418.

Speca S, Giusti I, Rieder F, Latella G (2012) Cellular and molecular mechanisms of intestinal fibrosis. World J Gastroenterol. 18(28):3635-3661.

Stergios K, Kontzoglou k, Pergialiotis V, Korou LM, Frountzas M, Lalude O, Nikiteas N, Perrea DN (2017) The potential effect of biological sealants on colorectal anastomosis healing in experimental research involving severe diabetes. Ann E Coll Surg Engl. 99(3):189-192.

Strup-Perrot C, Mathé D, Linard C, Violot D, Milliat F, François A, Bourhis J, Vozenin-Brotons MC (2004) Global gene expression profiles reveal an increase in mRNA levels of collagens, MMPs, and TIMPs in late radiation enteritis. Am J Physiol Gastrointest Liver Physiol. 287(4):G875-85.

Stumpf M, Klinge U, Wilms A, Zabrocki R, Rosch R, Junge K, Krones C, Schumpelick V (2005) Changes of the extracellular matrix as a risk factor for anastomotic leakage after large bowel surgery. Surgery. 137(2):229-34.

Su'a BU, Mikaere HL, Rahiri JL, Bissett IB, Hill AG (2017) Systematic review of the role of biomarkers in diagnosing anastomotic leakage following colorectal surgery. Br J Surg. 104:503-512.

Sueyoshi R, Ralls MW, Teitelbaum DH (2013) Glucagon like peptide 2 increases efficacy of distraction enterogenesis. J Surg Res. 184(1):365-73.

Tabola R, Cirocchi R, Fingerhut A, Arezzo A, Randolph J, Grassi V, Binda GA, D'Andrea V, Abraha I, Popivanov G, Di Saverio S, Zbar A (2017) A systematic analysis of controlled clinical trials using the NiTi CAR™ compression ring in colorectal anastomoses. Tech Coloproctol. 21(3):177-184.

Takeda N, Jain R, LeBoeuf MR, Wang Q, Lu MM, Epstein JA (2011) Interconversion Between Intestinal Stem Cell Populations in Distinct Niches. Science. 334:1420-1424.

Tappenden KA (2014) Intestinal Adaptation Following Resection. JPEN J Parenter Enteral Nutr. 38(1 Suppl):23S-31S.

Tasdelen A, Algin C, Ates E, Kiper H, Inal M, Sahin F (2004) Effect of leptin on healing of colonic anastomoses in rats. Hepatogastroenterology. 51:994–997.

Tei TM, Kissmeyer-Nielsen P, Flyvbjerg A, Christensen H (2006) Growth hormone is a stimulating but not an essential factor in healing of colon. A study in GH-deficient dwarf rats. Scand J Surg. 95:205-210.

Teke Z, Bostanci EB, Yenisey C, Kelten EC, Sacar M, Simsek NG, Duzcan SE, Akoglu M (2013) Caffeic acid phenethyl ester prevents detrimental effects of remote ischemia reperfusion injury on healing of colonic anastomoses. J Invest Surg. 26(1):16-29.

Theocharis AD, Skandalis SS, Gialeli C, Karamanos Nk (2016) Extracellular matrix structure. Advanced Drug Delivery Reviews. 97:4-27.

Tesori V, Puglisi MA, Lattanzi W, Gasbarrini GB, Gasbarrini A (2013) Update on small intestinal stem cells. World J Gastroenterol. 19(29):4671-4678.

Tetteh PW, Basak O, Farin HF, Wiebrands K, Kretzschmar K, Begthel H, van den Born M, Korving J, de Sauvage F, van Es JH, van Oudenaarden A, Clevers H (2016) Replacement of lost lgr5-positive stem cells through plasticity of their enterocyte-lineage daughters. Cell Stem Cell. 18(2):203-13.

Thompson SK, Chang EY, Jobe BA (2006) Clinical review: Healing in gastrointestinal anastomoses, Part I. Microsurgery. 2006;26:131-136.

Thulesen J, Hartmann B, Hare KJ, Kissow H, Ørskov C, Holst JJ, Poulsen SS (2004) Glucagon-like peptide 2 (GLP-2) accelerates the growth of colonic neoplasms in mice. Gut. 53:1145-1150.

Tian H, Biehs B, Warming S, Leong KG, Rangell L, Klein OD, de Sauvage FJ (2011) A reserve stem cell population in small intestine renders Lgr5-positive cells dispensable. Nature. 478(7368):255-9.

Tighe P, Negm O, Todd I, Fairclough L: Utility, reliability and reproducibility of immunoassay multiplex kits. Methods. 2013; 61:23–29.

Tomlinson MJ, Tomlinson S, Yang XB and Kirkham J (2013) Cell separation: Terminology and practical considerations. J Tissue Eng. 4:2041731412472690.

Trencheva K, Morrissey KP, Wells M, Mancuso CA, Lee SW, Sonoda T, Michelassi F, Charlson ME, Milsom JW (2013) Identifying important predictors for anastomotic leak after colon and rectal resection: prospective study on 616 patients. Ann Surg. 257(1):108–113.

Trivedi S, Wiber SC, El-Zimaity HM, Brubaker PL (2012) Glucagon-like peptide-2 increases dysplasia in rodent models of colon cancer. Am J Physiol Gastrointest Liver Physiol. 302:G840-9.

Turrentine FE, Denlinger CE, Simpson VB, Robert A Garwood RA, Guerlain S, Agrawal A, Friel CM, LaPar DJ, Stukenborg GJ, Jones RS (2015) Morbidity, mortality, cost, and survival estimates of gastrointestinal anastomotic leaks. J Am Coll Surg. 220:195-206.

Vakalopoulos KA, Bosmans JWAM, van Barneveld KWY, Vogels RRM, Boersema GSA, Wu Z, Gijbels MJJ, Jeekel J, Kleinrensink G, Bouvy ND, Lange JF (2017) Impact of tissue adhesives on the prevention of anastomotic leakage of colonic anastomoses: an in vivo study. Int J Colorectal Dis. 32:961-965.

Vakalopoulos KA, Daams F, Wu Z, Timmermans L, Jeekel JJ, Kleinrensink GJ, van der Ham A, Lange JF (2013) Tissue adhesives in gastrointestinal anastomosis: a systematic review. J Surg Res 180(2):290-300.

Vallance A, Wexner S, Berho M, Cahill R, Coleman M, Haboubi N, Heald RJ, Kennedy RH, Moran B, Mortensen N, Motson RW, Novell R, O'Connell PR, Ris F, Rockall T, Senapati A, Windsor A, Jayne DG (2016) A collaborative review of the current concepts and challenges of anastomotic leaks in colorectal surgery. Colorectal Disease. 19:O1-12.

van Es JH, Sato T, van de Wetering M, Lyubimova A, Nee AN, Gregorieff A, Sasaki N, Zeinstra L, van den Born M, Korving J,Martens AC, Barker N, van Oudenaarden

A, Clevers H (2012) Dll1+ secretory progenitor cells revert to stem cells upon crypt damage. Nature Cell Biol. 14:1099–1104.

Van Landeghem L, Blue RE, Dehmer JJ, Henning SJ, Helmrath MA, Lund PKI (2012a) Localized intestinal radiation and liquid diet enhance survival and permit evaluation of long-term intestinal responses to high dose radiation in mice. PLoS One. 7(12): e51310.

Van Landeghem L, Santoro MA, Krebs AE, Mah AT, Dehmer JJ, Gracz AD, Scull BP, McNaughton K, Magness ST, Lund PK (2012b) Activation of two distinct Sox9-EGFP-expressing intestinal stem cell populations during crypt regeneration after irradiation. Am J Physiol Gastrointest Liver Physiol. 302(10):G1111-32.

Van Landeghem L, Santoro MA, Mah AT, Krebs AE, Dehmer JJ, McNaughton K, Helmrath MA, Magness ST, Lund PK (2015) IGF1 stimulates crypt expansion via differential activation of 2 intestinal stem cell populations. FASEB J. 29(7):2828-2842.

van Praagh JB, Goffau MC, Bakker IS, Harmsen HJM, Olinga P, Klaas Havenga K (2016) Intestinal microbiota and anastomotic leakage of stapled colorectal anastomoses: a pilot study. Surg Endosc. 30:2259-2265.

van Rooijen SJ, Huisman D, Stuijvenberg M, Stens J, Roumen RMH, Daams F, Slooter GD (2016) Intraoperative modifiable risk factors of colorectal anastomotic leakage: Why surgeons and anesthesiologists should act together. Int J Surg. 36:183e200.

Vanuytsel T, Senger S, Fasano A, Shea-Donohue T (2013) Major signaling pathways in intestinal stem cells. Biochim Biophys Acta. 1830(2):2410-2426.

Wallis K, Walters JR, Forbes A (2007) Review article: Glucagon-like peptide 2- current applications and future directions. Aliment Pharmacol Ther. 25(4):365-72.

Wang F, Scoville D, He XC, Mahe MM, Box A, Perry JM, Smith NR, Lei NY, Davies PS, Fuller MK, Haug JS, McClain M, Gracz AD, Ding S, Stelzner M, Dunn JC, Magness ST, Wong MH, Martin MG, Helmrath M, Li L (2013) Isolation and characterization of intestinal stem cells based on surface marker combinations and colony-formation assay. Gastroenterology. 145(2):383-95.e1-21.

Wang L, Fang F, Lu C, Wang D, Li P, Fu P (2014) Safety of fast-track rehabilitation after gastrointestinal surgery: Systematic review and meta-analysis. World J Gastroenterol. 20(41):15423-15439.

Wang S, Liu J, Wang S, Zhao H, Ge S, Wang W (2017) Adverse effects of anastomotic leakage on local recurrence and survival after curative anterior resection for rectal cancer: A systematic review and meta-analysis. World J Surg 41:277–284.

Wang P, Wang J, Zhang W, Li Y, Li J (2009) Effect of the combination of fibrin glue and growth hormone on intestinal anastomoses in a pig model of traumatic shock associated with peritonitis. World J Surg. 33:567-576.

Wiest R, Rath HC (2003) Gastrointestinal disorders of the critically ill. Bacterial translocation in the gut. Best Pract Res Clin Gastroenterol. 17(3):397-425.

Wu Z, Boersema GS, Kroese LF, Taha D, Vennix S, Bastiaansen-Jenniskens YM, Lam KH, Kleinrensink GJ, Jeekel J, Peppelenbosch M, Lange JF (2015) Reducing colorectal anastomotic leakage with tissue adhesive in experimental inflammatory bowel disease. Inflamm Bowel Dis. 21(5):1038-46.

Wu Z, Boersema GS, Vakalopoulos KA, Daams F, Sparreboom CL, Kleinrensink GJ, Jeekel J, Lange JF (2014) Critical analysis of cyanoacrylate in intestinal and colorectal anastomosis. J Biomed Mater Res B Appl Biomater. 102(3):635-42.

Yamaguchi R, Terashima H, Yoneyama S, Tadano S, Ohkohchi N (2012) Effects of platelet-rich plasma on intestinal anastomotic healing in rats: PRP concentration is a key factor. J Surg Res. 173:258-266.

Yan D, Liu S, Zhao X, Bian H, Yao X, Xing J, Sun W, Chen X (2017) Recombinant human granulocyte macrophage colony stimulating factor in deep second-degree burn wound healing. Medicine. 96:22(e6881).

Yan KS, Chia LA, Li X, Ootani A, Su J, Lee JY, Su N, Luo Y, Heilshorn SC, Amieva MR, Sangiorgi E, Capecchi MR, Kuo CJ (2012) The intestinal stem cell markers Bmi1 and Lgr5 identify two functionally distinct populations. Proc Natl Acad Sci U S A. 109(2):466-471.

Yang J, Su Y, Zhou Y, Besner GE (2014) Heparin-binding EGF-like growth factor (HB-EGF) therapy for intestinal injury: Application and future prospects. Pathophysiology. 21(1):95-104.

Yarimkaya A, Apaydin B, Unal E, Karabicak I, Aydogan F, Uslu E, Erginoz E, Artis T, Eyuboglu E (2003) Effects of recombinant human growth hormone and nandrolone phenylpropionate on the healing of ischemic colon anastomosis in rats. Dis Colon Rectum. 46:1690-1697.

Yauw STK, Wever KE, Hoesseini A, Ritskes-Hoitinga M, van Goor H (2015) Systematic review of experimental studies on intestinal anastomosis. Br J Surg. 102(7):726-734.

Yazbeck R, Howarth GS, Abbott CA (2009) Growth factor based therapies and intestinal disease: Is glucagon-like peptide-2 the new way forward? Cytokine Growth Factor Rev. 20(2):175-184.

Yildiz R, Can MF, Yagci G, Ozgurtas T, Guden M, Gamsizkan M, Ozturk E, Cetiner S: The effects of hyperbaric oxygen therapy on experimental colon anastomosis after preoper ative chemoradiotherapy. Int Surg. 2013;98(1):33-42.

Yilmaz ÖH, Katajisto P, Lamming DW, Gültekin Y, Bauer-Rowe KE, Sengupta S, Birsoy K, Dursun A, Yilmaz VO, Selig M, Nielson GP, Mino-Kenudson M, Zukerberg L, Bhan A, Deshpande V, Sabatini DM (2012) mTORC1 in the Paneth cell niche couples intestinal stem cell function to calorie intake. Nature. 28;486(7404):490–495.

Yol S, Tekin A, Yilmaz H, Küçükkartallar T, Esen H, Caglayan O, Tatkan Y (2008) Effects of platelet rich plasma on colonic anastomosis. J Surg Res. 146:190–194.

Zacharakis E, Demetriades H, Kanellos D, Sapidis N, Zacharakis E, Mantzoros I, Kanellos I, Koliakos G, Zaraboukas T, Topouridou K, Betsis D (2007) Contribution of insulin-like growth factor I to the healing of colonic anastomoses in rats. J Invest Surg. 20:9–14.

Zacharakis E, Demetriades H, Pramateftakis MG, Lambrou I, Zacharakis E, Zaraboukas T, Koliakos G, Kanellos I, Betsis D (2008) Effect of IGF-I on healing of colonic anastomoses in rats under 5-FU treatment. J Surg Res. 144:138-144.

Zhang YE (2018) Mechanistic insight into contextual TGF-β signaling. Curr Opin Cell Biol. 51:1-7.

Zhao WT, Li NN, He D, Feng JY (2017a) Transanal tube for the prevention of anastomotic leakage after rectal cancer surgery: A systematic review and meta-analysis. World J Surg. 41(1):267-276.

Zhao L, Zhou Y, Song C, Wang Z, Cuschieri A (2017b) Predicting burst pressure of radiofrequency-induced colorectal anastomosis by bio-impedance measurement. Physiol Meas. 38(3):489-500.

Zhou B, Ren J, Ding C, Wu Y, Chen J, Wang G, Gu G, Li J (2014) Protection of colonic anastomosis with platelet-rich plasma gel in the open abdomen. Injury. 45:864-868.

Zubaidi AM, Hussain T, Alzoghaibi MA (2015) The time course of cytokine expressions plays a determining role in faster healing of intestinal and colonic anastomatic wounds. Saudi J Gastroenterol. 21(6):412-7.

Zubaidi A, Buie WD, Hart DA, Sigalet D (2010) Temporal expression of cytokines in rat cutaneous, fascial and intestinal wounds: a comparative study. Dig Dis Sci. 55:1581-1588.

Supplementary data

Table S1. Search strategy for the literature review on growth factors and hormones as adjuvants of the intestinal anastomotic healing

Data	Description
Database	PubMed version of Medline database
Interval	From January 1, 2000 and to July 22, 2017
Search #1	(((surgical anastomosis[MeSH Terms] OR anastomo*[Title] OR anastomo*[Abstract]) AND (intestin*[Title] OR intestin*[Abstract] OR colon[Title] OR colon[Abstract] OR enteral[Title] OR enteral[Abstract] OR ileum[Title] OR ileum[Abstract] OR colon[Title] OR colon[Abstract] OR colorectal[Title] OR colorectal[Abstract] OR colonic[Title] OR colonic[Abstract] OR rectal[Title] OR rectal[Abstract] OR rectum[Title] OR rectum[Abstract] OR colon[MeSH Terms] OR ileum[MeSH Terms] OR rectum[MeSH Terms] OR intestines[MeSH Terms] OR colocolost*[Title] OR colo-colost*[Title] OR colocolost*[Abstract] OR colo-colost*[Abstract] OR anastomotic leak [MeSH Terms] OR wound healing[MeSH Terms])) AND (growth factor[Title] OR growth factor[Abstract] OR growth factors[Title] OR growth factors[Abstract]))
Search #2	(((surgical anastomosis[MeSH Terms] OR anastomo*[Title] OR anastomo*[Abstract]) AND (intestin*[Title] OR intestin*[Abstract] OR colon[Title] OR colon[Abstract] OR enteral[Title] OR enteral[Abstract] OR ileum[Title] OR ileum[Abstract] OR colon[Title] OR colon[Abstract] OR colorectal[Title] OR colorectal[Abstract] OR colonic[Title] OR colonic[Abstract] OR rectal[Title] OR rectal[Abstract] OR rectum[Title] OR rectum[Abstract] OR colon[MeSH Terms] OR ileum[MeSH Terms] OR rectum[MeSH Terms] OR intestines[MeSH Terms] OR colocolost*[Title] OR colo-colost*[Title] OR colocolost*[Abstract] OR colo-colost*[Abstract] OR anastomotic leak[MeSH Terms] OR wound healing[MeSH Terms])) AND (Glucagon-Like Peptide 2[MeSH Terms] OR Insulin-Like Growth Factor I[MeSH Terms] OR Insulin-Like Growth Factor II[MeSH Terms] OR Heparin-binding EGF-like Growth Factor[MeSH Terms] OR Fibroblast Growth Factor 1[MeSH Terms] OR Fibroblast Growth Factor 2[MeSH Terms] OR Platelet-Derived Growth Factor[MeSH Terms] OR Transforming Growth Factor beta[MeSH Terms] OR Vascular Endothelial Growth Factor A[MeSH Terms] OR Vascular Endothelial Growth Factor D[MeSH Terms] OR Vascular Endothelial Growth Factor C[MeSH Terms] OR Vascular Endothelial Growth Factor B[MeSH Terms] OR Fibroblast Growth Factor 7[MeSH Terms] OR Fibroblast Growth Factor 10[MeSH Terms] OR Platelet-Rich Plasma[MeSH Terms] OR Granulocyte-Macrophage Colony-Stimulating Factor[MeSH Terms]))

Referent to **Chapter 3:** *Response of putative intestinal epithelial stem cells to teduglutide on animal model of intestinal anastomosis*

Table S2. Characteristics of the putative intestinal epithelial stem cell surface markers used in the study[a]

Cell marker	Characteristics
Lgr5/Gpr49	Wnt/β-catenin-target gene that encodes a receptor for the wnt-agonists R-spondins. Specific marker of crypt base columnar intestinal stem cells.
Bmi1	Polycomb ring finger oncogene that encrypts a component of the polycomb repressive complex 1. Modulation of stem cells self-renewal, pluripotency and lineage specification in several tissues. Involvement in cancer initiation and progression and in embryonic development. Most widely recognized marker of "position +4" intestinal epithelial stem cells.
CD44	Class I transmembrane glycoprotein with several isoforms. Cell surface molecule whose role is primarily governed by various posttranslational modifications. Receptor for hyaluronic acid in the extracellular matrices. Induction of adhesion and migration. Ubiquitous expression in many normal cell types, including in most epithelial and lymphatic tissues; and, also, in human hematopoietic, mesenchymal and adipose-derived stem cells. No expression in undifferentiated human embryonic stem cells. Variant 9 emerged as marker of cancer stemness in a variety of solid tumors; other variants were suggested as cancer stem cell surface markers in several tumors (head and neck squamous cell, breast, colon, liver, ovarian, pancreas and gastric cancers).
CD24	35-60 kDa glycosyl phosphatidylinositol-linked sialoprotein. Role in cell-cell and cell-matrix interactions. Rare expression in normal tissues except B-cell precursors, neutrophils, neuronal cells, and certain epithelial cells. High expression in undifferentiated human embryonic stem cells. Cancer stem cell surface marker expressed in breast, gastric and pancreatic cell cancers.
CD166/Alcam	Type I membrane glycoprotein, which is a member of the immunoglobulin superfamily. Participates in cell-cell and cell-matrix interactions. Expression detected in many epithelial cells. Weak expression in undifferentiated human embryonic stem cells. Marker for human adipose-derived stromal stem cells and intestinal stem cells. Marker of colorectal cancer stem cells.
Grp78	Endoplasmic reticulum chaperone that assists proper protein conformation. Repressor of the unfolded protein response that plays an important role in the early regulation of intestinal stem cells differentiation. Marker of endoplasmic reticulum stress and activity of unfolded protein response that seems to be induced at the transition from stem cell to transit-amplifying cells in the beginning of the differentiation process.

Bmi1, Polycomb ring finger oncogene (B cell-specific Maloney murine leukemia virus integration region 1); CD24, Cluster of differentiation 24; CD44, Cluster of differentiation 44; CD166/Alcam, Cluster of differentiation 166/Activated leukocyte cell adhesion molecule; Grp78, 78 KDa glucose-regulated protein; Lgr5, Leucine-rich repeat-containing G-protein coupled receptor/G protein-coupled receptor 49; Wnt, wingless. [a] Data from references Kim and Ryu, 2017; Barker, 2014; Clevers *et al.*, 2013; Wang *et al.*, 2013; Barker *et al.*, 2012; Levin *et al.*, 2010; Rajasekhar *et al.*, 2007

Table S3. Monoclonal antibodies used in the characterization of rats' small intestine cells by flow cytometry

Purpose	Antibody name	Manufacturer
Lgr5 (Gpr49)	Anti-Gpr49/Lgr5 (Alexa Fluor 488)	Antibodies-online
Bmi1	Bmi1 Polycomb Ring Finger Oncogene antibody	Antibodies-online
Secondary antibody	Rabbit F(ab')2 anti-goat IgG H&L (Phycoerythrin)	Abcam
CD45 (LCA)	PerCP/Cy5.5 anti-rat CD45	Biolegend
CD31 (Pecam-1)	Mouse anti-rat CD31 (Alexa Fluor 647)	AbD Serotec
Desmin	Anti-desmin (Alexa Fluor 488)	Antibodies-online
CK18	Anti-cytokeratin 18 (RGE53PE)	Santa Cruz Antibodies
α-Sma	Anti-alfa-smooth muscle actin (EPR5368)	Abcam
Secondary antibody	Goat anti-rabbit IgG-PerCP-Cy5.5	Santa Cruz Antibodies
Vimentin	Vimentin (D21H3) XP Rabbit mAb (Alexa Fluor 647 Conjugate)	Cell Signaling Technology
Grp78	Anti-Grp78 (10C3) antibody (DyLight 488)	Abcam
CD166 (Alcam)	Mouse/rat Alcam/CD166 antibody	R&D Systems
Secondary antibody	Rabbit F(ab')2 anti-goat IgG H&L (Phycoerythrin)	Abcam
CD24	PerCP/Cy5.5 anti-mouse CD24	BioLegend
CD44	APC anti-mouse/human CD44	BioLegend

α-Sma, α-smooth muscle actin; APC, Allophycocyanin; Bmi1, Polycomb ring finger oncogene (B-cell-specific Moloney murine leukemia virus insertion site 1); CK18, Cytokeratin 18; CD24, Cluster of differentiation 24; CD31, Cluster of differentiation 31; CD44, Cluster of differentiation 44; CD45, Cluster of differentiation 45; CD166, Cluster of differentiation 166; Grp78, 78 KDa glucose-regulated protein; LCA, Leukocyte common antigen; Lgr5, Leucine-rich repeat-containing G-protein coupled receptor 5; PE, Phycoerythrin; PerCP-Cy5.5, Peridinin cholorophyll protein complex with cyanin-5.5

Table S4. Distribution of the antibodies used in the characterization of rats' small intestine cells by flow cytometry

Detection channel	Vial 1	Vial 2	Vial 3
FL 1	Anti-Lgr5	Anti-desmin	Anti-Grp78
FL 2	Anti-Bmi1+Rabbit anti-goat IgG PE	Anti-CK18	Anti-CD166+Rabbit anti-goat IgG PE
FL 3	Anti-CD45	Anti-α-Sma+Goat anti-rabbit IgG-PerCP-Cy5.5	Anti-CD24
FL 4	Anti-CD31	Anti-vimentin	Anti-CD44

α-Sma, α-smooth muscle actin; Bmi1, Polycomb ring finger oncogene (B-cell-specific Moloney murine leukemia virus insertion site 1); CK18, Cytokeratin 18; CD24, Cluster of differentiation 24; CD31, Cluster of differentiation 31; CD44, Cluster of differentiation 44; CD45, Cluster of differentiation 45; CD166, Cluster of differentiation 166; FL, Fluorescence detector; Grp78, 78 KDa glucose-regulated protein; Lgr5, Leucine-rich repeat-containing G-protein coupled receptor 5; PE, Phycoerythrin; PerCP-Cy5.5, Peridinin cholorophyll protein complex with cyanin-5.5

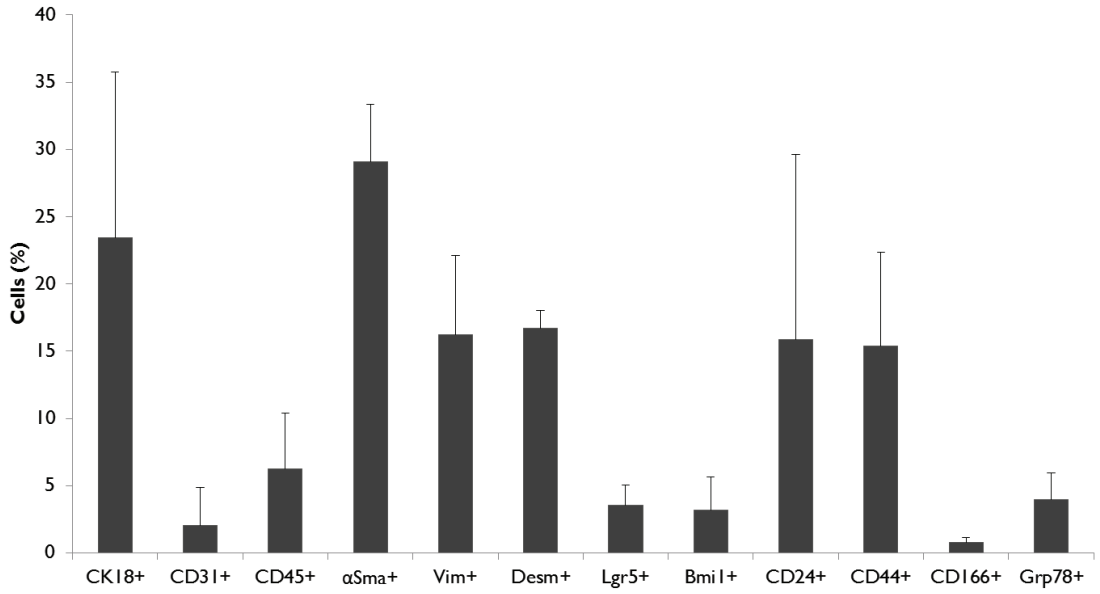

Figure S1. Flow cytometry expression profile of cells isolated from rats' ileum at the baseline (*n*=28). Results were presented in percentage (%) of cells expressing the specific marker and corresponded to the median (±interquartile range). α-Sma, α-smooth muscle actin; Bmi1, Polycomb ring finger oncogene (B-cell-specific Moloney murine leukemia virus insertion site 1); CK18, Cytokeratin 18; CD24, Cluster of differentiation 24; CD31, Cluster of differentiation 31; CD44, Cluster of differentiation 44; CD45, Cluster of differentiation 45; CD166, Cluster of differentiation 166; Desm, Desmin; Grp78, 78 KDa glucose-regulated protein; Lgr5, Leucine-rich repeat-containing G-protein coupled receptor 5; Vim, Vimentin

Referent to **Chapter 5:** *Effects of the perioperative administration of teduglutide on the cellular viability and death, oxidative stress and inflammatory response*

S1. Determination of cytokines concentrations in the rats' homogenized intestinal tissue and in the plasma

Expression of inflammatory cytokines was performed by multiplex cytokine bead array approach, using the Rat Cytokine 5plex Kit FlowCytomix (eBioscience, Affymetrix, Vienna, Austria) produced for quantification of rats' homogenized tissue and plasma levels of interleukine-1α (IL-1α), macrophage chemo-attractant protein (MCP-1), tumour necrosis factor-α (TNF-α), interferon-γ (IFN-γ) and interleukine-4 (IL-4).

Biological samples standardization was attentive to increase stability and representativeness of the cytokine measurement. Reagents were prepared following the manufacturer's recommendations. Assay buffer, the biotin-conjugate mixture and the bead mixture were prepared by adding the assay buffer concentrate (phosphate buffered saline with 10% bovine serum albumin; 10x) to distilled water (50:450 ml), diluting each biotin-conjugate (1:20) and diluting each bead set (1:20) and washing it once with rat reagent dilution buffer (RRDB), respectively. Standard mixture was prepared by reconstituting the lyophilized standard with distilled water, making a 1:20 dilution of the reconstituted standards all diluted in the same vial to get Standard 1 and proceeding to further serial dilutions. Streptavidin-phycoerythrin solution was prepared by adding 176 μl of the streptavidin-phycoerithrin concentrate to 5324 μl of the assay buffer (1x). Diluted standard mixture (25 μl) dilution "1" to "7" was pipetted into designated tubes. Procedure included addition of 25 μl of the assay buffer (1x) to the blank tubes, of 25 μl of the standard mixture dilution "1" to the tube which is designated for cytometer setup, of 25 μl of the sample (supernatant from the intestinal tissue homogenization or plasma) to designated tubes, of 25 μl of bead mixture to all tubes and of 50 μl of biotin-conjugate mixture to all tubes. Tubes were then incubated two hours at room temperature (18° to 25°C) protected from light. One milliliter of the assay buffer (1x) was added to all tubes, which were then washed twice by centrifugation (five minutes at 200 x g) discarding the supernatant carefully and leaving 100 μl of liquid in each tube; streptavidin-phycoerithrin solution (50 μl) was added to

all tubes followed by incubation for one hour at room temperature (18 to 25°C) protected from light. This procedure was repeated once except for adding 500 μl of the assay buffer (1x) to the 100 μl of the liquid remaining in each tube (instead of the streptavidin-phycoerithrin solution) and the samples were ready for analysis on the flow cytometer. Standard and test samples were analyzed using a FACSCalibur flow cytometer (Becton Dickinson, San Jose, California, USA) as stated in the producer's recommendations. Mean fluorescence intensities (MFIs) of the serially diluted standard samples were calculated and used to generate the standard curves of each cytokine that model protein concentration as a function of the MFI. Cytokine concentrations present in the test sample were calculated, using the corresponding standard curves and dilution factors.

Referent to **Chapter 6:** *Tissue growth factors profile after teduglutide administration on an animal model of intestinal anastomosis*

Table S5. Primers used in gene expression analysis of growth factors and Glp2 receptor by qRT-PCR

Gene*	GenBank Accession nº	Orientation	Sequence	Size (bp)
Rat Igf1	NM_001082477	Forward	GCCATTAGCCCTGCCCTTTCTT	78
Rat Igf1	NM_001082477	Reverse	GCCACCCAGTTGCTATTGCTTTCG	
Rat Vegfa	NM_001110333	Forward	CAGCGACAAGGCAGACTATTC	193
Rat Vegfa	NM_001110333	Reverse	CCGAAGTAATTTGAGGGAGTGAAG	
Rat Tgfb1	NM_021578	Forward	GTGGACCGCAACAACGCAATCT	100
Rat Tgfb1	NM_021578	Reverse	GTTCTGGCACTGCTTCCCGAATG	
Rat Ctgf	NM_022266	Forward	TGCCGGTAACAAGCCAGATT	394
Rat Ctgf	NM_022266	Reverse	GCAGCAAACACTTCCTCGTG	
Rat Fgf2	NM_019305	Forward	TGCTCTAGGGGACTGGAGATT	86
Rat Fgf2	NM_019305	Reverse	GACCAGCCTTCCACCCAAAG	
Rat Fgf7	NM_022182	Forward	TGGCAATCAAAGGGGTGGAA	249
Rat Fgf7	NM_022182	Reverse	TAGGAAGAAAGTGGGCCGTT	
Rat Egf	NM_012842	Forward	TGACCTTAGAACCACCGAGACCAT	92
Rat Egf	NM_012842	Reverse	TCTGCTGTGCTGTGACACTGAG	
Rat Hbegf	NM_012945	Forward	AGAGAGGACGGATGAGTGGT	99
Rat Hbegf	NM_012945	Reverse	GGAGGGTCCAAACAGCAGAT	
Rat Pdgfb	NM_031524	Forward	GCACAGAGACTCCGTAGAC	77
Rat Pdgfb	NM_031524	Reverse	CCGACTCGACTCCAGAATG	
Rat Glp2r	NM_021848	Forward	ACCTGTTCGCTTCGTTCA	106
Rat Glp2r	NM_021848	Reverse	GACATCCATCCACTCTCATCAT	
Rat Hprt1	NM_012583.2	Forward	CTCCTCAGACCGCTTTTC	86
Rat Hprt1	NM_012583.2	Reverse	CTGGTTCATCATCACTAATCAC	

* *Igf1: Insulin-like growth factor 1, transcript variant 1, mRNA; Vegfa: Vascular endothelial growth factor A, transcript variant 2, mRNA; Tgfb1: Transforming growth factor, beta 1, mRNA; Ctgf: Connective tissue growth factor, mRNA; Fgf2: Fibroblast growth factor 2, mRNA; Fgf7: Fibroblast growth factor 7, mRNA; Egf: Epidermal growth factor, mRNA; Hbegf: Heparin-binding EGF-like growth factor, mRNA; Pdgfb: Platelet-derived growth factor beta polypeptide, mRNA; Glp2r: Glucagon-like peptide 2 receptor, mRNA; Hprt1: Hypoxanthine phosphoribosyltransferase 1, mRNA* (housekeeping gene) (Rattus *norvegicus*)

S2. Protocol of analysis of gene expression levels of growth factors and glucagon-like peptide 2 receptor by quantitative real-time reverse-transcription polymerase chain reaction (qRT-PCR)

RNA extraction

Total RNA was extracted from the homogenates of the longitudinal strips of ileum using the Isolate II RNA Mini Kit (Bioline, London, UK). Succinctly, biological samples were first lysed and homogenized in the presence of guanidinium thiocyanate, a chaotropic salt that immediately deactivated endogenous RNases to ensure purification of intact RNA. After homogenization, ethanol was added to the sample. Lysate was filtered and the RNA adjusted to RNA binding conditions. Sample was then processed through a spin column containing a silica membrane to which the RNA binds. Genomic DNA contamination was removed by a DNase I digestion during the preparation. Any impurities such salts, metabolites and cellular components were removed by simple washing steps of the silica membrane with two different buffers. High-quality purified total RNA was then eluted in RNase-free water and stored at -80°C.

In particular, pellet obtained in the previously outlined protocol of intestinal tissue homogenization was sonicated twice with one short pulse of 10 seconds followed by cooling intervals of 30 seconds. According to the protocol, up to $5x10^6$ eukaryotic cells were collected by centrifugation and all supernatant was removed. Cells were directly lysed by adding 600 μl of lysis buffer RLY (with a guanidine salt) and 6 μl of β-mercaptoethanol, a denaturing agent, to the cell pellet and vortexed vigorously. Lysate was loaded on an Isolate II filter placed on a collection tube (2 ml) and a centrifugation for one minute at 11,000x *g* was performed to obtain a clear lysate with reduced viscosity to facilitate efficient binding of RNA to the column membrane. Isolate II filter was discarded, the flow-through was transferred into a new 1.5 ml microcentrifuge tube; 350 μl of 70% ethanol was added and mixed by vortexing (2 x 5 seconds). One Isolate II RNA mini column was placed in a collection tube (2 ml) for each preparation. Lysate was pipetted up and down two to three times and all loaded onto the column. A centrifugation for 30 seconds at 11,000x *g* was performed and the column was

placed in a new collection tube (2 ml). A 350 μl of membrane desalting buffer (MEM) was added and a centrifugation at 11,000x *g* for one minute was done to dry the membrane. DNase I (RNase-free) stock solution was prepared by reconstitution of lyophilized DNase I in RNase-free water (adding 540 μl of water for the 250 preparations kit), incubation for one minute at room temperature and mixing by gently swirling. A DNase I reaction mixture was prepared in a sterile 1.5 ml microcentrifuge tube. For each isolation, 10 μl of reconstituted DNase I was added to 90 μl of reaction buffer for DNase I (RDN) and mixed by gently flicking the tube. DNase I reaction mixture (95 μl) was applied directly onto the center of silica membrane. Incubation at room temperature for 15 minutes was done. Then, the silica membrane was washed and drying (three steps): wash buffer RW1 (200 μl) was added to the Isolate II RNA mini column (to inactivate the DNase I), a centrifugation for 30 seconds at 11,000x *g* was done and the column was placed into a new collection tube (2 ml); wash buffer RW2 (600 μl), prepared by adding 96-100% ethanol to wash buffer RW2 concentrate (100 ml x 3 for the 250 preparations kit), was added to the Isolate II RNA mini column, a centrifugation for 30 seconds at 11,000x *g* was done, the flow-through was discarded and the column was placed back into the collection tube; wash buffer RW2 (250 μl) was added to the Isolate II RNA mini column, a centrifugation for two minutes at 11,000x *g* was done (to dry the membrane completely) and the column was placed into a nuclease-free (1.5 ml) collection tube. RNA was eluted with 60 μl of RNase-free water and centrifuged at 11,000x *g* for one minute. Eluted RNA was placed on ice immediately to prevent degradation by RNases and freeze at -80°C for long-term storage.

Reverse-transcription (conversion of RNA to cDNA)

The Tetro cDNA Synthesis Kit (Bioline) was used for reverse-transcription. According to the protocol, priming premix was prepared on ice, in a RNase-free reaction tube, with total RNA (1 μg), random hexamer primer mix as a primer (1 μl), free nucleotides (dNTP) mix 10 mM (1 μl), Reverse-transcription buffer (5x) (4 μl), ribosafe RNase inhibitor (1 μl), tetro reverse transcriptase (moloney strain of murine leukemia virus reverse transcriptase; 200 U/μl; 1 μl) and diethylpyrocarbonate-treated

water (up to 20 μl) (Bioline). Solutions were vortex and centrifuged briefly before use. Mixture was mixed gently by pipetting and samples were incubated for 10 minutes at 25°C followed by 30 minutes at 45°C. Reaction was terminated by incubation of the mixture five minutes at 85°C and chilling on ice.

Real-time polymerase chain reaction

Quantitative RT-PCR was performed on a Bio-Rad iQ5 real-time PCR instrument (BioRad, Hercules, California, USA) using the SensiFAST SYBR & Fluorescein Kit (Bioline).

During the procedure, distinct areas were maintained for reaction set-up and PCR amplification to prevent any DNA contamination. One microliter of the reverse-transcription product of each sample was used for real-time PCR. A PCR mastermix was prepared by mixing 2x SensiFAST SYBR & fluorescein mix (10 μl; 1x), 10 μM forward primer (0.8 μl; 400 nM), 10 μM reverse primer (0.8 μl; 400 nM), template (100 ng cDNA *per* reaction) and water up to 20 μl. Magnesium chloride concentration in the (1x) reaction mix is 3 mM. A two-step cycling was performed and included one cycle of polymerase activation (two minutes at 95°C) and 40 cycles of denaturation (five seconds at 95°C), annealing and extension (20 seconds at 60°C). After the reaction had reached completion, a melting point analysis was performed. Melt peak chart was established following the instruments instructions (checking every 0.5°C between 50 and 95°C with intervals of one second). Quality control of the procedure was done, including the detection of the presence of contaminating DNA that may affect the reliability of the data; accordingly, no-reverse-transcriptase and no-template controls were set up. Purity of each PCR product was checked by analyzing the amplification plot and dissociation curves. Each sample was monitored for fluorescein and signals were regarded as significant if the fluorescence intensity exceeded 10-fold of the standard deviation of the baseline fluorescence, defined as threshold cycles (C_T). C_T were selected in the line in which all samples were in the logarithmic phase. For each sample, PCR was performed in duplicate. Data were analyzed by relative quantification.

S3. Protocol for determination of glucagon-like peptide 2 plasma concentrations by competitive enzyme immunoassay

Plasma levels of glucagon-like peptide 2 (glp-2) were determined by competitive enzyme immunoassay (EIA) using the Glp-2 EIA Kit 96-Well Plate (Phoenix Europe GmbH, Karlsuhe, Germany).

Following the manufacturer's protocol, procedure began with extraction of peptides from plasma. Rats' plasma collected, as stated before, was acidified with 1% trifluoroacetic acid and centrifuged at 3000x *g* for 20 minutes at 4°C; supernatant acidified plasma solution was loaded onto a pre-equilibrated SEP-column containing 200 mg of C-18; eluent collected into a polystyrene tube was evaporated to dryness using a centrifugal concentrator and then lyophilized.

Enzyme immunoassay protocol began with standard peptide and quality controls preparation. Assay buffer solution (1x), used to dilute or reconstitute all other reagents and samples, was prepared by dilution of the assay buffer concentrate (20x; 50 ml) with 950 ml of distilled water and mixing. Standard peptide was centrifuged, diluted with 1 ml of assay buffer solution (1000 ng/ml), vortexed gently and allowed to sit for at least 10 minutes at room temperature; standard peptide was centrifuged and vortexed immediately before use. Assay buffer (0.9 ml) was added to each of five tubes. Serial dilutions were prepared by adding 0.1 ml of the prepared standard to Tube 1 (100 ng/ml) and mixing well; transferring 0.1 ml of Tube 1 to Tube 2 (10 ng/ml), mixing well; transferring 0.1 ml of Tube 2 to Tube 3 (1 ng/ml), mixing well; transferring 0.1 ml of Tube 3 to Tube 4 (0.1 ng/ml), mixing well and transferring 0.1 ml of Tube 4 to Tube 5 (0.01 ng/ml) and mixing well. Positive control was centrifuged and rehydrated with 200 μl of the assay buffer solution, allowed to sit for at least five minutes and mixed thoroughly.

Primary antibody (rabbit anti-peptide IgG) and biotinylated peptide were reconstituted with 5 ml of the assay buffer solution, allowed to sit for at least five minutes and mixed thoroughly. Enzyme solution was prepared by pipetting 12 μl of the streptavidin-horseradish peroxidase into 12 ml of the assay buffer solution, after centrifugation (3000-5000 rpm) during five seconds, and voxtexing thoroughly.

Fifty microliters of prepared peptide standards (#1 to 5), rehydrated positive control and plasma sample were added to the designated wells (in duplicate) leaving two wells as "blank" and two wells as "total binding" (exclusively with the assay buffer solution). Reconstituted primary antibody and prepared biotinylated peptide (25 μl of each) were added to each well except the "blank". Immunoplate was sealed with the acetate plate sealer and incubated for two hours, at room temperature (20 to 23°C) with orbital shaking at 300 to 400 rpm. Next, plate sealer was removed and solutions were decanted from the plate. Four careful washes were performed, with 350 μl of the assay buffer solution *per* well, decanting and tapping firmly after each wash to remove residual buffer. Streptavidin-horseradish peroxidase solution (100 μl) was added to each well. Plate was covered with sealer and incubated for one hour, at room temperature, with moderate shaking (300 to 400 rpm) on the microtiter plate shaker. Plate sealer was removed and solutions decanted from the plate. Four careful washes were performed, with 350 μl of the assay buffer solution *per* well, decanting and tapping firmly after each wash to remove residual buffer. The 3,3',5,5'-tetramethylbenzidine substrate solution (100 μl) was added to each well, avoiding unnecessary exposure to light; plate was covered with sealer and incubated for one hour, at room temperature, with moderate shaking (300 to 400 rpm) on the plate shaker. Blue color was formed in wells of the peptide standards with intensity inversely proportional to the concentration of the peptide. Sealer was removed and 100 μl of stop solution (2N hydrochloric acid) was added to each well; plate was shaken by hand to ensure complete mixing of solution in all wells. Blue color turned to yellow after acidification. Absorbance (optical density) was read at 450 nm in a microtiter plate reader within 20 minutes. Difference of absorbance units was recorded.

A standard curve was constructed using the serial dilutions of peptide standards (known concentrations of standard peptide on a logarithmic scale *versus* its corresponding optical density reading on a linear scale). This analysis modeled the peptide concentration as a function of the optical density. Standard curve showed reverse sigmoidal shape and an inverse relationship between peptide concentrations and the corresponding absorbance. As the standard concentration increases, the yellow color decreases, thereby reducing the optical density absorbance. Then, the

Glp-2 plasma concentrations were calculated using the corresponding standard curve and the microplate reader with Gen5 software (Synergy HT, Biotek, Winooski, Vermont, USA), and expressed in ng/ml.

Referent to **Chapter 7:** *Teduglutide effects on gene regulation of fibrogenesis on an animal model of intestinal anastomosis*

Table S6. Primers used in gene expression analysis of extracellular matrix components by qRT-PCR

Gene*	GenBank Accession nº	Orientation	Sequence	Size (bp)
Rat Col1a1	NM_053304.1	Forward	GTGCGATGGCGTGCTATG	111
Rat Col1a1	NM_053304.1	Reverse	ACTTCTGCGTCTGGTGATACA	
Rat Col3a1	NM_032085.1	Forward	GTGTGATGATGAGCCACTAGACTG	98
Rat Col3a1	NM_032085.1	Reverse	GAATGACAGGAGCAGGTGTAGAAG	
Rat Col4a1	NM_001135009.1	Forward	TCTTCCACCCTCTACACAGA	108
Rat Col4a1	NM_001135009.1	Reverse	TCCACAGAAAGCCATGACTT	
Rat Col5a1	NM_134452.1	Forward	CAGCAGAACATCACCTACAA	87
Rat Col5a1	NM_134452.1	Reverse	CAAGAAGCGGATAGCCTTAT	
Rat Timp1	NM_053819.1	Forward	CATCCTCCTGTTGCTATCATTG	149
Rat Timp1	NM_053819.1	Reverse	GCTGGTATAAGGTGGTCTC	
Rat Timp2	NM_021989.2	Forward	TCAGCAGACAGCAGCATTA	104
Rat Timp2	NM_021989.2	Reverse	CGGCTACACAGTCTTATAACAAC	
Rat Mmp1	NM_001134530.1	Forward	ATGGACCTGAATATGGACTTG	188
Rat Mmp1	NM_001134530.1	Reverse	GAACATTAGTGCTCCTACATCTC	
Rat Mmp2	NM_031054.2	Forward	CACCAAGAACTTCCGACTATCCA	88
Rat Mmp2	NM_031054.2	Reverse	ACCAGTGTCAGTATCAGCATCAG	
Rat Mmp3	NM_133523.2	Forward	TCCCTGAAACCGTCCAGAAGA	174
Rat Mmp3	NM_133523.2	Reverse	CATCCACCTTTGTGCCAATGC	
Rat Mmp9	NM_031055.1	Forward	TGGACAGCGAGACACTAA	103
Rat Mmp9	NM_031055.1	Reverse	TTATGATGGTGCCACTTGAG	
Rat Mmp12	NM_053963.2	Forward	CGATGTGGAGTGCCTGATGTA	111
Rat Mmp12	NM_053963.2	Reverse	ACGCTTCATGTCTGGAGTGTAAT	
Rat Mmp13	NM_133530.1	Forward	CGTTCAAGGAATCCAGTCTCT	106
Rat Mmp13	NM_133530.1	Reverse	AATGGCATCAAGGGATAGGG	
Rat Mmp14	NM_031056.1	Forward	GGCATTTCCAGGAGCAATTC	75
Rat Mmp14	NM_031056.1	Reverse	GTCTTCTAAAGGAACGGAATGTGA	
Rat Hprt1	NM_012583.2	Forward	CTCCTCAGACCGCTTTTC	86
Rat Hprt1	NM_012583.2	Reverse	CTGGTTCATCATCACTAATCAC	

**Col1a1: Collagen, type I, alpha 1, mRNA (coding for collagen alpha-1(I) chain); Col3a1: Collagen, type III, alpha 1, mRNA; Col4a1: Collagen, type IV, alpha 1, mRNA; Col5a1: Collagen, type V, alpha 1, mRNA; Timp1: TIMP metallopeptidase inhibitor 1, mRNA (coding for metalloproteinase inhibitor 1); Timp2: TIMP metallopeptidase inhibitor 2, mRNA; Mmp1: Matrix metallopeptidase 1 (interstitial collagenase), mRNA; Mmp2: Matrix metallopeptidase 2, mRNA; Mmp3: Matrix metallopeptidase 3, mRNA; Mmp9: Matrix metallopeptidase 9, mRNA; Mmp12: Matrix metallopeptidase 12, mRNA; Mmp13: Matrix metallopeptidase 13, mRNA; Mmp14: Matrix metallopeptidase 14 (membrane inserted), mRNA; Hprt1: Hypoxanthine phosphoribosyltransferase 1, mRNA* (housekeeping gene) (Rattus *norvegicus*)

Table S7. Relevant correlations between putative intestinal epithelial stem cells and other parameters[a]

(σ / *p*)	Lgr5$^+$/Bmi1$^-$ cells	Lgr5$^-$/Bmi1$^+$ cells	Lgr5$^+$/Bmi1$^+$ cells	Lgr5$^+$ or Bmi1$^+$ cells
Viability and death				
Viability index	55.9% *p*=0.0001			
Early apoptosis index	-39.8% *p*=0.002			
Late apoptosis/necrosis index	-40.2% *p*=0.002			
Necrosis index	-37.3% *p*=0.004			
Oxidative stress				
Cytosolic peroxides	61.7% *p*=0.0001	-48% *p*=0.0001		
Mitochondrial reactive species	72.9% *p*=0.0001	-42.8% p=0.001		
Cellular reduced glutathione	-64.6% *p*=0.0001	40.9% *p*=0.001		
Mitochondrial membrane potential	-63.2% *p*=0.0001	36.9% *p*=0.004		
Tissue cytokines level				
[IL-1α]	47.2% *p*=0.0001	-29.9% *p*=0.021		
[MCP-1]	48.7% *p*=0.0001			
[TNF-α]	53.1% *p*=0.0001			27.2% *p*=0.037
[IFN-γ]	-27.4% *p*=0.036			
[IL-4]	29.5% *p*=0.023		51.9% *p*=0.0001	49.3% *p*=0.0001
Plasma cytokines concentration				
[IL-1α]	29.9% *p*=0.024			
[MCP-1]	27.5% *p*=0.038	-34.6% *p*=0.008		
[TNF-α]		-35.3% *p*=0.007		
[IFN-γ]		28.4% *p*=0.032		
[IL-4]	-33.2% *p*=0.012			-38.2% *p*=0.003

[a] Relevant correlations of the proportion of putative intestinal epithelial stem cells isolated from rats' ileum, at the moment of sacrifice, in all the studied animals (*n*=59), as determined by flow cytometry, *versus* cellular viability and death indexes, oxidative stress parameters, tissue and plasma levels of cytokines. Samples recovered at the sacrifice in rats submitted to ileal resection corresponded to the anastomotic segment. Viability and death analysis was performed by flow cytometry with Annexin-V/Propidium iodide; cytokines levels were determined by flow cytometric bead assay; peroxides production in the cytosol, reactive species generation in the mitochondria, mitochondrial membrane potential and cellular reduced glutathione content were evaluated by the DCF expression, DHR123 production, aggregates/monomers ratio of JC-1 probe and mercury orange staining determined by flow cytometry, respectively. Spearman's correlation coefficent (σ) and value of significance (*p*) were presented

Table S8. Relevant correlations between putative intestinal epithelial stem cells and tissue gene expressions of growth factors and plasma levels of glucagon-like peptide 2[a]

σ / *p*	Lgr5^{+}/Bmi1^{-} cells	Lgr5^{-}/Bmi1^{+} cells	Lgr5^{+}/Bmi1^{+} cells	Lgr5 or Bmi1^{+} cells
Gene expression of growth factors/receptor				
Igf1				
Vegfa	62.5% *p*=0.0001			
Tgfb1	-39.7% *p*=0.002			
Ctgf		30.7% *p*=0.019	43.5% *p*=0.001	54.7% *p*=0.0001
Fgf2				30.6% *p*=0.02
Fgf7	-36% *p*=0.005	51.9% *p*=0.0001		
Egf		53.3% *p*=0.0001		43.9% *p*=0.001
Hbegf				
Pdgfb	-37.8% *p*=0.003		-26,1% *p*=0.048	
Glp2r		49.7% *p*=0.0001		34.5% *p*=0.008
Plasma Glp2 levels				
[Glp2]		-57% *p*=0.0001		-49.7% *p*=0.0001

[a] Relevant correlations of the proportion of putative epithelial stem cells isolated from rats' ileum, at the moment of sacrifice, in all the studied animals (*n*=59), as determined by flow cytometry, *versus* relative gene expressions of growth factors and glucagon-like peptide 2 receptor (Glp2r), and postoperative plasma levels of glucagon-like peptide 2 (Glp-2). Relative gene expressions of growth factors and Glp2r and postoperative plasma levels of Glp-2 were determined by quantitative real-time reverse-transcription polymerase chain reaction (qRT-PCR) and by competitive enzyme immunoassay, respectively. Samples recovered at sacrifice in rats submitted to ileal resection corresponded to the anastomotic segment. Spearman's correlation coefficent (σ) and value of significance (*p*) were presented